Université de Montréal

AXL receptor tyrosine kinase in breast cancer: Defining novel substrates and pathways involved in cell motility and invasion

Par Afnan Abu-Thuraia

Programmes de Biologie Moléculaire

Faculté de Médecine

Thèse présentée
en vue de l'obtention du grade de de doctorat
en Biologie Moléculaire

August 2018

Résumé

Le cancer du sein est le cancer le plus fréquemment diagnostiqué et le plus mortelle chez la femme, où sa progression vers le stade métastatique constitue une menace pour la vie des patientes. La présence de métastases représente le défi clinique central de l'oncologie des tumeurs solides, de sorte que les mécanismes et les voies sous-jacents au processus métastatique doivent être mieux définis. L'expression aberrante du récepteur tyrosine kinase (RTK) AXL a été liée cliniquement à la formation de métastases et à l'acquisition d'une résistance aux médicaments contre le cancer. AXL est un membre de la sous-famille des récepteurs tyrosine kinase TAM et intervient dans plusieurs processus biologiques tels que l'atténuation de la réponse immunitaire, l'élimination des cellules apoptotiques et la promotion de la survie cellulaire. L'expression d'AXL dans les tumeurs primaires humaines corrèle avec la faible survie des patients. Malgré sa régulation positive préférentielle dans les lignées cellulaires triple négatives / basales B, des études ont montré que l'expression d'AXL est indépendante du sous-type de la tumeur mammaire des patients. AXL peut être activé par son ligand GAS6 ou par d'autres RTK. Lors de son activation, AXL induit une signalisation en aval entraînant l'activation d'intermédiaires de signalisation canoniques, notamment MAPK, AKT et PI 3-kinases. Cependant, les voies de signalisation spécifiques engagées par AXL pour conférer un tel pouvoir pro-invasion ne sont pas connues. Ainsi, le but de cette thèse est d'identifier des substrats spécifiques d'AXL et des voies en aval qui jouent un rôle important dans le maintien d'un état « EMT » et d'un renforcement du phénotype mésenchymal dans les cellules cancéreuses.

À la recherche de régulateurs en amont du complexe ELMO/DOCK1 impliqués dans l'activation de RAC, nous présentons au chapitre 2 les protéines d'échafaudage ELMO en tant que substrats directs et partenaires de liaison d'AXL. Grâce à des approches de protéomique et de mutagenèse, nous révélons que la kinase AXL phosphoryle ELMO1/2 sur un résidu tyrosine carboxy-terminal conservé. Dans les cellules cancéreuses du sein, l'activation d'AXL dépendante de GAS6 a conduit à la phosphorylation endogène d'ELMO2 sur Tyr-713, menant ainsi à la formation du complexe AXL/ELMO. En outre, l'activation de RAC induite par GAS6 dans les cellules cancéreuses du sein dépendait de l'expression d'ELMO2. Semblable au blocage

d’AXL, l'inhibition d’ELMO2 ou l'inhibition pharmacologique de DOCK1 supprime l'invasion des cellules du cancer du sein, qui, selon nous, dépendait de l'état de phosphorylation d'ELMO. Notre travail au chapitre 2 définit un nouveau mécanisme par lequel AXL favorise la prolifération et l'invasion cellulaire et identifie l'inhibition de la voie ELMO/DOCK comme une cible thérapeutique potentielle pour arrêter les métastases induites par AXL.

Bien qu'il soit encore difficile de savoir comment les signaux d’AXL induisent son phénotype pro-invasif, notre travail au chapitre 3 vise à identifier des substrats et des voies de signalisation spécifiques qui sont significativement modulés lors de l'activation d'AXL. Pour y remédier, nous avons défini le phosphoprotéome de la régulation d’AXL dans des cellules cancéreuses du sein triple-négatives en utilisant une approche quantitative. Nous révélons qu’AXL module de manière robuste, parmi de nombreux processus et voies biologiques importants, la phosphorylation d'un réseau de protéines d'adhésion focale (FA) aboutissant à un désassemblage plus rapide des FA. De manière intéressante, nous avons trouvé que la modulation de la voie FA était unique à AXL par rapport à d'autres RTK tels que l'EGFR. En particulier, nous avons trouvé qu’AXL phosphoryle la protéine NEDD9, modulant la formation du complexe NEDD9/CRKII/DOCK3, qui orchestre la phosphorylation de la pseudo-kinase PEAK1 médiée par AXL. Nos données révèlent un mécanisme distinct par lequel les complexes PEAK1 avec la kinase CSK médient la phosphorylation de PXN et le renouvellement des FA induit par AXL. En utilisant l'injection orthotopique de cellules cancéreuses du sein dans le tissu adipeux mammaire des souris et dans la veine de la queue, nous révélons que l'inactivation de PEAK1 par CRISPR diminue la croissance tumorale et les métastases *in vivo*. De plus, notre travail au chapitre 3 révèle une contribution unique et inattendue de la signalisation d’AXL à la dynamique des FA, révélant un mécanisme longtemps recherché sous-tendant l'activité invasive d'AXL. Cette compréhension approfondie des réseaux de signalisation régulés par AXL identifie PEAK1 comme une nouvelle cible thérapeutique dans les tumeurs AXL positives.

En conclusion, cette thèse a identifié, pour la première fois, le phosphoprotéome d’AXL et des voies de signalisation spécifique à AXL, pouvant justifier le rôle du récepteur en tant que promoteur de métastases et de résistance aux médicaments. Notre travail révèle de nouvelles cibles thérapeutiques qui pourraient avoir un grand potentiel si elles sont utilisées en thérapie

combinatoire avec l'inhibition d'AXL pour prévenir la formation de métastases des tumeurs AXL positives.

Mots clés: Métastases, Voies de signalisation récepteur de tyrosine tinase, Protéomique, Adhésion focale, Cancer du sein, Invasion cellulaire

Abstract

Breast cancer is the most frequently diagnosed cancer in women where its progression to the metastatic stage poses a threat to the life of patients. The metastatic disease represents the central clinical challenge of solid tumor oncology such that mechanisms and pathways underlying the metastatic process must be better defined. The aberrant expression of the receptor tyrosine kinase (RTK) AXL has been linked clinically to metastasis and acquisition of drug resistance. AXL is a member of the TAM subfamily and functions in several biological processes such as dampening the immune response, clearing apoptotic cells and promoting cell survival. Despite its preferential upregulation in triple negative/basal B cell lines, studies have shown AXL expression in the clinic to be subtype independent. AXL can be activated by its ligand GAS6 or by a crosstalk with other RTKs. Upon its activation, AXL induces downstream signaling resulting in the activation of canonical signaling intermediates including MAPKs, AKT and PI 3-kinases. However, the specific signaling pathways engaged by AXL to confer such enhanced pro-invasion power are not known and the goal of this thesis is to identify AXL-specific substrates and downstream pathways that are behind AXL's significant role in maintaining an EMT state and reinforced mesenchymal phenotype in cancer cells.

In search of upstream regulators of ELMO/DOCK1 complex involved in RAC activation, we reported ELMO scaffolds as direct substrates and binding partners of AXL. Through proteomics and mutagenesis approaches, we revealed phosphorylation of ELMO1/2 by AXL kinase on a conserved carboxyl-terminal tyrosine residue. In breast cancer cells, GAS6-dependent activation of AXL led to endogenous ELMO2 phosphorylation on Tyr-713 and AXL/ELMO complex formation. In addition, GAS6-induced RAC activation in breast cancer cells was dependent on ELMO2 expression and phosphorylation. Our work in chapter 2 defines a new mechanism by which AXL promotes cell proliferation and invasion and identifies inhibition of ELMO/DOCK pathway as a potential therapeutic target to stop AXL-induced metastases.

While it still remains elusive how AXL signals to induce its pro-invasive phenotype, our work strove to identify specific substrates and signaling pathways that are significantly modulated upon AXL activation using a quantitative phosphoproteomics approach. By

generating GAS6-induced AXL phosphoproteome, we found that AXL robustly modulates, among many different significant biological processes and pathways, the phosphorylation of a network of focal adhesion (FA) proteins culminating in faster FA disassembly. Interestingly, we found AXL modulation of FA pathway to be unique to AXL in comparison with other RTKs such as EGFR. NEDD9 FA protein was identified to be a direct substrate of AXL, where its phosphorylation modulates its complex formation with CRKII/DOCK3, and this subsequently orchestrates the AXL-mediated phosphorylation of the pseudo-kinase PEAK1. Our data revealed a distinct mechanism by which PEAK1 complexes with CSK kinase, mediating PXN phosphorylation and AXL-induced FA turnover. Using *in vivo* assays such as tail-vein metastasis assay and tumor growth assay, we revealed that gene inactivation of PEAK1 by CRISPR CAS9 decreased tumor growth and metastasis. Furthermore, our work in chapter 3 uncovers an unexpected and unique robust contribution of AXL signaling to FA dynamics revealing a long sought-after mechanism underlying AXL pro-invasive activity. This in-depth understanding of AXL regulated signaling networks identifies PEAK1 as a new therapeutic target in AXL positive tumors.

In conclusion, this thesis identified, for the first time, AXL phosphoproteome and AXL specific downstream signaling pathways that may justify AXL's role as a promoter of metastasis and drug resistance. Our work reveals novel therapeutic drug targets that may hold a great potential if used in combinational therapeutics with AXL inhibition to prevent metastasis of AXL positive tumors.

Keywords: Metastasis, RTK signaling, Proteomics, Focal adhesion, Breast Cancer, Cell invasion

Preface

This thesis is written in a manuscript format by articles and is divided into three chapters followed by a discussion. It contains one published article and two articles prepared for submission.

CHAPTER 1: INTRODUCTION

Section 1.1, 1.3, and 1.4 contain a literature review on breast cancer and metastasis, dynamics of actin cytoskeleton, and cancer cell migration and invasion, respectively. Section 1.5 contains our research hypothesis and objectives. Section 1.2 contains a manuscript of a review to be submitted for publication:

Abu-Thuraia A*, Goyette MA*, Delliaux C and Côté JF (2018) Dissecting AXL's role in cancer progression. *Equal contribution

CHAPTER 2: AXL phosphorylates ELMO scaffold proteins to promote RAC activation and cell invasion.

This chapter contains a published article:

Abu-Thuraia A, Gauthier R, Chidiac R, Fukui Y, Screaton RA, Gratton JP and Côté JF (2015). Axl phosphorylates Elmo scaffold proteins to promote Rac activation and cell invasion. **MCB** 35, 76-87.

CHAPTER 3: AXL confers cell migration and invasion by hijacking a PEAK1-regulated focal adhesion protein network.

This chapter contains a submitted manuscript to Nature Communication and is in revision:

Abu-Thuraia A, Goyette MA, Delliaux C, Boulais J, Chidiac R, Bagci H, Davidson D, Veillette A, Daly RJ, Gingras AC, Gratton JP and Côté JF (2018).

Table of Content

List of tables

List of figures

List of abbreviations

ABP: Actin Binding Proteins

ADAM10: ADAM Metallopeptidase Domain 10

ADAM17: ADAM Metallopeptidase Domain 17

ADP: Adenosine Diphosphate

AKT: AKT Serine/Threonine Kinase

ALK: Anaplastic Lymphoma Kinase, RTK

ARMs: Armadillo Repeats

ATP: Adenosine Triphosphate

AXL: AXL Receptor Tyrosine Kinase

BAD: BCL-2 Associated Agonist of Cell Death

BAX: BCL-XL Associated Protein

BCAR1: Breast Cancer Antiestrogen Resistance 1

BCL-2: B-cell CLL/Lymphoma-2

BCL-XL: BCL-2 Like Protein

B-CLL: B-cell Chronic Lymphocytic Leukemia

βPIX: β-PAK Interacting Exchange Factor

C1-TEN: C1-Domina containing Phosphatase and Tensin Homolog

CAF: Cancer-Associated Fibroblasts

CBLB: CBL proto-oncogene B

CRKII: CRK proto-oncogene, Adaptor protein

CSK: C-terminal SRC Kinase

CTC: Circulating Tumor Cells

CXCR4: C-X-C Motif Chemokine Receptor 4

DH: Dbl Homology

DHR: Dbl Homology Region

DOCK: Dedicator of cytokinesis

DTC: Disseminated Tumor Cells

ECM: Extracellular Matrix

EGFR: Epidermal Growth Factor Receptor

EID: ELMO Inhibitory Domain

ELMO: Engulfment and cell motility

EMT: Epithelial-to-Mesenchymal Transition

EPHA2: Ephrin Receptor 2

ER: Estrogen Receptor

ERK: Extracellular Signal-Regulated Kinase

FA: Focal Adhesions

FAK: Focal Adhesion Kinase

FRA-1: FOS Related Antigen-1

GAP: GTPase Activating Protein

GAS6: Growth Arrest Specific 6

GDI: GDP Dissociation Inhibitor

GDP: Guanosine Diphosphate

GEF: Guanine nucleotide Exchange Factor

GIT1: G-protein coupled receptor kinase Interacting ArfGAP1

GnRH: Gonadotropin-Releasing Hormone

GPCR: G-Protein Coupled Receptor

GRB2: Growth Factor Receptor Bound Protein 2

GTP: Guanosine Triphosphate

HER2: Human Epidermal Growth Factor Receptor 2

HR: Homologous Recombination

KID: Kinase Insert Domain

KO: Knockout

LPA: Lipoprotein A

MCL1: Myeloid Cell Leukemia 1

MEK: MAPK/ERK kinase

MERTK: MER Proto-oncogene, Receptor Tyrosine Kinase

MET: Mesenchymal-to-Epithelial Transition

MET: MET proto-oncogene

MHC1: Major Histocompatibility Complex 1

MMP: Matrix Metallopeptidase

MYPT1: Myosin phosphatase, Target Subunit 1

NCK: NCK adaptor protein

NEDD9: Neural precursor cell Expressed, Developmentally Downregulated 9

NF-KB: Nuclear Factor Kabba B subunit

NK: Natural Killer Cells

OPCML: Opioid Binding Protein/Cell Adhesion Molecule-Like

PAK: P21 Activated Kinase

PDGFR: Platelet Derived Growth Factor Receptor

PD-L1: Programmed Death-Ligand 1

PEAK1: Pseudopodium Enriched Atypical Kinase 1

PI3K: Phosphatidylinositol-4,5-Bisphosphate 3-Kinase

PKA: Protein Kinase A

PKC: Protein Kinase C

PLC-γ: Phospholipase C-γ

PR: Progesterone Receptor

PRAG1: PEAK1 Related-Kinase Activating Pseudokinase 1

PRR: Proline-Rich Region

PS: Phosphatidyl Serine

PTK2: Protein Tyrosine Kinase 2

PTPRG: Protein Tyrosine Phosphatase, Receptor Type G

PUMA: P53 Up-regulated Modulator of Apoptosis

PXN: Paxillin

PyMT: Polyoma Middle T oncoprotein

RAS: RAS proto-oncogene GTPase

RBD: Ras binding domain

RTK: Receptor Tyrosine Kinase

SDF-1α: Stromal cell-Derived Factor 1α

SH3: SRC Homology Domain 3

SH2: SRC Homology Domain 2

SRC: SRC proto-oncogene, nonreceptor tyrosine kinase

STAT: Signal Transducer and Activator of Transcription

TAM: Tyro3 AXL MER

TGF-β: Transforming Growth Factor β

THBS2: Thrombospondin 2

TKD: Tyrosine Kinase Domain

TKI: Tyrosine Kinase Inhibitor

TLR: Toll-Like Receptor

TMA: Tissue Microarray

TNBC: Triple Negative Breast Cancer

TYRO3: TYRO3 Protein Tyrosine Kinase

VEGFR-2: Vascular Endothelial Growth Factor Receptor - 2

VSMC: Vascular Smooth Muscle Cells

WASP: Wiskott-Aldrich Syndrome Protein

WAVE2: Wiskott-Aldrich Syndrome Protein family member 2

ZEB1/2: Zinc Finger E-box Binding Homeobox 1/2

To my dear family

Acknowledgments

First and foremost, I would like to thank GOD for giving me the will and power to believe in myself and pursue my goals in attaining a doctorate degree. I could never have done this without the faith I have in you.

I take immense pleasure to express my sincere gratitude to my guiding supervisor and mentor Dr. Jean-Francois Cote for his continuous guidance and mentorship, for believing in who I can become, and for his creative suggestions and motivation throughout my doctoral research. I thank him for developing my scientific curiosity and critical thinking. I submit my humble thanks to him for bringing my dreams into reality.

I offer my gratitude to the members of my thesis committee, Dr. David Hipfner, Dr. Peter Siegel and Dr. Philippe Roux, for their support and encouragement, as well as their continuous interest and follow up in my doctoral work.

Thanks to our funding agencies, CIHR and Quebec Breast Cancer Foundation, who this work would not have been possible without. I also want to thank the funding who provided my doctoral scholarships: Internal IRCM award offered by Emmanuel Triassi and FRQS doctoral award. In addition, thanks to Universite de Montreal and IRCM for the poster and oral talk awards I received throughout my doctoral years during conferences.

I would like to extend my gratitude to Universite de Montreal and the department of Biologie Moleculaire for supporting me in attaining my doctoral degree. I am also thankful to the IRCM community for making these past 6 years memorable, Virginie Leduc for her help and cooperation to reach my academic expectations and IRCM platform facilities, specifically Dr. Dominic Filion in Microscopy platform and Dr. Denis Faubert in Proteomics department. Huge thanks go to Dr. Jonathan Boulais, our computational analyst, who helped in analyzing my mass spectrometry data and bringing it into a visual model. Without them, our work wouldn't have advanced technically.

Thanks to our collaborators: Dr. Jean-Philippe Gratton, Dr. Rob Screaton, Dr. Roger Daly, Dr. Andre Veillette, Dr. Yoshinori Fukui and Dr. Anne-Claude Gingras for their time and

resources. Special thanks go to Rosemarie Gauthier, Dr.Halil Bagci, Dr. Rony Chidiac and Dr. Carine Delliaux for their contributions in our work.

I sincerely acknowledge my previous and current colleagues that shared with me, the ups and downs, throughout my doctoral years. Thanks to Marie-Anne for the good teamwork on collaborations we have made as well as the insightful discussions on our protein AXL. Thanks to Viviane for always making me critical of my data and for being interested to give me some scientific input. Thanks to Noumeira for being a friend and for sharing a cup of coffee or a walk with me. Thanks to our previous and current research assistants, Ariane Pelletier, and Marie-Pier Thibault, for their continuous support, availability, and interest.

I cherish friendship and will take this opportunity to thank my friends and specifically Kathy Malas who has been an encouragement every time and who put confidence in me and helped me reach here. Thank you for your continuous support, whole-hearted solidarity and for bearing with me throughout my tough days.

Thank you to my amazing husband Mohamed, who has supported me and pushed me throughout these years to be my best. I could not have done this without his support, love, and encouragement.

Last but not least, my greatest gratitude and for whom I owe so much, is my beloved parents, Nabil Abu-Thuraia and Shamieh Al-Khatib. I can not find the words to express the wisdom, love, and support I have had from them throughout my bachelor, master, and Ph.D. I am in debt for your unconditional love, encouragement, and endurance. You have always been there with me and my family and supported us throughout those years. Without them, I would have never achieved what I achieved today. My heartful gratitude also goes to my beautiful siblings who always have been there through the thick and thin. Thank you for continuous support and encouragement!

There are so many others whom I may have not mentioned, and I sincerely thank all of them for their support.

CHAPTER 1

INTRODUCTION

1.1 The Central Dogma of Cancer

Cancer is a neoplastic disease that is very complex. It consists of an uncontrolled growing tumor that represents a complex tissue where multiple cell types are involved participating in heterotypic interactions with one another. Cancer occurs when a normal cell acquires a neoplastic state due to oncogenic and tumor suppressor mutations that will enable it to become tumorigenic and malignant. To understand the complexity of this disease, hallmarks of cancer have been proposed and comprise of eight biological capabilities that are acquired during the progress of the disease. These hallmarks include sustaining proliferative signaling, evading growth suppressors, resisting cell death, enabling replicative immortality, reprogramming of energy metabolism, evading immune destruction, inducing angiogenesis, activating invasion and metastasis and cellular dormancy [1-3]. These biological capabilities allow the cancer cell to survive, proliferate and disseminate via distinct mechanisms in diverse tumor types at various times during the process of tumorigenesis. The acquiring of these hallmarks is made possible by the enabling characteristics of the neoplasia. One of which is genome instability and mutability in the cancer cells, which generates random mutations and genetic alterations including chromosomal rearrangements, that will allow tumor progression [2, 3]. These will in turn foster and orchestrate the hallmark capabilities. Another enabling feature or characteristic of the neoplasia involves the inflammatory state of the premalignant neoplasia that is driven by the innate immune cells to promote inflammation that will support multiple hallmark capabilities.

Apart from these biological capabilities acquired by the cancer cells, normal cells in the vicinity of the cancer cells are also used by the cancer cells to contribute to tumorigenesis and acquire their hallmarks. These cells are known to create what is known as “tumor-associated stroma” or “tumor microenvironment” [2, 3]. This tumor microenvironment consists of many different cell types such as cancer-associated fibroblasts, cancer stem cells, endothelial cells, pericytes, and immune inflammatory cells. The interactions and associations between these diverse cell types in a tumor environment are orchestrated and maintained by heterotypic signaling interactions that are of a great importance for tumor progression. Interestingly, these heterotypic intracellular signaling are not static and change along the way the tumor progresses due to the reciprocal interactions between the cancer cells and the stromal cells, where stromal cells enhance the neoplastic phenotypes of the cancer cells and the cancer cells evolve to

reprogram the stromal cells to support the neoplasm growth and ultimately its dissemination into adjacent tissues.

1.1.1 Metastasis

Metastasis is the final stage of multistep tumor progression. It is divided into two steps: the step where the tumor disseminates from its primary tissue and colonize into a distant tissue and the step where the disseminated tumor has to successfully colonize and form metastases. The process of dissemination starts when the epithelial cancer cell becomes invasive and goes through a process of alterations in shape and its attachment with other cells and the extracellular matrix (ECM). One of the best-characterized features of this process is the change in expression of an adhesion molecule named E-Cadherin, which is responsible for the formation of adherens junctions in cell-cell contact. Reduction of its expression is known to potentiate the process of invasion and metastasis [4, 5]. In contrast, another adhesion molecule named N-Cadherin, known to be expressed in migrating neurons and mesenchymal cells is upregulated in invasive tumor cells.

The invasion metastasis cascade is a multistep process [6, 7] (**Figure 1.1.1**). In specific, epithelial cells in primary tumors invade locally the surrounding tissue by degrading the ECM and the stromal cell layer. They then intravasate into the lumina of the blood vessels and survive in the circulation to adhere to the vessel at a distant organ site to extravasate into the parenchyma of the distant tissue. Once extravasated, the tumor cells must survive the foreign environment in order to colonize and form micrometastases. To further grow and form macrometastases, the tumor needs to go through a step named metastatic colonization, where the tumor cells reinitiate their proliferative programs to grow and proliferate. These steps of the invasion metastasis cascade are influenced by intrinsic molecular pathways orchestrated in the carcinoma cells, as well as extrinsic signaling cascades from non-neoplastic stromal cells [7].

Furthermore, epithelial cells co-opt a cell biological process named Epithelial-Mesenchymal Transition (EMT) that facilitates its invasion process throughout the metastatic cascade. This process involves the dissolution of cell-cell contact, cell-ECM attachment and loss of cell polarity [8]. Several transcription factors such as SNAIL, SLUG, TWIST, and ZEB1/2 have been characterized and identified as the major players behind the EMT process

[9]. Among the biological traits evoked by these transcription factors, are the downregulation of E-Cadherin and upregulation of N-Cadherin expression, expression of matrix metalloproteases, increased invasiveness and resistance to apoptosis.

Another factor that contributes to the invasion metastasis cascade is heterotypic interactions of cancer cells with the stromal cells, mentioned above [10]. The reciprocal interactions between cancer and the stromal cells that defined the multistep progression of the tumor at the primary site can be reinitiated in the distant tissue to promote the colonization of the disseminated cancer cell at the new organ sites. In comparison to this logic, others have stated that microenvironments of certain tissues named “metastatic niches”, can support the growth of the seeded cancer cells at distant sites, independent of the cancer cell-induced stroma [11, 12]. Furthermore, for the cells to grow and colonize at distant sites, cancer cells might revert from the invasive phenotype and go through the reversible process of EMT named “Mesenchymal-to-Epithelial Transition” (MET) or they can colonize and grow independently of MET due to acquired genetic alterations that confer all the necessary traits for metastatic seeding. Mesenchymal cells are known to cycle slowly or are dormant and reverting back to MET from EMT has been proven necessary for the mesenchymal dormant cell to become reactivated and proliferate rapidly at the distant site [13]. In MET-independent metastasis, genetic alterations or epigenetic reprogramming can induce a state in which EMT-fixed cells have a high invasive and proliferative potential which will lead them to become more aggressive and more likely to seed at a different organ. Altogether, both mechanisms of metastasis can then subsequently result in colonization and the formation of macrometastases.

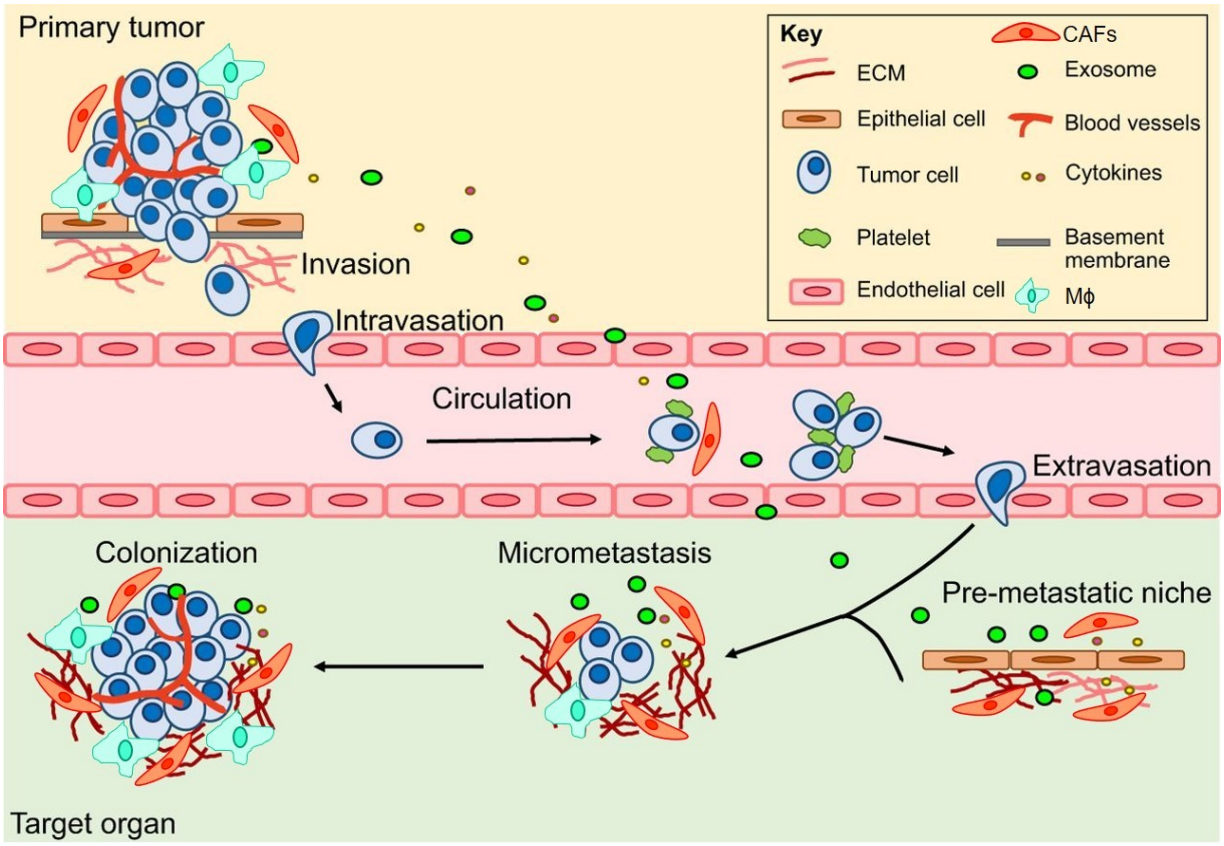

Figure 1.1.1 The invasion-metastasis cascade

Adapted from Laura Gómez-Cuadrado et al. in Dis. Model Mech. Review 2017 [14]

Metastasis is a multistep process. Initially, tumor cells migrate into adjacent tissues, referred to as local invasion. This involves the breakdown of the basement membrane and invasion into the surrounding ECM. In fact, invasive tumor cells recruit macrophages (Mϕ) and cancer-associated fibroblasts (CAFs), which are part of the tumor microenvironment, to produce promigratory and pro-invasive factors and cytokines that will facilitate their invasion and metastasis. Intravasation then allows cells to enter the circulation. In blood vessels, circulating tumor cells exist as single cells or clusters, coated with platelets. They need to survive shear stress and evade clearance by the immune system to successfully reach distant organs. Tumor cells then attach to endothelial cells, which facilitates their extravasation. After settling in the metastatic target organ, tumor cells must survive in this foreign environment and establish micrometastases. These disseminated tumor cells (DTCs) can remain dormant for many years before proliferating into large macrometastases in a process termed colonization. The primary site also regulates the development of metastasis via secretion of factors (such as cytokines and exosomes) that can prime a pre-metastatic niche and support survival of DTCs.

1.1.2 Breast Cancer and its molecular subtypes

Breast cancer is the most frequently prevalent cancer in woman and is the most leading cause of cancer death in most developed countries [15]. It is now recognized that breast cancer is not a single disease and comprises of many biological entities. Studies have shown that breast cancer with different biological and histopathological features exhibit different behaviors and thus respond differently to treatments. Hence breast cancer is grouped into different subtypes to provide a more efficient therapeutic strategy. The classification of breast cancer into various subtypes is determined by the molecular and genetic features of the tumor cells (**Figure 1.1.2**). It is classified into Luminal A and Luminal B, which are hormone receptor-positive tumors (Estrogen Receptor+ or Progesterone Receptor+), HER2+ and Basal-like or Triple negative (TNBC; ER-, PR-, HER2-). Several groups have put some effort into identifying further varying gene signatures that define each of these molecular subtypes [16]. With the development of tissue microarray technology (TMA), these gene signatures of the different molecular subtypes have been validated at the translational level, confirming the biological heterogeneity of breast cancer. Interestingly, Luminal A and B cancers have the highest prevalence and the best prognosis. Among breast cancers, HER2+ and TNBC subtypes have a poor prognosis due to their tendency for metastasis. In HER2+ cancer, HER2 receptor which is an EGFR receptor tyrosine kinase family member is amplified or overexpressed to transmit signals that will mediate tumor growth, invasion, and metastasis. However, TNBC subtype of breast cancer represents 10-20% of breast cancer diagnosis and has the worst prognosis in the clinic. In comparison to other breast cancer subtypes, TNBC breast cancer lacks any targeted therapy treatment. The only effective therapy for TNBC breast cancer in the clinic is currently chemotherapy and unfortunately, 50% of the patients develop resistance and relapse to develop metastasis. Hence, it still remains elusive and is of a great significance to investigate in defining the molecular mechanisms that are behind TNBC aggressiveness and what novel key players could be used as future drug targets for therapy.

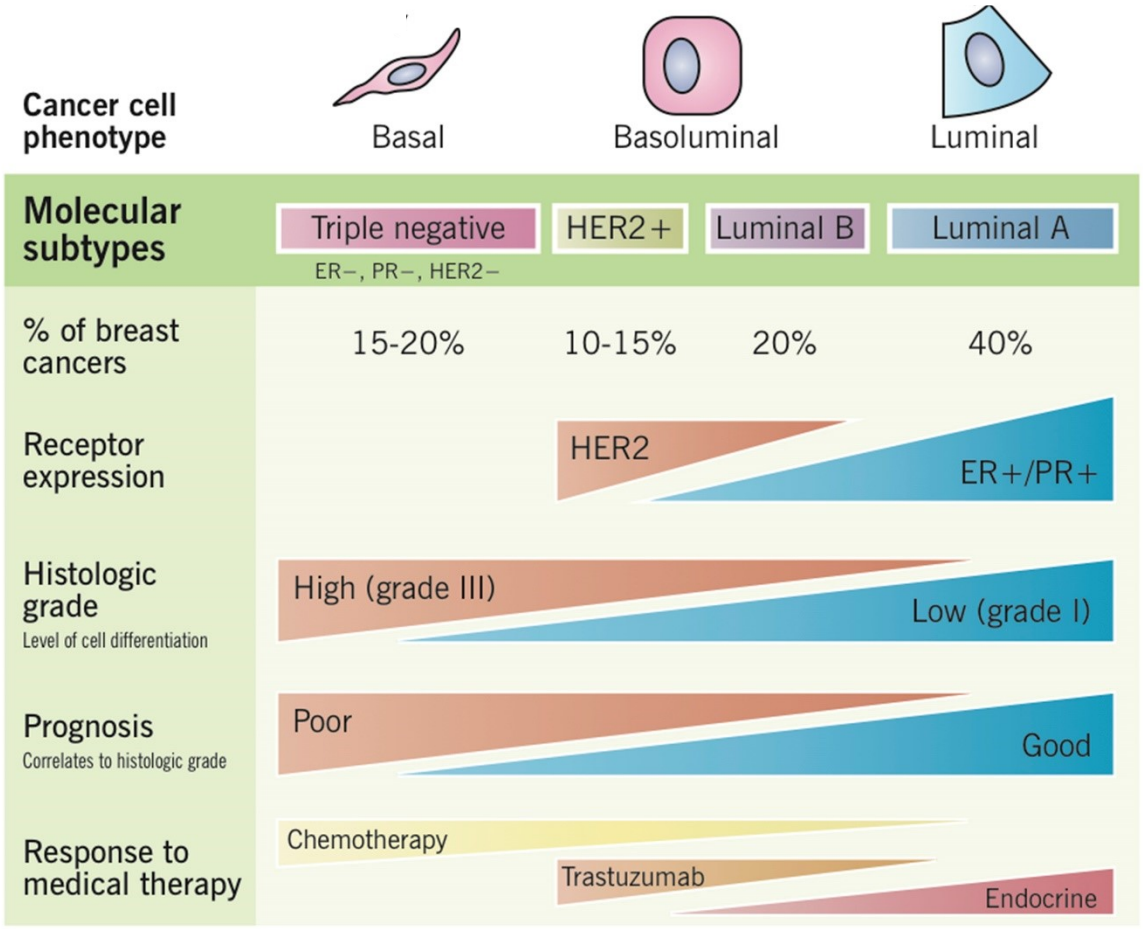

Figure 1.1.2 Molecular subtype of breast cancer

Adapted from McMaster Pathophysiology Review by Eric Wong and Jenna Rebelo 2012.

1.1.3 Receptor Tyrosine Kinases: key players in cancer biology

Receptor protein tyrosine kinases (RTKs) are a subclass of tyrosine kinases that are cell surface receptors and are known to be key regulators of different cellular processes such as cell migration, cell cycle, cell survival, metabolism, and differentiation [17]. Overexpression of many RTKs such as epidermal growth factor receptors (EGFRs), vascular endothelial growth factor receptors (VEGFRs) and platelet-derived growth factor receptors (PDGFRs) have been found in many types of cancer, such as breast cancer, and are correlated with cancer aggressiveness and decreased overall and disease-free survival [18]. They are known to respond to environmental cues to initiate the appropriate signaling pathways in tumor cells. In fact, RTKs may transduce their downstream signal via another class of protein tyrosine kinases named non-RTKs, which are predominantly cytoplasmic and contain a kinase domain with a catalytic activity regulated by phosphorylation upon external cues. Moreover, RTKs regulate many signaling pathways that may play a pivotal role in regulating cancer stemness, angiogenesis, and metastasis.

RTKs consist of 58 members that are subdivided into 20 subfamilies (**Figure 1.1.3A**) [19]. They all possess an extracellular domain, containing different components, that bind an activating ligand, a single transmembrane helix and an intracellular domain that contains the tyrosine kinase domain (TKD). In some cases, TKD is interrupted by a sequence known as a kinase insert domain (KID) that can regulate the function of TKD. Generally, all RTKs are activated upon growth factor binding that induces receptor dimerization. It is important to note, however, that some RTKs form oligomers in the absence of a ligand. Whether the "inactive" RTK is in a monomer or an oligomer form, the binding of a bivalent ligand is still required to induce a structural change in the "inactive" state which will stimulate the tyrosine kinase activity and become "active" to subsequently serve as a site of assembly for intracellular proteins to induce downstream cell signaling. Extensive structural studies have shown a range of mechanisms for ligand-induced dimerization of the extracellular regions of RTKs. This dimerization could be ligand-mediated, receptor-mediated or a combination of ligand- and receptor-mediated [19]. In all cases, the dimerization of the extracellular domain leads to the activation of the intracellularly TKD. All TKDs contain an N-lobe, a C-lobe and an activation loop. The N-lobe contains a glycine-rich loop which is followed by a lysine that is important for

ATP binding. The C-lobe however, contains a conserved aspartic acid that is important for the catalytic activity of the TKD. These residues are required for ATP binding, metal ion (Mg+) binding, and phosphoryl group transfer. Some kinases lack at least one of the motifs required for catalysis and have been termed pseudokinases [20]. They are seen as signal transducers by bringing together components of signaling complexes. However, it still remains elusive whether pseudokinases are true pseudokinases and lack any catalytic activity since some have reported some pseudokinases to have catalytic activity under certain conditions [20]. Hence, pseudokinases should be studied individually by probing for their activity with direct methods and having their structures determined.

Furthermore, before activation of an RTK, each TKD is cis-autoinhibited by intramolecular interactions unique for each receptor, which is released by ligand binding and dimerization of the extracellular regions of RTKs. Three different forms of cis-autoinhibition exist that are induced by various intramolecular interactions (**Figure 1.1.3B**) [19]. TKD autoinhibition is mediated by the activation loop occluding the ATP and substrate binding sites. This form of autoinhibition could be stabilized by the juxtamembrane regions of the kinase that can make extensive contacts with the TKD domain to stabilize the activation loop in an inactive conformation. In addition, the C-terminal tail can also play a role in cis-autoinhibition of TKD by blocking the substrate binding pocket. Releasing all these forms of autoinhibition by ligand binding and dimerization of the extracellular regions of RTKs can lead an active form of a TKD that can bind ATP and a substrate of interest to induce downstream signaling.

Under normal physiological conditions, RTKs function is tightly balanced. When they acquire transforming abilities through different mechanisms such as gain-of-function mutations, genomic amplifications, chromosomal rearrangements, or autocrine activation by an upregulation of their ligands, this will lead to the dysregulated function of the RTKs and their constitutive activation [21]. This can ultimately trigger oncogenic properties and RTK-induced oncogenesis. Due to the pivotal roles, they play in tumorigenesis and metastasis in breast cancer, RTKs are used as drug targets for therapy. However, resistance to anti-RTK therapy has been prevalent due to the acquired mechanisms they uptake to remain constitutively active.

A)

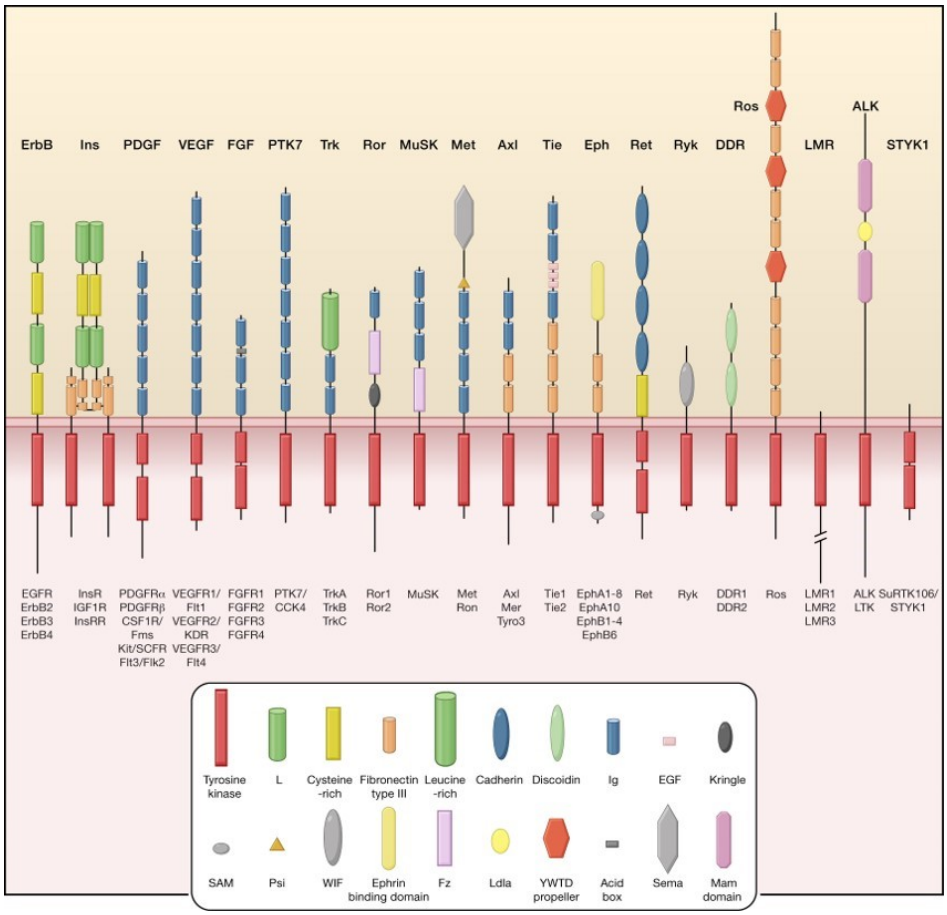

B)

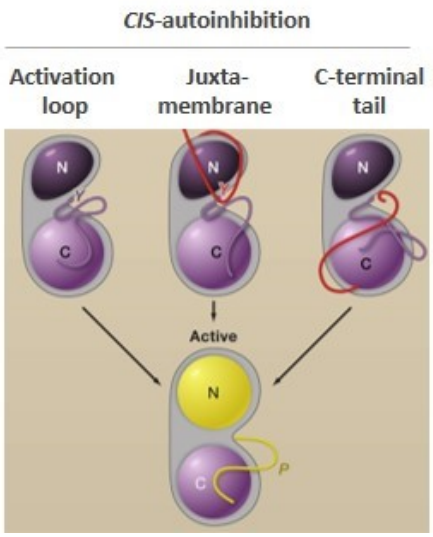

Figure 1.1.3 Receptor tyrosine kinases

Adapted from Mark A. Lemmon and Joseph Schlessinger in Cell Reviews (2010) [19]

A) Human receptor tyrosine kinases (RTKs) contain 20 subfamilies, shown here schematically with the family members listed beneath each receptor. Structural domains in the extracellular regions, identified by structure determination or sequence analysis, are marked according to the key. The intracellular domains are shown as red rectangles. **B)** Activation loop inhibition: In the activation loop interacts directly with the active site of the kinase and blocks access to protein substrates or to both ATP and protein substrates. Phosphorylation of key tyrosines ("Y") disrupts these autoinhibitory interactions and allows the kinase to "relax" to the active state. Juxtamembrane inhibition: the juxtamembrane region (red) interacts with elements within the active site of the kinase (including the αC helix and the activation loop) to stabilize an inactive conformation. Phosphorylation of key tyrosines in the juxtamembrane region destabilizes these autoinhibitory interactions and allows the TKD to assume an active conformation. C-terminal tail inhibition: C-terminal tail (red) interacts with the active site of the TKD to stabilize an inactive conformation.

1.2 Dissecting AXL's role in cancer progression

Preface

A review to be submitted once CHAPTER 3 of my thesis is in the revisions process of a publication.

Dissecting AXL's role in cancer progression

Afnan Abu-Thuraia[1,2*], **Marie-Anne Goyette**[1,2*], Carine Delliaux[1], Jean-Francois Côté[1,2,3,4#]

[1] Montreal Clinical Research Institute (IRCM), Montréal, QC, H2W 1R7, Canada.

[2] Molecular Biology Programs, Université de Montréal, Montréal, QC, H3T 1J4, Canada.

[3] Department of Anatomy and Cell Biology, McGill University, Montréal, QC, H3A 0C7, Canada.

[4] Department of Biochemistry and Molecular Medicine, Université de Montréal, Montréal, QC, H3C 3J7, Canada.

[*]First co-authors, contributed equally to the work

[#]Corresponding author:

Jean-François Côté

IRCM

110 avenue des Pins Ouest

Montréal (QC) Canada

H2W 1R7

Email: jean-francois.cote@ircm.qc.ca

Phone: (514) 987-5647

Introduction

The TAM receptor tyrosine kinases (RTKs) comprised of TYRO3, MER and AXL are one of the latest family of RTKs to evolve and be identified since they are not known as strong oncogenic drivers [22, 23]. They have been largely identified in neoplastic cell lines, yet they are not frequently mutated in cancer. TAMs are known for their involvement in inflammation, autoimmunity and recently in cancer progression. They are ectopically expressed and highly expressed in many cancer types. TAMs are defined by their similar overall domain structure and a unique KWIAIES, a conserved amino acid sequence found in their catalytic kinase domain [24] (**Figure 1.2.1**). Their extracellular domain consists of two tandem immunoglobulin-like domains (Ig1 and Ig2) followed by two tandem Fibronectin type 3 (FN-III)-like domains. Their ligands for their activation are Growth Arrest Specific factor 6 (GAS6) and Protein S, which require Vitamin-K dependent γ-Carboxylation to have the ability to activate the TAMs [25]. Their structure consists of an N-terminal γ-carboxyl glutamic acid (GLA) domain, 4 tandem Epidermal Growth Factor (EGF)-like repeats, and a C-terminal Sex Hormone-Binding Globulin-like region consisting of two tandem Laminin G-like (LG) repeats. They bind the receptor with their carboxy-terminal domain and are known to bind the lipid moiety Phosphatidylserine (PS) with their amino terminus. PS is abundant in the body but can only activate TAMs when externalized on apoptotic cell membranes, aggregating platelets, exosomes, and invading virus envelopes [26-28]. While GAS6 and Protein S share common domains and require γ-carboxylation to activate TAM receptors, they have different affinities to different TAM receptors. GAS6 binds all TAM receptors, with the highest affinity for AXL, whereas Protein S only binds MER and TYRO3 [25]. PS increases GAS6 and Protein S activation of MER and to a lesser degree TYRO3. However, it still remains unknown and requires further experimentation how the PS/Gla binding translates into the LG binding to the receptor to induce receptor activation. Other than GAS6 and Protein S, novel TAM ligands have been identified recently that are tissue and receptor-specific [29-31].

Regulation of TAM Expression

TAMs overexpression has been observed in many cancer types promoting the survival, chemo-resistance, motility, and invasion of the tumor cells. Their expression has been shown to

correlate with poor prognosis in various tumor types. For example, MER kinase is aberrantly expressed in B-cell acute lymphoblastic leukemia (B-ALL) and T-ALL, whereas AXL is less observed in ALL, but highly observed in acute myeloid leukemia (AML) and chronic lymphoid leukemia (CLL) and chronic myeloid leukemia (CML) [24]. In addition, TYRO3 is also observed to be expressed in some leukemia samples. Hence, there seems to be a preferential for TAM receptor expression in different types of cancers. However, it still remains understudied how TAM expression is induced in cancer cells. Some evidence suggests that the expression of the different TAM receptors is regulated differently. For instance, dexamethasone increases MER expression and eliminates AXL expression in bone-marrow derived macrophages, yet TLR agonists increase AXL expression without altering MER expression [32]. In addition, previous studies have shown MER kinase transcription is upregulated in macrophages upon Liver X receptor (LXR) activation by its ligand, where ligand-bound LXR binds to the promoter of MER to enhance transcription [33]. Epstein-Barr virus (EBV) lytic transcription factors have been also demonstrated to substantially increase MER expression as well [34]. In terms of AXL expression, hypoxic conditions in the tumor increase HIF1α expression levels, which directly binds to the promoter of AXL to induce its expression [35]. TYRO3 also contains similar HIF1α responsive elements in its promoter, suggesting its expression upregulation under hypoxic conditions. Moreover, epigenetic regulation of expression has been observed in relapsed AML patients where hypomethylation of AXL promoter was shown to correlate with its high expression [36]. In addition, MZF1 transcription factor has been shown to bind AXL promoter to result in a dose-dependent increase in AXL mRNA levels [37]. TAM expression can also be regulated post-transcriptionally by miRNAs, where for instance, miRNA 355 known to negatively regulate MER kinase, is suppressed in breast cancer [38-42].

Although TAMs are overexpressed in multiple tumor types, genetic mutations or amplification of the genes encoding TAM RTKs are relatively rare. In some instances, point mutations and translocations creating fusion genes have been reported [24], yet the functional importance of these mutations remains elusive.

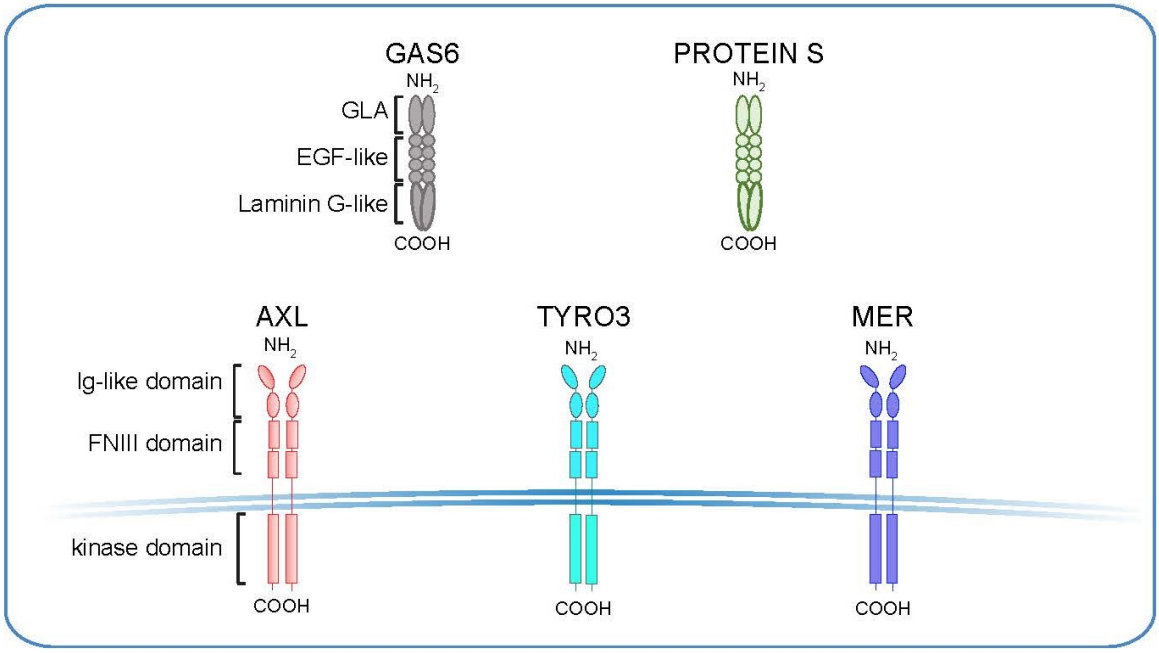

Figure 1.2.1 Schematic representation of TAM family of receptors and their ligands

Mechanisms of activation

Ligand-dependent

AXL activation mechanisms are unique and can be achieved in many ways **(Figure 1.2.2**). To become active, AXL binds the C-terminal of its ligand GAS6, an interaction that is of a strong affinity and independent of the presence of GAS6 γ-carboxylated N-terminal Gla domain [43]. However, this ligand interaction does not translate into AXL autophosphorylation and activation since Vitamin K-dependent γ-carboxylation of GAS6 Gla domains is necessary for GAS6-induced AXL autophosphorylation and activation [44, 45]. In fact, there is some evidence showing that warfarin treatment, which depletes Vitamin K levels, decreases the γ-carboxylation process of GAS6 and inhibits AXL autophosphorylation [46]. Upon GAS6 binding to AXL, GAS6 induces AXL homodimerization in a 2:2 stoichiometry where one GAS6 binds one AXL monomer, and this leads to its homodimerization, autophosphorylation, and activation to induce downstream signaling [43]. GAS6 binding and induced homodimerization of AXL is a unique activation mechanism to AXL that is different from MER and TYRO3 where GAS6 binds in a 1:1 stoichiometry manner. To become activated, AXL is auto-phosphorylated on Y702/Y703 in mammals, which then leads to the autophosphorylation of three other tyrosine residues in its intracellular domain (Y779, Y821, Y866) that act as scaffold hubs for proteins such as p85 (the regulatory subunit of PI3K), Grb2, and phospholipase C-γ (PLC-γ) to induce downstream signaling [47].

The γ-carboxylated Gla domain of GAS6 is known to bind, in a Ca^{2+}-dependent manner, the lipid moiety phosphatidylserine (PS), which is externalized on membranes of apoptotic cells, exosomes, and enveloped viruses [48]. It is believed that PS exposed membranes facilitate the dimerization or oligomerization of MER and TYRO3 to induce signaling [24]. However, there seems to be a controversy for the role of PS in AXL activation. Some have shown that GAS6-induced activation of AXL requires the PS binding to GAS6 to have complete activation of AXL [32, 49]. They suggest that AXL is assumed to be constitutively in complex with GAS6 due to their high-affinity binding and act as a hybrid receptor to detect PS and subsequently become activated [32, 50]. Others, however, have shown that GAS6-induced activation of AXL does not require PS binding to GAS6 and was not further enhanced by the presence of PS [43]. A

more recent study has demonstrated a model that provides a quantitative and mechanistic understanding of efficient GAS6 activation of AXL [51]. They demonstrated AXL activation to be observed only when localized concentrations of GAS6 is high. This localized ligand concentration drives a diffusional influx of AXL from regions of low to high GAS6 concentrations which will allow GAS6 binding and result in receptor aggregation and dimerization to induce efficient AXL signaling. Ultimately, this localized signal of receptor function can be a marker for PS exposure in cell clearance.

Furthermore, AXL activation can also be achieved by forming heterodimers with other TAM members (MER or TYRO3) to induce signaling [52, 53]. This heterodimerization could be mediated by GAS6 binding, where AXL can bind GAS6 and activate MER or TYRO3 kinases, which have less affinity in GAS6 binding.

Ligand-independent

AXL activation could also be atypical and mediated by a ligand-independent approach. One way this can occur is by homophilic dimerization and autophosphorylation during pathophysiological conditions due to excess receptor expression or oxidative stress [54-56]. Another way GAS6-independent AXL activation can occur is by heterodimerizing or clustering with other RTKs, such as EGFR, MET, PDGFR and VEGFR-2, to become auto-phosphorylated and activated to induce downstream signaling [57-61]. In the squamous cell cancer of head and neck, AXL heterodimerizes with EGFR to confer resistance to PI3K inhibition. A similar mechanism was seen also in EGFR-mutant lung cancer, whereupon EGFR tyrosine kinase inhibition, AXL dimerizes with MET receptor to bypass EGFR inhibition and confer resistance.

Furthermore, these molecular mechanisms of AXL activation shed light into the diverse approaches AXL can take to become activated and function to induce downstream signaling. It also complexifies the mechanisms of its regulation during physiological and pathophysiological conditions.

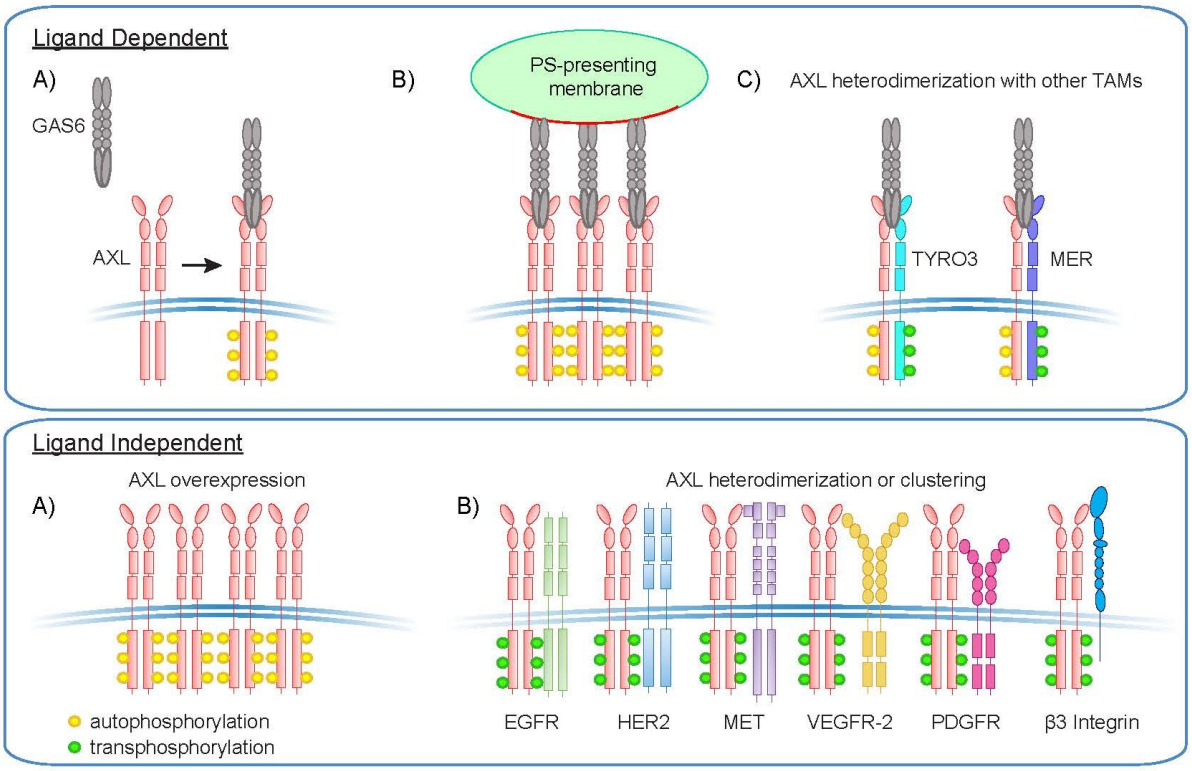

Figure 1.2.2 Mechanisms of AXL activation

AXL activation can take place in various manners. Ligand-mediated activation of AXL depends on AXL binding to GAS6 ligand to lead to its homodimerization and autophosphorylation (A). In addition, phosphatidylserine (PS) exposed on a membrane (ex. apoptotic cells) can induce GAS6 binding and lead to more efficient and localized AXL activation (B). In some cases, AXL can also heterodimerize with other TAM receptors in order to activate signaling (C). For cases when the ligand is absent, AXL can be activated in a ligand-independent manner in several ways. When AXL is expressed at high levels due to a disease condition or is induced by a specific stimulus, its high expression can lead to its dimerization and autophosphorylation (A). In many cancers, AXL has been shown to be transphosphorylated by many RTKs such as EGFR, HER2, MET, VEGFR-2 and PDGFR to diversify signaling. In ovarian cancer, AXL has been shown to converge with β3 signaling to induce tumor cell adhesion.

Regulation of activation

AXL activation and function can regulate cytoskeletal functions, intracellular signaling and gene expression [24]. Its aberrant expression or activity can dysregulate physiological functions and lead to a disease. Thus, the regulation of its activity is a crucial process to keep AXL function appropriate. Upon its activation, AXL has been shown to be negatively regulated in several ways. The proteolytic shedding of its extracellular domain mediated by the metalloproteinases ADAM10 and ADAM17 has been shown to play a role in decreasing its activity at the membrane [62]. In fact, MEK inhibitor resistance was associated with a decreased circulating level of AXL ectodomain in melanoma patients, which represents reduced RTK shedding as a mechanism in which cancer cells bypass signaling to attain high AXL activity and drug resistance. This suggests that soluble AXL ectodomain could be used as a diagnostic biomarker for clinical use.

In addition to AXL shedding, AXL can be negatively regulated by its binding partner C1 domain-containing phosphatase and tensin homolog (C1-TEN). C1-TEN can negatively regulate AKT activation downstream of AXL activation to inhibit survival and motility [63, 64]. Moreover, AXL, MER, and TYRO3 are targets of E3 ubiquitin ligase CBLB [46]. A study has emphasized on the role of TAM RTK ubiquitination by CBLB ligase in natural killer (NK) cells. Genetic deletion of *cblb* in NK cells prevented TAM RTK ubiquitination and degradation and hence inhibited NK cell activity in rejecting tumor and metastatic growth and this was reversed by TAM RTK inhibition [46]. Recently, another study has identified a novel mechanism in negatively regulating AXL oncogenic signaling in ovarian cancer by the GPI-anchored tumor suppressor OPCML [65]. Once activated by GAS6, AXL directly interacts with OPCML and subsequently gets accumulated in cholesterol-rich lipid domains where OPCML resides. This brings AXL in proximity with a lipid residing phosphatase named PTPRG, where AXL gets dephosphorylated by this phosphatase and can not transactivate other RTKs such as MET and EGFR to induce ERK signaling to induce EMT and cell invasion.

It still remains elusive how the cell can shuttle and traffic AXL from the cell membrane to regulate its activity. In addition, it will be interesting to explore if AXL once shuttled, gets

degraded in the endosomes via lysosomal degradation or continue to signal intracellularly in the endosome vesicles until vesicles merge back with the cell membrane.

Signaling in cancer

Several studies in many cancers have shown different roles of AXL signaling in cancer cells that positively correlate with chemo-resistance, targeted-therapy resistance, metastasis, and poor patient outcome. AXL signaling in cancer is deregulated and is known to induce downstream oncogenic signaling in the cell that leads to the promotion of survival and motility of the tumor cells (**Figure 1.2.3**).

Survival

AXL was first shown to play a role in survival in leukemia cells in which GAS6 stimulation prevented apoptosis upon growth factor deprivation [66, 67]. Treatment of B-CLL cells with AXL tyrosine kinase inhibitor led to apoptosis induction [68]. Another study demonstrated that inhibition of AXL expression by shRNA in leukemia cells decreased the cells ability to form colonies [69]. As with other RTKs, AXL promotes survival and proliferation by harnessing the RAS/ERK cascade and PI3K/AKT kinase pathway [70, 71]. AXL inhibition in cancer cells abrogates the activation of these pathways upon ligand stimulation [66, 72-75]. In fact, AXL induces a survival signal by upregulating the expression of anti-apoptotic proteins such as BCL-2, BCL-XL, MCL1 and SURVIVIN, and inhibiting the proapoptotic protein Caspase-3, BAD, BAX, and PUMA [68, 76-79]. For instance, AKT signaling downstream of AXL led to the increase of BCL-2 levels and inactivated the pro-apoptotic BAD proteins [78]. In addition, STAT proteins are also involved in the transcription of survival genes. AXL activation induces tyrosine phosphorylation of STAT3 to regulate its transcriptional activity [23, 38, 80]. Other pathways are also stimulated including those that involve NF-kB and p38 signaling that leads to the promotion of survival and regulation of pro-survival and pro-migratory gene expression [23, 81, 82]. Notably, NF-kB activity in schwannoma cells has been shown to be a mediator of GAS6/AXL induced overexpression of pro-survival genes to enhance survival of merlin-deficient tumors [82]. Altogether, these pathways induced downstream of

AXL activation in many cancer types play a role in promoting cancer cell survival in response to apoptotic stimuli.

Migration

Apart from survival signaling, AXL has been shown to play a significant role in the metastasis of many cancer types. Whether it's in patient samples or cell lines, AXL expression correlates with invasion and metastasis [24]. Initially, AXL was first demonstrated to play a role in cell migration of GnRH neurons to the hypothalamus [83, 84]. Another study in AXL-expressing glioblastoma cells portrayed the role of AXL in cell migration, where transfection of the dominant negative form of AXL lacking the kinase domain resulted in reduced motility and filopodia formation and loss of cell-cell contact [85]. In fact, AXL activity in glioblastoma cells was shown to play a role in tumor growth and invasion. Studies have further shown a role for AXL in a facilitating a process named epithelial-to-mesenchymal transition (EMT) that is required in metastasis. The first *in vivo* evidence that links AXL to metastasis was shown in breast cancer where dissemination of highly metastatic breast cancer cells and EMT-driven motility was AXL-dependent [86, 87]. Similarly, AXL inhibition in ovarian cancer prevented dissemination and establishment of metastatic lesions [88]. EMT gene expression inducers such as TWIST, SNAIL, and SLUG are induced upon AXL activation or overexpression. These transcription factors, TWIST, and SNAIL, in return, can induce the expression of AXL as a positive feedback loop system to reinforce EMT [72, 89-91]. In fact, a positive correlation between AXL expression and mesenchymal phenotype was present in human cancer cell lines, particularly in breast cancer and non-small cell lung cancer [92]. A study has defined the mesenchymal subtype tumor cells of ovarian cancer to have an enrichment of AXL expression that positively correlated with EMT and poor patient outcome [93]. In this mesenchymal subtype of ovarian tumor cells, AXL co-clusters with and activates EGFR, HER2 and MET to induce protracted ERK signaling to promote motility and invasion by inducing the expression of the ERK pathway effector FRA-1, which in return can induce the gene expression of the EMT inducer SLUG [94]. Overall, AXL expression and signaling in many cancer types is necessary, not only to sustain an EMT state and allow cancer cells to disseminate and invade to form metastatic lesions but also to acquire resistance to targeted drug therapies.

The mechanisms in which AXL sustains an EMT state remain to be elusive. Initially, AXL signaling through PI3K/RAC pathway was shown to cause actin rearrangement and an increase in motility [83, 84]. This was recently explained in part in breast cancer cells where AXL mediated phosphorylation of ELMO proteins bound to DOCK1, promoted RAC-mediated cytoskeleton changes and induced breast cancer cell migration [95]. In addition, AXL was reported to regulate cell adhesion by modulating the signaling complex ILK/PINCH/PARVIN found at adhesion sites via its interaction with NCK2 protein [96]. It has also been shown to localize to active myosin filaments and phosphorylate tropomyosin at sites critical for adhesion [97]. In fact, a recent study has demonstrated how AXL signaling in ovarian cancer can sustain an EMT state by converging with β3 integrin signaling pathway to promote adhesion to the extracellular matrix and induce invasion [98]. These different mechanisms may suggest AXL as a regulator of cell adhesion during cell invasion process. In support of this notion, AXL invasive activity in tumor cells was further demonstrated to be mediated through the activation of matrix metalloproteases (MMPs) which are required to break down the extracellular matrix during cell adhesion process. Indeed, AXL activation enhances the expression of MMP9, known to promote tissue remodeling and invasion, and this was shown to be reversed upon AXL inhibition [99].

These attempts in defining mechanisms behind AXL's significant role in maintaining an EMT state and reinforced mesenchymal phenotype do not justify the role it plays in the invasiveness of the tumor to become invasive and metastasize. More recently, a novel approach was taken in defining signaling pathways and mechanisms that are specifically modulated by AXL activation. The first phosphoproteome of AXL was characterized in triple negative breast cancer cells where AXL is highly expressed. Interestingly, this study emphasized AXL's role in robustly regulating actin cytoskeleton rearrangements and in specific focal adhesion dynamics. Upon AXL activation or inhibition, focal adhesion disassembly rate was increased or decreased, respectively. The process of disassembly was found to be modulated by AXL-mediated recruitment of the disassembly complex GIT/βPIX/PAK to focal adhesions. Furthermore, the scaffold focal adhesion protein NEDD9 was identified as a novel direct substrate of AXL upon its activation by GAS6. AXL-mediated phosphorylation of NEDD9 induces its complex recruitment with CRKII/DOCK3 to induce RAC activation and modulate its role at focal

adhesions. This complex recruitment orchestrates AXL-mediated phosphorylation of the focal adhesion pseudokinase protein named PEAK1, via binding to the middle SH3 domain of CRKII. In this study, PEAK1, known to lack a kinase activity, was shown to recruit CSK kinase to modulate PAXILLIN phosphorylation levels at focal adhesion sites and regulate AXL-induced focal adhesion turnover. Notably, CRISPR CAS9 deletion of PEAK1 in triple negative breast cancer cells decreased tumor growth and metastasis *in vivo*. This study emphasizes AXL's role in exploiting NEDD9/CRKII/PEAK1/CSK module to regulate focal adhesion turnover in breast cancer cells to promote and sustain their mesenchymal phenotype and progress to metastasis. In addition to focal adhesion dynamics, other pathways and processes were revealed to be modulated by AXL activation such as RNA transport, vesicle trafficking, and phagocytosis. It remains elusive if these pathways modulated by AXL contribute to AXL-induced survival and migration in invasive cancer cells or affect a different biological process. Moreover, this is the first time that AXL effector pathways are defined in a quantitative manner that may explain and justify its invasive role in cancer cells. The global view of AXL signaling will aid in defining the mechanisms AXL acquires to promote metastasis and attain drug resistance. This will ultimately bring forward novel potential therapeutic targets that may hold promise in the clinic to be used in drug combination therapy.

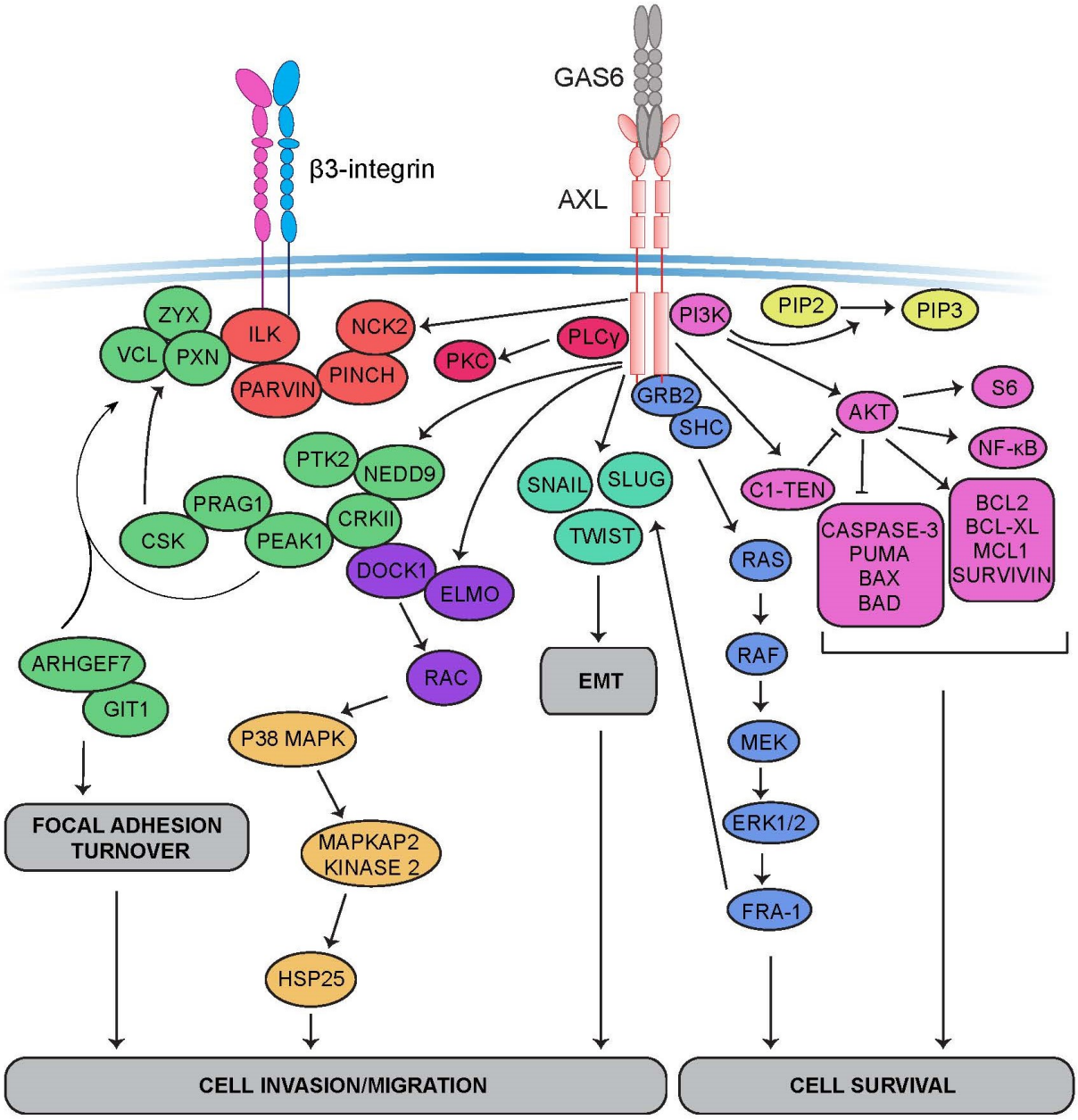

Figure 1.2.3 AXL signaling cascades

TAMs in human cancer

Expression of TAM receptor

TAM receptors and their ligands are expressed in a variety of human cancers and their expression correlates with a decrease in survival in solid malignancies and blood cancer. An exhaustive table of their expression in cancers and their significance in prognostic, function, metastasis and chemoresistance roles was reviewed in [24]. However, GAS6 contribution during cancer progression in human cancer still remains to be unclear. In non-small cell lung cancer, its expression was linked to increased metastasis and AXL decoy receptors that trap GAS6 were shown to reduce metastasis *in vivo* [100, 101]. On the other hand, other studies have shown GAS6 expression to correlate with a positive outcome in breast cancer and we have recently shown that GAS6 was not required, in contrast to AXL, for the metastatic progression of HER2+ breast cancer *in vivo* [58, 102].

Tumor growth and survival

TAMs are defined as proto-oncogenes because their overexpression leads to signals that can contribute to cancer by various mechanisms like resistance to apoptosis and proliferation. Indeed, it was shown that tumor cells educate infiltrating leukocytes to secrete GAS6 to promote tumor cells proliferation via activation of the TAMs [103]. In addition, AXL and MER have been shown to be important for tumor growth of various cancers [73, 81, 104, 105]. However, AXL contribution to tumor growth seems to be context dependent. For instance, our group and others have observed that genetic ablation of AXL has no or minor effect on tumor growth and that its role is mostly on the metastatic progression [58, 86].

AXL as a prognostic marker

The question remaining unanswered in the field is whether the TAMs can be used as prognostic markers. Some studies strongly suggest that AXL can be used as a biomarker for the survival of different cancer types and a recent meta-analysis support these observations [100, 106, 107]. Nonetheless, a further large-scale analysis will be required to validate the prognostic value of AXL and its oncogenic status.

Metastatic progression of solid cancer

EMT and metastasis

Since 90% of cancer-related deaths are caused by metastasis, the role of TAMs in cancer spreading justifies their effect on patients' survival. It is now well established that TAM expression, particularly AXL, is linked to EMT and metastasis [58, 86, 108, 109]. We recently reported that AXL is essential for the metastatic progression of a transgenic mouse model of HER2+ breast cancer and its expression in patient samples correlates with EMT and TGF-β signaling [58].

AXL in multiple steps of the metastatic cascade

Metastasis is a multifaceted process which requires the adaptation of cancer cells through the different steps of the process. Firstly, the cells need to increase their invasion capacities in the primary tumor to enter the circulation, a process called intravasation. Once they reach their site of interest, the cancer cells exit the circulation to enter the distant organ parenchyma, in a process named extravasation. This metastatic cascade ends by the metastases growth at the new site [110]. A recent study has now recapitulated the role of AXL in this complex process.

In our recent study, we dissected this cascade in a HER2+ breast cancer mouse model and showed that AXL is required for intravasation, extravasation and metastatic growth in the lung [58]. A role for AXL was highlighted in this EMT-dependent process via TGF-β-reprogramming of cells for metastasis. We showed that AXL knockout cells are less prone to intravasate due to the loss of their ability to be mesenchymal and mobile. In addition, they were not responsive to TGF-β stimulation of cell invasion, suggesting AXL as a mediator of TGF-β-induced cell invasion

In the same study, AXL was revealed to be a mediator of TGF-β-induced extravasation for lung colonization in this context. Similarly, another study has also confirmed AXL's role in breast cancer cells extravasation to the lungs [87]. Furthermore, we demonstrated that this receptor contributes to the establishment of macrometastases once the cells are in the lung. A similar observation was also marked by another group, but this time in the context of PyMT

transgenic breast cancer model [111]. Using AXL+ tumor-initiating cells that display partial EMT, they suggested that AXL prepares the metastatic niche by promoting the activation of fibroblasts in the lung via the secretion of THSB2.

Dormancy

The metastatic cascade can also end by an alternative path where the cancer cells remain dormant in the new organ. Disseminated cells can survive without proliferating for years and wake-up to cause relapse in patients [112]. In the specific context of bone marrow metastasis of prostate cancer, AXL, GAS6, and MER have been implicated in dormancy. Osteoblasts have been shown to produce GAS6 that interacts with AXL or MER on the surface of nearby disseminated cancer cells to regulate the arrest of proliferation [66, 113, 114]. Recently, it was shown that AXL activation by GAS6 on prostate cancer cells induces the expression of TGF-β and TGF-βR that in turn leads to dormancy and cell growth suppression in the bone marrow niche [113] (**Figure 1.2.4**). This will, in turn, protect the cells from chemotherapy-induced apoptosis. This, in fact, is contradicting to AXL's role in inducing cell survival in the cancer cell at the primary site. Further work is needed to investigate whether AXL can induce dormancy in the niche of other metastatic sites. Since our work has demonstrated a role for AXL in the growth of macrometastasis in the lungs in HER2+ breast cancer model, it's possible that AXL, rather than inducing cell dormancy, may play a role in promoting cell growth.

Altogether, this extensive work on metastasis displays the requirement of AXL during the whole process of metastasis and strongly suggests that blocking this receptor could help decrease the metastatic burden at many stages of the disease.

Tumor microenvironment

Angiogenesis

TAMs and their ligands are expressed by different components of the cardiovascular system including endothelial cells, pericytes and vascular smooth muscle cells (VSMC) (**Figure 1.2.4**) [24]. However, in comparison to TAMs or GAS6 knockout mice, PROTEIN S knockout mice were embryonic lethal because of coagulation and blood vessel defects leading to

hemorrhages [115]. GAS6/AXL pathway has been shown to play a role in vasculogenesis due to its effect on migration and apoptosis of VSMC [116]. In contrary, PROTEIN S and MER have been shown to inhibit VEGF-A-induced angiogenesis [117]. Autocrine and paracrine GAS6/AXL signaling has been implicated in endothelial tube formation suggesting its role in angiogenesis [118, 119]. Indeed, inhibiting AXL *in vivo* via the small molecule inhibitor R428 leads to a reduction of tumor angiogenesis [89].

Antitumor immunity

TAM receptors are known for their function in immune homeostasis. Using inhibitory feedback mechanisms, TAMs reduce inflammation via phagocytosis of apoptotic cells and regulation of TLR and cytokine signaling [52, 120-122]. Indeed, the triple knockout mice are viable but suffer from chronic inflammation and systemic autoimmunity [123]. Thus, TAMs implication in immune regulation can be used to increase antitumor immune response.

In the immune system, TAMs are primarily expressed by antigen presenting cells (macrophages and dendritic cells) and NK cells (**Figure 1.2.4**) [24]. In macrophages, AXL and MER have been found to have distinct roles in the different context of phagocytosis. MER was presented as having a tolerogenic role during macrophage resting and immunosuppression, and AXL was associated with an inflammatory response because of its induction by proinflammatory stimuli [32]. Indeed, AXL signaling has also been associated with the polarization of macrophages toward a proinflammatory phenotype termed M2 in a cancer context [124, 125]. In addition, genetic ablation of MER in the immune system of PyMT breast cancer model led to a reduction of tumor and metastasis burden due to a difference in cytokines expression in leukocytes resulting in an increase of CD8+ lymphocytes infiltration [126].

Additionally, the TAMs act as a break for NK cells activation against metastatic tumor cells [46]. Thus, TAMs inhibition led to a decrease in the metastatic burden of murine mammary cancer and melanoma *in vivo* by enhancing NK cells activity. Moreover, TAMs have also been implicated in T cell regulation via their role in TLR signaling and type I IFNs production by dendritic cells [127]. To maintain homeostasis, TAMs are central to a negative feedback loop that prevents overactivation of the adaptive immunity. Once activated, T cells start to produce PROTEIN S that will activate the TAM receptors at the surface of dendritic cells to decrease

the dendritic cell activity [128]. Furthermore, GAS6/AXL axis has also recently been implicated in regulatory T cells (Tregs) suppressive activity. It was shown that AXL activation by GAS6 on Tregs leads to an increase in their immunosuppressive activity *in vitro* and *in vivo* [129]. All these evidence suggest that inhibiting TAMs could be a powerful approach to increase the efficiency of immunotherapy.

However, removing a homeostatic checkpoint on inflammation can also have the opposite effect on tumor progression. Indeed, the genetic ablation of AXL and MER in a mouse model of induced colon cancer promoted tumor growth [130]. In this context, the receptors inhibition led to the reduction of apoptotic neutrophils clearance in the intestine and increased proinflammatory cytokines that favored a tumor-promoting environment. Therefore, it is important to fully understand the role of those receptors in immunity to be able to modulate their activity toward enhancing antitumor responses.

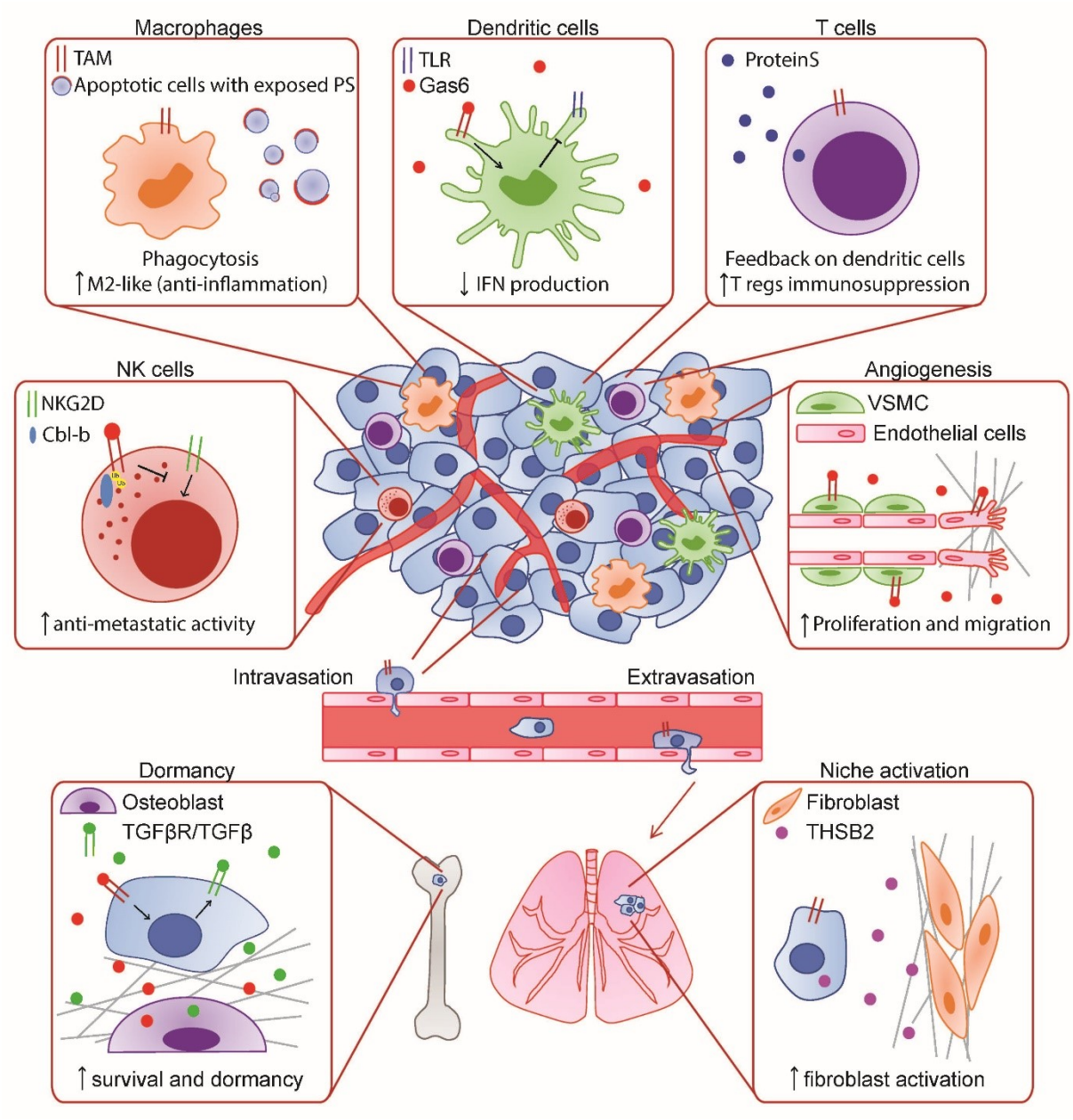

Figure 1.2.4 Role of AXL in metastasis and tumor microenvironment

Mediators of resistance

TAM overexpression has been linked to acquired resistance to conventional and targeted therapies in both solid and blood cancers. Therefore, increasing evidence suggests that they could be targeted to overcome the resistance of many types of anti-cancer strategies (**Figure 1.2.5**).

Chemotherapy and antimitotic drugs

AXL and MER have been found to be upregulated in chemoresistant cells in a variety of cancers. Many studies have shown a better drug sensitivity when combining AXL or MER inhibition with chemotherapeutic compounds such as Docetaxel, Cisplatin, Pemetrexel, Vincristine, Paclitaxel, Adryamicin or Gemcitabine [131-135]. Indeed, inhibiting AXL or MER promoted apoptosis that enhanced chemotherapeutic agents' effects mainly via the AKT pathway [73, 133, 136].

Mesenchymal cells are known to be more chemoresistant because of their stem-like properties. In cancer cells, chemotherapy induces EMT and AXL expression [80, 90, 92]. Indeed, AXL was shown to be associated with mesenchymal features in breast and lung cancer cells and AXL inhibition was able to synergize with antimitotic agents to induce cell death [92]. Recently, genetic or pharmacological inhibition of AXL was shown to revert EMT in pancreatic and prostate cancer cells and to modulate the expression of nucleoside transporters that impact chemotherapeutic response [131, 134]. Thus, it appears that blocking AXL or MER is able to improve the response to chemotherapies by reverting EMT and by blocking downstream pathways that lead to apoptosis and drug resistance.

Targeted therapy

TAM receptors expression has also been associated with targeted therapy resistance. Particularly, many pieces of evidence show that they mediate RTK inhibitors (TKI) resistance. For example, AXL was shown to be overexpressed in cell lines and in patients resistant to the multiple kinase inhibitor Imatinib [137]. In this context, knockdown of AXL reduced PKC and ERK activation leading to a sensitization of TKI-resistant cells.

Furthermore, AXL and MER were shown to be frequently overexpressed in a variety of cancer cells resistant to EGFR targeted therapies [38, 138-140]. Gefitinib resistant cells were shown to have AXL overexpression because of a slow turnover of the protein [140]. Additionally, many studies link the resistance to EGFR inhibitor Erlotinib to EMT and AXL overexpression [38, 139]. In this context, Erlotinib resistant cells displayed EMT features that could be prevented by AXL inhibition. AXL inhibition was then able to re-sensitize the cells to Erlotinib treatment. Likewise, the overexpression of AXL was sufficient to induce an acquired resistance to the anti-EGFR antibody Cetuximab [141]. AXL activation stimulated cell proliferation, EGFR activation, and MAPK signaling via a positive feedback loop that maintained EGFR activation by AXL. Indeed, AXL was shown to diversify EGFR signaling via heterodimerization which could lead to a lack of response to EGFR family of inhibitors [57]. On the other hand, EMT-associated drug resistance to Erlotinib with an increase of AXL expression was also shown to be independent of AXL, so the data are still controversial [92]. Moreover, AXL was also shown to be overexpressed in HER2 inhibitors (Lapatinib or Trastuzumab) resistant cells, and AXL inhibition was able to restore their sensitivity via inhibition of MAPK and AKT pathways [142]. Thus, AXL is now clearly linked with an acquired resistance to EGFR family of inhibitors and combining those therapies with AXL inhibitors could be a powerful approach to overcome the acquired resistance.

Other than TKIs, AXL has recently been shown to be implicated in the resistance to PI3Kα, ALK and PARP inhibitors among others [61, 143, 144]. The dimerization of AXL and EGFR has been associated with the activation of PLCγ-PKC leading to mTOR activation independently of the PI3K-AKT signaling pathway. Thus, inhibiting EGFR, PKC or AXL was able to revert resistance to PI3Kα inhibitors [61]. Crizotinib, an ALK inhibitor, was also linked with the activation of AXL and EMT. In this context, inhibiting AXL rescued ALK inhibitor resistance via the inhibition of ERK signaling [143]. Furthermore, the expression of AXL in patient samples was linked with the expression of DNA repair markers. Indeed, the inhibition of AXL reduced DNA repair genes and reduced homologous recombination (HR) in cancer cells. Thus, inhibiting AXL caused HR deficiency that increased the sensitivity to PARP1 inhibition [144].

Moreover, since AXL was implicated in tumor angiogenesis and VEGFR crosstalk, its role in angiogenesis inhibitors resistance was studied. Indeed, Sunitinib, an anti-angiogenic small molecule, was shown to increase AXL signaling [145, 146]. Chronic treatment with Sunitinib induced AXL, MET and EMT changes in expression leading to drug resistance. In this context, inhibition of AXL and MET kinases impaired Sunitinib acquired resistance *in vitro* and *in vivo* [146]. Thus, AXL emerges as a mediator of resistance to angiogenesis inhibitors and a strategy of a combination of inhibitors could be a solution to improve the efficiency of these treatments.

Immunotherapy and radiation

Cancer immunotherapy, using checkpoint inhibitors, is an emerging therapeutic option in the clinic, but a lot of patients are unresponsive. Mechanisms of evasion include adaptive immune resistance where tumor cells promote an immunosuppressive environment leading to T cell exclusion [147]. Since TAM inhibition promotes an antitumor microenvironment and an adaptive immune recruitment, combining those with immune checkpoint blockade could be a viable solution to increase their activity.

Combining radiation therapy and checkpoint immunotherapy have been suggested to treat various cancers and tumors resistant to this strategy have been shown to overexpress AXL [148]. In those tumors, AXL inhibition increased the sensitivity of this combined therapy by increasing CD8+ T cell response. AXL was associated with a reduction of antigen presentation via MHCI and an enhanced cytokine release that promoted a suppressive microenvironment, leading to a decrease in the efficiency of the treatment. Furthermore, several recent studies also linked AXL or MER activation with an increase of expression of PD-L1 by tumor cells [149-151]. Indeed, radiation resistant cells had an increase in this immune checkpoint molecule because of the AXL/PI3K pathway activation [149]. Hence, combining PD-L1 and AXL inhibition was able to synergize on antitumor efficacy *in vivo* [150]. In addition, MER and AXL have been shown to contribute to immune escape via modulation of efferocytosis depending on Phosphatidylserine (PS)/TAM signaling leading to AKT activation and upregulation of PD-L1. [151]. Thus, inhibiting the TAMs emerges as a good candidate for therapy to enhance the efficiency of this promising avenue to treat cancer.

In conclusion, TAM receptors are emerging as mediators of resistance for many types of antitumor strategies mainly via their link with other RTKs such as EGFR, HER2, MET, VEGFR or PD-L1 and their important role in EMT that is associated with a wide range of changes linked to stemness and various anti-tumor treatment resistance.

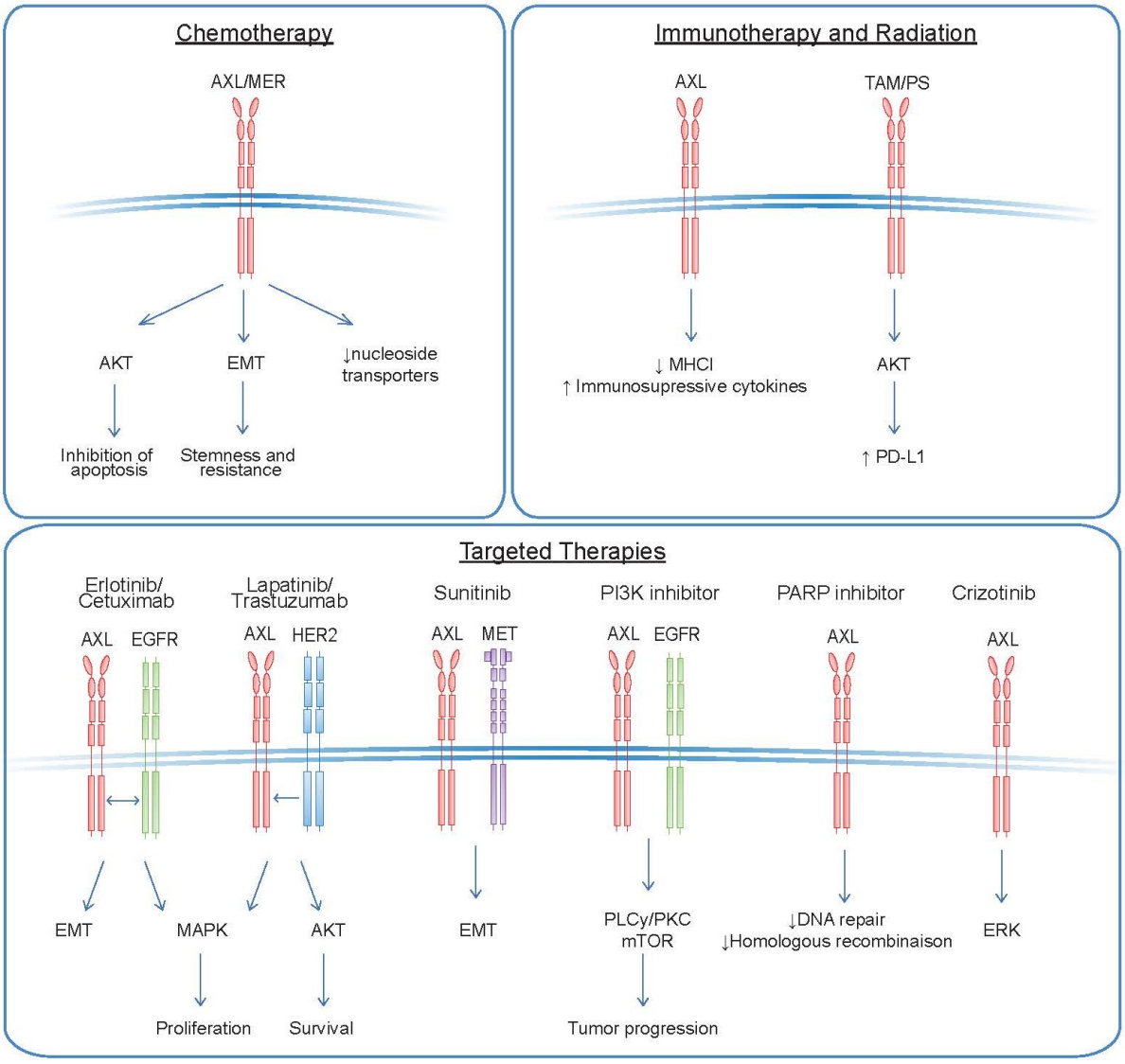

Figure 1.2.5 Mediators of Resistance

Future perspectives

See CHAPTER “Conclusion” of this thesis for a detailed perspective.

1.3 Dynamics of the actin cytoskeleton

The cytoskeleton is a dense network of elements consisting of microtubules, actin filaments and intermediate filaments that are found in the cytoplasm which provide structural support for the cells and permits directed movement of organelles, DNA and the cell itself. In specific, actin filaments consist of structural proteins named actin, where its monomeric globular form (G-actin) polymerize to form filamentous actin (F-actin) [152]. They constantly change in length which leads to their formation or dissolving. Actin is an ATPase protein that hydrolyzes an ATP upon its departing from a filament [153]. During the process of actin threadmilling, actin monomers join the barbed fast-growing end of the filament in its ATP state and depart the filament from the pointed end in an ADP state. This process of ATP hydrolysis plays a role in regulating the transition between polymerized and depolymerized actin, leading to changes in cell shape and movement, which will ultimately affect many biological processes such as embryonic morphogenesis, immune surveillance, angiogenesis, and tissue repair and regeneration [154-158].

1.3.1 Regulation of actin cytoskeleton dynamics

The cause of numerous diseases such as cancer, neurological disorders, cardiomyopathies, and Wiskott-Aldrich syndrome, is often the abnormal regulation or functioning of the actin cytoskeletal components since it affects many biological processes [152]. Hence, actin polymerization and depolymerization processes are tightly regulated by actin-binding proteins (ABP) [152]. Subsets of ABPs control many events during the dynamic process of actin threadmilling, including actin filament nucleation, elongation, severing, capping, crosslinking and actin sequestering [159]. ABPs are known to bind G-, F- actin or both. Some of which include, PROFILIN [160], COFILIN [161], WAVE/WASP [162], ENA/VASP [163] and FORMINs [164]. The dynamics of the actin rearrangements are regulated by signaling cascades that include kinases/phosphatases, and most notably RHO family small GTPases which act as GTP-dependent switchable molecules **(Figure 1.3.1**) [165]. Signals transmitted through these GTPases lead to actin rearrangement at the plasma membrane to induce different types of protrusions [166]. Generally, ABPs function as intermediate players which upon RHO GTPase activation, undergo conformational changes that will translate external cues or signals to changes in cytoskeletal rearrangements and membrane remodeling

[163]. Furthermore, RHO GTPase activation modulates the role of another protein family involved in the regulation of actin cytoskeleton dynamics, named BAR domain-containing proteins. BAR proteins contain a membrane-binding domain (BAR) and are known to link signaling pathways with actin rearrangements and membrane dynamics [167]. They also contain additional modules at the N- and C- terminal to the BAR domain, which play a role in diversifying their function, such as PH domains (phospholipid binding) [168], CRIB domain (RHO GTPase binding) [169], WH2 domain (actin binding) [170], and SH3 domains (proline-rich region binding) [169]. RHO GTPase binding to ABPs or BAR proteins leads to their activation by typically releasing their autoinhibition caused by internal interactions that will lead to their recruitment to a specific locus at the membrane [152]. Hence, this reveals RHO GTPases as significant players of actin cytoskeleton regulation that need to be tightly regulated to attain a controlled function of various cell processes.

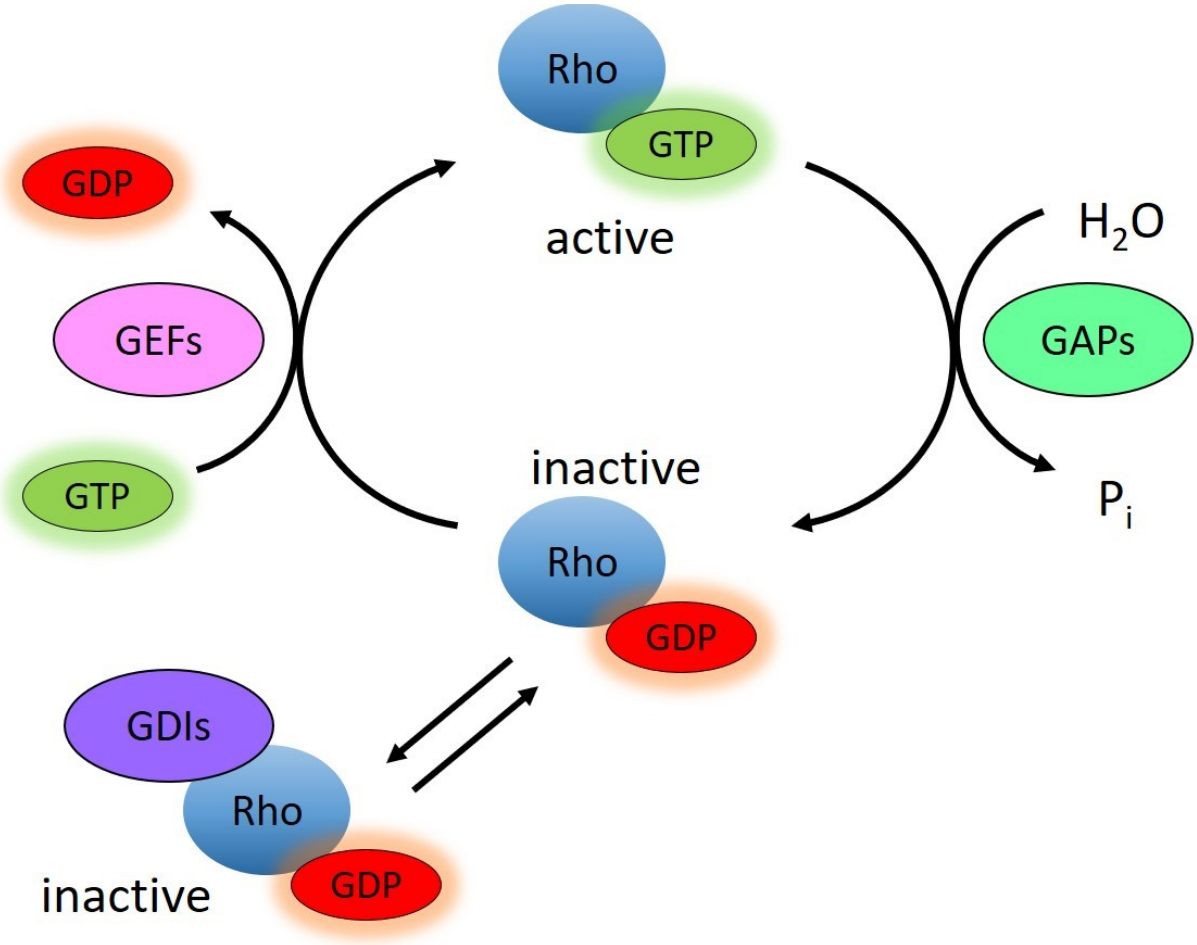

Figure 1.3.1 GDP-GTP cycle of RHO GTPases

RHO GTPases are known to cycle between an active (GTP-bound) form and an inactive form (GDP-bound). To activate RHO GTPases, guanine nucleotide exchange factors (GEFs) facilitate the exchange of GDP to GTP, whereas GTPase activating proteins (GAPs) promote the hydrolysis of GTP and inactivate the GTPase. Guanine nucleotide dissociation inhibitors (GDIs) are known to sequester the GTPase in a GDP-bound state in the cytosol.

1.3.1.1 RHO Family of GTPases

RHO family of GTPases are part of a superfamily named Ras-related small GTPases which are ubiquitously expressed. There are 23 members identified in mammals (**Figure 1.3.2**), 11 in *Drosophila melanogaster*, 10 in *Caenorhabditis elegans* and 5 in *Saccharomyces cerevisiae* [171-173]. They share a highly conserved GTPase domain and have small N- and C-termini, with a prenylated CAAX motif flanking its C-terminus allowing them to be anchored to the membrane to transduce signaling [172]. Because of their GTPase domain, they act as molecular switches to control signal transduction by cycling between a GTP form (active) and a GDP form (inactive) (Figure 1.3.1). Once they are GTP-bound, they interact with downstream targets named effectors to transduce their signal to a cellular process [174]. From the 23 members identified in mammals, RAC, RHO and CDC42 are the three most characterized members of the family where their function in regulating actin cytoskeleton was best characterized. In fibroblasts and many other cell types, using active and dominant negative forms, RHO was characterized to play a role in actomyosin contractility, whereas RAC and CDC42 play a role in actin polymerization in lamellipodia and filopodia membrane protrusions, respectively [175, 176]. In addition to actin cytoskeleton dynamics, RHO GTPases also regulate many other processes and signaling pathways such as cell polarity, gene transcription, cell cycle progression, microtubule dynamics, and vesicular transport [177]. The following table summarizes many function and roles of the cell that are regulated by specific GTPases and their effectors (**Table 1.I**).

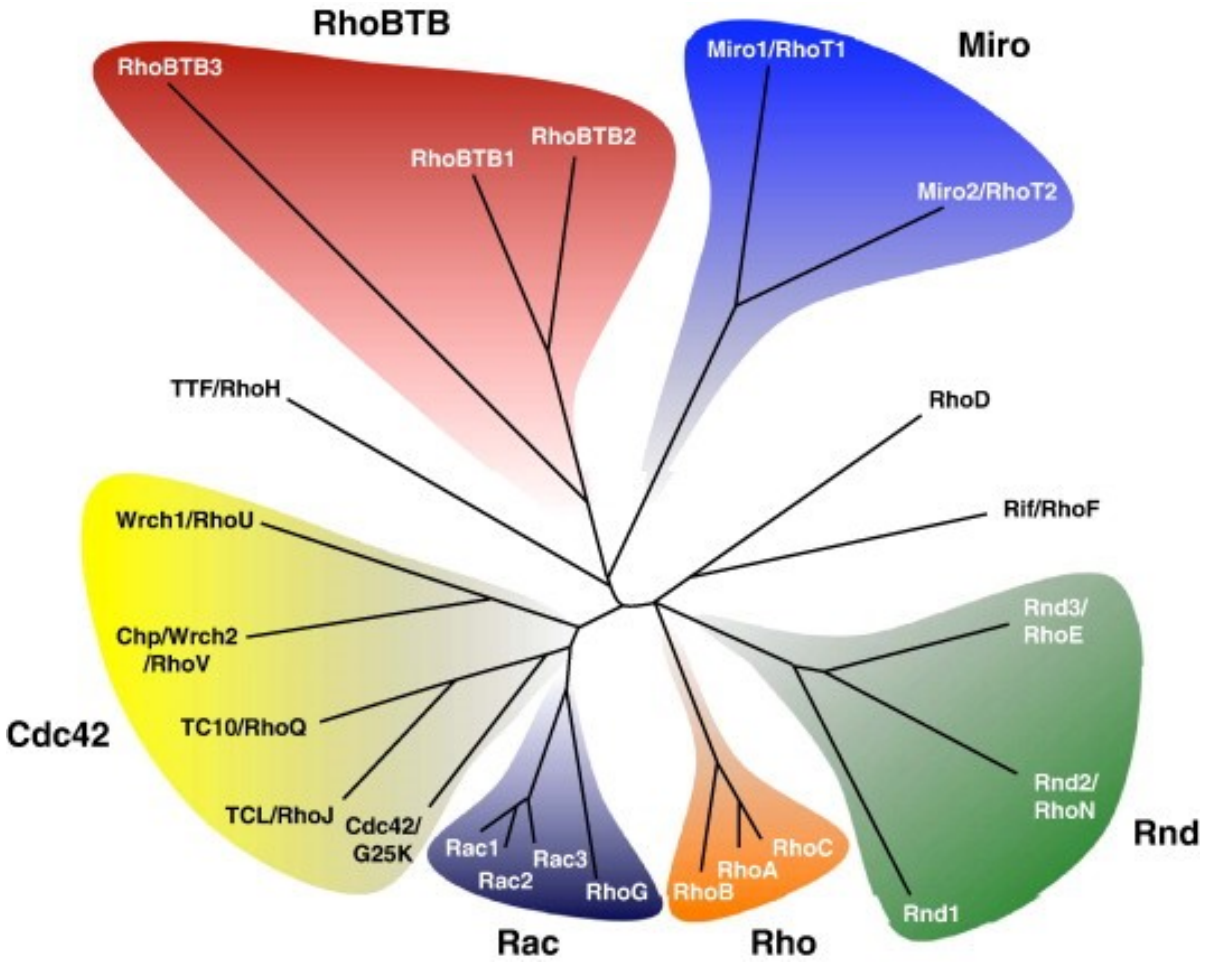

Figure 1.3.2 Phylogenetic tree of the RHO GTPase family

Adapted from Grise F, et al. Biochim Biophys Acta Review 2009 [178]

The 23 members of the family can be classified in 6 subfamilies (RHOA, RAC, CDC42, RHOBTB, MIRO, RND), shown in different colors. This tree is built based on their sequence identity. The amino acid sequences of human RHO GTPases were aligned using the ClustalW program and the phylogenetic tree was generated with the TreeView program [179].

Table 1. I Biological roles of GTPases in the cell

Role	Process	RHO GTPase involved	Effectors and other proteins involved
Morphology	Cell polarity	CDC42 [180]	PAR proteins, PKC kinase [181, 182]
	Cell shape	CDC42, RAC, RHOA [183-186]	PAR proteins, PKC kinase [187], LAMININ [188], RAL GTPase, SEC5 [189, 190]
Movement	Single-cell migration	RAC [191, 192], RHOA [193], CDC42 [194]	IRSp53, PIP5K, PAK1, LIM, ARP2/3 complex [195], DOCK180/CRKII [196], STATHMIN, ROCK1, mDIA [197]
	Coordinated cell migration	RHO [198], RAC, CDC42 [184]	PKN, ROCK1 [199], JNK/MAPK [200], DPP [201]
Behaviour	Contraction	RHO [202]	ROCK1 [203], THROMBIN [204]
	Phagocytosis	RAC, CDC42 [205, 206], RHOG [207], RHO [205]	FcR [205], PAK1 [208], ELMO1 [207], VAV [209], αMβ2 [205], CRKII, DOCK180 [196], ARP2/3 complex [210]
	Proliferation	RAC, RHO, CDC42 [211]	VAV, JNK/MAPK, NF-AT, IL2 [212], CYCLIN D2 [213], CYCLIN D1 [214], p21CIP [215]
	Regulated secretion	CDC42 [216], TC10 [217]	PAR proteins, PKC kinase [216] [216], GLUT4 [217]

1.3.1.1.1 Regulation of RHO GTPases

Alterations in RHO GTPase signaling can lead to many malignant transformation, neurological abnormalities, and immunological diseases. Hence tight regulation of RHO GTPase activity is critical for the normal function of various biological processes mentioned above. Their cycling process between GTP and GDP states is regulated by three families of proteins: Guanine nucleotide exchange factors (GEFs) which facilitate the exchange of GDP to GTP to activate the GTPase [218], GTPase activating proteins (GAPs) which promote the hydrolysis of GTP and inactivates the GTPase, and Guanine nucleotide dissociation inhibitors (GDIs) which sequester the GTPase in a GDP-bound state in the cytosol and prevent them from localizing at the membrane or being activated by GEFs [219] (**Figure 1.3.1**).

GEFs are divided between two families: DBL-Homology domain (DH) family and Dock Homology Region (DHR) domain or Dedicator of cytokinesis (DOCK) family. The majority of RHO GEFs are part of the DH family of GEFs which consist of more than 70 members. They contain a catalytic DH domain that is followed by a pleckstrin homology (PH) domain that facilitates their interaction with the plasma membrane and hence affects the catalytic activity of the DH domain [218, 220]. DOCK GEFs, however, which consist of 11 members are characterized by 2 conserved domains DHR-1 and DHR-2. DHR-2 domain binds the GDP form of GTPase to catalyze the exchange of GDP to GTP [221, 222], whereas DHR-1 domain binds PIP3 at the plasma membrane to facilitate GEF localization to the membrane. Moreover, GAPs and GDIs act as negative regulators of RHO GTPases. GAPs provide a catalytic group that can accelerate the intrinsic GTPase activity of the GTPase. They contain a GAP domain that binds the GTP-bound state of the RHO GTPase and catalyzes its GTPase activity [223]. On the other hand, GDIs control the cycling of the GTPases between cytosol and membrane and regulate their activation. GDIs family consist of 3 members that contain an N-terminal domain that binds RHO GTPases and a C-terminal domain that includes the geranylgeranyl-binding pocket that extracts geranylgeranylated RHO GTPases from the membrane to keep them inactive in the cytosol [224]. On the other hand, GDIs can also play the role of a GTPase activator by either acting as a chaperone in moving GTPases between membranes or by binding the GTPase and protecting them from proteasomal degradation by preventing ubiquitin ligase binding [225, 226].

In addition to their GDP/GTP cycling regulation, post-translational modifications of RHO GTPases such as lipid modification, phosphorylation, ubiquitination, and sumoylation are also known to regulate their signaling. RHO GTPases can also be regulated at the level of gene expression or post-transcriptionally by miRNAs. Examples and effects of these modifications on specific RHO GTPases are mentioned in **Table 1. II**.

Table 1. II Post-translational modifications of GTPases

Modification	RHO GTPase	Detail of modification	Outcome
Lipid Modification	All except RHOBTB1 and RHOBTB2	Prenylation: At the CAAX motif, irreversible prenylation on Cysteine by a farnesyl or a geranylgeranyl lipid followed by removal of AAX and methylation of the prenylated Cysteine [227, 228]	Localize them to certain membrane compartments
	RAC1 on Cys178 [229]	S-palmitoylation: a reversible addition of a palmitoyl group on a Cysteine	
	CDC42 on Cys189 [230]		
	RHOU [231]		
	RHOV [232]		
Phosphorylation	RAC1 on T108 [233], Y64 [234], S71 [235]	By kinase ERK, SRC/FAK, AKT	Targets RAC1 to the nucleus, negative regulation of RAC1 activity, inhibit GTP binding and a decrease in RAC1 activity
	CDC42 on Y64 [236], S185 [237]	By kinase SRC, PKA	Enhances GDI interaction and translocates to the cytosol
	RHOA on S188 [238, 239], T127 [240]	By kinase PKA and SLK, PKC	Enhances GDI interaction and translocates to the cytosol, protects GTP-bound form from proteasomal degradation, inhibit RHOA activity
	Atypical GTPases: RND3 S240, S218, S210 [241-243], RHOU on Y254[244]	- By kinase ROCK1 and PKC - By kinase SRC	- Targets its binding to 14-3-3, rendering it inactive in the cytosol - Translocation from the plasma membrane to endosomes
Sumoylation	RAC1 on K183, 184, 186, 188 [245]	By SUMO E3 ligase PIAS3	Increases GTP binding and Rac1 activation
Ubiquitination	RHOA on K6, K7 [246], K135 [247]	By complex SCF, SMURF1, BACURD	Proteasomal degradation
	RHOBTB1 and RHOBTB2 [248]	By ligase CUL3	
	RND3 on K235 [249]	By complex SCF	
	RHOU on K177, K248 [250]	By ligase CUL5	
	RAC1 on K147 [251], K166 [252]	By complex XIAP, cIAP, SCF	
MiRNA	RHOA	miRNA-155 [253], miRNA-125a-3p [254], miRNA-185 [255]	mRNA degradation, inhibition of translation and decrease in expression
	CDC42	miRNA-185 [255], miRNA-29 [256]	

1.3.1.1.2 DOCK family of atypical GEFs

DOCK GEFs are referred to as "atypical" because they lack the typical Dbl-homology domains found in the typical DH GEFs. DOCK GEFs consist of 11 members that are classified into 4 subfamilies (**Figure 1.3.3**). Interestingly, they are all specific to RAC or CDC42 GTPases but not RHOA and the other members of RHO GTPases [257]. Besides their PIP3-binding domain (DHR-1) and GEF domain (DHR-2), 2 subfamilies of DOCK GEFs (DOCK-A and DOCK-B) contain an SH3 domain at the N-terminus, mediating their interaction with their binding partner, ELMO protein [222]. In addition, their C-terminus contains a PXXP motif where SH3-containing adaptors can bind such as CRKII. Following PI3-Kinase activation and PIP3 production upon an external signal or stimuli, DHR-1 facilitates the recruitment of DOCK GEFs to the membrane [258]. In addition to DHR-1, the polybasic region (PBR) of DOCK-A GEFs have been shown to mediate membrane localization by binding to phosphatidic acid (PA) [259]. Once recruited to the membrane, DOCK GEFs can mediate their GEF function on RAC or CDC42 GTPases near the membrane to induce actin cytoskeleton rearrangements. Recent studies *in vivo* have defined roles for DOCK GEFs in biological functions such as myoblast fusion, cardiovascular development, bone-resorption and immune homeostasis [260-263].

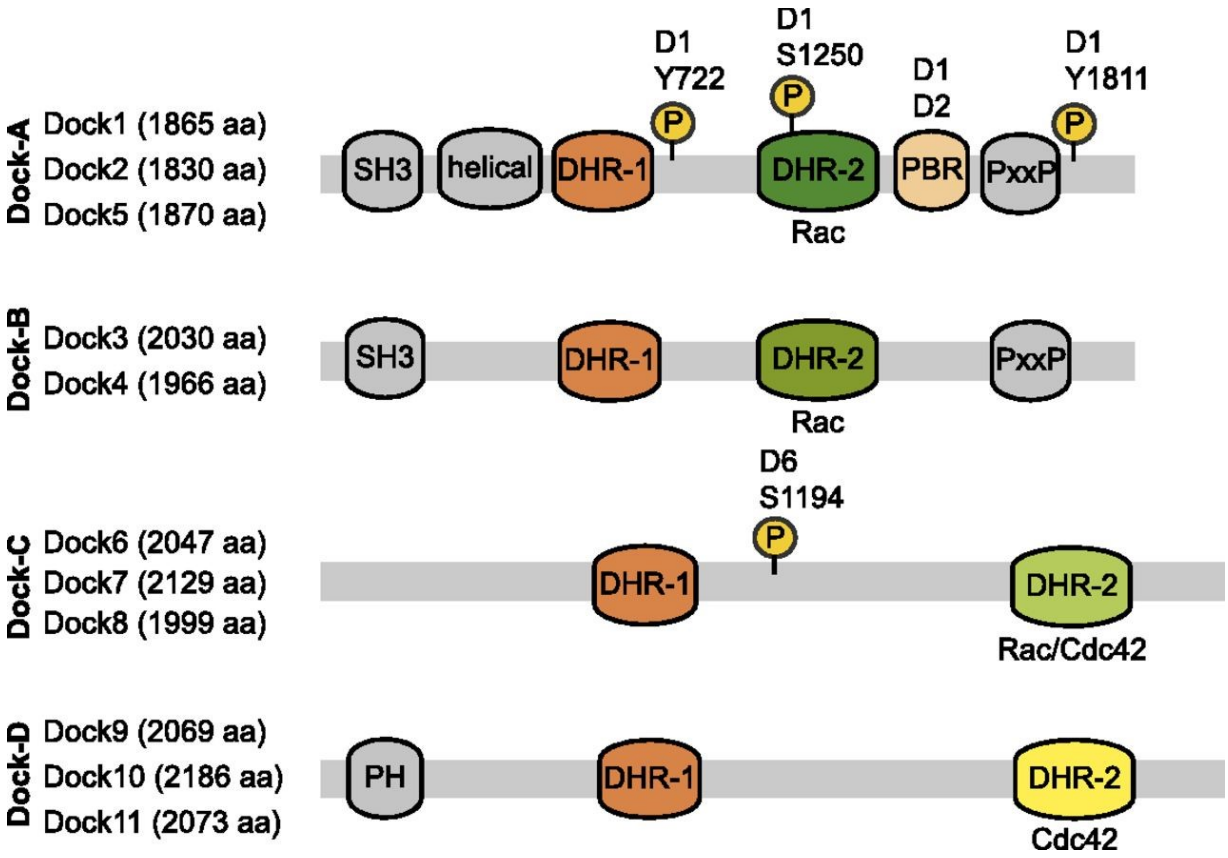

Figure 1.3.3 DOCK family of GEFs

Adapted from Mélanie Laurin and Jean-Francois Côté in Genes & Dev. Review 2014 [222]

DOCK proteins, subdivided into four subfamilies, are characterized by the evolutionarily conserved DHR-1, mediating binding to PIP3, and DHR-2, encompassing the GEF activity toward RAC/CDC42 GTPases. The N terminus of DOCK-A/B GEFs, including an SH3 domain, mediates their interaction with ELMO scaffolding proteins, while the C-terminal PXXP region coordinates interactions with SH3-containing adaptor proteins, such as CRK and GRB2. DOCK-D members have an N-terminal-localized PH domain involved in phosphoinositide binding for membrane translocation. Whereas the DHR-2 domain of DOCK-A/B is specific to RAC GTPase, DHR-2 domain of DOCK-C can mediate its GEF activity on RAC and CDC42 GTPases. Several studies have identified that DOCK GEFs are post-translationally modified by kinases and phosphatases. Of *in vivo* relevance, phosphorylation of DOCK1 (D1) on Y722, Y1811, or S1250 increases its GEF activity toward RAC and is elevated in brain cancers. AKT1 binds to DOCK6 (D6) and phosphorylates its S1194 to inhibit its GEF activity; binding of DOCK6 to the phosphatase PPP2CA counteracts this inhibition through dephosphorylation.

1.3.1.1.2.1 Binding Partners

DOCK1, also named DOCK180, in subfamily DOCK-A was initially identified as a binding partner to CRKII adaptor protein [264]. CRKII adaptor protein is known to complex with CAS family members p130CAS to induce RAC activation and cell migration [265], which have been shown to be dependent on DOCK1 expression [266]. Understanding the function of this pathway has been greatly explored in flies and worms. Its ortholog in *C. elegans* Ced-5 has been identified along with other six Ced genes to be involved in the engulfment of apoptotic cells [267, 268]. Along to Ced-5, Ced-2 and Ced-10, the worm orthologs of CRKII and RAC respectively, have also shown to play an important role in the migration of the distal tip cells in the gonads during *C. elegans* development. Further studies identified another gene Ced-12, the worm ortholog of ELMO, to bind Ced-5 (DOCK1) and to functionally cooperate with Ced-2 (CRKII) to regulate their complex [269, 270].

Engulfment and cell motility (ELMO) proteins are scaffold proteins that bind DOCK-A and DOCK-B family of DOCK GEFs. ELMO family of proteins consists of 3 mammalian members, ELMO1-3 (**Figure 1.3.4**). They are characterized by their C-terminus that contains an atypical PH domain that interacts with the α-helical region flanking the SH3 domain in DOCK proteins, followed by a proline-rich region (PRR or PXXP) that interacts with DOCK1 flanked SH3 domain. Their N-terminus, on the other hand, has been reported to bind RHOG, ERM proteins and BAI1 [271-273]. The central region of ELMO contains an ELM domain which has an unknown function [274]. Moreover, DOCK/ELMO complex formation has proven to be essential to achieve RAC-dependent actin cytoskeleton remodeling at the membrane protrusions which relies on microtubule stabilization mediated by the microtubule plus tip binding protein named ACF7, a binding partner of ELMO [257, 275-277]. In addition, other studies reported ELMO proteins to potentiate DOCK GEF activity on RAC [278]. This function of ELMO is proposed to be mediated by the PH domain which plays a role in stabilizing RAC interaction with DOCK1 at the DHR-2 domain, hence increasing the GEF activity and RAC GTP-loading [279]. Another strategy of how ELMO proteins can potentiate DOCK1 GEF activity could be by the ELMO-induced accumulation of DOCK1 protein levels in cells by preventing its proteasomal degradation [280].

A)

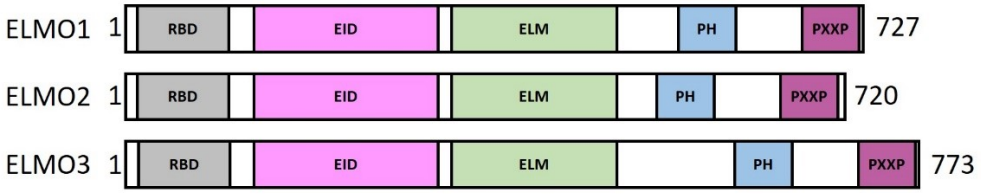

B)

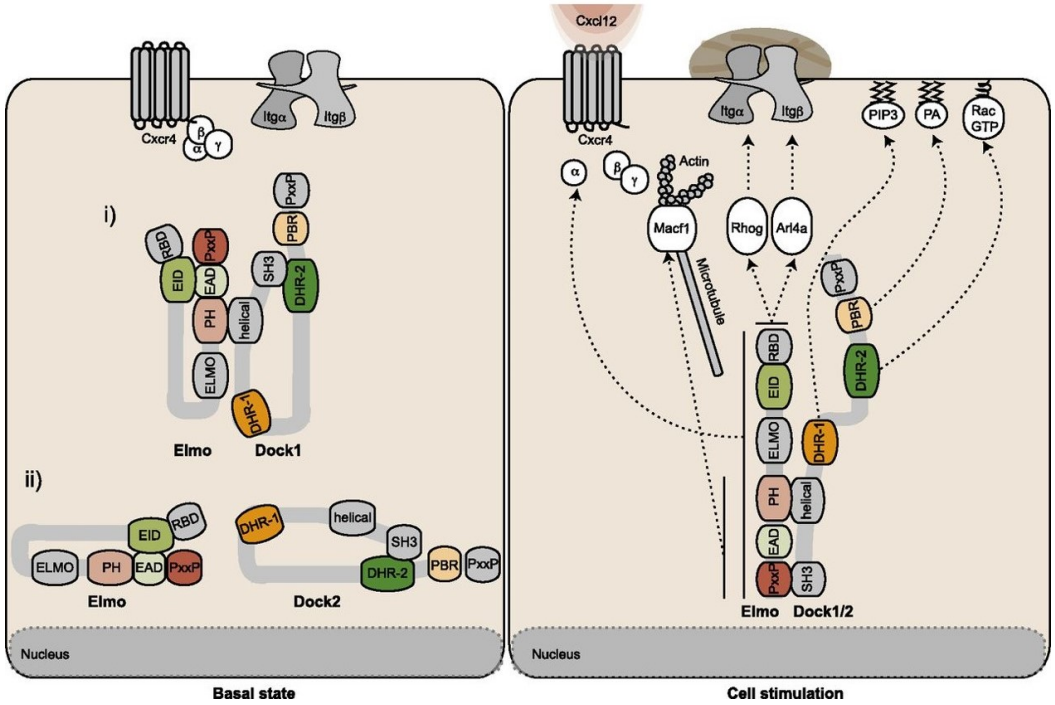

Figure 1.3.4 ELMO family of proteins and their regulation of DOCK protein localization

Adapted from Mélanie Laurin and Jean-Francois Côté in Genes & Dev. Review 2014 [222]

A) ELMO family of proteins consist of 3 members, ELMO1-3. They contain a Ras-binding domain (RBD) at their N-terminus that is known to bind activated RHOG and Arl4a. This domain is followed by an Elmo Inhibitory Domain (EID) that binds directly to the C-terminal domain between the PH and PXXP motif to regulate its open-closed conformation. The central region of ELMO proteins contains an ELM domain which has an unknown function. At the C-terminus, an atypical PH domain is presently followed by a proline-rich region (PXXP), which are both involved in binding to the α-helical region and the SH3 domain of DOCK proteins. **B)** Recent studies highlight the key role played by Elmo in positioning Dock1 after cell stimulation. At the basal state, ELMO and DOCK1 are found in complex and are proposed to be autoinhibited by intramolecular interactions. Uncomplexed ELMO and DOCK2 are also proposed to be autoinhibited, which is suggested to be released upon their interaction. Upon cell stimulation, the recruitment of the ELMO/DOCK complex at the membrane can be guided by ELMO's repertoire of interacting proteins.

1.3.1.1.2.2 Regulation of DOCK/ELMO complex

ELMO proteins can be regulated by intramolecular contacts where their N-terminal Armadillo Repeats (ARMs) named ELMO Inhibitory Domain (EID) directly binds the C-terminal region of ELMO between the PH and PXXP motifs. The disruption of this intramolecular interaction leads to changes in ELMO conformation. At basal state, ELMO has been proposed to be in a closed conformation and physically bound to DOCK proteins which are also in a closed conformation (**Figure 1.3.4)** [274, 281, 282]. Extracellular signals can release the autoinhibition of ELMO where Ras-binding domain (RBD) can bind the activated GTPases RHOG or ARL4A, change ELMO to an open conformation and hence facilitate the positioning of DOCK1 and RAC at the membrane to have increased and polarized RAC activation [271, 283]. Hence this autoinhibition relief seems to be dependent on a specific signal that will contribute to the promotion of a conformational change. This signal could be a direct or an indirect binding partner at its C-terminus or N-terminus or a post-translational modification that will induce the release of the autoinhibition. A study has shown ELMO proteins to be phosphorylated by the SRC kinase HCK [284]. Similar to ELMO, DOCK proteins have been shown to be phosphorylated by specific kinases and this phosphorylation led to the modulation of their GEF function. For instance, PDGFR-mediated phosphorylation of DOCK1 on Y1811 by SRC and EGFRvIII-mediated phosphorylation of DOCK1 on Y722 by SRC and S1250 by PKA, both found in brain tumors, increased DOCK GEF activity towards RAC and promoted the invasion and migration of EGFRvIII and PDGFR positive cells [285-287]. In addition, HER2-mediated tyrosine phosphorylation of DOCK1 on Y1811 has also been observed in HER2 breast cancer [288]. Inversely, DOCK6 phosphorylation by AKT on S1194 inhibits its GEF activity and prevents axon growth in neurons [289]. Another post-translational modification that can regulate DOCK function in cells is ubiquitination. A study has shown DOCK1 to be ubiquitinated upon EGF stimulation at the plasma membrane, and this ubiquitination was inhibited by ELMO expression [280].

Hence, it would be interesting to see if ELMO phosphorylation can lead to the release of EID intramolecular interaction. Investigating what protein partners can interact with ELMO either at N-term or C-term and what other kinases can phosphorylate ELMO can improve our understanding of how ELMO is activated and how it can regulate DOCK activity.

1.3.1.1.2.3 Role of DOCK/ELMO complex in cancer

DOCK proteins within subfamilies DOCK-A and DOCK-B, known to interact with ELMO, have shown to play a role in cancer growth and invasion. For instance, high levels of DOCK1 significantly associates with poor disease-free survival in HER2+ and basal breast cancer patients [288]. Its deletion has shown a decrease in Neu-induced mammary tumor burden and inhibition of lung metastasis. Similarly, in glioblastomas multiforme, DOCK1 has been shown to be highly expressed and its activation by either PDGFRA or EGFRVIII in glioblastoma cells have rendered cells to be more invasive [285-287]. Abrogating DOCK1 expression in these cells has led to a significant impairment in their proliferation when injected in the brain and their ability to invade the brain *in vivo*. Other studies reported urokinase-type plasminogen activator receptor (uPAR), a receptor highly expressed in many human cancers and correlating with poor prognosis of patients, to induce its invasive signaling by modulating DOCK1/CRKII/BCAR1 complex to induce tumor cell motility and invasion [290]. Another group has demonstrated a role for DOCK1/ELMO complex downstream of the GPCR CXCR4 in SDF-1α-induced breast tumor cell dissemination [291]. Upon CXCR4 activation by SDF-1α, DOCK1 is recruited to the plasma membrane via ELMO binding to Gαi2 subunit and activates RAC. This process was shown to be essential for breast tumor metastasis. A similar study has shown RAC activation by DOCK1 downstream of GPCRs led to the activation of the p110β subunit of PI3K [292]. RAC activation mediated by ELMO binding to Gβγ subunit downstream of LPA and S1P GPCR was shown to be necessary for LPA-stimulated cell migration. Altogether, these studies demonstrate cell surface receptors such as HER2, uPAR, CXCR4, EGFR, and PDGFR, exploit DOCK1/ELMO complex in their signaling pathways to mediate their role in tumor progression and metastasis in various types of cancer.

Metastatic cancer cells can move in two types of movements: mesenchymal and amoeboid in order to metastasize to secondary sites [293, 294]. During the mesenchymal movement, the cell adopts a RAC-induced elongated cell morphology with membrane ruffles formation at the leading edge. In contrast, amoeboid movement of the cell involves RHOA signaling to induce actomyosin contractility, where the cell becomes round shaped with membrane blebbing [293]. This change in movement mode is interconvertible depending on the microenvironment of the tumor cell. In search of regulators for these RHO GTPases, DOCK3

was identified as a regulator of mesenchymal movement in melanoma cells [295]. Suppression of DOCK3 led cells to migrate in an amoeboid manner. DOCK3 binds NEDD9 adaptor protein, a member of CAS family, and activates RAC to signal via WAVE2 to remodel actin cytoskeleton to induce a mesenchymal phenotype. It simultaneously suppresses amoeboid movement by decreasing the levels of phospho-myosin light chain-2 (pMLC2) and hence decreasing actomyosin contractility in the cells. During the amoeboid movement, RHOA-ROCK signaling is able to inhibit mesenchymal migration by ARH GAP22-mediated RAC inactivation. Hence, NEDD9/DOCK3/RAC/WAVE2 axis has been demonstrated to play a big role in the mesenchymal movement of melanoma cells. Similarly, others have shown this axis to play an invasive role in head and neck squamous cell carcinoma [296]. In this study, the authors have defined a novel role for TWIST protein, a regulator of EMT, in regulating DOCK3 and NEDD9 expression levels to promote a RAC-dependent mesenchymal migration. TWIST cooperates with BMI1, a polycomb group family member, to repress the expression of miRNA *Let7i*, to upregulate DOCK3 and NEDD9 expression levels and increase active RAC levels.

DOCK4, the other family member in DOCK-B subfamily, also plays a role in cancer cell migration. In complex with ELMO and SHY3YL proteins, DOCK4 induces RAC activation at the membrane sites where RHOG is activated to induce cortactin-rich protrusions [297-299]. In invasive breast cancer cells, EPHEXIN4 activates RHOG to recruit ELMO2/DOCK4 at the membrane to complex with EPHA2 and induce DOCK4-mediated RAC activation. Since EPHA2 is highly expressed in invasive breast cancers, we suggest DOCK4, therefore, can contribute to the invasiveness of EPHA2 overexpressing cancer cells.

1.3.2 Conclusion

As a summary, RHO GTPases are major players of actin cytoskeleton dynamics and their regulation is a necessary process in order to have a normal cell movement. GEFs, such as the atypical DOCK family of proteins, and their binding partners ELMO, are promoters of cell migration by inducing RHO GTPase activation. In fact, their de-regulation can lead to abnormal cell migration, which may facilitate the cancer cell dissemination process during metastasis. Hence the tight regulation of these proteins is of significant importance to maintaining normal cell migration and prevent cancer cell invasion. As mentioned earlier, DOCK proteins play a significant role in mediating cancer invasiveness. In specific, high expression of DOCK1 proteins has been shown to correlate with metastasis in breast cancer. Extensive studies have also shown the phospho-modulation of DOCK proteins downstream of RTKs and surface receptors promotes RAC activation and cancer cell movement. Since ELMO is a binding partner of DOCK proteins and can potentiate DOCK-mediated RAC activation levels, it is important to understand further how these proteins are regulated downstream of RTKs and whether they are post-translationally modified to enhance DOCK GEF activity in cancer cells.

1.4 Cancer Cell Migration and Invasion

Cell migration is a process that is critical for proper development and function of multicellular organisms. Many pathological conditions such as cancer, use the cell migration process for its tumor cells to invade and become a life-threatening disease. Cell migration is a multistep process that involves the activation of signaling pathways that control the dynamics of cytoskeleton and loss of cell-cell junctions in tumor cells [293, 300-303]. Tumor cells then acquire a migratory behavior to invade adjacent tissue or engage with blood and lymph vessels, penetrate through basement membranes and endothelial walls to disseminate into their lumen to colonize at distant organs [304, 305]. In fact, the interaction between the cancer cell and the extracellular matrix dictates the mechanism in which the cell will take to facilitate its migration and invasion process. The cells capacity to migrate is influenced by biological cues such as growth factors, and the underlying substrate on which they move, which would lead to the activation of diverse signaling pathways that mediate its movement [306]. Many mechanisms of cell movement have been identified in the past decades which include regulation of actin cytoskeleton and cell adhesion [302, 303]. Cancer cells can either migrate individually when cell-cell junctions are absent or collectively as a group when cell-cell junctions are retained [307]. For both mechanisms of migration, cells follow the paradigm of active cell migration, which involves multi molecular events that change the cell shape, its position and the tissue environment through which it migrates [301, 308-311] (**Figure 1.4.1**). Firstly, the cytoskeleton polarizes and forms the leading protrusion at the front edge of the cell towards its migratory track [312, 313]. The leading-edge protrusion then communicates with the extracellular matrix to recruit cell surface receptors to form focalized adhesion clusters which will couple the extracellular matrix to the interior of the cell to generate force to move [314]. Simultaneously, local proteolysis of the extracellular matrix takes place to modify the tissue and provide some space for the cell to maneuver [309]. Subsequently, RHO GTPases induce actin contractility inside the cell leading to the turnover of the adhesion complexes at the trailing end of the cell.

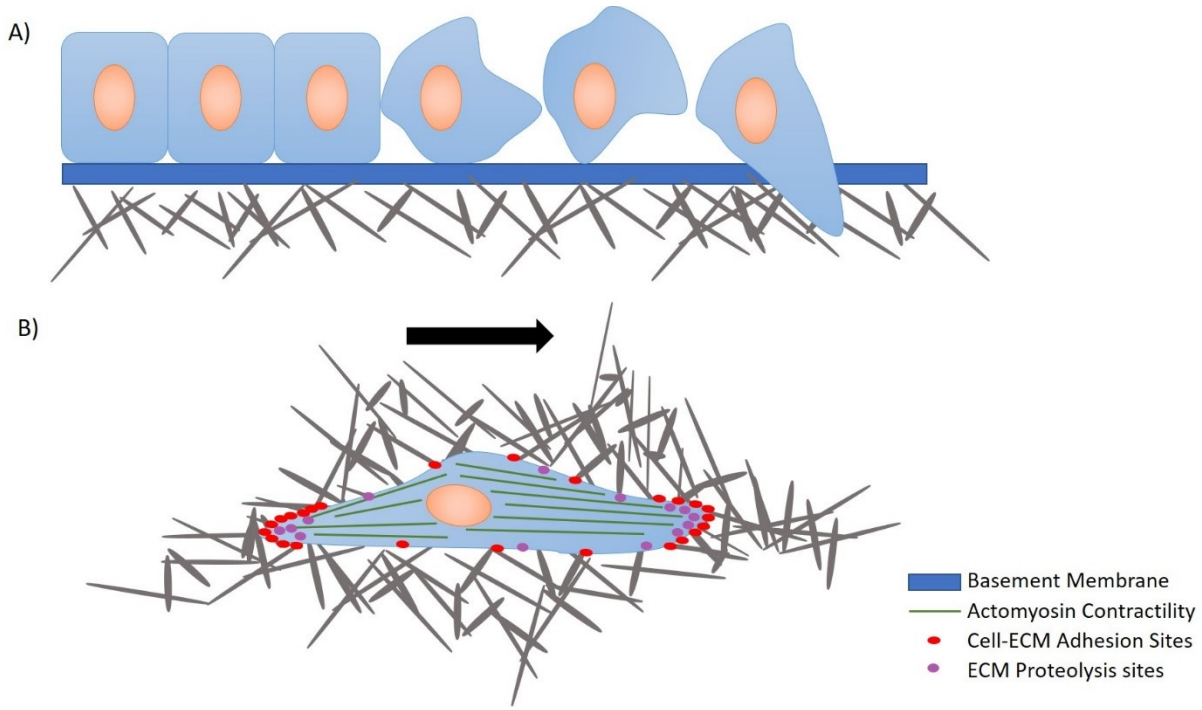

Figure 1.4.1 Cell movement mechanism

A) Upon a migration stimulus, epithelial cells retaining their cell-cell and cell-basement membrane adherence, go through a change in cell shape and position in order to invade their surrounding environment. **B)** The cell protrudes towards the migratory track and forms a cell protrusion or the leading edge. Once formed, the migratory cell can form new adhesion sites that can allow it to adhere to the ECM and move forward. Simultaneously, focalized proteolysis takes place where cell degrades the ECM in order to make space to maneuver. Actin contractility will then take place in order to generate the force inside the cell which allows the cell to move forward and lead to the turnover of the adhesion complexes at the back of the cell, also named the trailing edge.

1.4.1 Cell Polarization and Protrusions

Cell polarity is a fundamental event that plays a role in eukaryotic cells in shaping tissues during development, intracellular transport, cell division, differentiation and directed cell migration [315]. Regularly, the polarization of the cell occurs when a polarization cue dictates an asymmetric recruitment and activation of adhesion complexes, cytoskeleton structures and traction forces inside the cell which leads to the translation of a functional asymmetry [316]. This ultimately induces the polarized signals that result in the generation of a protrusion and acquiring a leading and a trailing edge or a front-rear polarity axis. Leading-trailing edge cell polarity does not only occur in singly migrating cells but also in collective migrating cells during morphogenesis, wound healing and tissue renewal in adult life and is involved in cancer spreading [315]. A leading edge is formed when the cytoskeleton assembles to push the membrane forward to expand and produce a protrusion [317]. This process of cell polarity requires a particular organization and orientation of the cytoskeleton and adhesive structures [315]. The actin cytoskeleton rearrangements at the leading edge of the cell determine the overall shape of the cell and can give rise to the formation of different membrane protrusions mentioned in **Table 1.III**.

Table 1. III Various types of protrusions formed by the cell upon cell movement

Type of Structure	Description	Proteins involved	Purpose
Lamellipodia [318, 319]	Broad, flat, sheet-like membrane extensions at the leading edge	- RAC1 [320]/RHOG [321], COFILIN [322]/FORMIN [323] - CORTACIN [324], ARP2/3 [325, 326] - VASP/WAVE [326]	Drivers of migration, determines the direction of movement and requires the attachment to the ECM
Filopodia [327]	Thin, cylindrical, needle-like membrane projections at the leading edge	- FASCIN [328], CDC42 [329]/RHOF [330] - ENA/VASP [331, 332], IRSp53 [329] - MYOSIN X [333], mDIA2 [334], PROFILIN, ARP2/3 [335]	Carry an exploratory function enabling the cell to probe its local environment
Invadopodia [336-338]	Finger-like ventral membrane protrusions	- MT1-MPP [339], VIMENTIN [340] - ARP2/3 [337], WASP/WAVE [337] - CDC42 [341], mDIA [342], CIP4 [343], FASCIN [328]	Matrix degrading structures involved in ECM proteolysis
Pseudopodia [344]	Cylindrical finger-like protrusions that protrude and retract at the leading edge	- ARP2/3, WAVE [345] - EPS8, CORTACTIN [158] - LIM kinase, IQGAP1 [346], FASCIN [347],	The first event formed after cell polarization before ECM recognition
Blebs [348]	Curves in membrane induced by the local weakening of the plasma membrane/cortical actin interactions	- DAPK [349], ROCK [350], RHOA [351] - FORMIN/PROFILIN [352], MYOSIN II [350]	Allows cytoplasmic flow, when the plasma membrane is detached to push the membrane outwards, does not adhere to ECM

1.4.2 Focal Adhesions

Following the formation of a polarized protrusion, the leading edge of the cell attaches to the substratum in the extracellular matrix to generate adhesion or attachment sites. These adhesion sites are known for two properties: to transmit a signal from the cell cytoskeleton to the ECM and to dynamically respond to tension stress generated by mechanical forces in the interior and exterior of the cell [353]. They are predominantly formed by adhesion receptors called integrins, which are coupled with cytoskeletal and signaling proteins, and act as sensors of the ECM environment [316, 354-356]. Integrins are expressed on the cell surface and exist as heterodimers comprising of α and β subunits. Both subunits are type I transmembrane proteins consisting of a large extracellular domain that interacts with the ECM and a cytoplasmic tail that interacts with intracellular proteins. Once the cell attaches to ECM, integrins cluster at the cell surface and recruit scaffolds/adaptors and signaling proteins to the inner side of the plasma membrane where they form a structure named Focal Adhesion (FA) [357-359] **(Figure 1.4.3**). The proteins found in the FAs such as TALIN, VINCULIN, α-ACTININ, and KINDLIN, provide a strong linkage to the actin cytoskeleton, hence firming the cell-ECM connection [360-362]. Among these FA proteins, TALIN is a key regulator or the rate-limiting step of the FA assembly process where it links Integrins to the actin filaments [363-365]. Subsequent steps include the recruitment of VINCULIN protein which triggers the clustering of the integrins and strengthens the actin-integrin link [360, 365, 366]. This initial structure formed is named a nascent FA, some of which grow and form mature FAs, which are more stable [316]. Since integrins lack enzymatic activity, many signaling proteins such as kinases and phosphatases are recruited to the FA sites to transmit ECM derived signals, which will induce the activation of RHO GTPases mediated pathways to result in actin cytoskeleton rearrangements and generation of a mechanical force [316]. In turn, the formation of the integrin-mediated cell adhesion structures leads to a global change of the cell shape and motility. For the cell to migrate efficiently, cells must also detach from the ECM and disassemble the FA structures to migrate. At the leading edge of the cell in a directional movement, FAs are formed underneath the lamellipodia to generate a force inside the cell to move the cell body forward [367]. Subsequently, FAs at the leading and trailing end of the cell must disassemble to accompany

the formation of new protrusions and to release the cell from the ECM attachment, respectively [367, 368] (**Figure 1.4.4**). Therefore, the continuous formation and turnover of these FAs structures is crucial for the cells to adhere to ECM and move in a directional manner, and must be a tightly regulated process, that is driven by the balance of actin polymerization and actomyosin contraction [302].

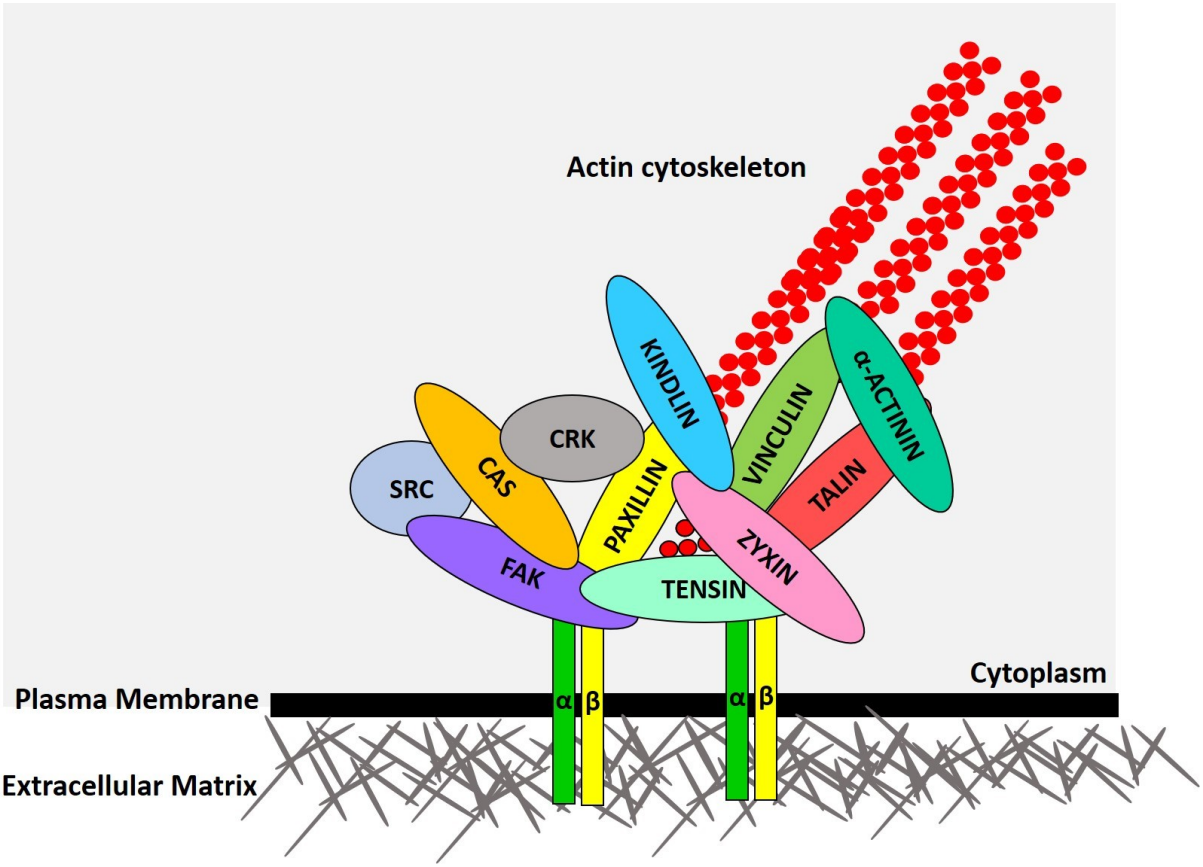

Figure 1.4.3 Focal Adhesion Structure

Inspired by Nicholas O.Deakin and Christopher E. Turner in J Cell Sci 2008 [369]

The focal adhesion is a structure that provides the cell with a link between the ECM and the actin cytoskeleton inside the cell. It also serves as a signaling hub for the cell to facilitate cell movement. The cell adheres to the ECM by its transmembrane integrin heterodimers, which leads to their activation and recruitment of the many intracellular proteins to the plasma membrane. Depicted above are some of the proteins found at focal adhesion sites that may play a structural or regulatory role.

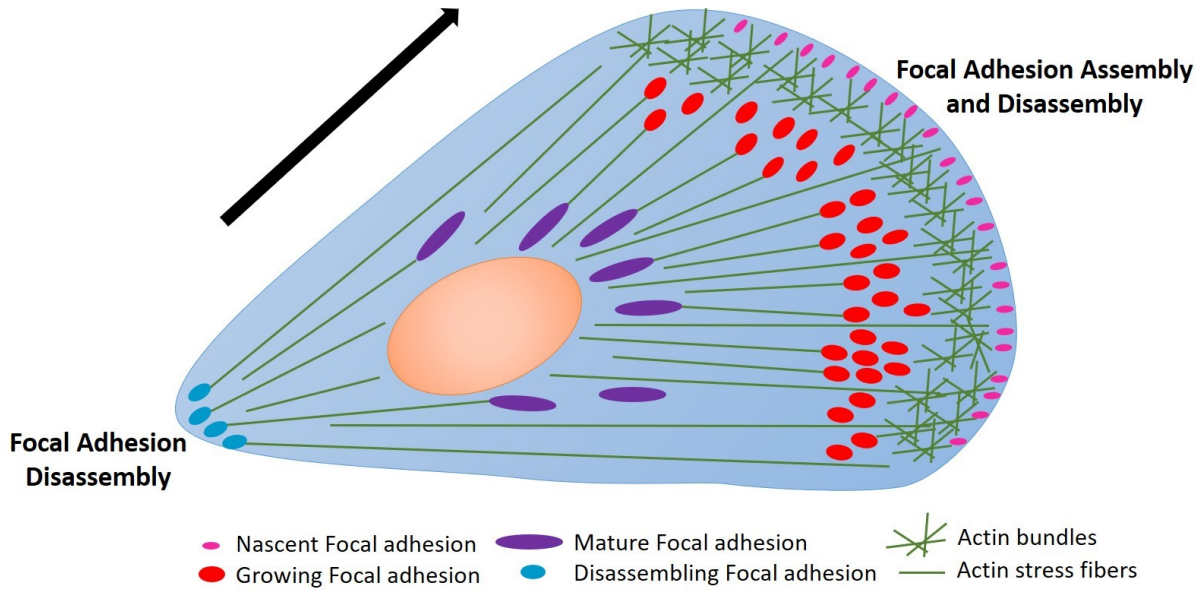

Figure 1.4.4 Focal adhesions turnover in a directed cell migration

In a migrating cell, focal adhesion turnover is necessary for the cell to make new attachments (focal adhesion assembly) on the cell-substratum at the front leading edge of the cell and release the adhesions (focal adhesion disassembly) at the rear end of the cell. The branched actin bundles that are formed to support the front leading edge are stabilized by the formations of nascent focal adhesions that are known to rapidly disassemble. Once a focal adhesion is linked to a stress fiber, it becomes stable and is termed a “growing focal adhesion”. Once grown and become named “mature focal adhesions”, their link with the actin stress fibers allows them to generate a force that will allow the cell to move forward. In contrast to the front leading edge of the cell, the rear end of the cell goes through a disassembly of the focal adhesions to detach the cell from the substratum and allow the release of the cell from substrate attachment.

1.4.2.1 Regulation

Focal adhesions are transient structures that can either form and develop into mature FAs or disassemble and disappear. The molecular nature of this transient mechanism involves different protein compositions and phosphorylation dynamics. RHO GTPases have been shown to play a major role in regulating adhesion dynamics, not only by controlling actin-mediated protrusions but also by inducing MYOSIN II-mediated contraction [173, 177, 370, 371]. RAC and CDC42 activation induce protrusions by activating WASP and WAVE complexes to induce actin polymerization by ARP2/3 complex [159, 372]. On the other hand, the maturation or formation of FAs is regulated by RHOA activation and it's kinase ROCK that activates MYOSIN II by inactivating MYOSIN II phosphatase, MYPT1 [302]. The actin stress fibers formed by MYOSIN II activation stabilize FAs by linking the stress fibers to the clustered integrins at the cell surface and by inducing actin bundling [373, 374]. In fact, the MYOSIN-mediated tension in the cell leads to a conformational change of proteins in the FAs [353, 374]. For example, recruitment of VINCULIN to TALIN is driven by changes in tension, where VINCULIN binding sites on TALIN are exposed upon tension generation [375]. In contrast to actin stress fibers, microtubule binding to FAs regulates their turnover by inducing the internalization and recycling of the integrins by an endocytosis protein named DYNAMIN which has been shown to be recruited to FAs by a kinase named Focal Adhesion Kinase (FAK) or Protein Kinase 2 (PTK2) [376, 377]. Many other proteins such as scaffolds/adaptors, kinases, phosphatases, GEFs and GAPs have been shown to play a role in the regulation of FA maturation and turnover and are summarized in **Table 1. IV.**

Table 1. IV Major players involved in the regulation of Focal Adhesion dynamics

Name of protein	Type of protein	Function	Role in FA: Maturation or Turnover
PIX proteins	RHO GEF	Binding partners of PAK, contain a DBL homology domain and is a GEF for RAC and CDC42 [378-381]	Turnover
p190RHOGEF	RHO GEF	Binds to FAK, becomes activated upon cellular interaction with ECM, activates RHOA and increases stress fiber formation [382]	Maturation
DOCK180	RHO GEF	Following integrin activation, forms a complex with CAS proteins and CRK to promote membrane ruffling and protrusion. It only activates RAC and not CDC42 or RHOA [257, 383]	Turnover
p190RHOGAP	RHO GAP	Used by RAC to inhibit RHOA and reduce tension at the front end of the cell to promote protrusion [384]	Turnover
ARHGAP22	RHO GAP	Activated by RHOA to inhibit RAC to stimulate mechanical tension [295]	Maturation
GIT	Scaffold/adaptor	The binding partner of PIX proteins and links PIX proteins to focal adhesion molecules by binding to PAXILLIN [378, 381, 385]	Turnover
BCAR1, NEDD9	Scaffold/adaptor	Binds to FAK and when phosphorylated recruits CRK and other adhesion-associated proteins [386, 387]	Turnover, Maturation
CRK	Scaffold/adaptor	SH2- and SH3-containing protein that interacts with CAS proteins to recruit additional adhesion proteins [369, 386, 388, 389]	Turnover, Maturation
PAXILLIN	Scaffold/adaptor	Adhesion molecule is known to be phosphorylated by SRC kinase to go through a conformational change and recruit other adhesion molecules [390-392]	Turnover, Maturation
PEAK1	Adaptor/pseudokinase	Scaffold molecule is known to be associated with the actin cytoskeleton and focal adhesions. Known to be phosphorylated by SRC to induce migration and FA turnover [393]	Turnover, Maturation
FAK	Kinase	Bind, phosphorylate and activate GEFs and GAPs. Its activation upon adhesion leads to the recruitment of SRC kinase to mediate phosphorylation of itself, PAXILLIN and CAS proteins [394-396]	Turnover, Maturation
ILK	Kinase	Forms a ternary complex with PINCH and PARVIN to link focal adhesions (integrins) to cytoskeleton [397]	Maturation
SRC, FYN, ABL	Kinase	Phosphorylates adhesion proteins such as FAK, PAXILLIN, VINCULIN, CAS to mediate the recruitment of other FA proteins [398-400]	Turnover
PTP-PEST	Phosphatase	Dephosphorylates FAK at Tyr397 upon activation by RAS-induced signal [401-403]	Turnover
SHP2, SHP1	Phosphatase	Dephosphorylates FAK at Tyr397 upon GAB2 binding on its N-terminus to release its intramolecular inhibition of the phosphatase activity [400, 401, 404-406]	Turnover
PTP-1B	Phosphatase	Dephosphorylates FAK at Tyr397, SRC at Tyr527 and α-ACTININ at Tyr12 [401, 407, 408]	Turnover

1.4.3 Conclusion

Overall, the cell movement mechanism is a complex process that comprises several steps where each plays a significant role in order for the cell to move forward. In cancer, cell migration and invasion are the rate-limiting steps of the metastatic cascade explained previously. To understand and investigate how they are regulated is of a great importance in order to prevent the process of cancer cell dissemination and subsequent metastasis. In a mesenchymal cancer cell, which is highly motile and invasive, many signaling pathways including kinases and phosphatases are known to induce this invasive phenotype. However, the exact mechanism of how the cell becomes polarized and what leads the FAs to mature or turnover holds great interest for investigation. In specific, how cell polarity and FA proteins are modulated and complex into structures to induce cell migration and invasion still remains elusive and will bring great knowledge in identifying key players of the process of cell invasion which can be used as a mean for targeted therapy in metastatic patients.

1.5 Research hypothesis and objectives

AXL has been identified clinically as a promoter of metastasis and its expression has been correlated with poor patient survival and drug resistance. However, the underlying mechanisms behinds its invasive role remain elusive. Since little is reported on AXL-specific signaling pathways in comparison to other oncogenic RTKs, we hypothesized that AXL engages AXL specific pro-invasive pathways to promote invasion and metastasis.

Objective 1 (CHAPTER 2):

Since upstream regulators of DOCK1, such as EGFR, PDGFR and HER2 were reported to play a role in DOCK1 phosphorylation, we were interested in defining upstream regulators of ELMO proteins, which may affect RAC activation downstream of DOCK1. Our objective for this chapter was to define upstream regulators of the ELMO/DOCK180/RAC pathway. We identified AXL-family of proteins as RTKs proficient to phosphorylate ELMO proteins and hypothesized that phosphorylation of ELMO by AXL may engage the ELMO/DOCK180/RAC pathway and is, therefore, a strong candidate signaling event to mediate AXL-dependent cell migration/invasion. This chapter defines a new mechanism by which AXL promotes cell proliferation and invasion and identifies inhibition of the ELMO-DOCK pathway as a potential therapeutic target to stop AXL-induced metastases.

Objective 2 (CHAPTER 3):

Our objective for this chapter was to further uncover GAS6/AXL specific and direct substrates and pathways. Using an unbiased quantitative proteomics screen in triple negative breast cancer cells, we were able to identify global signaling pathways engaged by GAS6-induced AXL activation which may define the mechanisms AXL acquires to attain a pro-invasive role. In this chapter, we defined focal adhesions, among others, to be the most significant modulated pathway upon AXL activation. Indeed, using biochemical, functional and proteomics approaches, we defined a mechanism where AXL hijacks the NEDD9/CRKII/PEAK1 complex to modulate focal adhesion turnover and ultimately metastasis. This study allowed us to identify PEAK1, as a novel therapeutic target downstream of AXL signaling that may modulate the AXL invasive role.

CHAPTER 2

AXL phosphorylates ELMO scaffold proteins to promote RAC activation and cell invasion

Contributions

Figure 2.1 (A): Afnan Abu-Thuraia

Figure 2.1 (B-C): Rosemarie Gauthier

Figure 2.2 (A): Afnan Abu-Thuraia

Figure 2.2 (B): Rosemarie Gauthier

Figure 2.3 (A, C-E): Afnan Abu-Thuraia

Figure 2.3 (B): Rosemarie Gauthier

Figure 2.4 (A-C): Afnan Abu-Thuraia

Figure 2.5 (A-C): Afnan Abu-Thuraia

Figure 2.5 (D-E): Afnan Abu-Thuraia, Rony Chidiac

Figure 2. S1 (A-C): Rosemarie Gauthier

Figure 2. S1 (D): Afnan Abu-Thuraia

Figure 2. S2 (A-B): Afnan Abu-Thuraia

Figure 2. S3: Afnan Abu-Thuraia

Figure 2. S4 (A-B): Rosemarie Gauthier

Figure 2. S4 (C): Afnan Abu-Thuraia

Figure 2. S5 (A-C): Afnan Abu-Thuraia

Figure 2. S6 (A-B): Afnan Abu-Thuraia

*Jean-Francois Côté designed the research

*Afnan Abu-Thuraia, Rosemarie Gauthier, Rony Chidiac, Robert A. Screaton and Jean-Francois Côté performed the research

*Afnan Abu-Thuraia, Rosemarie Gauthier, Rony Chidiac, Yoshinori Fukui, Robert A. Screaton, Jean-Philippe Gratton, and Jean-Francois Côté analyzed the data

*Jean-Francois Côté wrote the manuscript with the contribution of all authors

AXL phosphorylates ELMO scaffold proteins to promote RAC activation and cell invasion

Afnan Abu-Thuraia[1,2], Rosemarie Gauthier[1], Rony Chidiac[3], Yoshinori Fukui[4], Robert A. Screaton[5], Jean-Philippe Gratton[6,] and Jean-François Côté[1-2,7-8 #]

[1]Institut de Recherches Cliniques de Montréal (IRCM), Montréal, QC, Canada.

[2]Département de Médecine (Programmes de Biologie Moléculaire), Université de Montréal, Montréal, QC, Canada.

[3]Département de Pathologie Biologie Cellulaire, Université de Montréal, Montréal, QC, Canada.

[4]Division of Immunogenetics, Department of Immunobiology and Neuroscience, Medical Institute of Bioregulation, Kyushu University, Fukuoka, Japan.

[5]Children's Hospital of Eastern Ontario Research Institute, Ottawa, ON, Canada.

[6]Département de Pharmacologie, Université de Montréal, Montréal, QC, Canada.

[7]Département de Biochimie, Université de Montréal, Montréal, QC, Canada.

[8]Department of Anatomy and Cell Biology, McGill University, Montréal, QC, Canada.

Running Title: Axl promotes invasion by phosphorylation of Elmo

Address correspondence to Jean-François Côté, jean-francois.cote@ircm.qc.ca

**Manuscript published in MCB (2015)

Abstract

The receptor tyrosine kinase Axl contributes to cell migration and invasion. Expression of Axl correlates with metastatic progression in cancer patients yet the specific signaling events promoting invasion downstream of Axl are poorly defined. Herein, we report Elmo scaffolds as direct substrates and binding partners of Axl. Elmo proteins are established to interact with Dock-family guanine nucleotide exchange factors to control Rac-mediated cytoskeletal dynamics. Proteomics and mutagenesis studies reveal that Axl phosphorylates Elmo1/2 on a conserved carboxyl-terminal tyrosine residue. Upon Gas6-dependent activation of Axl, endogenous Elmo2 becomes phosphorylated on Tyr-713 and enters in physical complex with Axl in breast cancer cells. Interfering with Elmo2 expression prevented Gas6-induced Rac1 activation in breast cancer cells. Similarly to blocking Axl, Elmo2 knockdown or pharmacological inhibition of Dock1 abolishes breast cancer cell invasion. Interestingly, Axl or Elmo2 knockdown diminishes breast cancer cell proliferation. Rescue of Elmo2 knockdown cells with the wild-type protein, but not with Elmo2 harboring Tyr-713-Phe mutations, restores cell invasion and cell proliferation. These results define a new mechanism by which Axl promotes cell proliferation and invasion, and identifies inhibition of the Elmo-Dock pathway as a potential therapeutic target to stop Axl-induced metastases.

Keywords: Axl/ Elmo / Rac / cell migration / phosphorylation / cell proliferation

Introduction

Tyro3, Axl and Mer (TAMs) belong to a family of receptor tyrosine kinases (RTKs) characterized by an extracellular part formed by two Immunoglobulin-like domains and two Fibronectin Type III domains followed by a transmembrane region and an intracellular tyrosine kinase module [23, 409]. Like the majority of RTKs, TAMs are activated by ligands which include the vitamin K-dependent coagulation factor-like Growth Arrest Specific 6 (Gas6) and Protein S in addition to unconventionally secreted Tubby/Tubby-like proteins [31, 410-412]. While these ligands activate TAMs in a canonical manner when presented in free forms, they also bridge phosphatidylserine (PS) exposed on the outer surface of apoptotic cells such that TAMs on phagocytes promote prompt clearance of dying cells [413-416]. TAMs are also activated in a ligand-independent manner either by overexpression or transphosphorylation by other RTKs [54, 417, 418]. A number of signaling pathways are activated following engagement of TAMs including Phosphatidylinositol (PI) 3-kinase/Akt, Ras/Mapk, Stat3 and Rac [419]. Together, these pathways are thought to integrate Axl-induced proliferation, survival, cytoskeletal remodeling and cell migration responses depending on the biological context [419]. Moreover, the normal biological functions of TAMs are complex. Individual inactivation of TAMs in mice does not impair development and a panel of mild defects is observed in adult animals [120, 123, 420]. The most striking defect among them is blindness in Mer mutant animals arising from abnormal clearance of photoreceptor outer segments by retinal pigment epithelial cells [421]. Studies of triple mutant animals lacking TAMs also revealed their role in limiting macrophage response and this has important consequences such as the development of autoimmune diseases [123, 420].

Among TAMs, Axl is highly expressed in various invasive cancers [422]. High expression of Axl in breast tumors associates with metastasis and poor patients' outcome [86]. Notably, expression levels of Axl correlate with an invasion potential of breast cancer cell lines [86], where silencing its expression, or blocking its activity through a pharmacological inhibitor or blocking antibodies, impairs breast cancer cell invasion [86, 118, 423, 424]. In addition, *in vivo* experiments suggest that downregulation of Axl in human breast cancer cells drastically

blocks metastasis without considerably affecting tumor growth [86, 119]. Within basal/triple-negative human breast cancer cell lines, Axl signaling promotes the expression of an epithelial to mesenchymal gene signature including the upregulation of Slug, Snail and Vimentin and the downregulation of E-cadherin that are important for ensuring a stem cell and invasive phenotype [86, 90]. Notably, the signaling pathways engaged by Axl to promote such aggressive migration and invasive behaviors remain to be fully defined as it may uncover new targets for anti-metastatic treatments.

Evolutionarily conserved Dock-family guanine nucleotide exchange factors (GEFs) activate Rac or Cdc42 GTPases through a unique Dock Homology Region 2 domain to promote cytoskeletal rearrangements [278, 425, 426]. Elmo1-3 are auto-regulated scaffold proteins that interact with Dock1-5 to spatiotemporally organize Rac signaling [275, 276, 282, 298]. *In vivo*, in mice, Dock1 and Elmo1 promote migration, engulfment of apoptotic cells and myoblast fusion during development and adult life (reviewed in [222]). High expression of Dock1 in breast cancer tumors correlates with a poor probability of survival for HER2+ or Basal-like breast cancer patients [288]. Deletion of Dock1 in mouse mammary gland protects mice from developing lung metastasis in a model of HER2 breast cancer [288]. In addition, activation of Dock1 by the PDGF Receptor or the EGFRvIII Receptor promotes cancer cells dissemination in distinct subclasses of gliomas and correlate with poor patient survival [285, 286, 427]. Likewise, interfering with Dock1 or Elmo expression in human breast cancer cell lines impairs invasion [290, 291]. These results point to Dock1 and Elmo as potentially important proteins to promote Rac1-dependent cell migration and invasion during metastasis.

Here, we present evidence that Axl orchestrates breast cancer cell invasion by phosphorylating Elmo proteins. Our results demonstrate that Elmo2 is required for Axl-induced Rac activation. We identify Tyr 713 on Elmo2, homologous to Tyr 720 in Elmo1, as the phosphorylation site by Axl kinase and their mutation abolishes cell invasion and proliferation. Collectively, our efforts uncover a long sought after a signaling pathway operating downstream of Axl to promote cell invasion and proliferation.

Results

A kinase screen uncovers Elmo proteins as direct substrates of Tyro3, Axl and Mer receptor tyrosine kinases (TAMs).

Dock1 is activated by phosphorylation to promote cell migration and invasion [285, 286, 288, 427]. Previously, we reported that mRNA expression levels of Dock1 correlate with poor patient outcome in HER+ and basal/triple-negative breast cancer subtypes [288]. Because Elmo proteins are bound to Dock1 and regulate Rac signaling [274], we aimed to identify novel regulators of the Elmo/Dock1 complex by carrying out a screen designed to uncover kinases that could phosphorylate Elmo1. To this end, a panel of 180 GST-tagged human kinases, composed of representative members of each kinase subfamilies, was expressed in HEK293T cells as previously reported [428] (see **Table 2. SI** for a full list of kinases). Following cell lysis, each GST-kinase was recovered in a glutathione-coated well as depicted in **Figure 2.1A**. To carry out *in vitro* kinase (IVK) assays, immobilized kinases were mixed with recombinant purified Elmo1, Myelin Basic Protein (MBP) and [γ-^{32}P] ATP (**Figure 2.1A**). Seven putative candidate kinases that phosphorylate Elmo1 were identified including five Ser/Thr kinases (Pftaire1, Camkk2, Dclk1, Prpf4b, and Ttbk2) and two tyrosine kinases (Blk and Tyro3) (see **Table 2. SII).** A secondary screen on selected candidates revealed that GST-tagged Camkk2 and Pftaire1 cannot phosphorylate Elmo1; instead, they co-migrated with recombinant Elmo1 and their auto-phosphorylation led us to conclude that they were false positives (not shown). Although we have not re-tested Blk's ability to phosphorylate Elmo1, another Src family kinase, Hck, has been reported to do that efficiently [284]. Instead, we chose to further study Elmo1 phosphorylation by the RTKs of the TAM family (including Tyro3, Axl and Mer) due to their involvement in biological processes similarly controlled by Elmo/Dock1 including cell migration, cell invasion, and phagocytosis of apoptotic cells [23, 429].

Since Axl and Mer were not part of the initial screen, we extended our analyses to test if, as seen for Tyro3, they could phosphorylate Elmo proteins indicating this as a conserved feature of TAMs. We conducted IVK assays using purified recombinant kinase domains of

Tyro3, Axl and Mer to test their ability to directly phosphorylate Elmo1-3 proteins. We found that all three TAMs preferentially phosphorylate Elmo1 and Elmo2, yet phosphorylation of Elmo2 seems to be less than that of Elmo1 (**Figure 2.1B**). We also found that full-length TAMs, but not kinase-dead mutants, also phosphorylate recombinant Elmo1 *in vitro* (**Figure 2. S1A**). To confirm these results in cells, we co-expressed TAMs with Myc-Elmo1 and examined the phosphorylation status of immunoprecipitated Myc-Elmo1 using an anti-phosphotyrosine antibody. In a cellular context, we similarly found that TAMs, but not their kinase-dead mutants, promote tyrosine phosphorylation of Myc-Elmo1 (**Figure 2.1C** and **Figure 2. S1B-C**). Collectively, these results establish Elmo1 and Elmo2 as previously unidentified direct substrates of TAMs and raise the question as to whether TAMs could exploit the Elmo/Dock1 complex to promote migration and invasion.

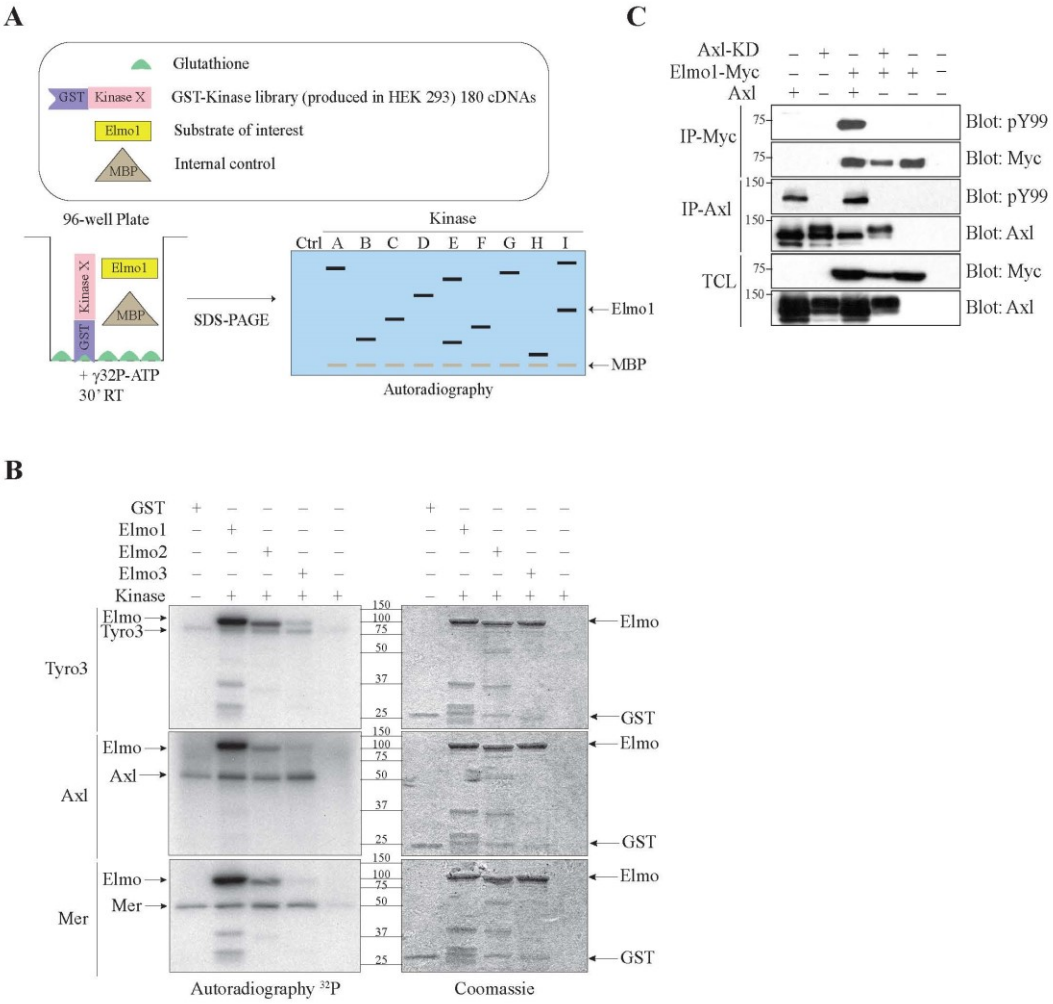

Figure 2.1 The TAM receptors phosphorylate Elmo proteins

(A) Schematic overview of the kinase screen. Elmo1 is the substrate of interest and MBP1 is used as a positive control. (B) Elmo is phosphorylated *in vitro* by the TAMs. An *in vitro* kinase assay was performed where 2µg of GST-Elmo proteins were incubated with 0.05µg of the kinase domains of Tyro3, Axl and Mer and γ_{32}-ATP. The expression of the proteins was analyzed by Coomassie staining and the phosphorylation by autoradiography. (C) Elmo1 phosphorylation in cells is dependent on Axl catalytic activity. Lysates of HEK293T cells transfected with the indicated plasmids were immunoprecipitated with an antibody against the Myc-epitope (Elmo1) and with an antibody against Axl. The phosphorylation and expression levels of Elmo1 and Axl were analyzed via immunoblotting with anti-Myc (Elmo1) and anti-Axl antibodies, respectively.

TAMs phosphorylate two tyrosine residues on Elmo1/2

To gain mechanistic insights on the effect of tyrosine phosphorylation of Elmo proteins, a proteomics approach was used to map the tyrosine residues of Elmo1 targeted by TAMs. First, *in vitro* phosphorylated Elmo1 was obtained by mixing bacterially produced and purified Elmo1 with Tyro3 immunoprecipitated from HEK293T lysates and cold ATP (as done in **Figure 2. S1A**). Second, a cellular phosphorylated Myc-Elmo1 was generated by co-expression with Tyro3 and immunoprecipitation with an anti-Myc antibody (as done in **Figure 2. S1B**). Both phosphorylated Elmo1 samples were subjected to proteomics analysis and 9 phosphorylated tyrosine sites were identified (18, 48, 216, 352, 395, 511, 576, 588, 720) (**Figure2.2A**). We also included in our analysis Tyr 724 of Elmo1 as a residue potentially phosphorylated by TAMs as we could not rule it out from the mass spectrometry spectrum that identified Tyr 720. We generated single Tyr to Phe mutants of Elmo1 for each site identified by proteomics and narrowed our focus on Tyr 720 as the major site targeted by Axl by performing IVK assays (**Figure 2.2B**). The residual phosphorylation on Elmo1 Tyr 720 mutant was attributable to Tyr 724 as the double mutant 720/724 failed to become phosphorylated upon incubation with Axl (**Figure 2.2B**). In contrast, mutation of Tyr 352 did not affect the residual phosphorylation signal observed for the Tyr 720 mutant (**Figure 2.2B**). Tyr 720 is highly conserved between Elmo1 and Elmo2 but not Elmo3 proteins (**Figure 2. S1D**), explaining the differential phosphorylation of Elmo family proteins by TAMs observed in **Figure 2.1B**. Together, these results demonstrate that TAMs specifically phosphorylate Elmo1 on Tyr 720/724.

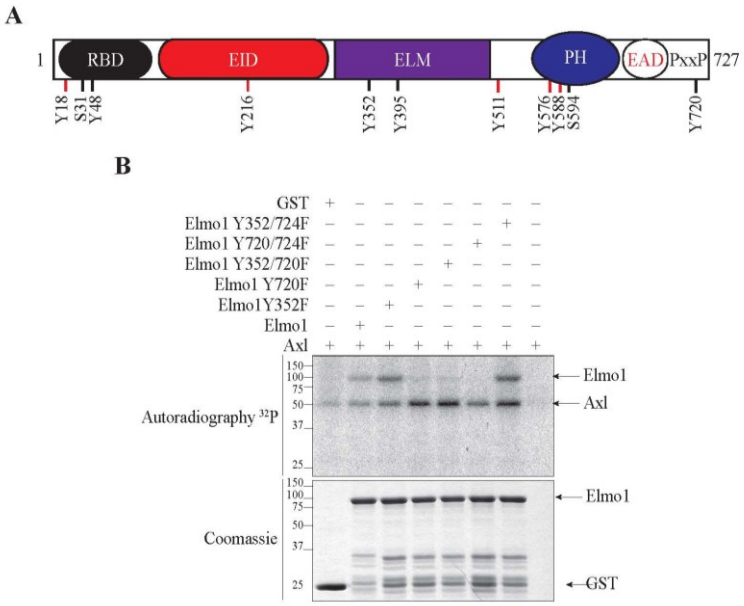

Figure 2.2 Elmo1 is phosphorylated on Tyrosine 720 and 724 by TAM receptors

(A) Elmo1 phosphorylation sites identified by mass spectrometry by the Tyro3 kinase. Lysates of HEK293T cells were transfected with c-Myc Elmo1 and were either subjected to an *in vitro* kinase assay with GST-Tyro3 or co-transfected with GST-Tyro3 and subjected to immunoprecipitation of c-Myc Elmo1. Phosphorylated sites on Elmo1 by Tyro3 were identified by mass spectrometry. Sites depicted in red were identified by both experiments whereas the sites depicted in black were only identified in the c-Myc Elmo1 immunoprecipitation. RBD: Ras-binding domain, EID: Elmo Inhibitory Domain, ELM: Elmo domain, PH: atypical Pleckstrin Homology domain, EAD: Elmo Autoregulatory Domain, PxxP: proline-rich region. (B) Elmo1 is phosphorylated on Tyrosine 720 and 724. An *in vitro* kinase assay was performed where 3µg of GST-Elmo1 protein or Y-F mutants were incubated with 0.025µg of the Axl kinase domain and γ_{32}-ATP. The expression of the proteins was analyzed by Coomassie staining and the phosphorylation by autoradiography

Axl interacts with and phosphorylates Elmo proteins

We investigated whether Elmo recognition by Axl could involve the formation of a physical RTK-substrate complex. In cells co-expressing Axl and Myc-Elmo1, we found that Myc-Elmo1 specifically co-immunoprecipitated with Axl (**Figure 2.3A**). However, the binding of Myc-Elmo1 to Axl was lost when kinase-dead Axl was immunoprecipitated. We raised a phospho-specific antibody against Tyr 720 of Elmo1 (Tyr 713 in Elmo2) to monitor the phosphorylation of this site in cells (see **Figure 2. S2** for antibody characterization). As shown in **Figure 2.3A**, co-expression of Axl with Myc-Elmo1 promoted the phosphorylation of Tyr 720 and this increase was not observable with kinase-dead Axl. To further validate the interaction between Elmo and Axl, we performed *in vitro* binding assays using GST Elmo1 fusion proteins and found that full-length Elmo1 and the N-terminus of Elmo1 (aa 1-495), but not the C-terminus of Elmo1 (aa 532-727), were able to bind to Axl (**Figure 2.3B**). We also tested if Elmo2 was a binding partner of Axl and found that it co-immunoprecipitated with Axl, but not the kinase-dead mutant, when the two proteins were co-expressed in HEK293T cells (**Figure 2.3C**). In addition, by monitoring Elmo2 phosphorylation on Tyr 713 (Tyr 720 in Elmo1; see **Figure 2. S1D**) with our phospho-specific antibody, we similarly found that Axl, but not the kinase-dead mutant, promoted phosphorylation of this site (**Figure 2.3C**). We next used a pharmacological inhibitor against Axl R428 [423] to investigate whether inhibiting the kinase activity would be sufficient to abrogate Elmo2 phosphorylation and binding to Axl. Treatment of HEK293T cells expressing Axl and Myc-Elmo2 with R428 prevented Elmo2 phosphorylation on Tyr 713, but surprisingly, did not inhibit the interaction of Axl to Elmo2 (**Figure 2.3D**).

In an effort to understand if adaptor proteins could facilitate Elmo2 coupling to Axl, we mutated Tyr in Axl (779, 821 and 866), known to be involved in binding the SH2 adaptor proteins Grb2 and PI 3-kinase [47, 430], to Phe and found that this did not abrogate Axl-Elmo2 association (**Figure 2. S3**). From these results, it is still unclear how Elmo2 is recruited to Axl receptor and remains to be investigated.

Moreover, we found that Elmo2 is the only Elmo family member expressed in MDA-MB-231 and Hs578T basal breast cancer cell lines ([277]; **Figure 2. S4A**). We also observed that Hs578T cells only expressed Axl whereas MDA-MB-231 expressed both Axl and Mer (**Figure 2. S4B**). Tyro3 was not expressed in either cell lines. Using these basal breast cancer cell line models, we next investigated if endogenous Axl can phosphorylate and bind Elmo2. To this end, we treated serum starved MDA-MB-231 cells with recombinant Gas6 to activate Axl. As expected, immunoprecipitation of Axl revealed that it becomes globally phosphorylated on Tyr residues following 5 and 30 min treatments with Gas6 suggesting that the RTK is activated (**Figure 2.3E**). An increase in Akt phosphorylation, a known target of Axl, confirmed the activation of downstream signaling following Gas6 treatments (**Figure 2.3E** and **Figure 2. S4C**). We also found that endogenous Elmo2 in MDA-MB-231 and Hs578T cells co-precipitated minimally with Axl at basal state and this interaction is enhanced transiently at 5 min after Gas6 treatment (**Figure 2.3E**). Blotting of total cell lysates with Elmo2 pTyr 713 phospho-specific antibody revealed an increase in Elmo2 phosphorylation at this site after 5 and 30 min of Gas6 treatments (**Figure 2.3E**). We found that Axl is the major kinase promoting Gas6 signaling since siRNA-mediated knockdown of Axl completely prevented Akt phosphorylation after stimulation with Gas6 (**Figure 2. S4C**). Identical results were observed in MDA-MB-231 cells. Collectively, these data demonstrate that Axl phosphorylates and interacts with Elmo2 in invasive breast cancer cells.

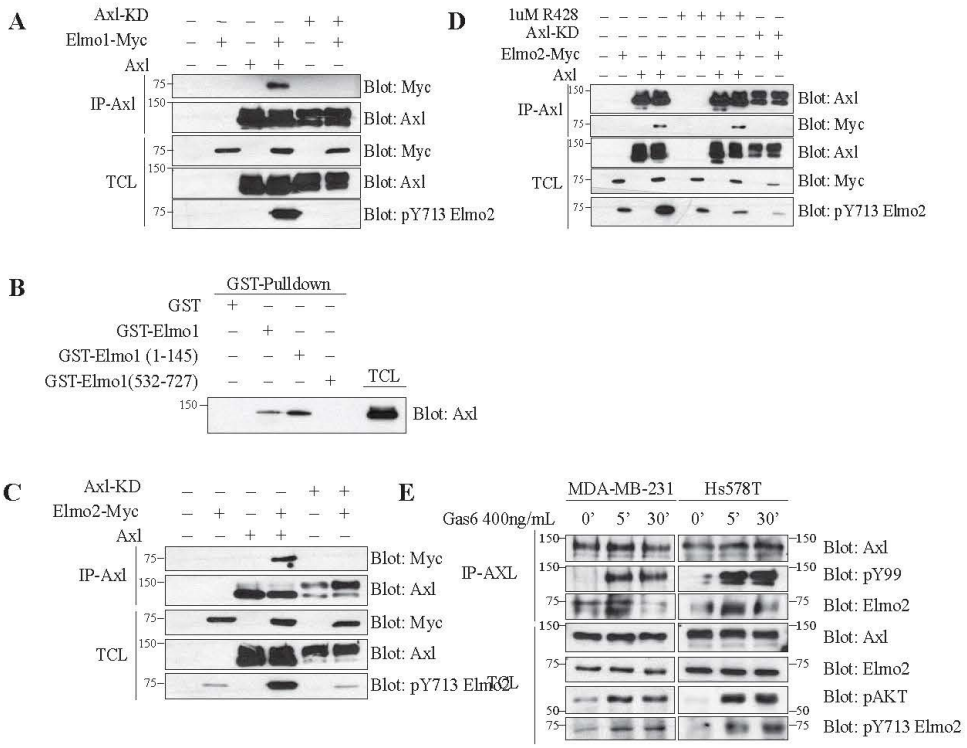

Figure 2.3 Elmo Modulation by Axl is dependent on Axl's catalytic activity

(A, C) Axl wild-type and not kinase-dead interacts with and phosphorylates Elmo1 (A) and Elmo2 (C). Lysates of HEK293T cells transfected with the indicated plasmids were co-immunoprecipitated with an antibody against Axl. The co-precipitation and expression levels of the Axl proteins and Elmo1 (A) or Elmo2 (C) were analyzed via immunoblotting with anti-Myc (Elmo) and anti-Axl antibodies. (B) The interaction between Elmo1 and Axl is mediated by the N-terminus of Elmo1. Lysates from transfected HEK293T cells with Axl were incubated with 3 µg of GST-Elmo1 full-length protein or fragments. The binding of Axl to Elmo1 fragments and the expression levels were analyzed via immunoblotting with the anti-Axl antibody. (D) Inhibition of Axl activity with R428 abolishes Elmo2 phosphorylation by Axl. Transfected HEK293T cells with the indicated plasmids were serum starved prior to treatment with either DMSO or 1µM of the Axl inhibitor R428 for 1h. Lysates were co-immunoprecipitated with an antibody against Axl. The co-precipitation and expression levels of the Axl proteins and Elmo2 was analyzed via immunoblotting with anti-Myc (Elmo2) and anti-Axl antibodies, respectively. Protein expression and Elmo2 phosphorylation were analyzed by immunoblotting with anti-Myc, anti-Axl, and anti-pY713 Elmo2. (E) Axl interacts with and phosphorylates endogenous Elmo2 in basal breast cancer cell lines. MDA-MB-231 and Hs578T cells were treated with 400ng/mL of Gas6, for the indicated time points, they were subjected to co-immunoprecipitation of Axl using anti-Axl antibody. The precipitation of Elmo2 by Axl was detected by immunoblotting with the anti-Elmo2 antibody. The protein expression levels were also analyzed via immunoblotting with anti-pAKT, anti-pY99, anti-Elmo2, anti-Axl, and anti-pY713 Elmo2 antibodies.

Elmo2 is required for Axl-induced Rac activation

Axl promotes neuron migration by activating Rac [431]. We investigated if Elmo2 functions as a scaffold protein to connect Axl to the Rac GEF Dock1 in breast cancer cells. Immunoprecipitation of Flag-Dock1 revealed the formation of a multi-protein complex with Axl (**Figure 2. S5A**). Surprisingly, and in addition to Elmo, Dock1 also appears to make its own contacts with Axl as this interaction was neither enhanced nor reduced by the expression of wild-type Myc-Elmo1 or a mutant Myc-Elmo1 (αN/PXXP) that is not able to bind Dock1 (**Figure 2. S5C**). Interestingly, Dock1 might contribute to guiding Elmo for phosphorylation by Axl since the phosphorylation of the Elmo1 mutant (αN/PXXP), which is not interacting with Dock1, is decreased (**Figure 2. S5C**). We also found that mutating Tyr 713 to Phe in Elmo2 did not impact the formation of an Elmo2/Dock1 complex (**Figure 2. S5A**). This was also observed when Elmo1 was co-expressed, where wild-type and the mutant of Elmo1 on Tyr 720 or Tyr 720/724 bound similarly to Axl and Dock1 (**Figure 2. S5B**). Because Rac is a key molecule in promoting cell migration, we, therefore, investigated the possibility that Axl might employ the Elmo-Dock1 complex to promote Rac activation in invasive breast cancer cells. To test this, serum starved Hs578T cells were stimulated with Gas6 and Rac GTP-loading was monitored by affinity precipitation with a GST PAK-PBD fusion protein. Treatment of Hs578T cells with Gas6 induced Rac activation that peaked at 10 min (**Figure 2.4A**). To confirm that Gas6 mediates Rac activation in these conditions through Axl, we found that treatment of Hs578T cells with R428 prevented Rac activation (**Figure 2.4B**). In addition, interfering with Elmo2 expression by siRNA or with Dock1 GEF activity with the small molecule inhibitor CPYPP [432], prevented Gas6-induced Rac activation (**Figure 2.4A-C**). It is noteworthy that depletion of Elmo2 by siRNA in MDA-MB-231 led to a partial decrease in expression of Dock1, and the closely related member Dock5 and this could explain at least in part the decrease in Rac activation observed following Gas6 treatment in Elmo2 depleted cells (**Figure 2. S6A**). We reproducibly found that downregulation of Elmo2 and inhibition of Dock1 GEF activity impaired maximal activation of Akt following Gas6 treatment (**Figure 2.4A-C**), suggesting that Elmo2-Dock1-RacGTP might be involved in stimulating a PI 3-kinase.

Axl promotes the expression of epithelial to mesenchymal transition (EMT) markers in invasive breast cancer cells [86]. Rac signaling is also found to contribute to the maintenance of

the mesenchymal and stem cell phenotype of cancer cells [296, 433]. Therefore, we investigated the possibility of Elmo and Dock1 (or Dock5) playing a role downstream of Axl in promoting a mesenchymal phenotype in MDA-MB-231 cells via Rac activation either by suppressing the expression of E-Cadherin or inducing the expression of mesenchymal markers. To test this, we inhibited Axl and Dock GEF activity using R428 and CPYPP, respectively (**Figure 2. S6B**). In addition, we blocked the expression of Axl, Elmo2, Dock1 and Dock5 using a siRNA approach (**Figure 2. S6A**). The expression of the epithelial marker E-Cadherin was rescued neither by blocking the expression of Axl, Dock1, Dock5, and Elmo2 nor by inhibiting their activity (**Figure 2. S6A-B**). Interestingly, the expression of the mesenchymal marker Vimentin was significantly reduced by the knockdown of Axl, Elmo2, and Dock1 expression, and by inhibiting Dock GEF activity in MDA-MB-231 cells (**Figure 2. S6A-B**). However, knockdown of Dock5 and R428 treatment were not able to reduce Vimentin expression levels (**Figure 2. S6A-B**). Collectively, these results uncover the Elmo2-Dock1 complex as a key signaling module for Rac activation and in promoting the expression of mesenchymal markers downstream of Axl in invasive breast cancer cells.

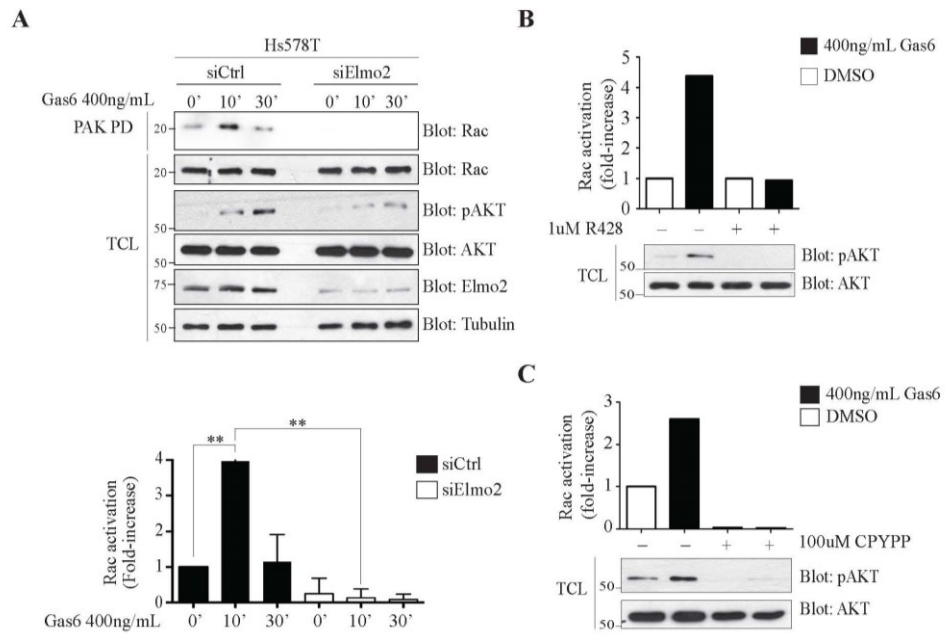

Figure 2.4 Rac activation in Hs578T cells is Axl- and Elmo2-dependent

(A) Elmo2 is required for Rac activation upon Gas6 stimulation. Hs578T cells transfected with 60nM NON-targeting or ON-target smart pool Elmo2 siRNA prior to being treated with 400ng/mL of Gas6 for the indicated time points were assayed for Rac activation by precipitation of Rac with the purified p21-Binding domain of PAK protein kinase expressed as a GST fusion protein (GST-PAK-PBD) (n=6). The amount of Rac in pulldowns and in total cell lysates (TCL) was detected by immunoblotting with an anti-Rac antibody. Expression levels of the various proteins and equal loading of Rac in all samples were analyzed by immunoblotting of the TCL using anti-Rac, anti-Tubulin, anti-Elmo2, anti-pAKT, and anti-AKT. (B-C) Axl and Dock1 inhibition reduce Rac activation upon Gas6 stimulation. Hs578T cells were treated with 1μM R428 (B) or with 100μM CPYPP (C) for 1hr followed by 400ng/mL Gas6 for 20min. Rac activation was assayed by precipitation with the purified p21-Binding domain of PAK protein kinase expressed as a GST fusion protein (GST-PAK-PBD) (n=5). The amount of Rac in pulldowns and in total cell lysates (TCL) was quantified by the software Image J. Expression levels of the various proteins were analyzed by immunoblotting of the TCL using anti-pAKT and anti-AKT. Data are shown as mean ± SD; **p < 0.0001; one-way ANOVA

Phosphorylation of Elmo2 on Tyr 713 is required for cell invasion and cell proliferation

We aimed to define if phosphorylation of Elmo2 by Axl is a required signaling event to promote cell invasion. We first confirmed previous observations suggesting that MDA-MB-231 and Hs578T cells invade through Matrigel in an Axl-dependent manner [86, 423, 434]. We treated MDA-MB-231 cells with R428 or siRNA against Axl and found that both treatments blocked cell invasion (**Figure 2.5A-B**). We next assayed the role of Elmo2 in breast cancer cell invasion by a siRNA approach. Knockdown of Elmo2 robustly inhibited migration of MDA-MB-231 cells across a Matrigel barrier (**Figure 2.5C**). In an effort to determine if phosphorylation of Elmo is important for cell invasion, we performed rescue experiments in Elmo2 knockdown cells with a construct encoding for either Myc-Elmo1 wild-type or a Myc-Elmo1 Y720F mutant. We re-expressed Elmo1 since the exogenous Myc-Elmo2 was difficult to express in siRNA Elmo2 treated cells (the human Elmo2 SmartPool siRNA also targets the murine mRNA). We also previously reported that Elmo1 and Elmo2 biological functions in myoblast fusion are interchangeable [435]. We observed that expression of Myc-Elmo1 in Elmo2 knockdown cells completely restored the invasion to an extent comparable to cells expressing a control siRNA (**Figure 2.5C**). In contrast, re-expression of Myc-Elmo1 Y720F in Elmo2 knockdown cells failed to re-establish cell invasion despite its identical expression to the wild-type protein (**Figure 2.5C**).

We next aimed to define if Elmo, i.e. Rac signaling, downstream of Axl contributes to the proliferation of these cells. We assayed proliferation by BrdU staining and found that knockdown of Axl or Elmo2 robustly inhibited the proliferation of MDA-MB-231 cells (**Figure 2.5D**). To determine if Elmo phosphorylation is important for proliferation, we performed rescue experiments as mentioned above. We observed that expression of Myc-Elmo1 in Elmo2 knockdown cells partially restored the proliferation of these cells (**Figure 2.5E**). In contrast, expression of Myc-Elmo1 Y720F in Elmo2 knockdown cells failed to re-establish cell proliferation despite its identical expression to the wild-type protein (**Figure 2.5E**). Globally, our findings demonstrate a central role for Axl-mediated phosphorylation of Elmo2 in promoting proliferation and invasion of basal breast cancer cells.

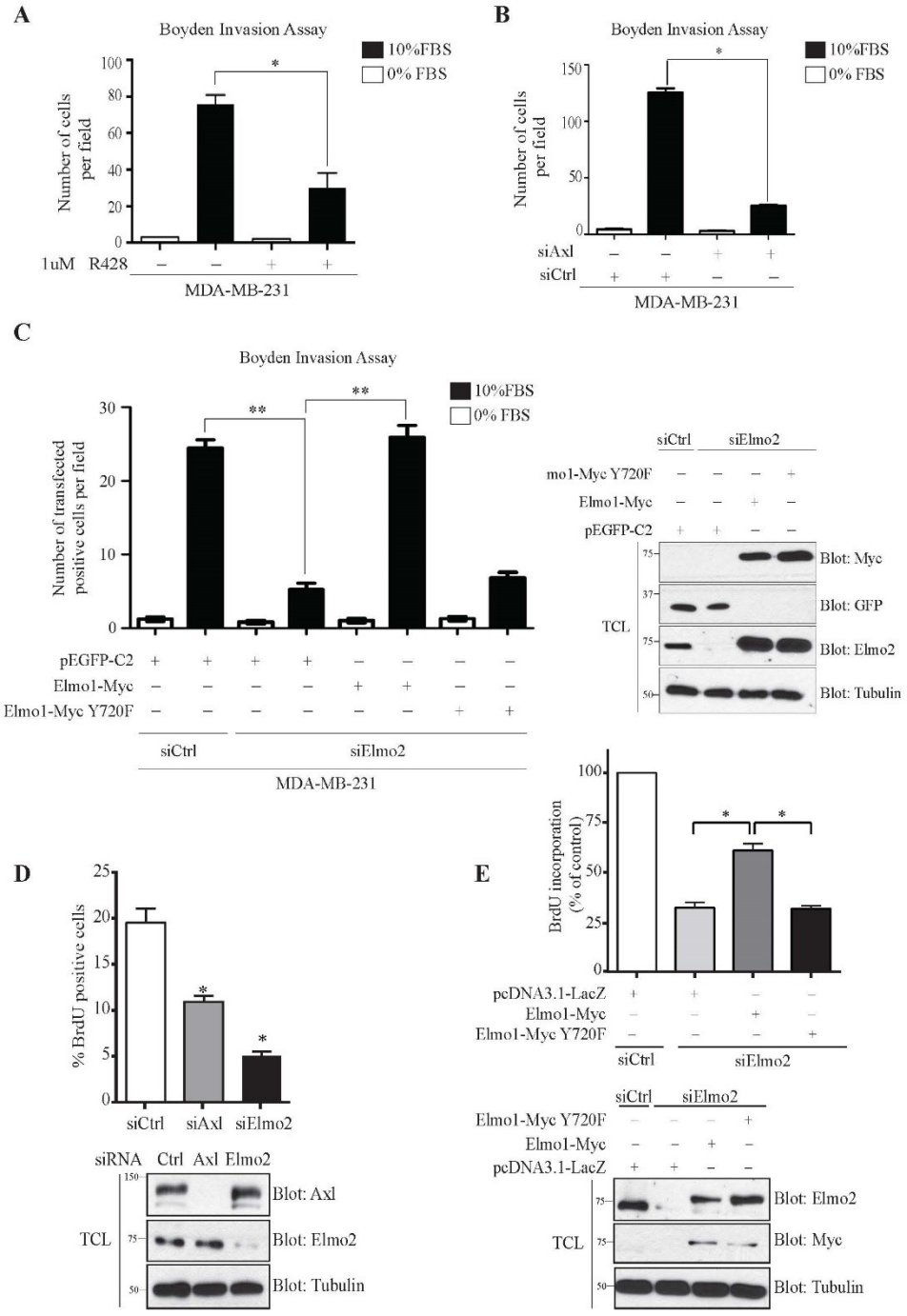

Figure 2.5 Cell invasion and proliferation of MDA-MB-231 cells is Elmo2 and Axl dependent

(A-B) Axl activity or expression inhibition reduces cell invasion. Serum-starved MDA-MB-231 cells treated with 1μM R428 (A) or transfected with 100nM NON-targeting or ON-target smart pool Axl siRNA (B) were detached and placed in the upper compartment of a Boyden chamber. Cells were allowed to invade through the Matrigel for 16hrs. The invasion assay was performed in triplicate, and data are shown as mean ± SEM; *p < 0.001; one-way ANOVA. (C) Elmo1 phosphorylation site

Tyr 720 is required for cell invasion in MDA-MB-231 cells. Serum-starved MDA-MB-231 cells transfected with 60nM NON-targeting or ON-target smart pool Elmo2 siRNA and rescued 24hrs later with either 1µg GFP or 1µg Elmo1 WT or 2 µg Elmo1 Y720F mutant, were detached and placed in the upper compartment of a Boyden chamber. Cells were allowed to invade through the Matrigel for 16hrs and then were fixed and stained with anti-Myc and anti-GFP. GFP and Myc positive cells that invaded the Matrigel to the underside of the membrane were counted from photographs taken at 20x magnification. The invasion assay was performed in triplicate, and data are shown as mean ± SD; **$p < 0.0001$; one-way ANOVA. Expression levels of the transfected proteins for invasion assays were analyzed by immunoblotting cell lysates with anti-Elmo2, anti-Myc, anti-GFP, and anti-Tubulin antibodies, as indicated. (D-E) Axl and Elmo1 phosphorylation site Tyr 720 is required for cell proliferation in MDA-MB-231 cells. Cells transfected with 100nM NON-targeting, 100nM ON-target smart pool Axl siRNA or 60nM ON-target smart pool Elmo2 siRNA were detached 24hrs later and plated on fibronectin-coated glass slips. Transfected MDA-MB-231 cells with 60nM NON-targeting or ON-target smart pool Elmo2 siRNA were rescued 24hrs later with either 1µg pcDNA3.1-LacZ or 1µg Elmo1 WT or 2 µg Elmo1 Y720F mutant prior to being plated on fibronectin-coated glass slips (E). Cells were allowed to grow for 24hrs and then were stained with BrdU for 30min. The BrdU positive cells were counted and the percentage of BrdU positive cells versus total cells stained for DAPI were calculated in 5 different fields of each condition. Three experiments were performed and the percentage of BrdU positive cells was calculated for each experiment and used for the final quantification. For rescue experiments (E), the BrdU incorporation was expressed as a percentage of decrease relative to control (n=3). Values are reported as mean ± SEM. Expression levels of the transfected proteins for proliferation assays were analyzed by immunoblotting cell lysates with anti-Elmo2, anti-Myc, anti-Axl, and anti-Tubulin antibodies, as indicated.

Discussion

Axl is a potent promoter of invasion and metastasis in experimental models and its expression correlates with the poor outcome of breast cancer patients. Therefore, defining the molecular pathways by which this RTK promotes invasion is essential to interfere with downstream signaling. We report here a previously unrecognized molecular mechanism by which Axl uses Elmo scaffold proteins to signal to the Rac pathway to promote cell invasion. Despite the identification of many Axl interacting proteins, Elmo1 and Elmo2 may be the first identified *bona fide* direct substrates of this RTK and we show that their interaction with Axl and phosphorylation on carboxyl-terminal tyrosine residues is essential for invasion of basal breast cancer cells. Early studies exploiting an EGFR-Axl chimeric protein had identified unknown proteins of approximately 45 and 80 kDa that became robustly tyrosine phosphorylated in response to EGF stimulation [47]. Elmo proteins are approximately 80 kDa and may represent the proteins observed in that study. In addition, early studies in *Drosophila* demonstrated that Myoblast City, the fly orthologue of mammalian DOCK1, acts downstream of the receptor tyrosine kinase PDGF/VEGF Receptor to promote the Rac-dependent migration of border cells [436]. In our study, we present evidence that the Elmo/Dock1 complex likewise acts as a signaling mediator downstream of receptor tyrosine kinases of the TAM family receptors which are not found in *C. elegans* or *Drosophila*.

Our knockdown of Elmo2, in parallel to rescue assays with Elmo1, demonstrates that Elmo2 is required for basal breast cancer cell invasion and proliferation. Likewise, a recent study demonstrated that stable knockdown of Elmo2 prevents metastasis of MDA-MB-231 cells to lungs in experimental tail vein assays [291]. However, we find here that rescuing Elmo2 with Elmo1 lacking Y720 completely prevented cell invasion. These data point to a critical role for this residue in transmitting signaling. Exactly how phosphorylation of Elmo2 promotes cell invasion is not fully understood. We previously reported that Elmo proteins are regulated by intramolecular interactions that prevent aberrant Rac signaling [282]. In particular, expression of Elmo with mutations maintaining it in an open conformation can increase migration in cells

and biological activity *in vivo* [282, 437]. Through the use of a conformational state biosensor for Elmo2 that we previously described [282], we failed to detect changes in Elmo2 conformation when it enters in a complex with and is phosphorylated by, Axl (data not shown). Another mechanism could be that the tyrosine phosphorylated residue Y713 in Elmo2 becomes a docking site for other signaling molecules, but we deemed this hypothesis unlikely as bioinformatics analysis conflicts with these sites being strong candidates for SH2 or PTB domain-containing proteins. Recent studies also demonstrated that phosphorylation of Dock1 on Serine and Tyrosine residues can increase Rac binding and GEF activity [285, 286, 288, 427]. One hypothesis is that this phosphorylation site on Elmo can transmit signals to Dock1 and enhance its GEF activity, such as relieving Dock1 from its auto-inhibited state, which may explain why we found the Elmo/Dock1 complex stable whether or not the proteins are phosphorylated.

Moreover, guanine nucleotide exchange factors for Rho GTPases operating downstream of Axl have not been previously described. They have been neglected as signaling intermediates that are important in defining the mechanism whereby this RTK promotes metastasis. Through an interaction with Elmo2, or potentially through another mechanism, we report here that Axl can form a complex with the Rac regulator Dock1. We demonstrated, using the CPYPP small molecule inhibitor, that Dock1, a member of the Dock-A subfamily (Dock1, Dock2, and Dock5), mediates Axl-induced Rac activation. Because this inhibitor also targets hematopoietic cell-specific Dock2 and ubiquitous Dock5, we cannot rule out that Dock5 is also recruited to Axl via an interaction with Elmo2 since it is also expressed in basal breast cancer cells. Similarly, Dock4, which belongs to the Dock-B subfamily (Dock3, Dock4), is another broadly expressed Elmo-binding GEF that may contribute to Axl signaling since it has been shown recently to promote MDA-MB-231 cell migration through activation of Rac [297]. In the case of Mer TAM family member, it has been reported to recruit the classical GEF Vav1 for activating Rac during engulfment of damaged photoreceptors [438]. Interestingly, Mer can also recruit Dock1, but in this context through an interaction with the scaffolding protein p130Cas and the adaptor protein CrkII, to promote engulfment of apoptotic cells [414]. We did not investigate if CrkII can complex with tyrosine phosphorylated Axl through its SH2 domain; if

that was the case, CrkII, or other SH2/SH3 adaptors, could also cooperate with Elmo proteins, to facilitate the recruitment of Dock GEFs to the RTK.

Previous studies have shown that high Axl expression in breast cancer patients is correlated with poor patient survival [86]. Similarly, the Axl ligand Gas6 has been shown to be a target for overexpression and amplification in breast cancer [102]. However, some studies have shown upregulation of Axl in breast cancer cells led to an increase in Axl activity independently of Gas6 binding confirming the constitutive activation of Axl in these cells [90]. Because we detect Axl phosphorylation at basal levels prior to Gas6 stimulation in serum-starved cells in MDA-MB-231, our data suggest that Axl in basal breast cancer cells is constitutively active and may act independently of its ligand, which may be the reason why we observe an Elmo2/Axl complex at basal levels prior to Gas6 stimulation.

Our data highlight a previously unsuspected role of Axl and Elmo in the proliferation of invasive breast cancer cells. Previous studies did not detect a reduction in proliferation upon Axl and Elmo expression knockdown using shRNA [86, 291]. A transient siRNA approach may have not allowed enough time for alternative pathways to rescue proliferation, which allowed us to identify a role for Elmo tyrosine site Y713 in promoting proliferation. Similarly, we showed in another study Dock1-null mammary tumors' growth was reduced compared to Dock1-WT mammary tumors, indicating a role for Dock1 in promoting cell proliferation [288].

Furthermore, it remains unclear at what step of breast cancer progression Axl is contributing. Knockout mouse models looking at this important question are missing. Recent data highlight that Axl expression is important in basal breast cancer cells to maintain a stem cell-like phenotype [86, 90]. In part, this is done through the expression of transcription factors that maintain a mesenchymal phenotype such as Snail and Slug. Our results revealing a role for Dock/Elmo proteins in EMT is novel and potentially unique for basal breast cancer cells. In a previous study, we found Dock1 *in vivo* not to be required for mesenchymal transition of cardiomyocytes [261]. Likewise, deletion of Dock1 in HER2 breast cancer tumors was found to

alter interferon gene expression but not EMT gene expression [288]. The pathophysiological importance of Vimentin expression by Elmo/Dock proteins remains to be fully explored in basal breast cancer cells. It will also be important to verify *in vivo* if Axl contributes to stem cells maintenance and if its role in sustaining epithelial to mesenchymal transition is directly linked to invasion.

Altogether, these results led us to propose that Axl may hijack the Rac activator Elmo/Dock complex to phosphorylate Elmo and promote cell invasion and cell proliferation. It also identifies inhibition of the Elmo-Dock pathway as a potential therapeutic target to stop Axl-induced cell proliferation, invasion, and metastases.

Methods

Antibodies

The antibodies against the following proteins were obtained commercially: Tyro3 (C-20), Axl (C-20), Myc (9E10), GFP (B-2), DOCK 180 (H-4) and pY99 (sc-7020) were from Santa Cruz Biotechnologies (Santa Cruz, CA); FLAG M2 and Tubulin were from Sigma (St.Louis, MO); Rac1 was from Millipore (Billerica, MA); $pAKT^{S473}$, AKT, pY100, and $pAxl^{Y702}$ were from Cell Signaling Technology (Danvers, MA); Vimentin, N-Cadherin, and E-Cadherin were from BD Biosciences (Franklin Lakes, NJ); Elmo2 was from Novus Biologicals (Littleton, CO); GST was from GE Healthcare (Buckinghamshire, UK); Mer and $pAxl^{779}$ were from R&D Systems (Minneapolis, MN); Mer and Twist1 were from Abcam (Cambridge, UK). Rabbit phosphospecific polyclonal antibody against pY713 Elmo2 was custom generated using the synthetic phospho-peptide CIPKEPSSpTyrDFVYHYG as an immunogen (GenScript, Piscataway, NJ). Specificity of the $pElmo2^{pY713}$ antibody was verified by dot blot against the phosphorylated and unphosphorylated peptides.

Plasmid Constructs

pCNX2 Flag-DOCK1 was from M. Matsuda (Kyoto University, Japan). pDEST27 Tyro3 was described in [428]. pCMVSport6 Axl was from Open Biosystems (Cat. MHS1010-7430144). pCMVSport6 Axl kinase-dead K561M was generated by site-directed mutagenesis (QuickChange; Stratagene) with primers specified in Table S3. pcDNA3.1 Myc-Elmo1, pcDNA3.1 Myc-Elmo2, and pcDNA3.1 Myc -Elmo3 plasmids were described previously [283, 425]. The Y-F mutants of Elmo1 and Elmo2 were generated by site-directed mutagenesis with the specified primers in Table S3. Elmo1-Myc αN/PxxP mutant plasmid was described previously [275]. pGEX-4T1-Elmo1 wild-type and mutants were subcloned XhoI/BamHI from pcDNA3.1 into pGEX-4T1 (Amersham, Piscataway, NJ). pGEX-4T1-Elmo2 and pGEX-4T1-Elmo3 were subcloned BamHI/XhoI into a pGEX-4T1 vector from pcDNA3.1.

Cell culture and Transfections

Cell lines (MDA-MB-231, Hs578T, and HEK 293T) were cultured in DMEM supplemented with 10% heat-inactivated fetal bovine serum (FBS) and 1% penicillin/streptomycin (Invitrogen-BRL, Carlsbad, CA) at 37°C in 5% CO_2 incubator. MDA-MB-231 and Hs578T cells were transfected with the indicated plasmids or siRNAs using Lipofectamine 2000 (Invitrogen). HEK 293T cells were transfected the indicated plasmids by the calcium phosphate method. Hs578T and MDA-MB-231 cells were transfected with ON-Target smart pool human siRNA (60nM of Elmo2, 100nM of Axl siRNA, 200nM of Dock1 and Dock5) (Dharmacon). Control cells were transfected with 60nM or 100nM NON-Targeting siRNA (Dharmacon). Biochemical and cell biological studies were performed 48 to 72h after transfection.

Kinase library screen

180 full-length human protein kinase cDNA clones derived from the MGC/ORFeome (Open Biosystems, Invitrogen) were Gateway-recombined with pDEST27 vector (Invitrogen) to generate in-frame glutathione S-transferase (GST)-kinase ORFs [428]. GST kinases encoded in plasmids were transfected into HEK293T and arrayed in 96-well plates. GST kinases were immobilized on glutathione-coated plates (Pierce) 24hrs later whose wells were previously rinsed and equilibrated with kinase buffer (25 mM Tris (pH 7.5), 5 mM β-glycerol phosphate, 1 mM $NaVO_4$) prior to adding 1 μg recombinant mouse Elmo1 substrate, 1 μg of MBP as internal control, and 2 μCi of [γ-^{32}P] ATP. Reactions were carried out at 30°C for 30 min and stopped with 2× SDS sample buffer; samples were boiled before separation on SDS/PAGE gels. Phosphorylated substrates were detected by autoradiography. pGEX-4T1 Elmo constructs were transformed in BL-21 for protein production. Exponentially growing BL-21 cultures (2-4L) were induced with 0.1 mM IPTG overnight at 25ºC. Cleared lysates were prepared and GST-Elmo1 was purified on GSTrap mini columns using an Äktaprime Plus chromatography system. The GST tag was cleaved by incubation with thrombin and the protease was removed by passing the sample on a HiTrap Benzamidine FF column. The sample was dialyzed against a phosphate buffer saline solution and passed on glutathione sepharose 4B to remove uncleaved GST-Elmo1 and the GST moiety. GST-Elmo1, and truncated proteins, in addition to GST-Elmo2-3, were

affinity purified on small amounts of glutathione sepharose 4B for small-scale pulldown (see below) [275].

Immunoprecipitation, GST-Fusion Protein Pulldowns, and Rac-GTP Assays

Cells were lysed for 10min in 150mM NaCl, 50mM Tris pH 7.5, 1% NP-40, 5mM NaF, 1mM Na_3VO_4, and 1X complete protease inhibitor (Roche, Indianapolis, IN). For immunoprecipitation, clarified cell lysates were incubated with the indicated antibodies, and the immune complex was allowed to form for 1hr at 4°C. Protein-A Agarose was added for 30 min to recover the immune complex. The beads were washed three times with lysis buffer, and bound proteins were analyzed by SDS-PAGE and immunoblotting. For GST-fusion protein pull-downs, the GST-fusion proteins were expressed in bacteria and purified on glutathione sepharose 4B as described above. Equal amounts of the various GST-fusion proteins bound to beads were next incubated with cell extracts (500µg of protein per condition). The *in vitro* kinase assays with the GST-fusion proteins and recombinant kinase domains of TAMs were carried out as described above. The kinase domains of the human TAMs were obtained from Signal Chem (Richmond, BC). Following IVK assays, the proteins were separated by SDS-PAGE and stained with Coomassie blue and the phosphorylated proteins were detected by autoradiography. For Rac activation assay, Hs578T cells were treated and lysed as described [288]. The GTP-loading status of Rac in was analyzed by GST-PAK-PBD affinity precipitation as described previously [425]. Equal amounts of protein lysates or pulldowns were separated by SDS/PAGE and Rac was detected by immunoblotting. Rac activation was quantified by densitometry analysis using ImageJ software (http://rsb.info.nih.gov/ij/).

Mass spectrometry

The human GST-Tyro3 kinase expressed in HEK293T cells was purified by affinity purification and used to phosphorylate 2 µg of recombinant mouse Elmo1 by IVK assay. To produce phosphorylated Elmo1 in cells, HEK293T cells were co-transfected with human GST-Tyro3 and mouse cMyc-Elmo1. 10mg of lysate was used for immunoprecipitation of Elmo1 with 10µg of anti-Myc antibody (9E10) bound to Proteins A beads. Samples were separated by SDS-

PAGE. The gel was stained in mass spectrometry compatible Coomassie and the band corresponding to Myc-Elmo1 was excised, destained extensively in water and in-gel digestion was then performed according to standard procedures. The peptide digestion products were extracted from the gel with an extraction buffer (1:2 (vol/vol) 5% formic acid/acetonitrile) and incubate for 15 min at 37 °C. Peptides were re-dissolved in 0.1% trifluoroacetic acid for LC-MS/MS analysis at the IRIC platform (Montréal, Qc).

RT-PCR

Total RNAs were extracted using TRIZOL (Invitrogen) and treated with DNAseI (Invitrogen) to remove genomic DNA. cDNA's were generated using the Superscript II Reverse Transcriptase (Invitrogen) and random primers (Invitrogen) as recommended by the manufacturer. The expression profiles of beta-actin, Elmo1, Elmo2, and Elmo3 were determined using specific primers shown in **Table 2. SIII**.

Boyden Chambers Invasion Assay

Cell invasion assays were performed using 8µm pores Boyden Chambers (Costar, Cambridge, MA) coated with 6µl of Matrigel (BD Biosciences, San Jose, CA) dissolved in 100µl of DMEM. Cells were detached and washed with DMEM 0.1% BSA as described in [439]. 100,000 cells were seeded in the upper chamber in duplicate for each condition in serum-starved DMEM and cells were allowed to invade for 16hrs toward the bottom chamber containing DMEM -/+ 10%FBS before fixation in 4% paraformaldehyde. Cells in the upper chambers were mechanically removed using cotton swabs. Invading cells were permeabilized with 0.2% Triton X-100 in PBS and blocked in PBS-1% BSA before staining with anti-cMyc and anti-GFP. The membrane was isolated and mounted on a microscope slide using SlowFade Gold reagent (Invitrogen). An aliquot of the cells was lysed to verify the expression levels of the exogenous proteins and the knockdown of Elmo2 by Western blotting. GFP-positive cells and c-Myc-positive cells that have invaded to the underside were counted from 8-10 independent fields on each membrane (20x).

BrdU Proliferation Assay

72hrs following siRNA transfection, cells were plated on fibronectin-coated glass slips for 24hrs. Cells were incubated with 0.03 mg/ml BrdU at 37°C for 30 minutes. Cells were then fixed with 70% ethanol for 5 minutes, rinsed with PBS (three times), denaturated with 1.5 M HCl for 30 minutes at room temperature and rinsed three times with PBS for 5 minutes each. After incubation with PBS-1%BSA to block non-specific staining for 60 minutes, cells were incubated with BrdU antibody (Cell Signaling Technology) overnight at 4°C. After three washes with PBS, cells were incubated with corresponding Alexa-Fluor-conjugated secondary (Invitrogen) for 2 hours. The samples were then counterstained with DAPI to stain the nuclei and analyzed with Zeiss Observer.Z1 microscope. The percentage of BrdU positive cells versus total cells was calculated in 5 different fields of each condition. The average of the percentage of BrdU positive cells calculated in the 5 images was used for the final quantification. Values are reported as mean ± SEM. Statistical differences were evaluated using ANOVA followed by Bonferroni's multiple comparisons posthoc test using Prism 6 software (GraphPad). A p-value less than 0.05 was considered as statistically significant. An aliquot of the cells was lysed to verify the expression levels of the exogenous proteins and the knockdown of Elmo2 or Axl by Western blotting.

Statistical Analysis

Statistical significance was determined using *Student's t-test* with p-values ≤ 0.05 considered as significant using Prism. In all tests, two groups with one changed parameter were compared. For invasion assays, ANOVA and all pairwise multiple comparison procedures (Holm-Sidak method) were performed (n=6 for each condition).

Acknowledgments

We are grateful to Dr. R. Birge (Rutgers New Jersey Medical School) for the gift of Mer plasmids. We thank members of the Côté lab for helpful discussions. We recognize the technical support of A. Pelletier, C. Julien, C. Meunier, and M. Al-Azzabi. We thank E. Boneil of the Mass spectrometry platform of IRIC (Montréal) for his assistance in mapping phosphorylation sites. This work was funded by a Quebec Breast Cancer Foundation grant to J.F.C and J.P.G; A.A.T was supported in part by the Programmes de Biologie Moléculaire funds from the Université de Montréal and was a recipient of a Ph.D. studentship from Emmanuel-Triassi-IRCM. R.G. was a recipient of an M.Sc. studentship from Wisent-IRCM. J.F.C. is a recipient of a Senior Investigator Award from the FRQ-S. RAS holds the Canada Research Chair in Apoptotic Signaling.

CONFLICT OF INTERESTS

The authors declare that they have no conflict of interest.

Supplementary Information

AXL phosphorylates ELMO scaffold proteins to promote RAC activation and cell invasion

Afnan Abu-Thuraia, Rosemarie Gauthier, Rony Chidiac, Yoshinori Fukui, Robert A. Screaton, Jean-Philippe Gratton, and Jean-François Côté

- **Supplementary Figures**
- **Supplementary Figure legends**
- **Supplementary Tables**

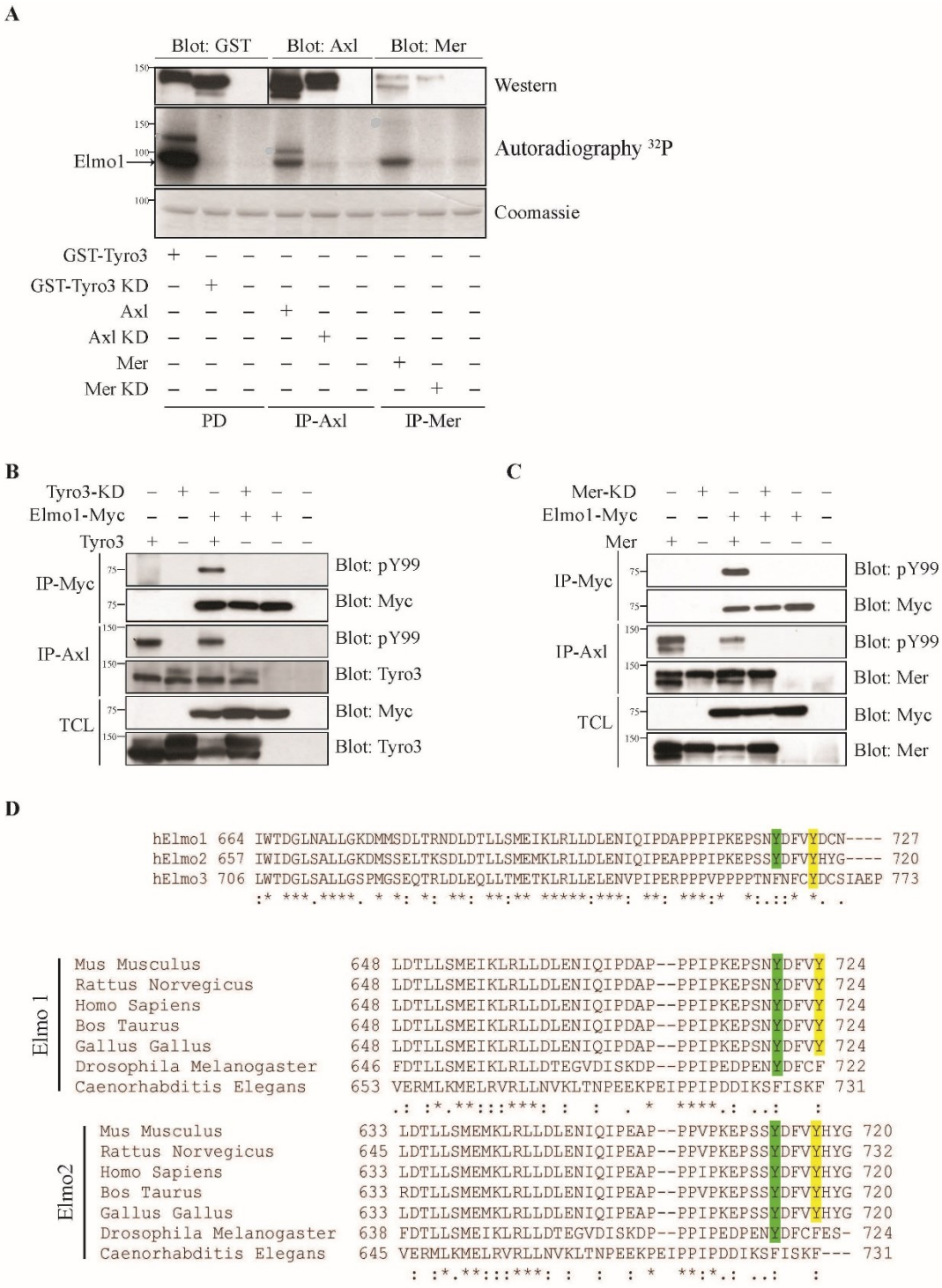

Figure 2. S1 Elmo phosphorylation by the TAM receptors

(A) Lysates of transfected HEK293T cells with indicated plasmids were either immunoprecipitated with antibodies anti-Axl or anti-Mer or glutathione-precipitated with GST-Tyro3 and were incubated with 5µg of GST-Elmo1 and γ_{32}-ATP. The expression of the proteins was analyzed by Coomassie staining and the phosphorylation by autoradiography (n=3). (B-C) Lysates of

HEK293T cells transfected with the indicated plasmids were immunoprecipitated with an antibody against the Myc-epitope (Elmo1) and with an antibody against Tyro3 (B) or Mer (C). The phosphorylation and expression levels of Elmo1, Tyro3 and Mer were analyzed via immunoblotting with anti-Myc (Elmo1) and anti-Tyro3 (B) or anti-Mer (C) antibodies, respectively. (D) Elmo protein sequence alignment in different species near identified phosphorylation sites Y720 (highlighted in green) and Y724 (highlighted in yellow).

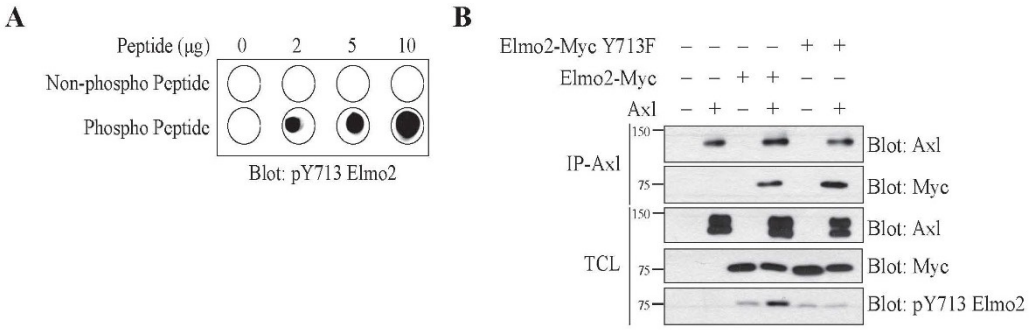

Figure 2. S2 Specificity of pY713 Elmo2 antibody

(A) The purified tyrosine 713 phosphospecific antibody was used for dot blot analysis of increasing amounts (0-10μg) of the phosphorylated and the non-phosphorylated immunogenic peptides used for affinity purification of the serum. (B) Elmo2 phospho-mutant Y720F is able to bind Axl and diminish phosphorylation detected by Elmo2 phospho-specific antibody anti-pY713. Lysates of HEK293T cells transfected with the indicated plasmids were co-immunoprecipitated with an antibody against Axl. The co-precipitation and expression levels of the Axl proteins and Elmo2 were analyzed via immunoblotting with anti-Myc (Elmo2) and anti-Axl antibodies, respectively. Phosphorylation of Elmo2 is detected by immunoblotting using anti-pY713 Elmo2 antibody.

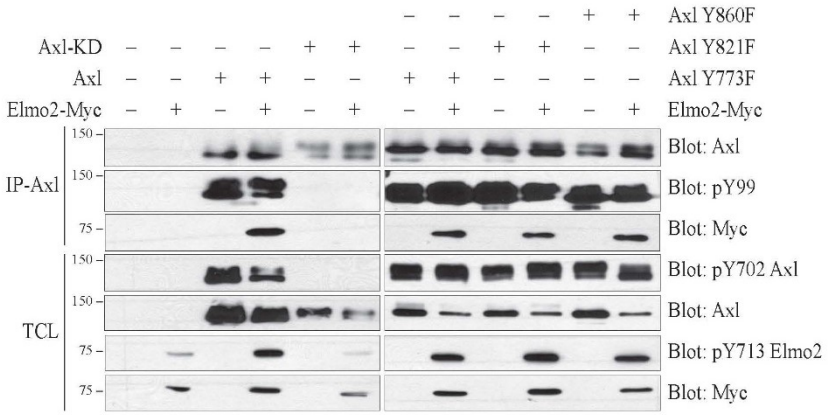

Figure 2. S3 Tyrosine 773, 821 and 860 in Axl C-terminal are not required for Elmo2 binding and phosphorylation

Lysates of HEK293T cells transfected with the indicated plasmids were immunoprecipitated with an antibody against Axl. The phosphorylation and expression levels of Elmo2, Axl and its mutants were analyzed via immunoblotting with anti-Myc (Elmo2), anti-Axl, anti-pY713 Elmo2, anti-pY99, and anti-pY702 Axl.

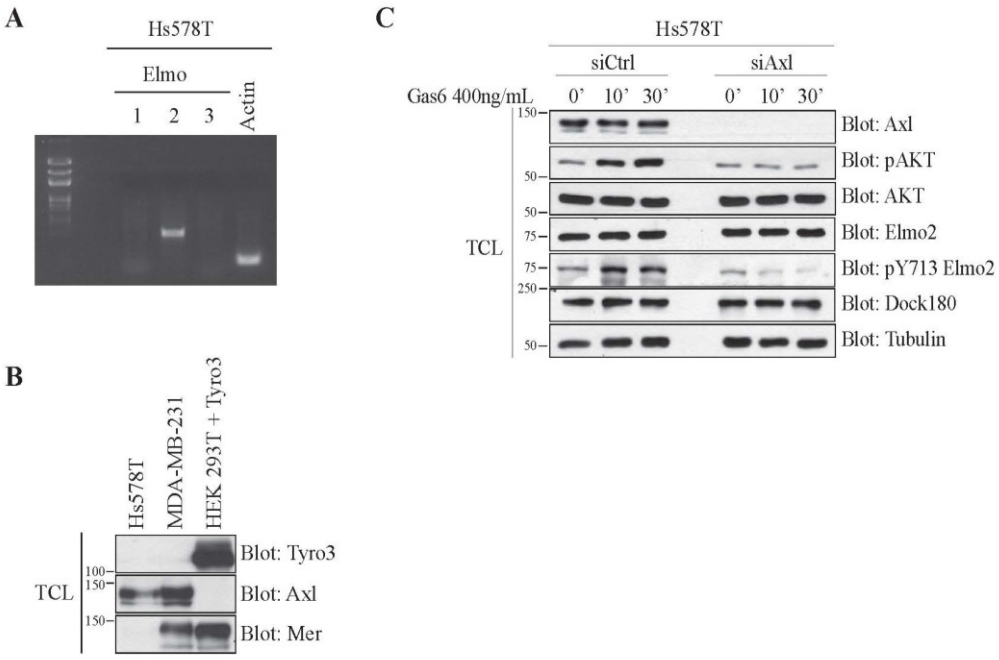

Figure 2. S4 Expression Profile of the TAM receptors and Elmo proteins in MDA-MB-231 and Hs578T cells

(A) RT-PCR analysis on RNA extracted from Hs578T cells using specific primers for Actin, Elmo1, Elmo2 and Elmo3 (Table 3) (B) Lysates of MDA-MB-231 cells, Hs578T cells and transfected HEK293T cells were analyzed for Axl, Tyro3 and Mer expression via immunoblotting using anti-Axl, anti-Tyro3, and anti-Mer. (C) Phosphorylation of Elmo2 in Hs578T cells is dependent on Axl expression. Hs578T cells were transfected with 100nM NON-targeting or ON-target smart pool Axl siRNA prior to being treated with 400ng/mL of Gas6 for the indicated time points. Cell lysates were analyzed via immunoblotting with anti-pAKT, anti-AKT, anti-Axl, anti-Elmo2, anti-pY713 Elmo2, anti-Dock180, and anti-Tubulin antibodies.

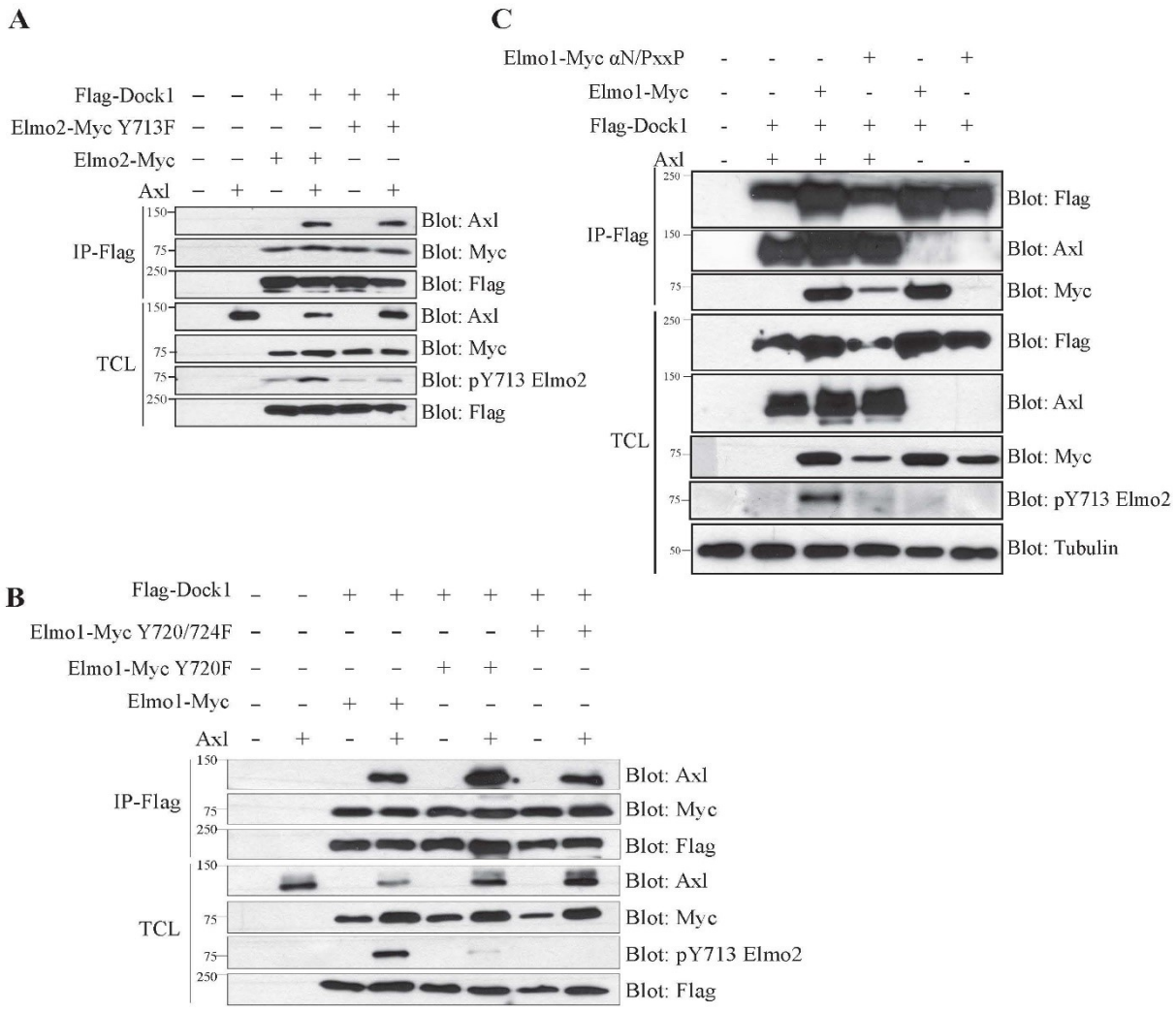

Figure 2. S5 Axl forms a complex with Elmo/Dock1

(A-B) Lysates of HEK293T cells transfected with the indicated plasmids were co-immunoprecipitated with an antibody against Flag-Dock180. The co-precipitation and expression levels of the Axl, Elmo1 (B), Elmo2 (A) and Dock180 were analyzed via immunoblotting with anti-Myc (Elmo), anti-Axl and anti-Flag antibodies. Phosphorylated Elmo in the lysates is detected with the antibody anti-pY713. (C) Lysates of HEK293T cells transfected with the indicated plasmids were co-immunoprecipitated with an antibody against Flag-Dock1. The co-precipitation and expression levels of the Axl, Elmo1, Tubulin, and Dock1 were analyzed via immunoblotting with anti-Myc (Elmo), anti-Axl, anti-Tubulin, and anti-Flag antibodies. Phosphorylated Elmo in the lysates is detected with the antibody anti-pY713 Elmo2.

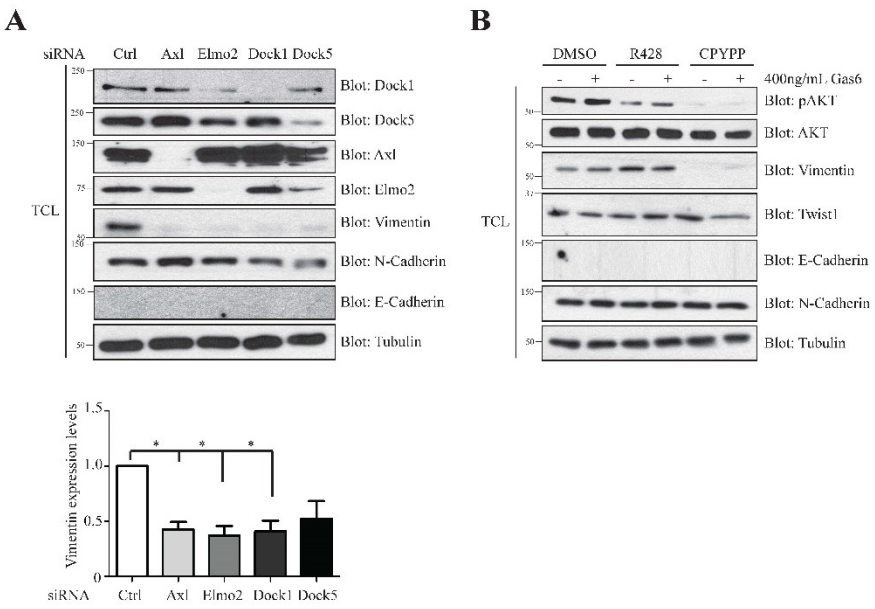

Figure 2. S6 Inhibition of activation or knockdown of Axl, Elmo2, Dock1, and Dock5 alter Vimentin Expression

(A) MDA-MB-231 cells were transfected with either 100nM NON-targeting siRNA, 100nM ON-target Axl siRNA, 60nM ON-target Elmo2 siRNA or 200nM ON-target Dock1 or Dock5 siRNA. The expression levels of Axl, Elmo2, Dock1, Dock5, N-Cadherin, E-Cadherin, Vimentin, and Tubulin were analyzed via immunoblotting with anti-Axl, anti-Elmo2, anti-Dock1, anti-Dock5, anti-N-Cadherin, anti-E-Cadherin, anti-Vimentin, and anti-Tubulin antibodies. The expression levels of Vimentin were quantified by the software Image J (n=3). Data are shown as mean ± SEM; *p < 0.05; one-way ANOVA. (B) Serum-starved MDA-MB-231 cells were treated with 100μM CPYPP or with 1μM R428 for 1hr followed by 400ng/mL Gas6 for 20min. Lysates were then analyzed for expression of Twist1, N-Cadherin, E-Cadherin, Vimentin, p-AKT, AKT and Tubulin via immunoblotting with anti-Twist1, anti-N-Cadherin, anti-E-Cadherin, anti-Vimentin, anti-pAKT, anti-AKT and anti-Tubulin antibodies.

Table 2. SI: GST-kinase library (List of human protein kinases in the GST-kinase expression library used in Figure 2.1 to screen.)

Gene Name	Gene Description
ABL2	v-abl Abelson murine leukemia viral oncogene homolog 2 (arg, Abelson-related gene)
ACVR1	activin A receptor, type I
ACVR1B	activin A receptor, type IB
ADCK4	aarF domain containing kinase 4
ADRBK1	adrenergic, beta, receptor kinase 1
AKT1	v-akt murine thymoma viral oncogene homolog 1
ALS2CR2	amyotrophic lateral sclerosis 2 (juvenile) chromosome region, candidate 2 (ALS2CR2)
ARAF	v-raf murine sarcoma 3611 viral oncogene homolog
AURKB	aurora kinase B (AURKB), mRNA
BLK	B lymphoid tyrosine kinase (BLK), mRNA
BMP2K	BMP2 inducible kinase
BMX	BMX non-receptor tyrosine kinase
BRAF	v-raf murine sarcoma viral oncogene homolog B1
BRD2	bromodomain containing 2
BUB1	BUB1 budding uninhibited by benzimidazoles 1 homolog (yeast)
BUB1B	BUB1 budding uninhibited by benzimidazoles 1 homolog beta (yeast)
C9orf96	chromosome 9 open reading frame 96
CAMK1G	calcium/calmodulin-dependent protein kinase IG
CAMK2G	calcium/calmodulin-dependent protein kinase (CaM kinase) II gamma
CAMK4	calcium/calmodulin-dependent protein kinase IV
CAMKK2	calcium/calmodulin-dependent protein kinase kinase 2
CAMKV	CaM kinase-like vesicle-associated
CDC2	cell division cycle 2, G1 to S and G2 to M
CDC2L6	cell division cycle 2-like 6 (CDK8-like)
CDK10	cyclin-dependent kinase (CDC2-like) 10
CDK2	cyclin-dependent kinase 2
CDK3	cyclin-dependent kinase 3
CDK4	cyclin-dependent kinase 4
CDK6	cyclin-dependent kinase 6
CDK7	cyclin-dependent kinase 7 (MO15 homolog, Xenopus laevis, cdk-activating kinase)

CDKL5	cyclin-dependent kinase-like 5
CHEK2	CHK2 checkpoint homolog (S. pombe)
CLK1	CDC-like kinase 1
CLK3	CDC-like kinase 3
CLK4	CDC-like kinase 4
CSNK1A1L	casein kinase 1, alpha 1-like
CSNK1D	casein kinase 1, Delta
CSNK1E	casein kinase 1, epsilon
CSNK1G2	casein kinase 1, gamma 2
CSNK2A1	casein kinase 2, alpha 1 polypeptide
DCAMKL2	doublecortin and CaM kinase-like 2
DLCK1	doublecortin and CaM kinase-like 1 (DCAMKL1)
DMPK	dystrophia myotonica-protein kinase
DYRK1B	dual-specificity tyrosine-(Y)-phosphorylation regulated kinase 1B
DYRK2	dual-specificity tyrosine-(Y)-phosphorylation regulated kinase 2
DYRK4	dual-specificity tyrosine-(Y)-phosphorylation regulated kinase 4
EEF2K	eukaryotic elongation factor-2 kinase
EIF2AK1	eukaryotic translation initiation factor 2-alpha kinase 1
EIF2AK2	eukaryotic translation initiation factor 2-alpha kinase 2
FASTK	Fas-activated serine/threonine kinase
FASTKD2	FAST kinase domains 2
FES	feline sarcoma oncogene
FGFR1	fibroblast growth factor receptor 1 (fms-related tyrosine kinase 2, Pfeiffer syndrome)
FRK	fyn-related kinase
FYN	FYN oncogene related to SRC, FGR, YES
GRK5	G protein-coupled receptor kinase 5
GRK6	G protein-coupled receptor kinase 6
GSK3A	glycogen synthase kinase 3 alpha
HCK	hemopoietic cell kinase
HIPK1	homeodomain interacting protein kinase 1
HIPK4	homeodomain interacting protein kinase 4
ICK	intestinal cell (MAK-like) kinase
ILK	integrin-linked kinase
IRAK3	interleukin-1 receptor-associated kinase 3

IRAK4	interleukin-1 receptor-associated kinase 4
JAK2	Janus kinase
KSR2	kinase suppressor of ras
LATS1	LATS, the large tumor suppressor, homolog 1 (Drosophila)
LYK5	protein kinase LYK5
MAP2K1	mitogen-activated protein kinase kinase 1
MAP2K2	mitogen-activated protein kinase kinase 2
MAP2K3	mitogen-activated protein kinase kinase 3
MAP2K4	mitogen-activated protein kinase kinase 4
MAP2K6	mitogen-activated protein kinase kinase 6
MAP3K11	mitogen-activated protein kinase kinase kinase 11
MAP3K14	mitogen-activated protein kinase kinase kinase 14
MAP3K8	mitogen-activated protein kinase kinase kinase 8
MAP4K2	mitogen-activated protein kinase kinase kinase kinase 2
MAP4K5	mitogen-activated protein kinase kinase kinase kinase 5
MAPK10	mitogen-activated protein kinase 10
MAPK11	mitogen-activated protein kinase 11
MAPK12	mitogen-activated protein kinase 12
MAPK13	mitogen-activated protein kinase 13
MAPK3	mitogen-activated protein kinase 3
MAPK8	mitogen-activated protein kinase 8
MAPK9	mitogen-activated protein kinase 9
MARK2	MAP/microtubule affinity-regulating kinase 2
MARK3	MAP/microtubule affinity-regulating kinase 3
MAST2	microtubule-associated serine/threonine kinase 2
MKNK1	MAP kinase interacting serine/threonine kinase 1
MYLK2	myosin light chain kinase 2, skeletal muscle
NEK2	NIMA (never in mitosis gene a)-related kinase 2
NEK3	NIMA (never in mitosis gene a)-related kinase 3
NEK4	NIMA (never in mitosis gene a)-related kinase 4
NEK6	NIMA (never in mitosis gene a)-related kinase 6
NEK8	NIMA (never in mitosis gene a)-related kinase 8
NLK	nemo-like kinase
NRBP1	nuclear receptor binding protein 1

NUAK1	NUAK family, SNF1-like kinase, 1 (ARK5)
NUAK2	NUAK family, SNF1-like kinase, 2 (SNARK)
OXSR1	oxidative-stress responsive 1
PAK1	p21/Cdc42/Rac1-activated kinase 1 (STE20 homolog, yeast)
PAK2	p21 (CDKN1A)-activated kinase 2
PAK4	p21 (CDKN1A)-activated kinase 4
PAK6	p21 (CDKN1A)-activated kinase 6
PAK7	p21 (CDKN1A)-activated kinase 7
PBK	PDZ binding kinase
PCTK1	PCTAIRE protein kinase 1
PCTK2	PCTAIRE protein kinase 2
PCTK3	PCTAIRE protein kinase 3
PDIK1L	PDLIM1 interacting kinase 1 like
PFTK1	PFTAIRE protein kinase 1
PIM1	pim-1 oncogene
PIM3	pim-3 oncogene
PKMYT1	protein kinase, membrane associated tyrosine/threonine 1
PKN3	protein kinase N3
PLK1	polo-like kinase 1 (Drosophila)
PLK2	polo-like kinase 2 (Drosophila)
PLK4	polo-like kinase 4 (Drosophila)
PNCK	pregnancy upregulated non-ubiquitously expressed CaM kinase
PRKACG	protein kinase, cAMP-dependent, catalytic, gamma
PRKAG1	protein kinase, AMP-activated, gamma 1 non-catalytic subunit
PRKC1B	protein kinase C, beta 1
PRKCA	protein kinase C, alpha
PRKCH	protein kinase C, eta
PRKCI	protein kinase C, iota
PRKCZ	protein kinase C, zeta
PRKD2	protein kinase D2
PRKRA	protein kinase, interferon-inducible double stranded RNA dependent activator
PRKX	protein kinase, X-linked
PRPF4B	PRP4 pre-mRNA processing factor 4 homolog B (yeast)
PSKH1	protein serine kinase H1

RAF1	v-raf-1 murine leukemia viral oncogene homolog 1
RAGE	renal tumor antigen
RIOK1	RIO kinase 1 (yeast)
RIOK2	RIO kinase 2 (yeast)
RIPK2	receptor-interacting serine-threonine kinase 2
RIPK3	receptor-interacting serine-threonine kinase 3
RPS6KA1	ribosomal protein S6 kinase, 90kDa, polypeptide 1
RPS6KL1	ribosomal protein S6 kinase-like 1
SCYL3	SCY1-like 3
SGK2	serum/glucocorticoid regulated kinase 2
SGK3	serum/glucocorticoid regulated kinase 3
SNF1LK	SNF1-like kinase
SRC	v-src sarcoma (Schmidt-Ruppin A-2) viral oncogene homolog (avian)
SRPK1	SFRS protein kinase 1
SRPK2	SFRS protein kinase 2
STK11	serine/threonine kinase 11
STK16	serine/threonine kinase 16
STK17A	serine/threonine kinase 17a
STK17b	serine/threonine kinase 17b
STK19	serine/threonine kinase 19
STK25	serine/threonine kinase 25
STK31	serine/threonine kinase 31
STK32A	serine/threonine kinase 32A
STK32B	serine/threonine kinase 32B
STK33	serine/threonine kinase 33
STK36	serine/threonine kinase 36 (fused homolog, Drosophila)
STK38	serine/threonine kinase 38
STK38L	serine/threonine kinase 38 like
STK40	serine/threonine kinase 40
SYK	spleen tyrosine kinase
TAF1	TAF1 RNA polymerase II, TATA box binding protein (TBP)-associated factor, 250kDa
TBK1	TANK-binding kinase 1
TESK1	testis-specific kinase 1
TLK1	tousled-like kinase 1

TNK2	Similar to activated p21cdc42Hs kinase
TP53RK	TP53 regulating kinase
TSSK1B	testis-specific serine kinase 1B
TSSK2	testis-specific serine kinase 2
TSSK6	testis-specific serine kinase 6
TTBK2	tau tubulin kinase 2
TTK	TTK protein kinase
TYK2	tyrosine kinase 2
TYRO3	TYRO3 protein tyrosine kinase
UHMK1	U2AF homology motif (UHM) kinase 1
ULK4	unc-51-like kinase 4 (C. elegans)
VRK1	vaccinia related kinase 1
WEE1	WEE1 homolog (S. pombe)
YES1	v-yes-1 Yamaguchi sarcoma viral oncogene homolog 1
YSK4	yeast Sps1/Ste20-related kinase 4 (S. cerevisiae)

Table 2. SII: List of kinases capable of phosphorylating Elmo1 identified in the screen for kinases.

Identified Kinase	Synonym	Kinase type	Validation IRCM
BLK (B-Lymphocyte Kinase)	p55-BLK	Non-receptor Tyr Kinase	Not tested
CAMKK2 (CaM-kinase kinase 2)	Calcium/calmodulin-dependent protein kinase, CaMKK beta, and KKCC2	Non-receptor Ser/Thr Kinase	Not tested
DCAMKL1	DCDC3A, DCLK1, DCAK1, CAM kinase-like 1 and KIAA0369	Non-receptor Ser/Thr Kinase	Negative
PFTAIRE1 (PFTAIRE protein kinase 1)	KIAA0834, PFT1, and PFTK1	Non-receptor Ser/Thr Kinase	Negative
PRP4 (pre-mRNA processing factor 4)	CBP143, KIAA0536, Pre-mRNA protein kinase, PRP4B, PRP4H, PRP4K, PRP4M, and PRPF4B	Non-receptor Ser/Thr Kinase	Not tested
TTBK2 (Tau-tubulin kinase 2)		Non-receptor Ser/Thr Kinase	Non tested
Tyro3 (Tyrosine kinase gene 3)	Sky, Brt (mouse), Rse, Etk-2 (mouse), Rek (chicken), DTK(mouse) and Tif	Receptor Tyrosine Kinase	Positive

Table 2. SIII: Primers used for different procedures

Procedure	Forward	Reverse
RT-PCR Human *β-Actin*	TGATGGTGGGCATGGGTCAGAA	TCCATGTCGTCCCAGTTGGTGA
RT-PCR Human *Elmo1*	CACGATCACAGTGCAGA	CAACTTTCAGCCCCTAGCTG
RT-PCR Human *Elmo2*	CGTTGCCAAACCCAGAGTAT	TGGAGGTGTGAGATGAGCTG
RT-PCR Human *Elmo3*	TGACGCACTCTGAGCGTTAC	CAAGGTCACACTCTCCAGCA
To generate Axl-KD (K561M)	CTCAAGGTCGCTGTGATGACCATGAAAATTGCC	GGCAATTTTCATGGTCATCACAGCGACCTTGAG
To generate Elmo1 Y352F	GAGAAACGCAAGTCCATGTTCACTCGGGATTATA AAAAAC	GTTTTTTATAATCCCGAGTGAACATGGACTTGCG TTTCTC
To generate Elmo1 Y720F	CCCAAGGAACCTAGCAACTTTGACTTTGTCTATG ACTGTAACTG	CAGTTACAGTCATAGACAAAGTCAAAGTTGCTAG GTTCCTTGGG
To generate Elmo1 Y724F	CCCAAGGAACCTAGCAACTATGACTTTGTCTTTG ACTGTAACTG	CAGTTACAGTCAAAGACAAAGTCATAGTTGCTAG GTTCCTTGGG
To generate Elmo1 Y720/724F	CCCAAGGAACCTAGCAACTTTGACTTTGTCTTTG ACTGTAACTG	CAGTTACAGTCAAAGACAAAGTCAAAGTTGCTA GGTTCCTTGGG

CHAPTER 3

AXL confers cell migration and invasion by hijacking a PEAK1-regulated focal adhesion network

Contributions

Figure 3.1 (a-b): Afnan Abu-Thuraia

Figure 3.1 (c): Jonathan Boulais

Figure 3.1 (d): Afnan Abu-Thuraia

Figure 3.1 (e): Carine Delliaux

Figure 3.2: Jonathan Boulais

Figure 3.3 (a-b): Afnan Abu-Thuraia

Figure 3.3 (c-g): Marie-Anne Goyette

Figure 3.4 (a-g): Afnan Abu-Thuraia

Figure 3.4 (h): Jonathan Boulais, Halil Bagci

Figure 3.5 (a-g): Afnan Abu-Thuraia

Figure 3.5 (h): Jonathan Boulais, Carine Delliaux

Figure 3.6: Afnan Abu-Thuraia

Figure 3.7: Afnan Abu-Thuraia

Figure 3.8 (a-b): Marie-Anne Goyette

Figure 3.8 (c-g): Afnan Abu-Thuraia

Figure 3.9 (a): Afnan Abu-Thuraia

Figure 3.9 (b-d): Marie-Anne Goyette

Figure 3.9 (e): Afnan Abu-Thuraia

Figure 3.9 (f-g): Marie-Anne Goyette

Figure 3.10: Jonathan Boulais, Afnan Abu-Thuraia

Figure 3. S1 (a): Afnan Abu-Thuraia

Figure 3. S1 (b-f): Rony Chidiac

Figure 3. S2: Jonathan Boulais

Figure 3. S3: Marie-Anne Goyette

Figure 3. S4: Afnan Abu-Thuraia

Figure 3. S5: Afnan Abu-Thuraia

Figure 3. S6 (a-e): Marie-Anne Goyette

Figure 3. S6 (f-h): Afnan Abu-Thuraia

Figure 3. S7: Afnan Abu-Thuraia

*Afnan Abu-Thuraia and Jean-Francois Côté designed the research

*Afnan Abu-Thuraia, Marie-Anne Goyette, Carine Delliaux and Halil Bagci performed the research

*Afnan Abu-Thuraia, Marie-Anne Goyette, Carine Delliaux and Halil Bagci, Jonathan Boulais and Rony Chidiac analyzed the data

*Afnan Abu-Thuraia and Jean-Francois Côté wrote the manuscript with contributions from all authors

AXL confers cell migration and invasion by hijacking a PEAK1-regulated focal adhesion network

Afnan Abu-Thuraia[1,2], Marie-Anne Goyette[1,2], Carine Delliaux[1], Jonathan Boulais[1], Rony Chidiac[3], Halil Bagci[1,4], Dominique Davidson[1], André Veillette[1,2], Roger J Daly[5], Anne-Claude Gingras[6,7], Jean-Philippe Gratton[3] and Jean-François Côté[1,2,4,8,*]

[1] Montreal Clinical Research Institute (IRCM), Montréal, QC, H2W 1R7, Canada.

[2] Molecular Biology Programs, Université de Montréal, Montréal, QC, H3T 1J4, Canada.

[3] Department of Pharmacology and Physiology, Université de Montréal, Montréal, QC, H3C 3J7, Canada.

[4] Department of Anatomy and Cell Biology, McGill University, Montréal, QC, H3A 0C7, Canada.

[5] Cancer Program, Biomedicine Discovery Institute and Department of Biochemistry and Molecular Biology, Monash University, Clayton, VIC 3800, Australia.

[6] Lunenfeld-Tanenbaum Research Institute, Sinai Health System, Toronto, ON, M5G 1X5, Canada.

[7] Department of Molecular Genetics, University of Toronto, Toronto, ON, M5S 1A8, Canada.

[8] Department of Biochemistry and Molecular Medicine, Université de Montréal, Montréal, QC, H3C 3J7, Canada.

*Corresponding author: Jean-François Côté

Email: jean-francois.cote@ircm.qc.ca, Phone: (514) 987-5647

**Manuscript submitted to Nature Communication and is under consideration (Nov 2018)

Abstract

The aberrant expression of the receptor tyrosine kinase (RTK) AXL is linked to metastasis and acquisition of resistance to cancer drugs. AXL can be activated by its ligand GAS6 or by a crosstalk with other RTKs. However, the signaling pathways engaged by AXL to confer such enhanced pro-invasion power are not known. To address this, we defined the AXL-regulated phosphoproteome in triple-negative breast cancer cells, which revealed that AXL robustly modulates the phosphorylation of a network of focal adhesion (FA) proteins culminating in faster FA disassembly. Interestingly, this signaling activity is unique to AXL in comparison to EGFR. In particular, AXL directly phosphorylates the FA protein NEDD9, promoting NEDD9/CRKII coupling, which orchestrates the AXL-mediated phosphorylation of the pseudo-kinase PEAK1. Our data reveal a distinct mechanism by which PEAK1 complexes with CSK kinase, mediating PAXILLIN (PXN) phosphorylation and AXL-induced FA turnover. Functionally, inactivation of *PEAK1* decreases tumor growth and metastasis *in vivo*. Together, our results uncover an unexpected and unique robust contribution of AXL signaling to FA dynamics revealing a long sought-after mechanism underlying AXL pro-invasive activity. This in-depth understanding of AXL regulated signaling networks identifies PEAK1 as a new therapeutic target in AXL positive tumors.

Introduction

Metastasis to secondary sites is the major cause of death of patients afflicted with breast cancer [441]. Metastasis is a complex process that involves the invasion of tumor cells from the primary site into the surrounding tissue, intravasation into the bloodstream and extravasation from the bloodstream into the secondary site [441]. Among breast cancer subtypes, HER2 positive and Triple-Negative (TNBC) are clinically more aggressive and prone to develop to a metastatic disease and patients show increased recurrence and a lower rate of survival [442]. While targeted therapies allow management of HER2 positive breast cancers, TNBC lacks the expression of Estrogen receptor, Progesterone receptor and HER2 such that they are typically treated by poorly effective standard chemotherapeutic regimens [443, 444]. Successful treatment of metastatic breast cancers is currently the central clinical challenge of solid tumor oncology. The progression of breast cancers often occurs when tumor cells re-activate the developmental epithelial-to-mesenchymal (EMT) program toward increased cell migration and invasion [445]. TNBC cells display robust EMT features and targeting pathways that promote cell migration and invasion would be valuable to decrease the metastatic burden associated with this subtype of the disease [446, 447]. A deep understanding of the molecular mechanism promoting metastasis is a priority to develop novel anti-metastatic approaches.

The TAM (TYRO3, AXL, MERTK) form a distinct group of receptor tyrosine kinases (RTKs) that are activated by atypical vitamin K-dependent and γ-carboxylated ligands known as Growth-Arrest Specific Protein 6 (GAS6) and Protein S (PROS) [44, 410]. These ligands, of higher molecular weights in comparison to other RTK ligands, use their LG domains to bind TAMs. The γ-carboxylated GLA domains are also needed for full activity of the ligands and are particularly important for recognizing phosphatidylserine exposed at the surface of apoptotic cells or vesicles [25]. As such, a fragment of AXL capable to trap soluble GAS6 has been developed as a tool to inhibit TAM signaling [101].

TAMs exert their functions in several biological processes such as dampening the immune response, in clearing apoptotic cells and in promoting cell survival [448]. Among TAMs, AXL

expression is strongly associated with metastasis in solid cancers of several origins and correlates with poor patient survival [24]. Despite its preferential overexpression in TNBC cell lines, studies have shown AXL expression to be subtype independent in patients' breast tumors [58, 449]. AXL is a particularly attracting therapeutic target in metastatic cancers since it is involved in EMT and is positively correlated with chemo-resistance and targeted drug resistance [92, 139, 141]. AXL activation in epithelial cancers is emerging to be complex and to involve crosstalk with other RTKs as an alternative to ligand-mediated activation. For example, AXL can be transactivated by HER2 and can function in a GAS6-independent manner to promote metastasis [58]. However, and in marked contrast with RTKs involved in cancer progressions such as EGFR and MET, little is known about the specific mechanisms induced upon AXL activation to promote tumor invasiveness, metastasis and other features such as drug resistance. Defining the signaling pathways engaged by AXL is essential toward developing efficient anti-AXL therapies to limit the progression of solid cancers.

Here, we used quantitative phosphoproteomics approaches to globally define the signaling pathways specifically modulated by activation AXL by GAS6 in a TNBC cell model. We now define a number of signaling pathways and biological processes that are impacted upon AXL activation. We identified a major contribution of AXL to the regulation of focal adhesion (FA) dynamics. We report a signaling pathway downstream of AXL activation that implicates the pseudokinase PEAK1 in coordinating FAs turnover through recruitment of the canonical FA turnover module composed of βPIX/GIT1/PAK to PAXILLIN (PXN). *In vivo*, cells, where PEAK1 was inactivated by CRISPR/CAS9, show impaired tumor growth and metastatic properties. Collectively, these results reveal a previously unknown contribution of AXL to the dynamics of FAs and expose new opportunities to limit AXL-driven cell invasion.

Results

Defining the GAS6-induced AXL phosphoproteome

AXL is a unique RTK that has been closely linked to metastasis but how it signals remains unexplored. To define the AXL-regulated phosphoproteome, we performed quantitative mass spectrometry (MS) using a stable isotope labeling by amino acids in cell culture (SILAC) approach [450] where the invasive TNBC cell line Hs578T cells were maintained either in media containing heavy Arginine ($^{13}C_6$ $^{15}N_4$) and Lysine ($^{13}C_6$ $^{15}N_2$) or in media containing light Arginine ($^{12}C_6$ $^{14}N_4$) and Lysine ($^{12}C_6$ $^{14}N_2$). These cells were used as a model due to their high expression of AXL and not the related RTKs TYRO3 or MERTK [95] (**Fig. 3.1a**). To specifically activate AXL, we produced the recombinant AXL ligand GAS6 by generating cells where GAS6-His is expressed and secreted in serum-free media containing Vitamin K3 in a tetracycline-inducible manner (**Supplementary Information, Fig. 3. S1a**). Subsequently, serum starved heavy isotope-labeled cells were treated with medium containing soluble GAS6 for 5, 10 or 20 min while the light isotope-labeled cells were treated with control medium (**Fig. 3.1a**) and these treatments promoted AXL auto-phosphorylation and activation of its downstream target AKT (**Fig. 3.1b**).

To globally map the phosphorylation events modulated by AXL activation, we performed phosphopeptide enrichment using TiO_2 chromatography and pY100 immunoaffinity on the mixed lysates of non-treated and GAS6 treated cells (**Fig. 3.1a-b**; **Supplementary Information, Fig. 3. S1b**). High-resolution liquid chromatography-tandem MS (LC-MS/MS) was employed to measure the relative phosphopeptide abundances enriched upon GAS6-induced AXL activation. Due to the short time treatments, protein abundances were presumed to be overall minimally affected. By combining data from all time points, we quantified 5065 unique phosphopeptides (in a total of 2059 proteins), among which a curtailed list of 701 phosphoproteins was found modulated at least 1.5-fold by GAS6 across the three time points (**Fig. 3.1c**; **Supplementary Information, Fig. 3. S1c-f**; **Appendix 1. Dataset I**). Among those, we identified and validated general targets of RTK pathways, including c-JUN, GSK3β, ERK, PI3KCA, JNK1, JNK2, GSK3α, and RAF (**Fig. 3.1d-e**). Interestingly, the phosphorylation

pattern obtained in the blots matched the SILAC ratios obtained in our phosphoproteomic dataset (**Appendix 1. Dataset I**), indicating that our phosphoproteomic dataset may reveal valid and novel signaling pathways modulated upon AXL activation.

Figure 1

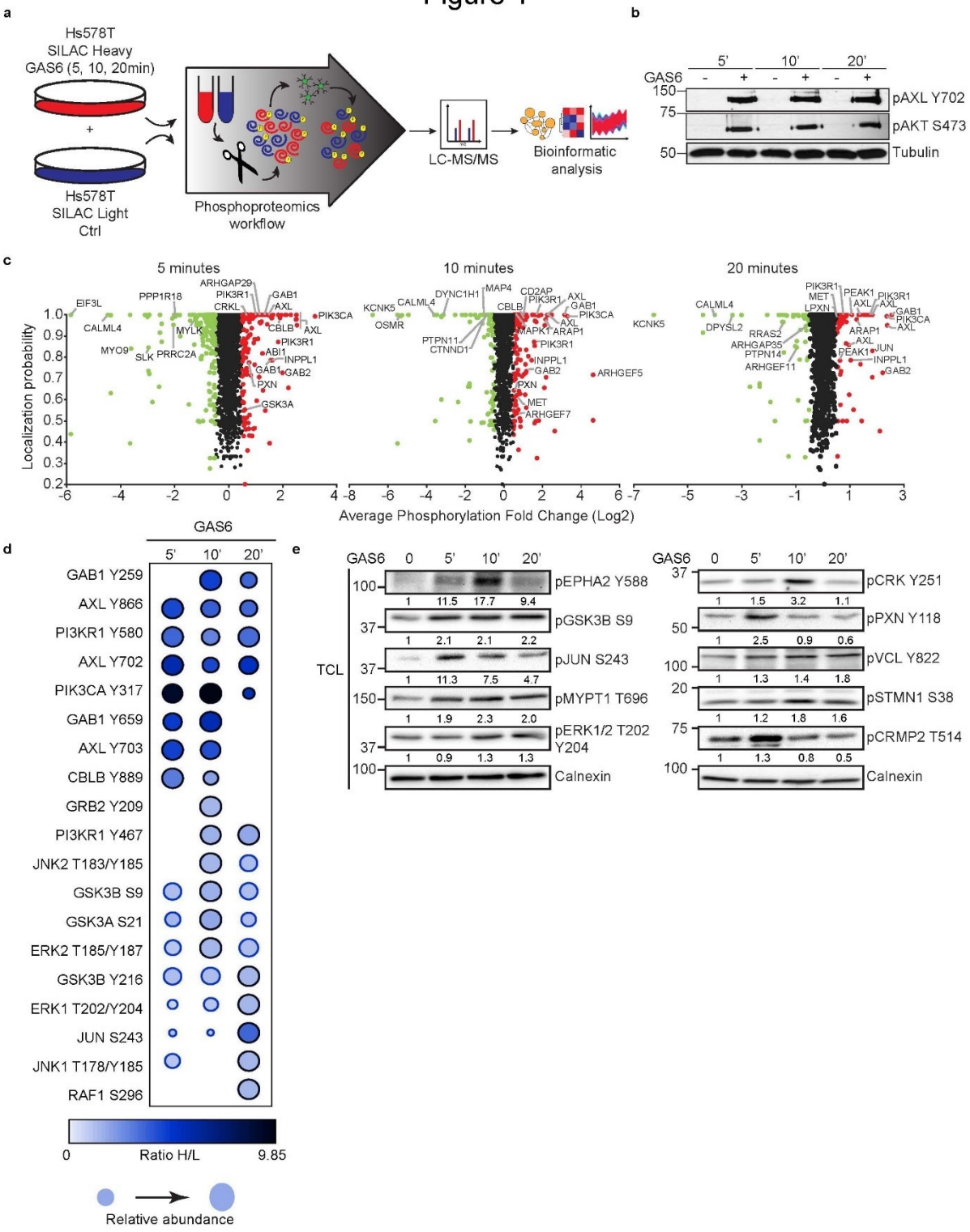
a
Hs578T
SILAC Heavy
GAS6 (5, 10, 20min)
+
Hs578T
SILAC Light
Ctrl
Phosphoproteomics
workflow
LC-MS/MS
Bioinformatic
analysis
b
GAS6
5'
10'
20'
pAXL Y702
pAKT S473
Tubulin
c
5 minutes
10 minutes
20 minutes
Localization probability
Average Phosphorylation Fold Change (Log2)
d
GAS6
5'
10'
20'
GAB1 Y259
AXL Y866
PI3KR1 Y580
AXL Y702
PIK3CA Y317
GAB1 Y659
AXL Y703
CBLB Y889
GRB2 Y209
PI3KR1 Y467
JNK2 T183/Y185
GSK3B S9
GSK3A S21
ERK2 T185/Y187
GSK3B Y216
ERK1 T202/Y204
JUN S243
JNK1 T178/Y185
RAF1 S296
0
Ratio H/L
9.85
Relative abundance
e
GAS6
TCL
pEPHA2 Y588
pGSK3B S9
pJUN S243
pMYPT1 T696
pERK1/2 T202 Y204
Calnexin
pCRK Y251
pPXN Y118
pVCL Y822
pSTMN1 S38
pCRMP2 T514
Calnexin

Figure 3.1 Phosphoproteomic analyses of the receptor tyrosine kinase AXL in TNBC model.

(**a**) Schematic workflow of Hs578T cell labeling, treatment and sample preparation for phosphopeptides enrichment and phosphoproteomic analyses. (**b**) Immunoblot analysis of SILAC labeled Hs578T cell lysates collected at different time points demonstrates the activation of AXL following GAS6 stimulation. (**c**) Graphs of differential phosphopeptide abundances and phosphorylation probabilities in GAS6 treated cells vs unstimulated cells. Phosphosites are deemed modulated if they exhibit SILAC ratios cutoffs of 1.5-fold increase or decrease, which is a phospho-modulation at a Log2 fold change ≥ 0.5 (phosphorylated – red circles) or ≤ 0.5 (dephosphorylated – green circles). (**d**) Dot plot representation of canonical phosphorylation sites regulated downstream of RTKs that were identified in our screen. The color of the circle represents the phosphorylation level (ratio H/L) at 5, 10 and 20 min. Border color of the circle depicts the significance of the modulation, whereas the size of the node indicates the relative abundance. (**e**) Lysates of Hs578T cells treated with GAS6 at three different time points were analyzed by immunoblotting for known targets of receptor tyrosine kinase signaling. Quantification of the western blot signal is indicated beneath each blot.

An overview map of signaling pathways regulated by AXL

Using the KEGG pathway database, analysis of the GAS6-modulated phosphoproteins revealed significant enrichment of potential pathways that could be regulated by AXL activity **(Fig. 3.2a**; **Supplementary Information, Fig. 3. S2**). We further generated a protein interactome based on our phosphoproteomic data, and for simplifying purposes, we headlined some of the significantly enriched protein subnetworks of relevant biological functions upon AXL activation (**Fig. 3.2a; Appendix 1. Dataset II**). In agreement with some of the established roles of AXL, we identified modulation in pathways including "Phagocytosis" and "mTOR signaling". Noteworthy, we also identified multiple novel pathways not previously linked to AXL signaling including "Focal adhesion", "RNA transport" and "Rap1 signaling" (**Fig. 3.2b**; **Appendix 1. Dataset II**).

Moreover, we focused on proteins involved in focal adhesion (FA) dynamics and regulation of the actin cytoskeleton as they were found to be the most phospho-modulated proteins by AXL and could be strong potential candidates in providing mechanistic insights for AXL's role in promoting cell migration and invasion. To investigate if FA dynamics is a process that is modulated specifically by AXL in comparison to other receptor tyrosine kinases, we compared our AXL phosphoproteomic dataset with EGFR phosphoproteomic datasets. Interestingly, when comparing the list of phosphoregulated proteins in our AXL dataset to previously generated

EGFR datasets in HeLa cells (with the caveat that different experimental approaches were employed) [451, 452], we defined a set of 331 unique and 195 shared phospho-modulated proteins (**Fig. 3.2c**). The unique AXL phospho-modulated proteins were significantly enriched for FAs in comparison to EGFR, where EGFR preferentially modulated proteins involved in adherens junctions (**Fig. 3.2d**). Hence, these data reveal that AXL, in contrast to EGFR, modulates uniquely and robustly the phosphorylation of FA proteins. Collectively, these experiments afford a unique and broad view of the phosphoproteome modulated by AXL activation.

Figure 2

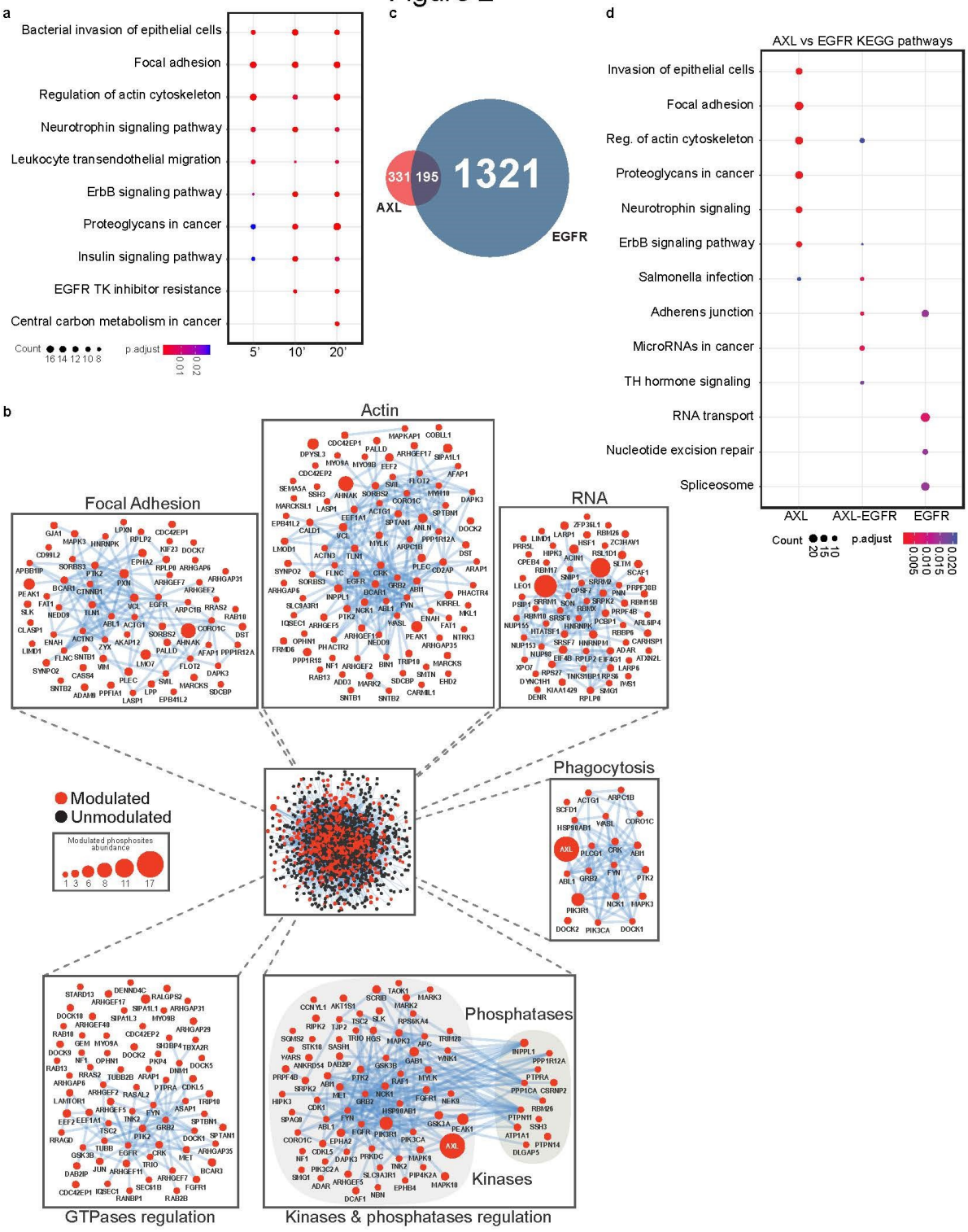
a
Bacterial invasion of epithelial cells
Focal adhesion
Regulation of actin cytoskeleton
Neurotrophin signaling pathway
Leukocyte transendothelial migration
ErbB signaling pathway
Proteoglycans in cancer
Insulin signaling pathway
EGFR TK inhibitor resistance
Central carbon metabolism in cancer
5'
10'
20'
Count
p.adjust
c
331
195
1321
AXL
EGFR
d
AXL vs EGFR KEGG pathways
Invasion of epithelial cells
Focal adhesion
Reg. of actin cytoskeleton
Proteoglycans in cancer
Neurotrophin signaling
ErbB signaling pathway
Salmonella infection
Adherens junction
MicroRNAs in cancer
TH hormone signaling
RNA transport
Nucleotide excision repair
Spliceosome
AXL
AXL-EGFR
EGFR
Count
p.adjust
b
Actin
Focal Adhesion
RNA
Modulated
Unmodulated
Modulated phosphosites abundance
Phagocytosis
Phosphatases
Kinases
GTPases regulation
Kinases & phosphatases regulation

Figure 3.2 High-resolution overview of AXL signaling revealed from a phosphoproteomic screen in TNBC cells

(**a**) Dot plot representation of top 10 significantly enriched KEGG pathways of GAS6-regulated phosphoproteins at the three different time points of stimulation. Circle sizes represent the number of regulated phosphoproteins associated with the specific pathway and the color of the circle represents the significant adjusted p-value. (**b**) Protein-protein interaction network analysis of GAS6-modulated (red nodes) and unmodulated phosphoproteins (black nodes). Surrounding subnetworks in zoom boxes highlight selected and relevant functions of modulated phosphoproteins. Node sizes represent the number of significantly modulated phosphosites. (**c**) A Venn diagram comparing the number of AXL phospho-modulated proteins detected versus the EGFR phospho-modulated proteins. (**d**) Dot plot representation of significantly enriched KEGG pathways of GAS6 regulated phosphoproteins and EGF regulated phosphoproteins. Circle sizes represent the number of regulated phosphoproteins associated with the specific pathway and the color of the circle represents the significant adjusted p-value.

AXL promotes focal adhesions turnover

The specific enrichment of FA proteins as targets of AXL signaling prompted us to investigate whether AXL itself is localized at FA sites in TNBC cells. Using proximity ligation assay (PLA) and PXN as a marker for FAs, a pool of AXL was indeed found to localize at PXN FAs (green signal), which was significantly decreased when cells were treated with the AXL inhibitor R428 [89] (**Fig. 3.3a, b**). We further quantified the number of PXN FAs following modulation of AXL kinase activity with either R428 or GAS6 and its expression levels by siRNA knockdown in MDA-MB-231 or Hs578T cells. In a motile cell, FA turnover is regularly recurrent leading to less stable adhesions. In contrast, serum starvation leads to a decrease in cell motility, and cells tend to have a high number of stable adhesions due to their slow turnover. Interestingly, we found AXL activation by GAS6 treatment of serum-starved cells led to a decrease in the number of FAs, whereas inhibiting its activity with R428 or decreasing its expression via siRNA knockdown led to an increase in the FA number (**Fig. 3.3c, d**; **Supplementary Information Fig. 3. S3a, b**). To test if AXL regulates FA turnover, we analyzed FA lifetime, assembly and disassembly times with a live cell imaging approach of MDA-MB-231 cells expressing GFP-PXN as an FA marker. An increase in AXL activity, in contrast to AXL inhibition or decrease in expression, led to a decrease in the lifetime and the disassembly time of FAs, without affecting the FA assembly time (**Fig. 3.3e-g; Supplementary Information, Video S1, S2**). Similar results were also obtained for Hs578T cells (**Supplementary Information, Fig. 3. S3c, d**).

Figure 3

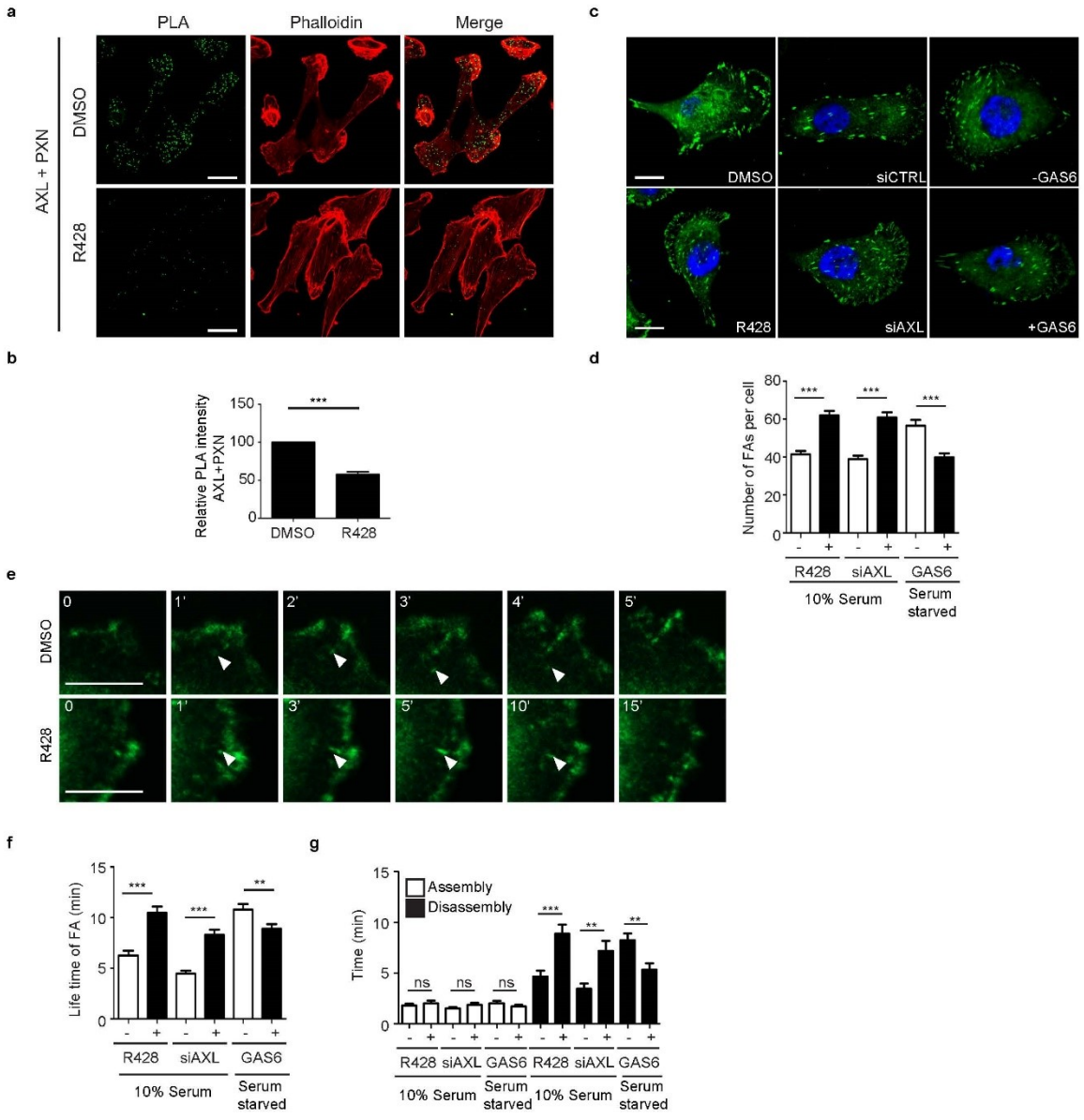
a
PLA
Phalloidin
Merge
AXL + PXN
DMSO
R428
c
DMSO
siCTRL
-GAS6
R428
siAXL
+GAS6
b
Relative PLA intensity AXL+PXN
150
100
50
0
***
DMSO
R428
d
Number of FAs per cell
80
60
40
20
0
***
***
***
- + - + - +
R428
siAXL
GAS6
10% Serum
Serum starved
e
DMSO
R428
0
1'
2'
3'
4'
5'
0
1'
3'
5'
10'
15'
f
Life time of FA (min)
15
10
5
0
***
***
**
- + - + - +
R428
siAXL
GAS6
10% Serum
Serum starved
g
Time (min)
15
10
5
0
Assembly
Disassembly
ns
ns
ns
***
**
**
- + - + - + - + - + - +
R428 siAXL GAS6 R428 siAXL GAS6
10% Serum
Serum starved
10% Serum
Serum starved

Figure 3.3 AXL localizes at FA sites and modulates their turnover.

(**a**) AXL localizes at FA sites. Representative confocal images of MDA-MB-231 cells treated either with DMSO or 1μM R428. PLA kit was used to analyze the localization of AXL at PXN positive FAs. (**b**) Quantifications of the number of PLA signals per cell per condition. *** $P < 0.001$. Scale bar, 20μm. (**c**) AXL modulates a number of FAs in the cell. Representative confocal images of MDA-MB-231 cells treated with DMSO or 1μM R428, transfected with 100nM of siCTRL or siAXL or serum-starved and treated with GAS6 for 20min. Cells were stained for PXN (green) and Dapi (blue). Scale bar, 20μm. (**d**) Quantification of the FA number per cell depicted in (c). *** $P < 0.0001$ (n=3 experiments with 30 cells per condition). (**e**) MDA-MB-231 GFP-PXN expressing cells treated with DMSO or 1μM R428 were imaged live by spinning disk microscopy for a period of 30min to assess the dynamics of FA turnover. White arrowheads point towards an FA that was followed for its assembly and disassembly times. Scale bar, 10μm. (**f-g**) Quantification of FA lifetime (f) and their assembly and disassembly times (g) of cells depicted in (e) and MDA-MB-231 GFP-PXN expressing cells treated with GAS6 for 30min or transfected with 100nM siAXL and imaged as mentioned in (e). *** $P < 0.0001$ (f), *** $P < 0.001$ (g), ** $P < 0.01$ (n=3 experiments with 90 FAs followed per condition).

NEDD9 is a direct AXL substrate mediating cell invasion and FA signaling in TNBC

We hypothesized that scaffold proteins that become tyrosine phosphorylated in response to GAS6 may orchestrate signaling by AXL to FA dynamics. Fitting this criterion, our dataset revealed PI3K regulatory subunits (AKT activation), GAB1/2 (PI3K and MAPK signaling), STAM1/2 (endosome trafficking) and the CAS family-proteins (p130CAS, NEDD9, and CASS4) that have previously been implicated in the regulation of actin and FA signaling. Of those, NEDD9, a scaffold protein downstream of integrin signaling, was particularly attractive since it is implicated in RAC-induced migration and metastasis [295, 453]. Since several NEDD9-binding proteins were also found differentially phosphorylated on tyrosine following AXL activation (BCAR3, CRK, DOCK1), we focused further on NEDD9.

Validating our phosphoproteomic data, AXL downregulation by siRNA in MDA-MB-231 cells resulted in a decreased tyrosine phosphorylation on NEDD9 (**Fig. 3.4a**). Conversely, GAS6 treatment of serum-starved cells increased NEDD9 phosphorylation (**Fig. 3.4b**). To test if NEDD9 could be a direct substrate of AXL, we carried out *in vitro* kinase assays using purified AXL (wildtype or kinase-dead) and recombinant NEDD9 substrate domain (SD) and C-terminal domain (CT) as substrates (**Supplementary Information, Fig. 3. S4a**). AXL phosphorylates NEDD9 on its substrate domain and either mutation of the kinase domain or addition of an AXL

or SRC inhibitor prevented this phosphorylation (**Supplementary Information, Fig. 3. S4b, c**). These results suggest that NEDD9 is a specific AXL substrate.

NEDD9 is known to associate with CRKII protein, to act as a molecular switch to activate RAC1 via DOCK3-CRKII complex[295]. The AXL-regulated tyrosine on NEDD9 (pY^{241}DFP) falls in the pYXXP consensus for interaction with CRK proteins. We tested if NEDD9 phosphorylation by AXL regulates complex formation with CRKII. Knockdown of AXL by siRNA in MDA-MB-231 cells led to a decrease in NEDD9 phosphorylation and a decrease in CRKII-binding to NEDD9 (**Fig. 3.4c**). Functionally, we further confirmed the canonical role of NEDD9 in promoting CRKII/DOCK3-induced RAC-mediated cell migration and invasion in a TNBC cell context (**Supplementary Information, Fig. 3. S4d-g**).

NEDD9 localizes to FAs in part through association with Focal Adhesion Kinase (FAK) [454]. To investigate whether AXL controls NEDD9 localization at FAs, Hs578T cells expressing GFP-NEDD9 were treated with AXL inhibitor R428 or transfected with siAXL. Using FAK as an FA marker, inhibition of AXL activity or decreasing its expression levels by siRNA led to an enrichment of NEDD9 at FAK FAs (**Fig. 3.4d, e**). We also noted an increase in NEDD9/FAK complex formation upon wild-type but not kinase-dead AXL overexpression (**Fig. 3.4f**). These results in positioning NEDD9 as a direct AXL substrate to regulate its localization at FA sites and RAC1-induced cell migration.

Figure 4

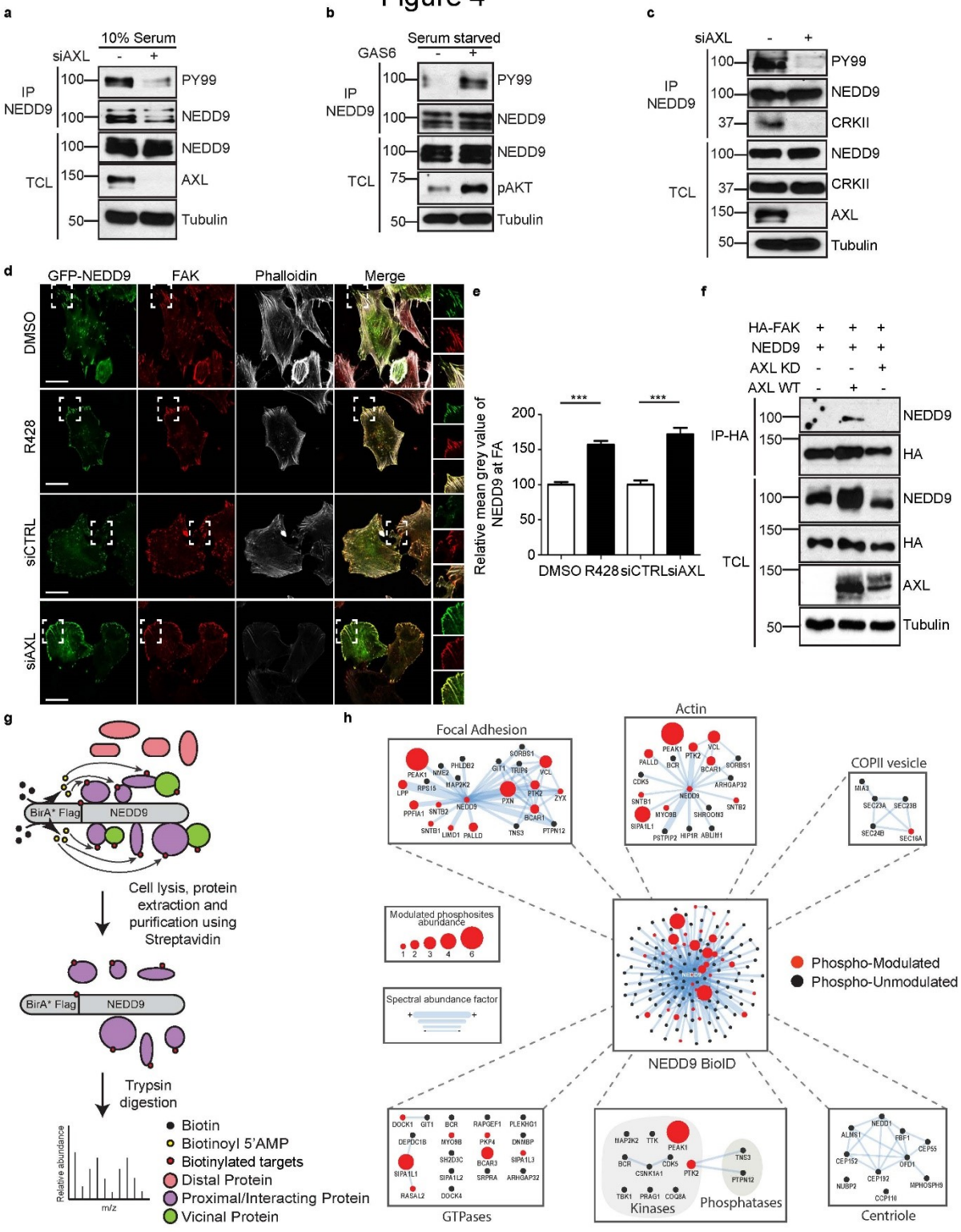
a
10% Serum
siAXL - +
IP NEDD9
100 PY99
100 NEDD9
TCL
100 NEDD9
150 AXL
50 Tubulin
b
Serum starved
GAS6 - +
IP NEDD9
100 PY99
100 NEDD9
TCL
100 NEDD9
75 pAKT
50 Tubulin
c
siAXL - +
IP NEDD9
100 PY99
100 NEDD9
37 CRKII
TCL
100 NEDD9
37 CRKII
150 AXL
50 Tubulin
d
GFP-NEDD9
FAK
Phalloidin
Merge
DMSO
R428
siCTRL
siAXL
e
Relative mean grey value of NEDD9 at FA
200
150
100
50
0
***
***
DMSO R428 siCTRL siAXL
f
HA-FAK + + +
NEDD9 + + +
AXL KD - - +
AXL WT - + -
IP-HA
100 NEDD9
150 HA
TCL
100 NEDD9
150 HA
150 AXL
50 Tubulin
g
BirA* Flag NEDD9
Cell lysis, protein extraction and purification using Streptavidin
BirA* Flag NEDD9
Trypsin digestion
Relative abundance
m/z
Biotin
Biotinoyl 5'AMP
Biotinylated targets
Distal Protein
Proximal/Interacting Protein
Vicinal Protein
h
Focal Adhesion
Actin
COPII vesicle
Modulated phosphosites abundance
1 2 3 4 6
Spectral abundance factor
NEDD9 BioID
Phospho-Modulated
Phospho-Unmodulated
GTPases
Kinases
Phosphatases
Centriole

Figure 3.4 AXL phosphorylates NEDD9 and regulates its localization at FA

(**a**) AXL knockdown decreases NEDD9 phosphorylation levels. MDA-MB-231 were transfected with 100nM siAXL. Following anti-NEDD9 immunoprecipitation, NEDD9 phosphorylation levels were determined by western blotting. (**b**) AXL activation increases NEDD9 phosphorylation levels. Serum-starved MDA-MB-231 cells were treated with GAS6 for 20min. Following anti-NEDD9 immunoprecipitation, NEDD9 phosphorylation levels were determined by western blotting. (**c**) AXL knockdown decreases NEDD9/CRKII complex formation. MDA-MB-231 were transfected with 100nM siAXL. Following anti-NEDD9 immunoprecipitation, levels of CRKII binding to NEDD9 was determined by western blotting. (**d**) NEDD9 localization at FAs is regulated by AXL. Representative confocal images of Hs578T cells transfected with GFP-NEDD9 plated on coverslips and either treated with DMSO or 1μM R428 or transfected with 100nM siAXL. Cells were then fixed and permeabilized and stained for GFP (green), FAK (red) and Phalloidin (grey). Dashed boxes are used to depict the location of the zoomed images. (**e**) Quantification of the mean grey value of NEDD9 at FAK positive FAs shown in (d). *** $P < 0.0001$ (n=3 experiments, 15 cells per condition per experiment). Scale bar, 20μm. (**f**) AXL kinase activity regulates NEDD9 complex formation with FAK. Lysates of 293T cells expressing indicated plasmids were subjected to anti-HA FAK immunoprecipitation. Co-immunoprecipitates were detected via western blotting. (**g**) Schematic workflow of the proximity-dependent biotinylation (BioID) proteomics approach performed with NEDD9 in Flp-In™ T-REx™ 293 cells. NEDD9 is fused to the promiscuous BirA* biotin ligase that can label the protein environment of the bait. (**h**) Network layout of the NEDD9 BioID dataset. Surrounding subnetworks in zoom boxes exhibit selected and relevant functions, such as «FA» and «Actin» where NEDD9 seems to play a central role. Node sizes represent the relative amount of GAS6-modulated phosphosites. Edge thickness represents the relative protein abundance depicted by the SAF (Spectral Abundance Factor) metric. The color of the node indicates if a NEDD9 prey has been phospho-modulated or not in the GAS6 phosphoproteomic screen.

AXL promotes the recruitment of the pseudokinase PEAK1, in proximity to NEDD9, to FAs

While NEDD9 localizes to FAs, how it contributes to the dynamics of these structures remains poorly understood. To address this, we sought to determine novel NEDD9 protein complexes. We exploited BioID, a proximity-dependent biotin labeling technique coupled to mass spectrometry that can capture interacting and proximal proteins of the BirA*-FLAG-NEDD9 bait in living cells [455] (**Fig. 3.4g**, **Supplementary Information, Fig. 3. S4h**). We generated Flp-In T-REx 293 cells to express BirA*-FLAG-NEDD9 in a tetracycline-inducible manner. Addition of biotin to cells led to biotinylation of BirA*-FLAG-NEDD9 and its bound proteins such that 133 high confidence proximal interactors were identified. While we identified 10 reported direct NEDD9-interactors (**Supplementary Information, Fig. 3. S4i**; **Appendix 1. Dataset III**), several of the novel NEDD9 BioID preys are known to be in complex with the previously reported interactors. NEDD9 proximal proteins were clustered based on their gene

ontology terms into their corresponding biological processes, which further cemented NEDD9 as a candidate for regulation of FA signaling (**Fig. 3.4h**; **Appendix 1. Dataset IV**).

To uncover the molecular mechanism of AXL-mediated FA dynamics, we intersected the AXL phosphoproteomic dataset with NEDD9 proximal interactors and this revealed PEAK1 as a previously unknown proximity partner to NEDD9 and a protein that is phosphotyrosine-modulated by AXL (**Fig 3.4h**; **Appendix 1. Dataset I, III**). PEAK1 is pseudo-kinase that has been linked previously to cell migration and FA turnover [393, 456-459], but how it achieves these functions is unresolved. While we could not detect a direct NEDD9/PEAK1 interaction, we detected an interaction of PEAK1 with AXL which led to its AXL-mediated phosphorylation (**Fig. 3.5a-c**). This phosphorylation likely occurs on multiple tyrosine residues since mutation of the PEAK1 phosphosite identified in our screen did not decrease its global tyrosine phosphorylation by AXL (**Supplementary Information, Fig. 3. S5a**). To determine whether AXL controls the cellular localization of PEAK1, we treated MDA-MB-231 cells with the AXL inhibitor R428 and found PEAK1 being redistributed from a cell periphery staining pattern to a more cytoplasmic staining following the treatment (**Fig. 3.5d, e**). Similarly, decreased PEAK1 localization at FAK FAs was also observed upon AXL inhibition (**Fig. 3.5f, g**). These data position PEAK1 as a candidate to mediate AXL signaling to FAs.

Figure 5

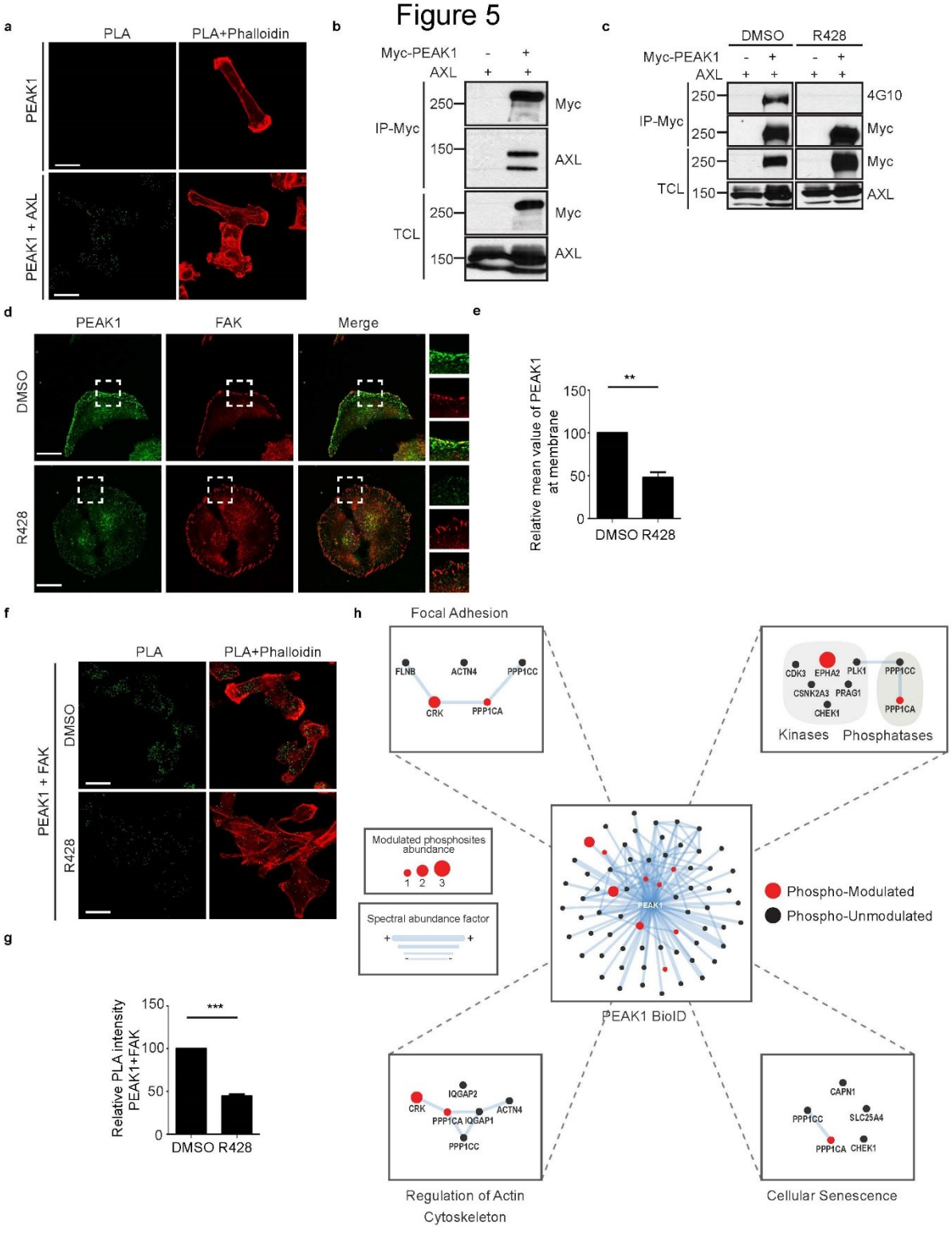
a
PLA
PLA+Phalloidin
PEAK1
PEAK1 + AXL
b
Myc-PEAK1
AXL
IP-Myc
TCL
250
150
Myc
AXL
c
DMSO
R428
Myc-PEAK1
AXL
IP-Myc
TCL
4G10
Myc
AXL
d
PEAK1
FAK
Merge
DMSO
R428
e
Relative mean value of PEAK1 at membrane
DMSO R428
f
PLA
PLA+Phalloidin
PEAK1 + FAK
DMSO
R428
g
Relative PLA intensity PEAK1+FAK
DMSO R428
h
Focal Adhesion
FLNB
ACTN4
PPP1CC
CRK
PPP1CA
Kinases
Phosphatases
CDK3
EPHA2
PLK1
CSNK2A3
PRAG1
CHEK1
Modulated phosphosites abundance
Spectral abundance factor
PEAK1
PEAK1 BioID
Phospho-Modulated
Phospho-Unmodulated
IQGAP2
IQGAP1
Regulation of Actin Cytoskeleton
CAPN1
SLC25A4
Cellular Senescence

Figure 3.5 AXL interacts with PEAK1 and modulates its phosphorylation and localization in the cell

(**a**) PEAK1 localizes with AXL in TNBC cells. Representative confocal images of MDA-MB-231 cells. PLA kit was used to analyze the localization of PEAK1 and AXL. (**b**) PEAK1 interacts with AXL. Lysates of 293T cells expressing the indicated plasmids were used for anti-Myc immunoprecipitation. Levels of AXL is detected via western blotting. (**c**) PEAK1 is phosphorylated by AXL. Lysates of 293T cells expressing the indicated plasmids and treated or not with 1μM R428 for 1 hour were subjected to anti-Myc immunoprecipitation. Levels of Myc-PEAK1 tyrosine phosphorylation was detected via western blotting. (**d**) PEAK1 recruitment to the cell membrane is AXL regulated. Representative confocal images of Hs578T cells treated with DMSO or 1μM R428. Cells were stained for PEAK1 (green) and FAK (red). Dashed boxes are used to depict the location of the zoomed images. (**e**) Quantification of the mean grey value of PEAK1 at the periphery of the membrane shown in (b). ** $P < 0.05$. (**f**) PEAK1 is localized at FA sites. Representative confocal images of MDA-MB-231 cells treated with DMSO or 1μM R428. PLA kit was used to analyze the localization of PEAK1 at FAK positive FAs. (**g**) Quantifications of the number of PLA signals per cell per condition. *** $P < 0.005$. (**h**) Network layout of the PEAK1 BioID dataset. Surrounding subnetworks in zoom boxes exhibit selected and relevant functions, such as «FA» and «Actin» where PEAK1 seems to play a central role. Node sizes represent the relative amount of GAS6-modulated phosphosites. Edge thickness represents the relative protein abundance depicted by the SAF (Spectral Abundance Factor) metric. The color of the node indicates if a PEAK1 prey has been phospho-modulated or not in the GAS6 phosphoproteomic screen.

CRKII is a PEAK1-binding protein mediating AXL signaling to FAs

We next defined the BirA*-FLAG-PEAK1 interactome by BioID proteomics to better understand how PEAK1 communicates with the FA machinery. The intersection of the AXL phosphoproteomic dataset with the PEAK1 BioID screen revealed a major proximal interactor, CRKII, that is also phospho-modulated by AXL activation (**Fig. 3.5h**; **Supplementary Information, Fig. 3. S5b**; **Appendix 1. Dataset V, VI**). The related CRKL was also identified in the BioID of PEAK1 but not in the AXL phosphoscreen. Since CRKII and CRKL adaptor proteins have been reported to assist in FA turnover [460] and emerged from these analyses, we further investigated their role in PEAK1 regulation of FA.

PEAK1 contains a putative proline-rich motif that fits the consensus for CRK-binding [456]. To test if this is the mechanism implicated for their interaction, we generated a mutant of PEAK1 in which this proline-rich region was disrupted (PEAK1 3PA) and we demonstrated that this was sufficient to almost completely disrupt PEAK1 binding to CRKII by both co-immunoprecipitation and GST-pulldown assays (**Fig. 3.6a, b**; **Supplementary Information, Fig. 3. S5c**). Further dissection of the complex by GST-pulldown assays defined that

PEAK1/CRKII coupling occurred via the CRKII middle SH3 domain (**Supplementary Information, Fig. 3. S5d**). These data were further confirmed by conducting a PEAK1 3PA mutant interactome by BioID that was compared with PEAK1 WT interactome and these analyses revealed PEAK1 3PA mutant loss of binding with CRKII and CRKL proteins (**Appendix 1. Dataset V**).

To characterize the functional role of the CRKII/PEAK1 complex formation, we found AXL-mediated phosphorylation of PEAK1 to be abolished upon mutation of the CRKII-binding domain of PEAK1, despite its correct localization in the cell, suggesting that PEAK1 phosphorylation downstream of AXL may require its coupling to CRKII (**Fig. 3.6c**; **Supplementary Information, Fig. 3. S5e**). In addition, localization of CRKII at FAK FAs was diminished upon knockdown of PEAK1 in MDA-MB-231 cells, suggesting that PEAK1/CRKII interaction is necessary for CRKII localization at FAs (**Fig. 3.6d, e**). CRK-PXN complex formation is known to be essential for increased FA turnover and induce cell migration [461]. Hence, we examined if CRKII recruitment to PXN is mediated by AXL. Indeed, co-immunoprecipitation revealed that CRKII interaction with PXN is indeed induced upon AXL overexpression and is dependent on AXL kinase activity, suggesting AXL mediated phosphorylation of CRKII may induce the coupling of CRKII/PEAK1 to PXN proteins at FAs (**Fig. 3.6f**).

Figure 6

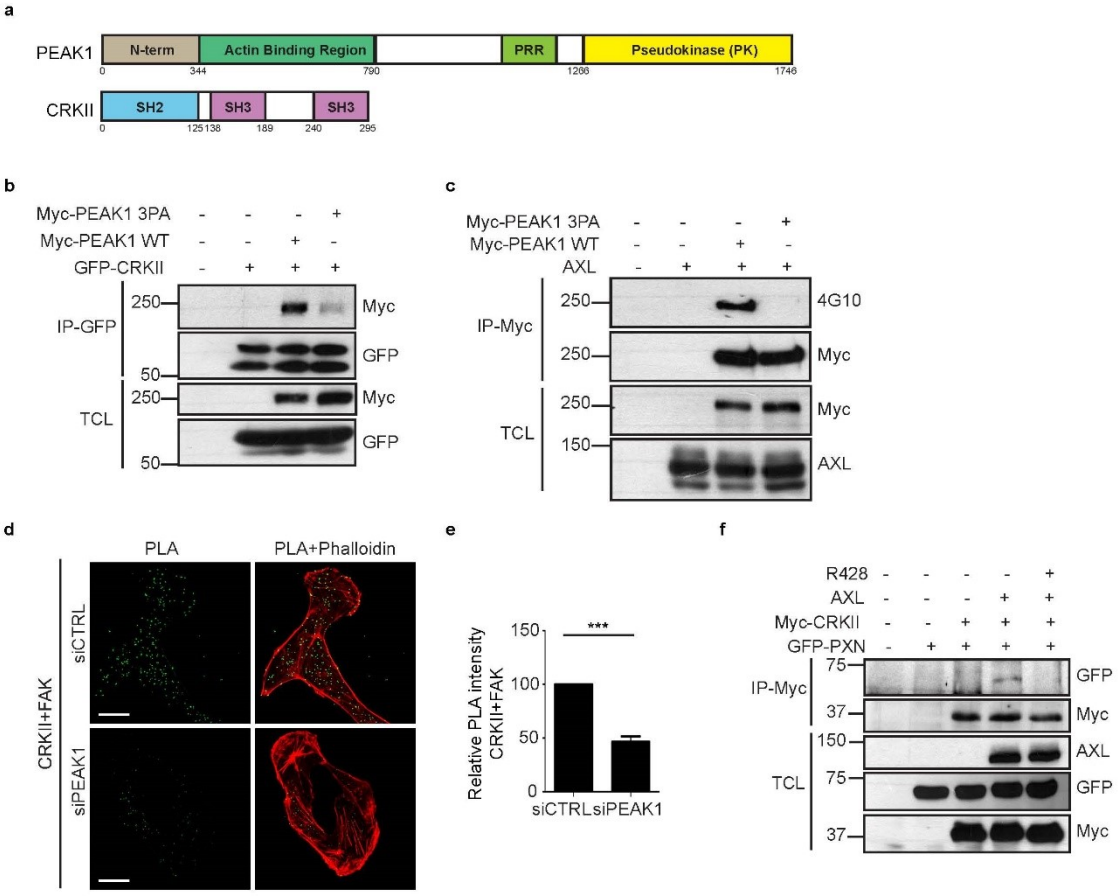

Figure 3.6 CRKII direct binding to PEAK1 is necessary for AXL-mediated PEAK1 phosphorylation and for CRKII localization at FA.

(**a**) Schematic of PEAK1 and CRKII domains. (**b**) CRKII binds PEAK1 proline-rich region. Lysates of 293T cells expressing the indicated plasmids were used for anti-GFP immunoprecipitation. Levels of Myc-PEAK1 is detected via western blotting. (**c**) Lysates of 293T cells transfected with the indicated plasmids were subjected to anti-Myc immunoprecipitation. Myc-PEAK1 phosphorylation levels were detected via western blotting. (**d**) PEAK1 regulates CRKII localization at FA sites. Representative confocal images of MDA-MB-231 cells transfected with either 100nM siCTRL or siPEAK1. PLA kit was used to analyze the localization of CRKII at FAK positive FAs. (**e**) Quantifications of the number of PLA signals per cell per condition. *** $P <$ 0.005. Scale bar, 20μm. (**f**) AXL modulates CRKII binding to PXN. Lysates of 293T cells expressing the indicated plasmids were used for anti-Myc immunoprecipitation. Levels of GFP-PXN is detected via western blotting.

PEAK1, in complex with PRAG1, orchestrates the phosphorylation of PAXILLIN via CSK

Accumulation of PXN phosphorylation at sites of FAs is an indicator of FA turnover. Since PEAK1 and PRAG1 are pseudo-kinases that associate with tyrosine kinase activity when phosphorylated [462], this led us to test if PEAK1 can orchestrate the phosphorylation of PXN. PEAK1 knockdown using siRNA eliminated PXN phosphorylation in TNBC cells (**Fig. 3.7a**) and an increase in PXN phosphorylation was observed following overexpression of PEAK1 (**Fig. 3.7b**). An *in vitro* kinase assay with GST-PXN N-terminus or C-terminus as substrates revealed the presence of a kinase activity able to phosphorylate N-terminus of PXN *in vitro* in PEAK1 immunoprecipitates (**Supplementary Information, Fig. 3. S5f, g**). A recent study has shown PRAG1, known to heterodimerize with PEAK1 [463], to induce tyrosine phosphorylation in human cells by associating with CSK tyrosine kinase [462]. We hypothesized that PRAG1 may bridge PEAK1 to CSK kinase to induce PXN phosphorylation at FA sites. Indeed, we confirmed that CSK kinase binds PEAK1 in an AXL-dependent manner in TNBCs (**Fig. 3.7c**) and that CSK can promote GFP-PXN phosphorylation (**Fig. 3.7d**).

In contrast to PEAK1 WT, PEAK1 3PA mutant failed to promote PXN phosphorylation, affirming the necessity of PXN/CRKII complex formation to mediate PXN phosphorylation (**Fig. 3.7e**). To address the necessity of PEAK1 in AXL-induced FA turnover, we depleted PEAK1 levels by siRNA in GFP-PXN expressing MDA-MB-231 cells and assessed the role of GAS6 on FA turnover by live cell imaging. The GAS6-mediated decrease in FA disassembly time and lifetime was not observed in PEAK1 knockdown GFP-PXN expressing MDA-MB-231 cells (**Fig. 3.7f, g**; **Supplementary Information, Fig. 3. S5h**), suggesting that AXL's regulation of FA turnover is mediated by PEAK1.

Figure 7

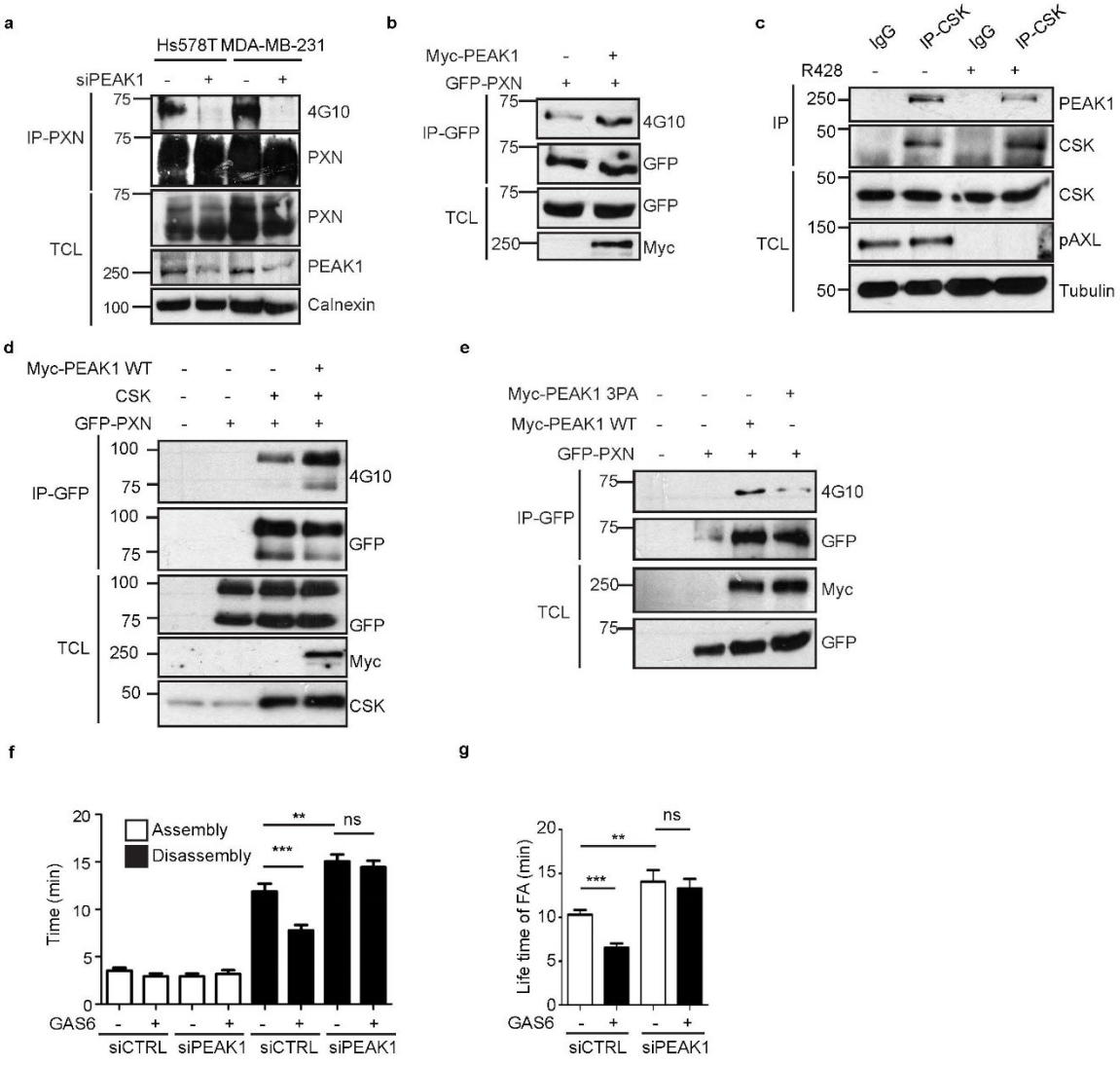
a
Hs578T MDA-MB-231
siPEAK1 - + - +
IP-PXN
TCL
4G10
PXN
PXN
PEAK1
Calnexin
b
Myc-PEAK1 - +
GFP-PXN + +
IP-GFP
TCL
4G10
GFP
GFP
Myc
c
IgG IP-CSK IgG IP-CSK
R428 - - + +
IP
TCL
PEAK1
CSK
CSK
pAXL
Tubulin
d
Myc-PEAK1 WT - - - +
CSK - - + +
GFP-PXN - + + +
IP-GFP
TCL
4G10
GFP
GFP
Myc
CSK
e
Myc-PEAK1 3PA - - - +
Myc-PEAK1 WT - - + -
GFP-PXN - + + +
IP-GFP
TCL
4G10
GFP
Myc
GFP
f
Assembly
Disassembly
Time (min)
GAS6
siCTRL siPEAK1 siCTRL siPEAK1
g
Life time of FA (min)
GAS6
siCTRL siPEAK1

Figure 3.7 PEAK1, in complex with CSK, regulates FA turnover by PXN phosphorylation downstream of AXL.

(**a**) PXN phosphorylation is PEAK1-mediated in TNBC cells. Hs578T and MDA-MB-231 cells were transfected with 100nM siCTRL or siPEAK1 and their lysates were used for anti-PXN immunoprecipitation. Phosphorylation levels of PXN were analyzed via western blotting. (**b**) PEAK1 expression increases PXN phosphorylation. Lysates of 293T cells expressing the indicated plasmids were used for anti-GFP immunoprecipitation. Levels of PXN phosphorylation is detected via western blotting. (**c**) PEAK1 interacts with CSK in an AXL dependent manner. Lysates of MDA-MB-231 cells treated or not with 1μM R428 were used for anti-CSK immunoprecipitation. PEAK1 levels in the IP were analyzed via western blotting. (**d**) Lysates of 293T cells transfected with the indicated plasmids were subjected to anti-GFP immunoprecipitation. GFP-PXN phosphorylation levels were detected via western blotting. (**e**) Lysates of 293T cells transfected with the indicated plasmids were subjected to anti-GFP immunoprecipitation. GFP-PXN phosphorylation levels were detected via western blotting. (**f-g**) AXL modulation of FA turnover is PEAK1-mediated. Quantification of assembly and disassembly time (f) and lifetime (g) of the FAs of GFP-PXN expressing MDA-MB-231 cells. *** $P < 0.001$, ** $P < 0.005$ (g), ** $P < 0.01$ (f).

AXL/PEAK1 coordinates the recruitment of the FA turnover machinery to PAXILLIN FAs

Since AXL activity led to the modulation of FA disassembly rate, we investigated whether this modulation is due to the recruitment of the disassembly complex machinery to FA. FA turnover is mediated by the recruitment of β-PAK1-interacting guanine-nucleotide exchange factor (βPIX)/GIT1/PAK1 complex into PXN FAs to induce disassembly of the FA structure [380, 464, 465]. Interestingly, our phospho-screen data revealed βPIX to be modulated by GAS6-induced AXL activation on S703, which falls on its RhoGEF domain (**Appendix 1. Dataset I**). Additionally, we found GAS6-mediated activation of AXL promotes PAK kinases activation while its inhibition by R428 decreases it (**Supplementary Information, Fig. 3. S6a**), suggesting that AXL modulation of βPIX/GIT1/PAK1 complex phosphorylation levels may regulate their recruitment and activity at FA sites. To determine if AXL modulates FA turnover by regulating the recruitment of this complex to FAs, we stained MDA-MB-231 cells, treated with R428, GAS6 or transfected with siAXL, for either GIT1 or βPIX, and assessed their localization at PXN FAs. Even though the number of PXN FAs is higher, a significant decrease in βPIX/GIT1 recruitment to PXN FAs upon R428 treatment or knockdown of AXL was observed, whereas GAS6 treatment increased the recruitment of this complex to the FA sites (**Fig. 3.8a, b**; **Supplementary Information, Fig. 3. S6b, c**). This suggests that AXL activity may induce FA turnover by modulating the recruitment of βPIX/GIT1/PAK1 complex to FA

sites. Similarly, knockdown of βPIX/GIT1/PAK1 and CDC42, a known target of βPIX and an activator of PAK kinases [466-468], in TNBC cells led to an increase in FA number and mechanistically to a slower disassembly, similar to what was observed previously with AXL inhibition. (**Supplementary Information, Fig. 3. S6d, e**). These results strengthen the connectivity and causality between AXL and βPIX/GIT1/PAK1 complex, signaling in a similar mechanism to promote FAs disassembly.

We hypothesized that CRKII-induced FA turnover could be mediated by PEAK1, where PEAK1 may function as a scaffold to coordinate the recruitment of the βPIX/GIT1/PAK1 complex to phospho-PXN downstream of AXL. In fact, complex formation between PEAK1 and βPIX or GIT1 was detectable (**Fig. 3.8c**; **Supplementary Information, Fig. 3. S6f**), and modulating PEAK1 expression levels via siRNA in MDA-MB-231 cells revealed a decrease in GIT1 recruitment (**Fig. 3.8d-g**) and βPIX localization to PXN FAs (**Supplementary Information, Fig. 3. S6g, h**). These data support a model where AXL signaling promotes the recruitment of the βPIX/GIT1/PAK1 into PXL focal adhesion through the CRKII/PEAK1 module.

Figure 8

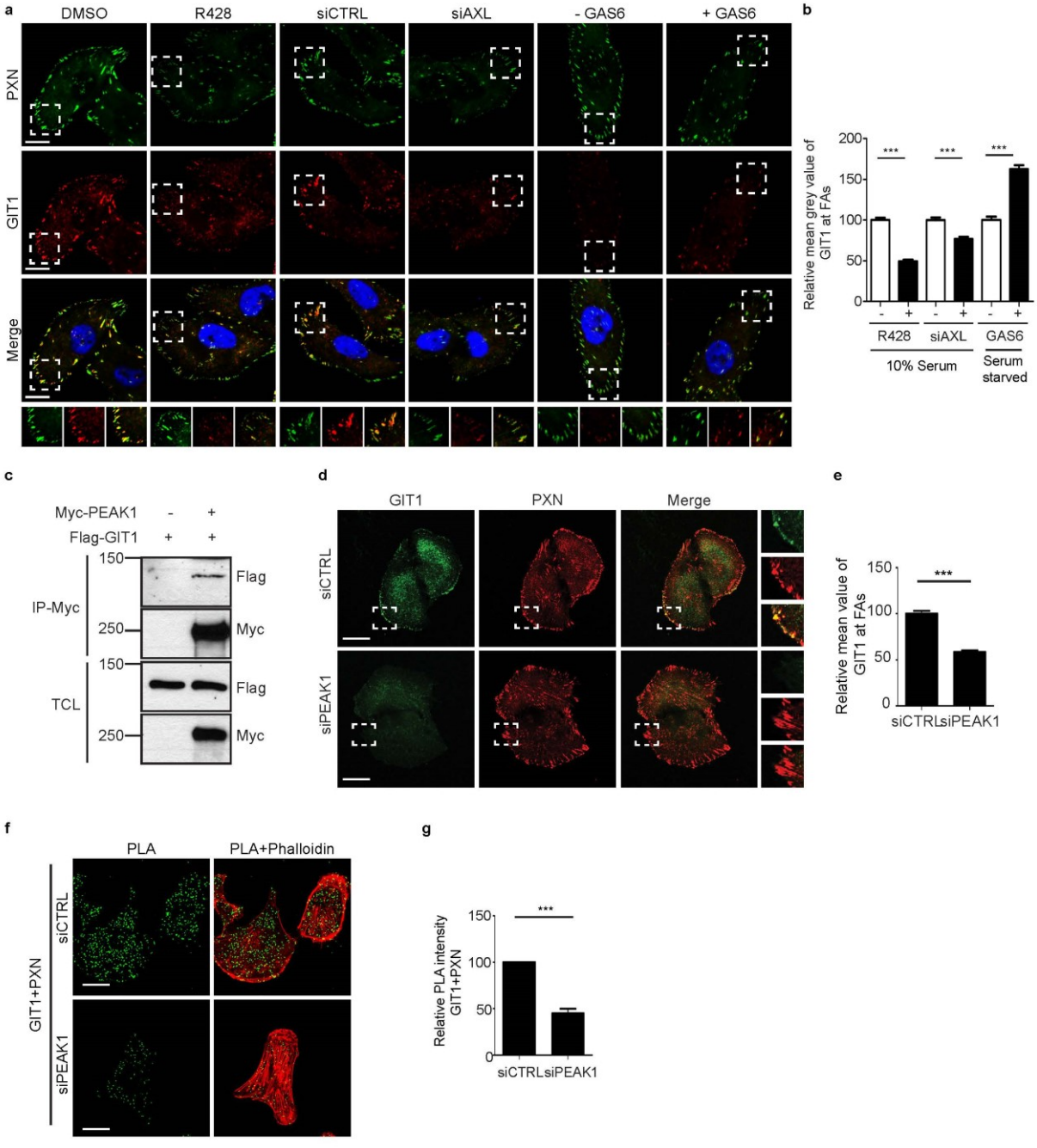
a
DMSO
R428
siCTRL
siAXL
- GAS6
+ GAS6
PXN
GIT1
Merge
b
Relative mean grey value of GIT1 at FAs
200
150
100
50
0
***
***
***
- + - + - +
R428
siAXL
GAS6
10% Serum
Serum starved
c
Myc-PEAK1 - +
Flag-GIT1 + +
150
250
IP-Myc
Flag
Myc
150
250
TCL
Flag
Myc
d
GIT1
PXN
Merge
siCTRL
siPEAK1
e
Relative mean value of GIT1 at FAs
150
100
50
0
***
siCTRL
siPEAK1
f
PLA
PLA+Phalloidin
GIT1+PXN
siCTRL
siPEAK1
g
Relative PLA intensity GIT1+PXN
150
100
50
0
***
siCTRL
siPEAK1

Figure 3.8 AXL/PEAK1 complex regulate recruitment of FA disassembly complex.

(**a**) Representative confocal images of MDA-MB-231 cells treated with DMSO or 1μM R428, transfected with 100nM of siCTRL or siAXL or serum-starved and treated with GAS6 for 20min. Cells were stained for PXN (green), GIT1 (red) and Dapi (blue). Dashed boxes are used to depict the location of the zoomed images. (**b**) Quantification of the mean grey value of GIT1 at PAXILLIN positive FAs shown in (h). *** $P < 0.0001$. Scale bar, 20μm. (**c**) PEAK1 interacts with GIT1. Lysates of 293T cells expressing the indicated plasmids were used for anti-Myc immunoprecipitation. Levels of Flag-GIT1 is detected via western blotting. (**d**) PEAK1 regulates GIT1 localization at FA sites Representative confocal images of MDA-MB-231 cells transfected with either 100nM siCTRL or siPEAK1. Cells were stained for GIT1 (green) and PXN (red). (**e**) Quantification of the mean grey value of GIT1 at PXN-FAs shown in (h). *** $P < 0.0001$. (**f**) PEAK1 expression levels modulate GIT1 recruitment to FA sites. Representative confocal images of MDA-MB-231 cells transfected with 100nM siCTRL or siPEAK1. PLA kit was used to analyze the localization of GIT1 at PXN-FAs. (**g**) Quantifications of the number of PLA signals per cell per condition. *** $P < 0.01$ (n=3 experiments, 15 cells per condition per experiment). Scale bar, 20μm.

Genetic inactivation of PEAK1 in TNBC cells decreases their tumor growth and metastasis *in vivo*

To assess the function of this pseudo-kinase in an *in vivo* context, we generated CRISPR-Cas9 PEAK1 knockout in MDA-MB-231 luciferase-expressing cells (PEAK1 KO) (Fig. 3.9a). PEAK1 KO cells displayed decreased ability to migrate and invade in comparison to control cells (**Supplementary Information, Fig. 3. S7a, b**). To investigate if PEAK1 plays a role in tumor growth and metastasis *in vivo*, PEAK1 KO cells from two different sgRNAs as well as control cells were injected into mammary fat pads of nude mice and tumor growth was followed for 4 weeks (**Fig. 3.9b**). PEAK1 KO cells showed delayed tumor growth, which was recapitulated *in vitro* in 2D and tumorsphere assays (**Fig. 3.9c**; **Supplementary Information, Fig. 3. S7c-f**). Mice bearing KO tumors for PEAK1 showed no lung metastases when compared with mice harboring wildtype tumors (**Fig. 3.9d**). The number of Circulating Tumour Cells (CTCs) was lower in mice bearing PEAK1 KO tumors in comparison to mice harboring wildtype tumors (**Fig. 3.9e**). To bypass the primary tumor growth defect, we conducted an *in vivo* experimental metastasis assay by injecting MDA-MB-231-Luc wildtype or PEAK1 KO cells into the lateral tail vein of nude mice. Metastasis progression was followed for 7 weeks by bioluminescence imaging. Knockout of PEAK1 in MDA-MB-231-Luc cells significantly repressed the ability of the cells to colonize lungs (**Fig. 3.9f, g**). Collectively, these data suggest that PEAK1 is required for both tumor growth and metastasis in TNBC cellular model.

Figure 9

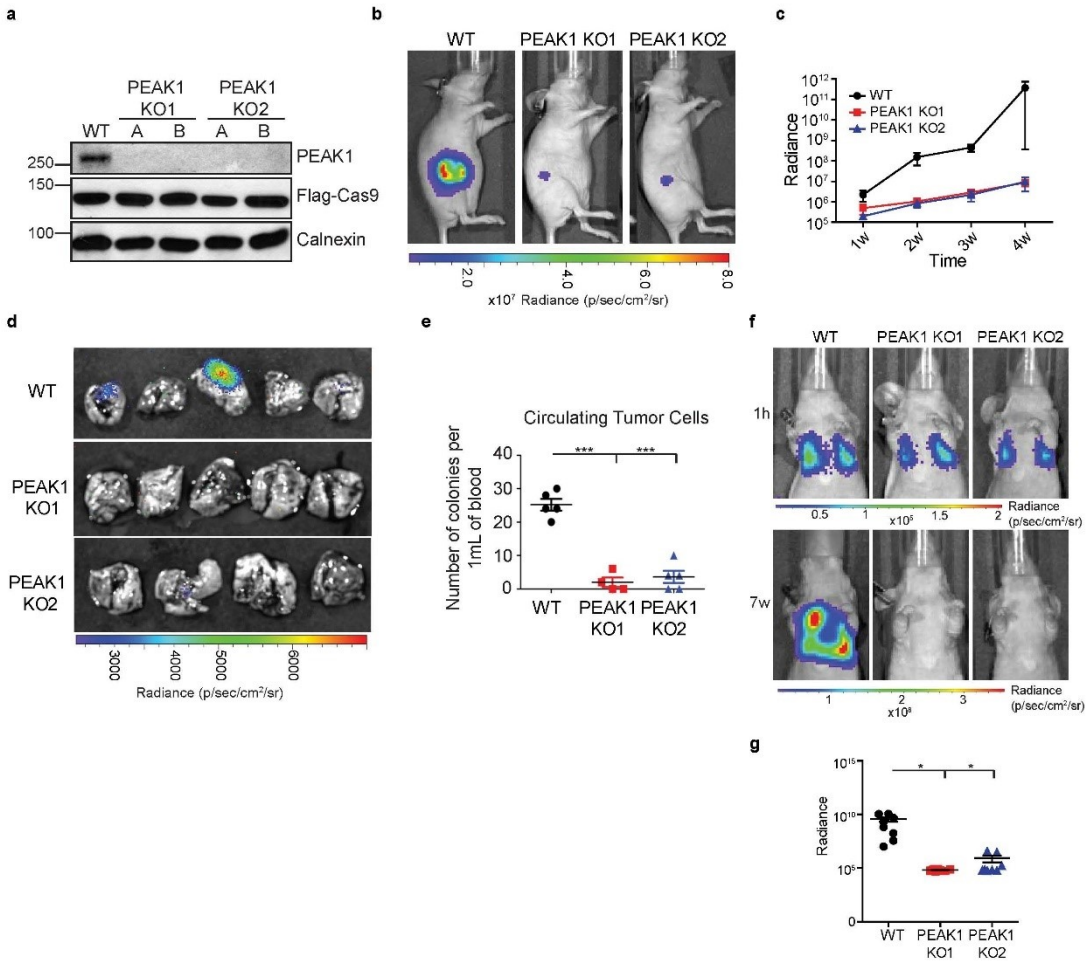

Figure 3.9 PEAK1 expression regulates tumor growth and metastasis of TNBC *in vivo.*

(**a**) Lysates of MDA-MB-231-Luc CRISPR PEAK1 knockout clones. (**b**) Representative in vivo bioluminescent images of fat-pad injected mice with MDA-MB-231-Luc WT or CRISPR PEAK1 KO cells 4 weeks post-injection. (**c**) Bioluminescence quantification of tumor growth at different weeks post-injection of mice bearing MDA-MB-231-Luc WT (n=5), PEAK1 KO1 (n=5) or PEAK1 KO2 (n=5). (**d**) Representative bioluminescent lung images of mice shown in (b). For the lungs of the mice bearing CRISPR PEAK1 KO tumors, lungs were dissected once the tumor reached the size of the WT tumors. (**e**) Circulating tumor cells isolated from mice-bearing MDA-MB-231-Luc WT or PEAK1 KO mammary tumors. *** $P < 0.0001$ (n=5 for each group). (**f**) PEAK1 regulates metastasis of TNBC cells *in vivo.* Representative in vivo bioluminescent images of tail-vein injected mice with MDA-MB-231-Luc WT or CRISPR PEAK1 KO cells 1hr and 7 weeks post-injection. (**g**) Bioluminescence quantification of lung metastases 7 weeks post-injection of mice bearing MDA-MB-231-Luc WT (n=8), PEAK1 KO1 (n=8) or MDA-MB- PEAK1 KO2 (n=8). * $P < 0.05$.

Figure 10

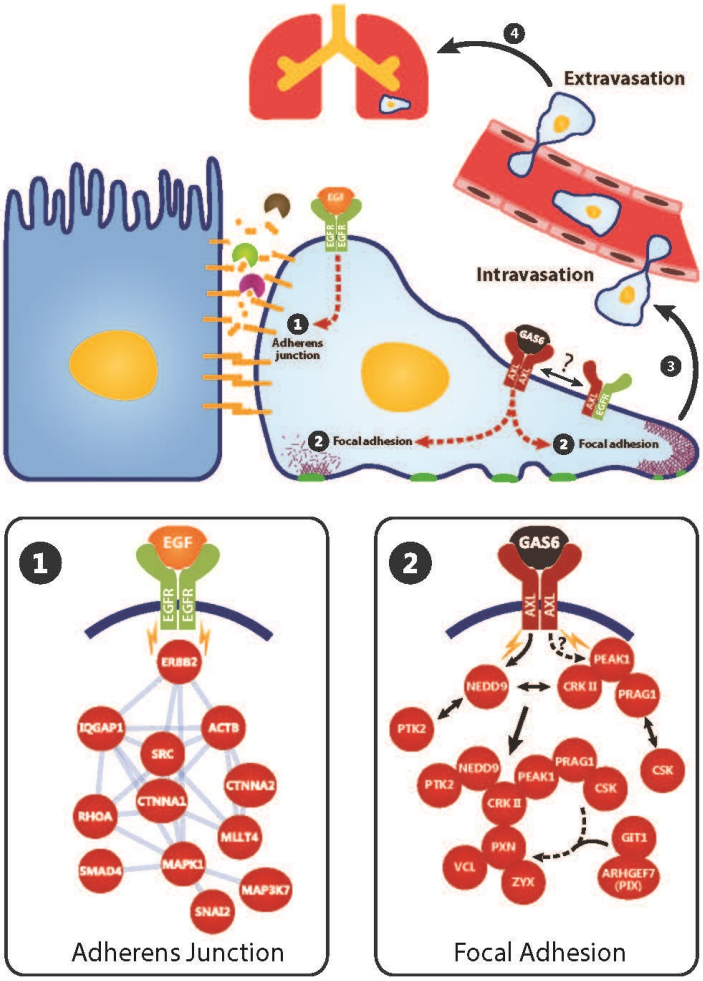

Figure 3.10 Schematic model of AXL and EGFR signaling in a cancer cell, where EGFR modulates adheren junctions and AXL modulates the FA turnover.

Upon EGF stimulation, EGFR induces the expression of MMPs to degrade the adheren junctions. Once cell-cell contact is lost, AXL activation by GAS6 or EGFR can lead to the modulation of FA turnover at the rear or front end of the cell. In specific, AXL directly phosphorylates NEDD9 to recruit its complex formation with PTK2 and CRKII. Simultaneously, AXL can phosphorylate (directly or indirectly) PEAK1, in complex with PRAG1 and CRKII, and recruit PTK2/NEDD9/CRKII/PEAK1/PRAG1 to PXN positive FAs. Upon PEAK1 phosphorylation, CSK is recruited to PEAK1/PRAG1 complex at FAs to induce tyrosine phosphorylation of PXN. In addition, PEAK1 can also recruit βPIX/GIT1 complex to PXN positive FAs to induce FA disassembly and hence turnover.

Discussion

The current view of AXL signaling is limited to the activation of downstream signaling intermediates shared with other RTKs [469], such as AKT, which fails to explain the unique pro-invasion influence of AXL. By performing an AXL phosphoproteomic screen, we explain how this RTK, in comparison to EGFR, facilitates cancer cell invasion and metastasis by strongly modulating the biological process of FA turnover. We report that AXL can be detected at FAs, and further work is required to determine how AXL traffics to these structures. At a molecular level, AXL activation leads to a modulation of the FA complex NEDD9/CRKII and their novel partner PEAK1. We reveal that phosphorylated PEAK1 at PXN FA sites is a major mediator of PXN tyrosine phosphorylation, via its complexing with PRAG1 atypical CSK-associated kinase activity. This recruits the FA disassembly complex βPIX/GIT1/PAK1 and ultimately increases FA turnover (**Fig. 3.10**). PRAG1 recently found to engage in a phosphotyrosine-dependent interaction with CSK, promotes CSK kinase activity, yet no specific substrate was identified [462]. Here, we find that PEAK1, in complex with PRAG1, phosphorylates PXN in a CSK-dependent manner, revealing the first specific substrate for this atypical pseudo-kinase/kinase complex. Interestingly, EPHA2 was found to be phosphorylated by AXL from our phosphoproteomic data and to interact with wildtype PEAK1 and not mutant from our BioID data. A recent study has shown EPHA2 signaling to promote cell motility by modulating FA dynamics [470]. This suggests that AXL may heterodimerize and transactivate EPHA2 to mediate PEAK1 phosphorylation and modulate FA turnover. Similar to AXL, PEAK1 expression in many cancer models correlates with mesenchymal features, disease relapse and therapy resistance [471, 472]. Developing strategies to interfere with a pseudo-kinase such as PEAK1, for example by pharmacologically targeting its bound kinases, may prove useful to block cell invasion and metastasis.

The effects of AXL activation are not limited to FA dynamics. We have also revealed links to regulation of the actin cytoskeleton, GTPase regulation, and phagocytosis. It will be important to compare the activation of these other networks by AXL and other RTKs and to probe their function in cell invasion. In addition, we used soluble GAS6 as a tool for AXL activation. Other sources of GAS6 can also be used such as PS liposomes that are bound to GAS6, where AXL

interaction with GAS6 can mediate its uptake in the cells to activate AXL [49, 51]. The experimental model that we chose here, namely activation of AXL by its ligand GAS6, has the advantage of being controllable *in vitro*, yet it is most likely a simplified model of the diversity of interactions that AXL can engage in at the cell surface to become activated. For instance, a pool of AXL is reported to co-signal with EGFR in TNBC cells to diversify signaling [57, 473]. Overall, defining the phosphoproteome of EGFR/AXL in the future may reveal additional therapeutic targets to limit metastasis.

Methods

Cell culture, treatments, transfections, and infections

MDA-MB-231, Hs578T, HEK293T (293T), and Hela cells were cultured in DMEM, supplemented with 10% fetal bovine serum (Gibco) and 1% Penicillin/streptomycin antibiotics (Wisent). Flp-In^{TM} T-REx^{TM} 293 cells were obtained from Life technologies. MDA-MB-231, Hs578T and Hela cells were obtained from ATCC and were transfected using Lipofectamine 2000 (Invitrogen) according to manufacturer instructions. 293T cells were transfected using Calcium phosphate. MDA-MB-231 and Hs578T cells were serum starved overnight prior to treatment with GAS6 recombinant media for the indicated time. These cells were also treated with 1μM R428 (Apexbio) for 1 hr. siRNA transfections were performed at a concentration of 100μM for 72 hours using the siRNA indicated in **Table 3. SII**. Lentiviral and retroviral infections were carried out by transfecting 293T cells using the plasmids indicated in **Table 3. SIII**. Viral supernatants were harvested 24hrs later and added to MDA-MB-231 cells in the presence of 10μg/mL of polybrene.

Plasmids

The plasmid pcDNA-hGAS6-His, a kind gift from Dr. Eric Maser, was used to generate pcDNA5-pDEST-hGAS6-His by Gateway cloning system using the primers indicated in **Table 3. SIV**, to produce the GAS6 conditioned media. pEGFP-NEDD9 and pcDNA3.1-HA-NEDD9 were a kind gift from Dr. Erica Golemis and were used to generate pcDNA5-pDEST-BirA*-Flag-N-ter NEDD9 by Gateway cloning system using the primers indicated in **Table 3. SIV**. pEGFP-NEDD9 was also used to generate pGEX4T1-hNEDD9 SD and pGEX4T1-hNEDD9 CT using the primers indicated in **Table 3. SIV** by Gibson Assembly cloning system. pOG44 and pcDNA5-pcDEST-BirA-Flag-N-ter were a kind gift from Dr. Anne-Claude Gingras to generate all BioID stable cell lines. pCIS2-HA-DOCK3 was a kind gift from Dr. David Schubert. pCMV-sport6-mouse AXL-WT was a kind gift from Dr. Rob Screaton. pRetroX-Sgk269 WT[458] was used to generate pcDNA5-pDEST-BirA*-Flag-N-ter PEAK1 WT,

pcDNA5-pDEST-BirA*-Flag-N-ter PEAK1 3PA, and pCS-6Myc-hPEAK1 using Gateway cloning system. pCS-6Myc-hPEAK1 3PA and pCS-6Myc-hPEAK1 Y531F were generated by site-directed mutagenesis using the primers indicated in **Table 3. SIV**. pCMV5-HA- ARHGEF7 was a kind gift from Dr. Liliana Attisano. pGEX2TK GST-PXN 1-313 and pGEX2TK GST-PXN 329-559, used in PXN *in vitro* kinase assay were generated as previously described [474]. pXM139-CSK was generated as previously described [475].

Stable Isotope Labelling by Amino acids in Cell culture (SILAC)

Hs578T cells were seeded in equivalent amounts for 50% confluency and let adhered to the plate. 24hrs later, media was changed in one plate with SILAC heavy media (500mL Arginine and Lysine free media (Cambridge isotope cat no. DMEM-500), 10% dialyzed fetal bovine serum (Invitrogen Cat no. 26400-036), 1% Penicillin/streptomycin antibiotics (Wisent), 50mg Proline (Cambridge Isotopes cat no. ULM-8333-0.1), 0.4mM heavy Arginine (Cambridge Isotopes cat no. CNLM-539-H-0.25), 0.275mM heavy Lysine (Cambridge Isotopes cat no. CNLM-291-H-0.25)) and the other with SILAC light media (500mL Arginine and Lysine free media (Cambridge isotope cat no. DMEM-500), 10% dialyzed fetal bovine serum (Invitrogen Cat no. 26400-036), 1% Penicillin/streptomycin antibiotics (Wisent), 50mg Proline (Cambridge Isotopes cat no. ULM-8333-0.1), 0.4mM Arginine (Cambridge Isotopes cat no. ULM-8347-0.1), 0.275mM heavy Lysine (Cambridge Isotopes cat no. ULM-8766-0.1)). Cells were passaged for 8 passages for heavy/light amino acids incorporation. The cell labeling was validated via mass spectrometry to have 99.9% incorporation.

SILAC sample preparation

SILAC cells were serum starved in Serum-free media for 24 hours. Heavy labeled cells were then treated with GAS6 recombinant media for 5, 10, or 20min and light labeled cells were treated with control media for the same time points. Cells were lysed with Urea lysis buffer (8M Urea (Sigma), 20mM HEPES pH 8.0, 10mM NaF, 1mM $Na_4P_2O_7$, 1mM NA_3VO_4, 1X complete protease inhibitor). Lysates were sonicated 3x at 30% amplitude for 30 seconds and cleared by centrifugation. Proteins were quantified via BioRad DC^{TM} Protein Assay reagents. An equal

quantity of proteins was mixed (light and heavy) for each time point. A total of 3mg or 20mg of protein was trypsin digested for the TiO_2 enrichment or pY100 immunoaffinity bead immunoprecipitation, respectively.

Trypsin digestion

Trypsin digestion was performed by adding 10 µl of trypsin to each sample (1 µg of trypsin [T6567-5×20µg, Sigma] in 200 µl of 20 mM Tris-HCl, pH 8.0). Beads (BioID) and whole lysates (Phosphoproteomics) were incubated at 37°C on a rotator for ~15-16 h. Next day, 1 µg of trypsin was added again for an additional 2h of trypsin digestion and samples were centrifuged for 1 min at 2000 RPM at RT. The supernatant was kept in a separate tube and beads were washed twice with 100 µl of water (8801-7-40, 4L, Caledon), while each supernatant was pooled with the collected supernatants. Formic acid (94318-250ml, Sigma) was added to the solution at a final concentration of 5%. Samples were centrifuged for 10 min at 16 000 g at RT. The supernatant was transferred and dried in a SpeedVac during 3h at 30°C. Samples were then resuspended in 15 µl of formic acid (5%) and stored at -80°C.

Phosphopeptide enrichment

For TiO_2 enrichment, titanium dioxide beads (Canadian Life Science) were resuspended in binding solution (80% Acetonitrile, 3%TFA, 290mg/mL DHB (Sigma) to have a final concentration of 200µg/µL. Digested peptides are also resuspended in 200µL of binding solution. Bead slurry (beads + binding solution) is added to the peptide solution in 1:2 ratio protein: beads (3mg of peptides:6mg of beads). The peptide-beads solution is incubated on a rotator for 30min at room temperature. Beads were then centrifuged at 5000xg for 1min and washed 3x with 75µL of 30% ACN, 3%TFA. Another 3 washes were carried out with 75µL of 80% ACN, 0.3%TFA. Beads are then eluted 2x with 75µL of 15%NH_4OH, 40% ACN. Eluted peptides are then dried by speed vacuuming for 2hrs. For phosphotyrosine enrichment, PTMScan® Phospho-Tyrosine Rabbit mAB (p-Tyr-1000) kit (Cell Signaling) was used according to manufacturers' instructions. TiO_2 enrichment and pY100 immunoaffinity precipitation were done in two biological independent replicates.

Phosphoproteomics

Phosphopeptides were analyzed by nano-LC-MS/MS on an Orbitrap Fusion (ThermoFisher Scientific, Bremen, Germany). A 120 minutes gradient was applied for the LC separation and standard proteomics parameters were used for a shotgun top 22 analysis and MS3 scanning upon detection of a phosphoric acid neutral loss. Phosphoprotein identifications and phospho-modulation analyses were performed using MaxQuant [476] (version 1.6.1.0) against the human RefSeq protein database (version July 29, 2016) and we considered as modulated phosphosites showing a normalized Log2 (Avg (H/L ratio)) ≤ -0.5 or ≥ 0.5 at either 5, 10 or 20 minutes. We compared our AXL phosphoproteomic data to a combination of two EGFR phosphoproteomic studies [451, 452]. This comparison was performed on AXL and/or EGFR phospho-modulated proteins showing a normalized Log2 (Avg (H/L ratio)) ≤ -0.5 or ≥ 0.5 at either time points.

Proximity-dependent biotin identification (BioID)

BioID experiments were carried out as described previously [477, 478]. Briefly, Flp-In^{TM} T-REx^{TM} 293 cells were engineered to express BirA*-Flag-NEDD9, BirA*-Flag-PEAK1 WT, BirA*-Flag-PEAK1 3PA or the control BirA*-Flag-EGFP in a *Tetracycline*-inducible manner (1 µg/ml) by transfecting Flp-In^{TM} T-REx^{TM} 293 cells with 2µg of pOG44 and 500ng of BirA*-Flag-NEDD9 or BirA*-Flag-PEAK1 using Lipofectamine 2000 (Invitrogen). Cells were then selected by Hygromycin for 12 days. Positive clones were grown in two 15-cm plates prior to treatments with Tetracycline and biotin (50 µM). After 24h of treatments, cells were harvested at ~90-95% confluence. The medium was discarded, the cells were washed with 5 ml ice-cold PBS and scraped from the plates to be transferred into 15 ml tubes. Tubes were centrifuged for 5 min at 500g at 4°C. This washing step was repeated two times and cell pellets were kept at -80°C. Later, a 50-ml stock of RIPA buffer was prepared and supplemented with 500 µl of 100 mM PMSF (P7626-1G, Sigma), 50 µl of 1M DTT (15508013, 5 g, Thermo Fisher) and 100 µl of protease inhibitor (P8340-1ml, Sigma). Cell pellets were thawed, resuspended in 1.5 ml of supplemented RIPA buffer and 1 µl of benzonase (71205-3, 250 U/µl, EMD Millipore) was added into each sample. Samples were sonicated three times during 30 secs at 30% amplitude

with 10-sec bursts and 2 seconds of rest in between. Samples were then centrifuged for 30 min at 16 000 g at 4°C. After centrifugation, 20 µl of supernatant was kept to evaluate levels of protein expression and biotinylation by immunoblotting. The remaining lysate was incubated with 70 µl of pre-washed streptavidin beads (17-5113-01, 5 ml, GE Healthcare) during 3 h on a rotator at 4°C. Samples were centrifuged for 1 min at 2000 RPM at 4°C and the supernatant was discarded. Beads were washed three times with 1.5 ml of RIPA buffer and centrifuged for 1 min at 2000 RPM at 4°C. Beads were washed three times by resuspending in 1 ml of 50 mM Ammonium Bicarbonate (ABC) (AB0032, 500G, Biobasic) and centrifuged for 1 min at 2000 RPM and 4°C. Samples were trypsin-digested (see Trypsin digestion method) and injected into an Orbitrap Velos Mass Spectrometer (Thermo Fisher). Peptides search and identification were processed using the Human RefSeq database (version 57) and the iProphet pipeline [479] integrated into Prohits [480]. The search engines were Mascot and Comet, with trypsin specificity and two missed cleavage sites allowed. The resulting Comet and Mascot search results were individually processed by PeptideProphet [481], and peptides were assembled into proteins using parsimony rules first described in ProteinProphet [482] into a final iProphet [479] protein output using the Trans-Proteomic Pipeline. For each duplicated bait, we used SAINTexpress (version 3.6.1, nControl:4, fthres:0, fgroup:0, var:0, nburn:2000, niter:5000, lowMode:0, minFold:1, normalize:1, nCompressBaits:2) on proteins with iProphet protein probability ≥ 0.85 with unique peptides ≥ 2, and considered statistically significant NEDD9 or PEAK1 interactors displaying a BFDR threshold ≤ 0.02 against 4 biological replicates of the BirA*-Flag-EGFP control. Prey's abundance was normalized by applying the SAF [483] (Spectral Abundance Factor) method. The SAF metric was calculated by dividing the protein's spectral count on the protein's length (from UniProt). We used ProHits-viz [484] to generate dot blot analyses.

Bioinformatics analyses

All proteomics data were imported into a local MySQL database. Graphical representations of protein-protein networks were generated with Cytoscape[485] (version 3.6.1) using the application GeneMANIA [486] (version 3.4.1 and its human database version 13 July 2017) or the built-in PSICQUIC client by merging networks generated from Intact, Mint, Reactome and

UniProt databases. Each protein was annotated in Cytoscape by importing the Gene Ontology Annotation Database (GOA) [487] and our phospho-modulation values, in order to identify relevant phospho-modulated functions. We also identified phosphatases and kinases families by importing the Phosphatome [488] and Kinome [489] classifications. Functional enrichment analyses of identified interactors were assessed with g: Profiler [490] against the Gene Ontology and KEGG [491] databases with moderate hierarchical filtering and by applying a statistical correction with the Benjamini-Hochberg FDR method. Dot plots of over-represented KEGG pathways (p-value cutoff = 0.05) were generated with the ClusterProfiler [492] package in R (www.r-project.org). Profiling of kinetic phosphorylation patterns was performed by fuzzy c-means clustering on modulated phosphosites (localization probability ≥0.7), in the R environment using the MFuzz package [493] with optimized parameters [494]. By using the *mestimate* function, we settled the appropriate fuzzifier parameter at 2.881. After establishing the right fuzzifier parameter, we evaluated the optimal number of clusters with the function *Dmin* by calculating the minimum distance between centroids from a range of 2 to 16 clusters with an increment of 1, and we established at six the optimal number of clusters. After filtering-in the six clusters' core at a membership value ≥ 0.5, we extracted a window of 17 amino acids surrounding each clustered phosphosites and characterized, with the probability logo generator pLogo [495], overrepresented sequence motifs matching known kinases substrate recognition motifs.

Production of PEAK1 KO cells via CRISPR/CAS9-mediated gene targeting

MDA-MB-231 cells were infected with the CAS9 plasmid cited in **Table 3. SIII** and selected with 10µg/mL Blasticidin for 10 days. MDA-MB-231-CAS9 cells were then infected separately with three different sgRNA plasmids described [496] in **Table 3. SIII**. These cells were selected with 1 µg/mL Puromycin for 3 days and were isolated in single cells in 2- 96 well plates. Single clones for each knockout were grown to maintain a homogenous pool of PEAK1 knockout cells. After testing multiple clones, we chose two clones for each knockout to further validate them. Cells that survived and grew colonies were tested for their efficiency of PEAK1 deletion via western blotting. To generate cells that are Luciferase positive, we infected the MDA-MB-231-CAS9 control and MDA-MB-231-CAS9 PEAK1 knockout cells with a luciferase plasmid

mentioned in **Table 3. SIII**. Cells were selected with 500µg/mL Hygromycin for 5 days. For animal experiments, 2 clones (A and B) of 2 (KO1 and KO2) out of the 3 different PEAK1 sgRNA knockout cells were mixed to create PEAK1 knockout pools (KO1 and KO2) to increase the heterogeneity of the model and decrease the specific off-target effects by the different sgRNA.

Immunofluorescence confocal microscopy

Cells plated on glass coverslips were fixed with 4% Paraformaldehyde (PFA) and permeabilized in 0.1% Triton in PBS. Cells were blocked with 2% BSA in 0.1% Triton and incubated with the indicated antibodies for one hour at room temperature. Cells were then washed 3 times with 0.1% Triton in PBS and incubated with the corresponding secondary antibody for 30min at room temperature. Following this incubation, cells were washed again 3 times with 0.1% Triton in PBS and stained for Phalloidin using the indicated antibody in **Table 3. SI** for 30min at room temperature. Cells were washed 3 additional times with 0.1% Triton in PBS and coverslips were mounted on slides using SlowFade Gold reagent (Invitrogen). Pictures were acquired with Zeiss LSM710 confocal microscope at objective 63X. Experiments were done in triplicates and 15 cells were used per condition per experiment for quantifications.

Proximity Ligation Assay (PLA)

Cells plated on glass coverslips were fixed, permeabilized, blocked and incubated with the indicated antibodies as mentioned in immunofluorescence. Proximity ligation assay was then performed using DuoLink in situ PLA detection kit (Sigma). Hybridization with PLA probes (plus and minus) for rabbit and mouse, ligation and amplification of the PLA signal were performed according to manufacturer instructions. Images were taken using Zeiss LSM710 confocal microscope at objective 63X. PLA signal was quantified per cell using ImageJ software. PLA signal is depicted in green and Phalloidin in red. Experiments were done in triplicates and 15 cells were used per condition per experiment for quantifications.

Boyden migration and invasion assay

Boyden assays were performed using 8 µm pores Boyden Chambers (24-well, Costar). For the invasion assays, upper chamber was coated with 6 µL of Matrigel (BD Biosciences) dissolved in 100 µL of DMEM. Cells were detached and washed with DMEM 0.1% BSA. 100,000 cells were seeded in the top chamber and allowed to migrate for 6hrs (migration) or 16hrs (invasion) toward the bottom chamber containing 10% FBS. Upper and lower chambers were then washed with 1xPBS and cells on the bottom side of the chamber were fixed with 4% PFA. Cells in the upper chambers were removed using cotton swabs and the membrane was mounted on a glass slide using SlowFade Gold reagent (Invitrogen). The average number of migrating cells in 10 independents 20× microscope fields were evaluated, and each experiment was performed in triplicates.

MTT proliferation assay

MDA-MB-231 cells were plated in 96well plate 5000 cells/100µL of regular culture media in 5 replicates (wells) for each cell type. 5-96well plates were plated for 5 different days of reading. MTT reaction mix (2.5mM MTT (Invitrogen), 15nM HEPES, red-phenol free and FBS free DMEM) was added to each well and incubated for 4hrs at 37 degrees for MTT incorporation. To stop the MTT reaction, stop solution (2% DMSO, 0.1M Glycine pH11) was added to each well for 5 min and the plate was read in an ELISA reader at 540nm wavelength. For the different day reading, the MTT reaction mix was added to the plate at the same time as the previous days for consistency. This experiment was performed in three independent replicates.

Tumorsphere formation Assay

MDA-MB-231 cells were plated in low adherence in DMEM/F12 media supplemented with 0.4% FBS, EGF (20ng/mL), FGF (10 ng/mL), Insulin (5 µg/mL) and B27 supplement (Invitrogen 17504-044) as described in (Lo et al., 2012). One week later, the quantification of tumorspheres formed was conducted using a DM IRE2 microscope (Leica).

Immunoprecipitation, GST-pulldown assay, and immunoblotting

Cells were lysed with either RIPA (50mM Tris pH7.6, 0.1%SDS, 0.5% sodium deoxycholate, 1%Nonidet P-40, 5mM EDTA, 150mM NaCl, 10mM NaF, 1mM $Na_4P_2O_7$, 1mM NA_3VO_4, 1X complete protease inhibitor) or 1%NP-40 (15mM NaCl, 50mM Tris pH7.5, 1% Nonidet P-40, 10mM NaF, 1mM $Na_4P_2O_7$, 1mM NA_3VO_4, 1X complete protease inhibitor) buffer and cell lysates were cleared by centrifugation. Proteins quantification was performed using DC™ Protein Assay reagents (Biorad). For immunoprecipitations, 1mg of protein lysate was incubated with the indicated antibody and corresponding agarose beads (Protein A or G) for 3 hrs at 4 degrees. Immunoprecipitates were then washed with the corresponding lysis buffer and denatured in 6X lysis buffer. For GST-pulldowns, 1mg of protein lysate was incubated with the corresponding GST-beads for 2 hrs at 4 degrees. Lysates, immunoprecipitates, and GST-complexes, were run on SDS-electrophoresis acrylamide gels at 180V and transferred on Nitrocellulose or PVDF for 3 hrs at 4 degrees at 50V or overnight at 4 degrees at 20V. Immunoblots are then blocked with 1% BSA and incubated with the indicated primary antibodies, mentioned in **Table 3. SI**, overnight at 4 degrees or room temperature. Immunoblots are then washed with 0.01% TBST three times and incubated with the corresponding secondary antibody for 30min at room temperature. Protein signals are then revealed via Clarity™ western ECL substrate (Biorad).

GST-protein purification

A strike of the glycerol stock of the GST-Protein is grown in LB with antibiotics overnight at 37%. 24hrs later, the bacteria culture is grown in 5x the volume of LB with antibiotics and 0.1M IPTG. This culture is then put to shake at 37% for 3hrs. Once the pellet is obtained by centrifugation, 4mL of lysis buffer (1xPBX, 1%Triton, 1x complete protein protease inhibitor) was used to lyse the cells. After rupturing the cell membranes by sonication 3x of 30s, a cell debris pellet is obtained by centrifugation. The supernatant containing the GST-Protein is incubated with GST-beads for 1hr to purify the GST-tagged protein. The GST-beads are then washed and resuspended in 0.1% PBS Triton. To purify the GST-protein, GST-protein is run on a column and is eluted with 10 aliquots of elution buffer (10mM Glutathione, 50mM Tris pH

8.0). Eluates are then quantified by Quick Start™ Bradford Dye Reagent (Biorad). Concentrated elutes containing protein are pooled and placed into a centrifugal filter unit and centrifuged for 10min at 4000rpm. The purified protein is collected and stocked at -80 degrees.

Live cell imaging

MDA-MB-231 cells were transfected with 1.5µg of GFP-PXN. 24hrs later, cells were plated on 35mm Fibronectin coated glass bottom plates (MatTek Corporation). Once adhered, cells were either serum starved for GAS6 stimulation or treated with AXL inhibitor R428 for 1hr at 1uM. Cells were then imaged while incubated with GAS6 or R428 using Carl Zeiss Spinning Disk Confocal microscopy and ZEN imaging program at 1min intervals for 30min, using the EGFP laser (488nm) at 3% strength. Videos and images were obtained using IMARIS 8.0 and analyzed via Image J software. The lifetime of the FAs was measured from the time an FA appeared to the time it disappeared. FA assembly rate is the time an FA takes to increase in size and intensity. Disassembly time is the time it takes an FA intensity decreases. Cells were performed in triplicates with 90 FAs followed per condition per experiment[392].

Animal Experiments

All animal experiments were approved by the Animal Care Committee of the Institut de Recherches Cliniques de Montréal and complied with the Canadian Council of Animal Care guidelines. Tail veins and graft experiments were conducted in athymic nude NU/J mice obtained from Jackson Laboratories and mice were housed in a specific pathogen-free (SPF) facility.

Experimental Metastasis, Mammary Fat Pad Grafts and Bioluminescence Imaging

Tail veins and fat pad grafts were conducted as in [58]. Briefly, for experimental metastasis assay, 10^6 cells resuspended in PBS were injected in the lateral tail vein of 6-8 weeks old nude mice. For fat pad grafts, 10^6 cells were injected in the mammary fat pad of 3 weeks old nude mice. Xenogen IVIS 200 (PerkinElmer) and Living Image 4.2 software were used for

bioluminescence imaging. 150mg/kg of Beetle Luciferin (Promega) solution (stock of 15mg/mL in PBS) was injected intraperitoneally 10 minutes before imaging and photon flux was calculated for each mouse using a region of interest.

Blood Burden Assay (Circulating Tumor Cells (CTCs))

The quantification of circulating tumor cells (CTCs) was performed as previously described [58]. Briefly, blood was drawn via heart puncture (0.5 mL) with a 25-gauge needle and a 1 mL syringe coated with Heparin (100U/mL). Blood was plated in DMEM/F12 20% FBS and media were changed every two days. After 8 days, tumor cell colonies in the dish were counted and the tumor blood burden was calculated as the total colonies divided by the volume of blood taken as described in [497].

Statistics

Phosphoproteomic data was done in duplicates (twice for TiO_2 enrichments and twice for pY100 immunoaffinity enrichment). Data are presented as mean ± SEM from at least 3 independent experiments. Statistical analyses were performed with the GraphPad Prism Software using the Student's t-test with either paired or unpaired t-test with a two-tailed p-value with 95% confidence interval.

Acknowledgments

We thank Drs. Elena Pasquale and Kristiina Vuori for critical reading of the manuscript. We thank Drs. Liliana Attisano, Christopher E. Turner, Edward Manser and Erica Golemis for providing plasmids. We thank Dr. Denis Faubert in the IRCM Proteomics facility for the processing of MS samples and Dr. Dominic Filion for microscopy assistance. This work was supported by operating grants from the Canadian Institute of Health Research (MOP-142425 to J.F.C. and J.P.G) and National Science and Engineering Research Council of Canada (RGPIN-2016-04808 to J.F.C). A.A. and H.B. are recipients of FRQS Doctoral studentship and M.A.G. is supported by a CIHR studentship. J.-F.C. holds the Transat Chair in Breast Cancer Research. J.-F.C. was supported by FRQS Senior investigator career award.

Data Availability

The raw proteomics data, which are presented in Fig. 1, 2, 4, and 5 will be uploaded to the MassIVE archive upon publication.

Supplementary Information

AXL CONFERS CELL MIGRATION AND INVASION BY HIJACKING A PEAK1-REGULATED FOCAL ADHESION PROTEIN NETWORK

Afnan Abu-Thuraia, Marie-Anne Goyette, Carine Delliaux, Jonathan Boulais, Rony Chidiac, Halil Bagci, Dominique Davidson, André Veillette, Roger J Daly, Anne-Claude Gingras, Jean-Philippe Gratton and Jean-François Côté

- **Supplementary Figures**
- **Supplementary Figure legends**
- **Supplementary Tables**

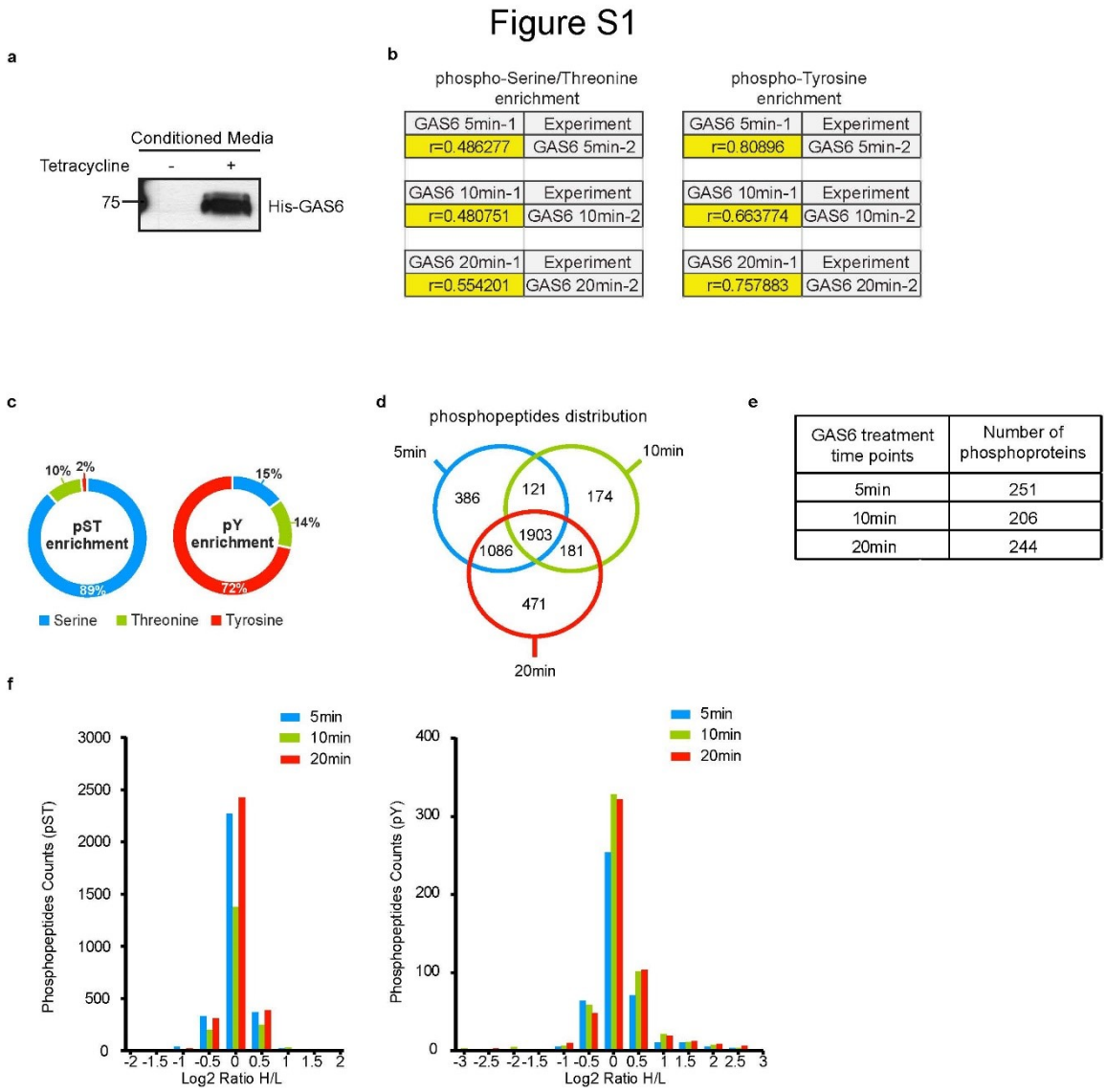

Figure 3. S1 Overview of the GAS6 phosphoproteome profiling and validations.

(**a**) Tetracycline-induced expression of His-GAS6 in the media of Flp-In™ T-REx™ 293 cells. Cells were treated with Tetracycline and Vitamin K for 24 hours. (**b**) Pearson Correlation Coefficient (r) between biological replicates of phospho-S/T and phospho-Y peptides enriched from GAS6-stimulated cells during 5, 10 and 20 min. (**c**) Pie charts indicating the percentage of Serine, Threonine, and Tyrosine phosphorylation sites identified in GAS6 treatment following pS/T and pY peptides enrichments. (**d**) Venn diagram showing the phosphopeptides distributions and overlaps between the three different time points of GAS6 stimulation. (**e**) Enumeration table of phosphoproteins identified at each GAS6 stimulation time point. (**f**) Log_2 ratio H/L distribution of pS/T or pY enriched peptides at 5, 10 and 20 min.

Figure S2

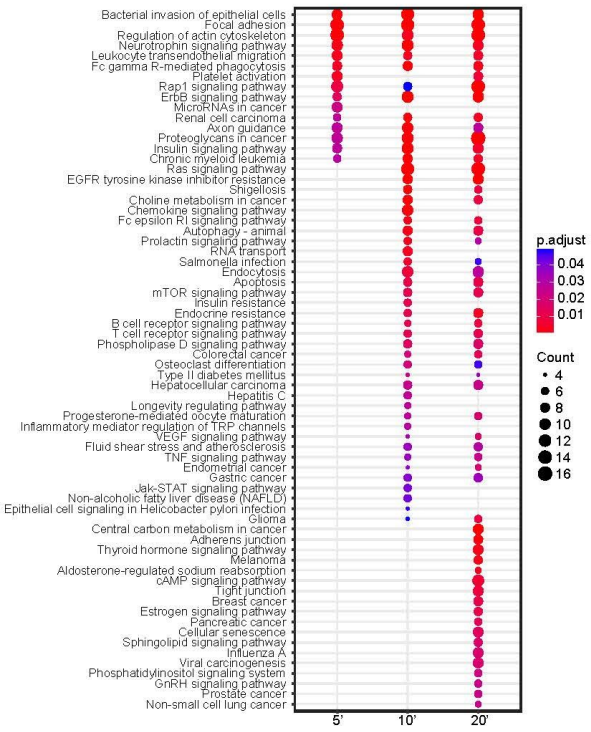

Figure 3. S2 Dot plot representation of significantly enriched KEGG pathways of GAS6 regulated phosphoproteins at the three different time points of stimulation

Circle sizes represent the number of regulated phosphoproteins associated with the specific pathway and the color of the circle represents the significant adjusted p-value.

Figure S3

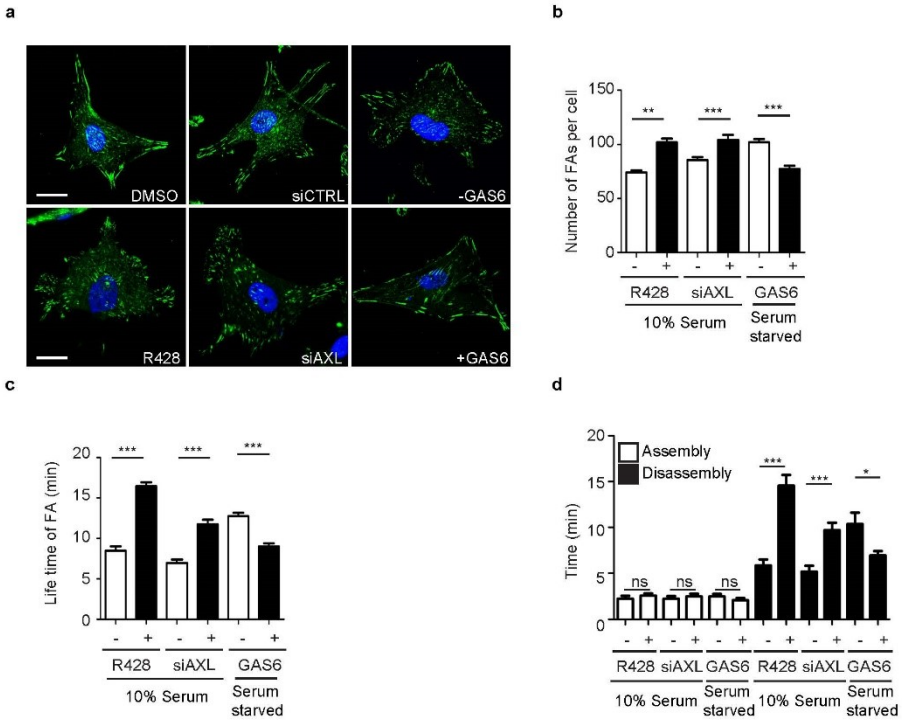

Figure 3. S3 AXL modulates FA turnover in Hs578T cells

(**a**) AXL regulates the number of FAs. Representative confocal images of Hs578T cells either treated with DMSO or 1µM R428, transfected with 100nM of siCTRL or siAXL or serum-starved and treated with GAS6 for 20min. Cells were stained for PXN (green) and Dapi (blue). (**b**) Quantification of the FA number per cell depicted in (a). ** $P < 0.005$ *** $P < 0.0001$ (n=3 experiments with 30 cells per condition). (**c-d**) Quantification of FA lifetime (c) and their assembly and disassembly time (d) of Hs578T cells transfected with GFP-PXN either treated with DMSO or 1µM R428, transfected with 100nM of siCTRL or siAXL or serum-starved and treated with GAS6 for 20min. *** $P < 0.0001$, * $P < 0.05$ (n=3 experiments with 90 FAs followed per condition).

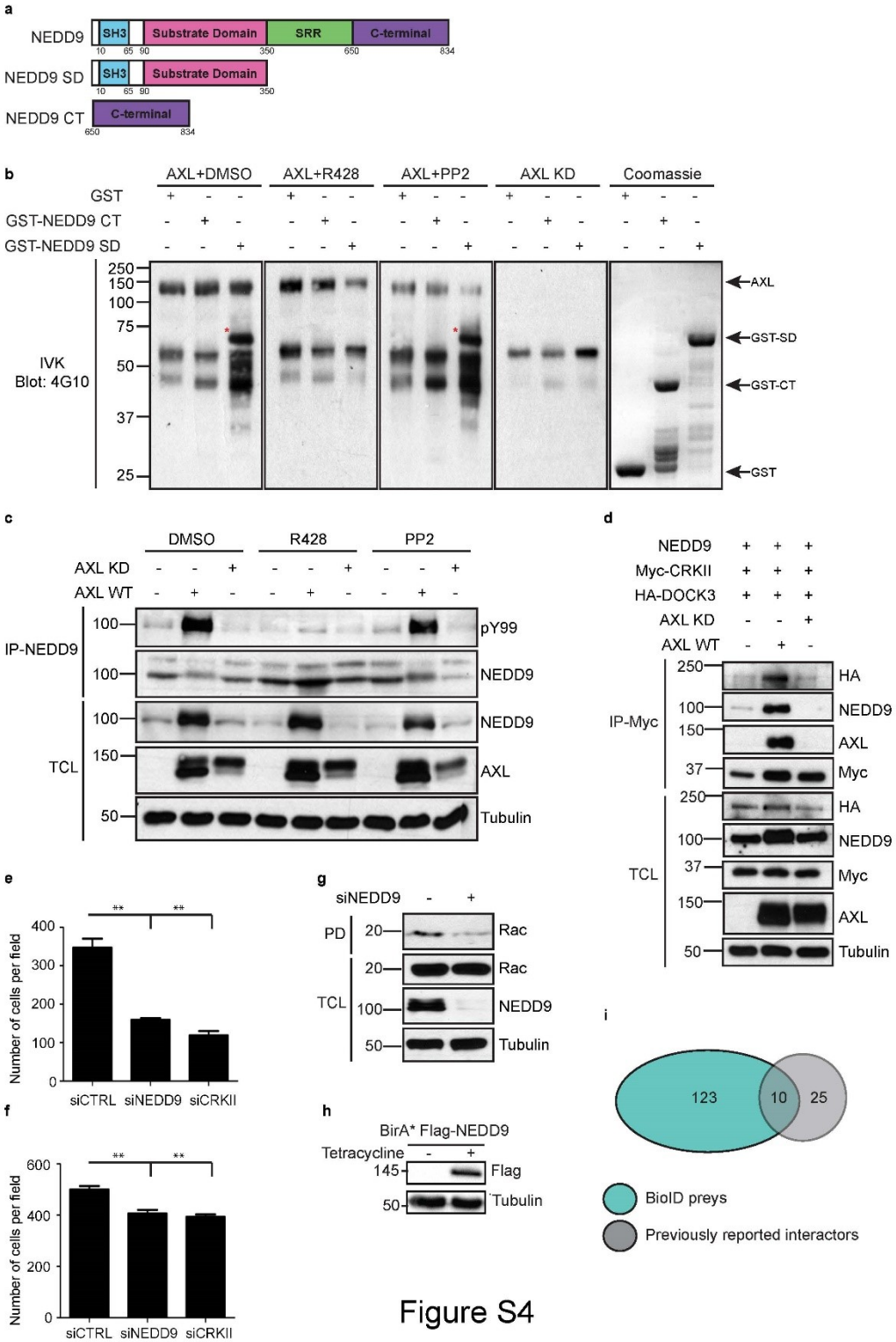
a
NEDD9
SH3
Substrate Domain
SRR
C-terminal
NEDD9 SD
NEDD9 CT
b
AXL+DMSO
AXL+R428
AXL+PP2
AXL KD
Coomassie
GST
GST-NEDD9 CT
GST-NEDD9 SD
IVK Blot: 4G10
AXL
GST-SD
GST-CT
GST
c
DMSO
R428
PP2
AXL KD
AXL WT
IP-NEDD9
pY99
NEDD9
TCL
AXL
Tubulin
d
Myc-CRKII
HA-DOCK3
IP-Myc
HA
Myc
e
Number of cells per field
siCTRL
siNEDD9
siCRKII
f
g
siNEDD9
PD
Rac
h
BirA* Flag-NEDD9
Tetracycline
Flag
i
123
10
25
BioID preys
Previously reported interactors

Figure S4

Figure 3. S4 AXL modulates NEDD9 phosphorylation levels *in vitro* and its complex formation

(**a**) NEDD9 constructs used for the Invitro kinase assay. (**b**) AXL phosphorylates NEDD9 *in vitro.* Lysates of 293T cells expressing AXL WT or KD (kinase dead) were used for anti-AXL immunoprecipitation. AXL immunoprecipitates were subjected to an in-vitro kinase assay using the constructs shown in (a) as substrates, in the presence of either AXL inhibitor (1μM R428) or Src inhibitor (5μM PP2). NEDD9 phosphorylation levels were detected via western blotting. (**c**) AXL phosphorylates NEDD9 in 293T cells. Lysates of 293T cells expressing indicated plasmids and treated with either DMSO, R428 or PP2 were subjected to anti-NEDD9 immunoprecipitation. Co-immunoprecipitates were detected via western blotting. (**d**) AXL kinase activity regulates NEDD9 complex formation with CRKII/DOCK3. Lysates of 293T cells expressing indicated plasmids were subjected to anti-Myc CRKII immunoprecipitation. Co-immunoprecipitates were detected via western blotting. (**e**) Boyden migration assay performed with MDA-MB-231 cells transfected with 100nM of siCTRL, siNEDD9 or siCRKII. The number of cells migrated was counted via DAPI staining of the membrane. ** $P < 0.0001$ (n=3, 10 fields used at 10X per condition per experiment). (**f**) Boyden invasion assay performed with MDA-MB-231 cells transfected with 100nM of siCTRL, siNEDD9 or siCRKII using Matrigel as a matrix. The number of cells invaded was counted via DAPI staining of the membrane. ** $P \leq 0.0001$ (n=3, 10 fields used at 20X per condition per experiment). (**g**) RAC1 activation levels are NEDD9 regulated in TNBC cells. MDA-MB-231 cells transfected with 100nM of siCTRL or siNEDD9 were subjected to a RAC activation Assay (GST-PAK1 PBD pulldown). RAC activation levels were detected via western blotting. (**h**) Tetracycline-induced expression of BirA-Flag-NEDD9 in Flp-In™ T-REx™ 293 cells. Cells were treated with Tetracycline for 24 hours. (**i**) A Venn diagram comparing the number of NEDD9 interactors detected in the BioID screen versus the previously reported ones.

Figure S5

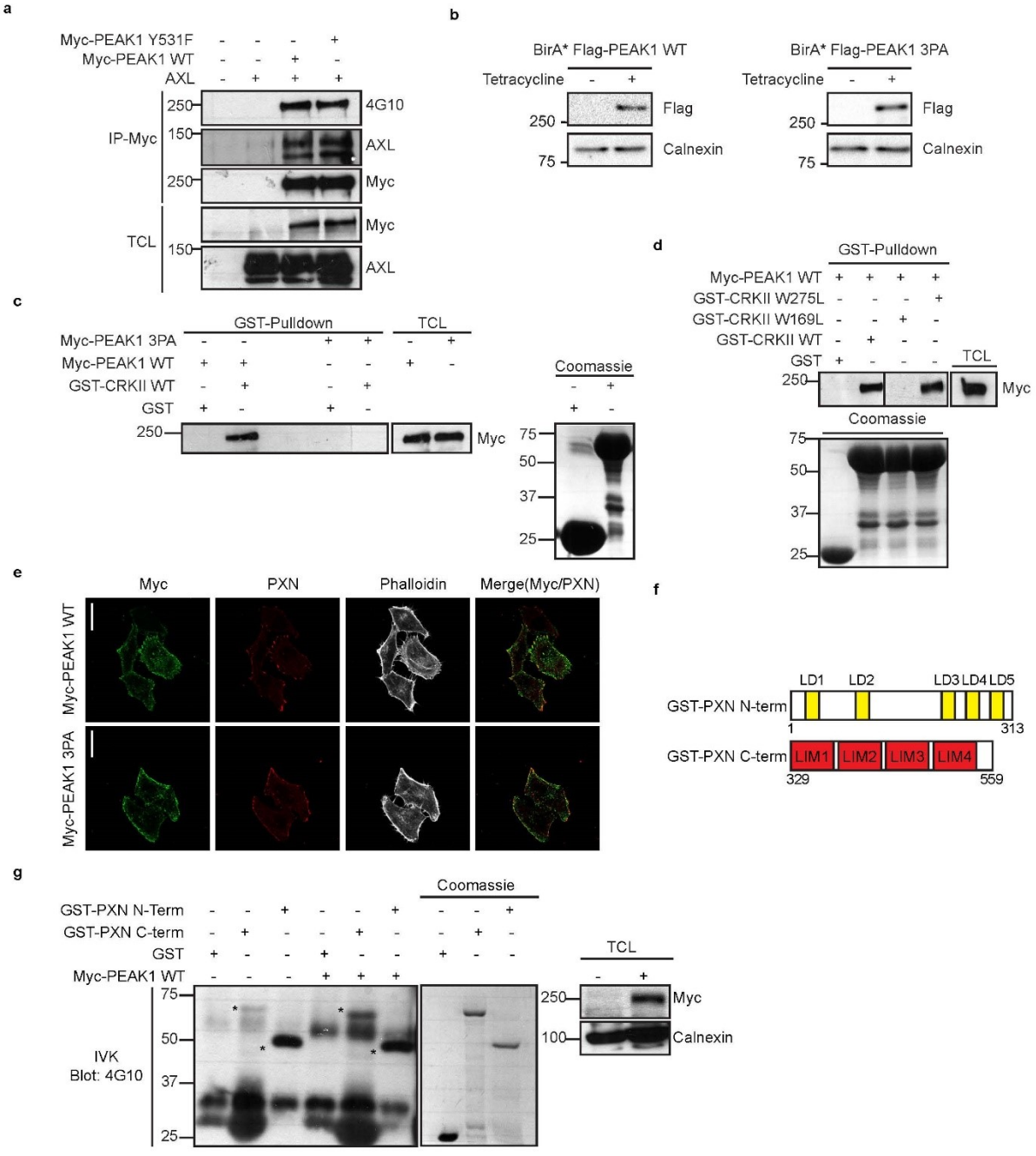
a
Myc-PEAK1 Y531F
Myc-PEAK1 WT
AXL
IP-Myc
TCL
4G10
AXL
Myc
Myc
AXL
b
BirA* Flag-PEAK1 WT
BirA* Flag-PEAK1 3PA
Tetracycline
Flag
Calnexin
c
GST-Pulldown
TCL
Myc-PEAK1 3PA
Myc-PEAK1 WT
GST-CRKII WT
GST
Coomassie
Myc
d
GST-Pulldown
Myc-PEAK1 WT
GST-CRKII W275L
GST-CRKII W169L
GST-CRKII WT
GST
TCL
Myc
Coomassie
e
Myc
PXN
Phalloidin
Merge(Myc/PXN)
Myc-PEAK1 WT
Myc-PEAK1 3PA
f
LD1
LD2
LD3
LD4
LD5
GST-PXN N-term
GST-PXN C-term
LIM1
LIM2
LIM3
LIM4
g
Coomassie
GST-PXN N-Term
GST-PXN C-term
GST
Myc-PEAK1 WT
IVK
Blot: 4G10
TCL
Myc
Calnexin

Figure 3. S5 PEAK1 interacts with CRKII and mediates PXN phosphorylation.

(**a**) Lysates of 293T cells expressing the indicated plasmids were used for anti-Myc immunoprecipitation. The levels of Myc-PEAK1 phosphorylation and AXL are detected via western blotting. (**b**) Tetracycline-induced expression of BirA-Flag-PEAK1 and BirA-Flag-PEAK1 3PA in Flp-In™ T-REx™ 293 cells. Cells were treated with Tetracycline for 24 hours. (**c**) Lysates of 293T cells expressing Myc-PEAK1 WT or 3PA mutant were used for GST-CRKII pulldown. Levels of Myc-PEAK1 is detected via western blotting. (**d**) PEAK1 binds CRKII middle SH3 domain. Lysates of 293T cells expressing Myc-PEAK1 were used for GST-CRKII pulldown using the different GST-CRKII constructs. Levels of Myc-PEAK1 is detected via western blotting. (**e**) Representative confocal images of HELA cells transfected with Myc-PEAK1 WT or 3PA mutant. Fixed cells were permeabilized and stained for Myc (green), PXN (red) and Phalloidin (grey). (n=3 experiments, 15 cells per condition per experiment). Scale bar, 20μm. (**f**) Schematic of GST-PXN domains. (**g**) PEAK1 induces phosphorylation of PXN *in vitro*. Lysates of 293T cells expressing or not Myc-PEAK1 were used for anti-Myc immunoprecipitation. Myc-PEAK1 immunoprecipitates were subjected to an in-vitro kinase assay using the GST constructs indicated as substrates, shown in Coomassie staining. PXN phosphorylation levels were detected via western blotting. The band of interest that corresponds to each substrate is indicated with a *.

Figure S6

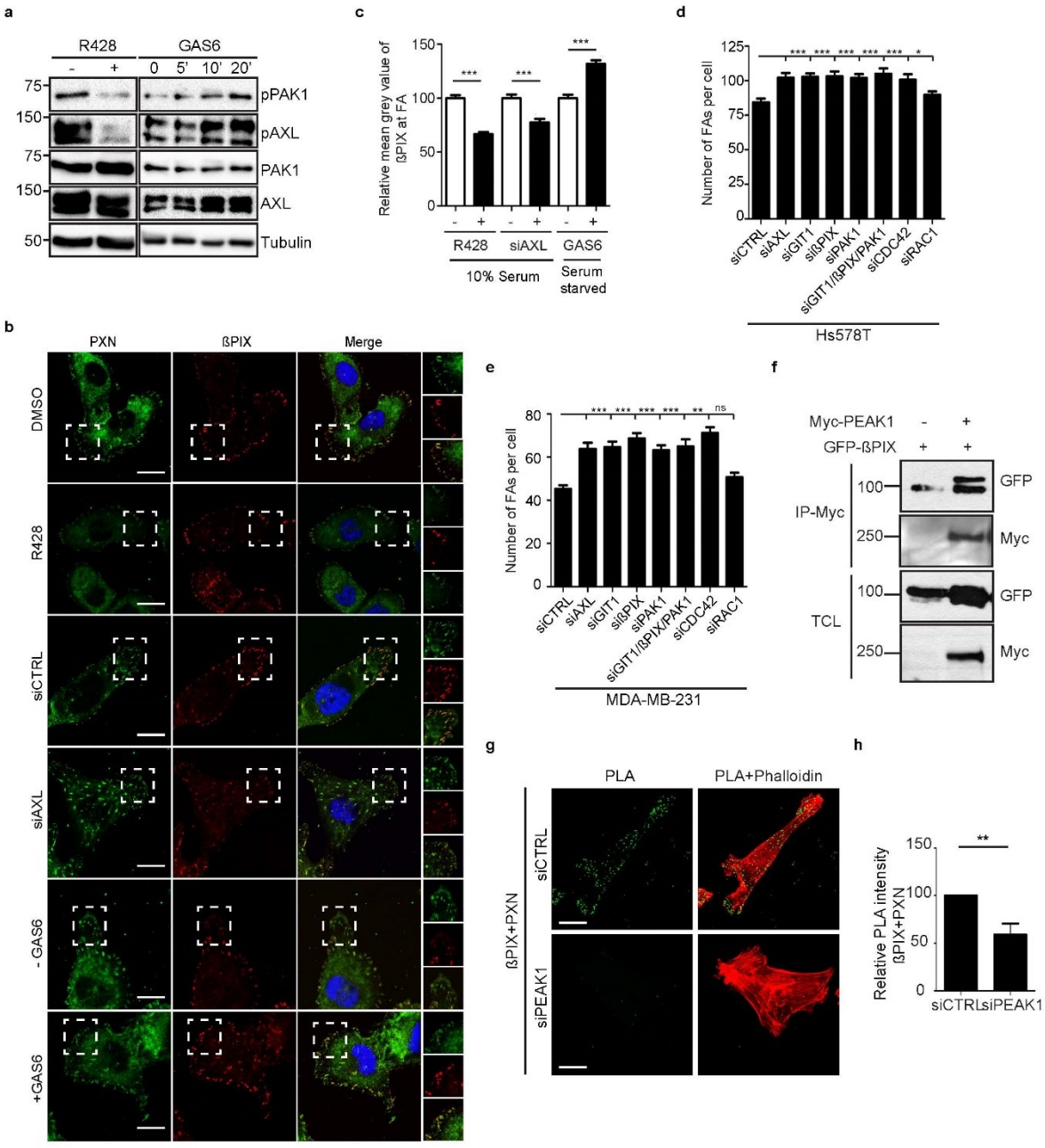
a
R428
GAS6
- + 0 5' 10' 20'
75
150
75
150
50
pPAK1
pAXL
PAK1
AXL
Tubulin
c
Relative mean grey value of ßPIX at FA
150
100
50
0
***
***
***
- + - + - +
R428
siAXL
GAS6
10% Serum
Serum starved
d
Number of FAs per cell
125
100
75
50
25
0
*** *** *** *** *** *
siCTRL
siAXL
siGIT1
sißPIX
siPAK1
siGIT1/ßPIX/PAK1
siCDC42
siRAC1
Hs578T
b
PXN
ßPIX
Merge
DMSO
R428
siCTRL
siAXL
- GAS6
+GAS6
e
Number of FAs per cell
80
60
40
20
0
*** *** *** *** ** ns
siCTRL
siAXL
siGIT1
sißPIX
siPAK1
siGIT1/ßPIX/PAK1
siCDC42
siRAC1
MDA-MB-231
f
Myc-PEAK1 - +
GFP-ßPIX + +
IP-Myc
100
250
GFP
Myc
TCL
100
250
GFP
Myc
g
PLA
PLA+Phalloidin
ßPIX+PXN
siCTRL
siPEAK1
h
Relative PLA intensity ßPIX+PXN
150
100
50
0
**
siCTRL
siPEAK1

Figure 3. S6 AXL/PEAK1 modulate βPIX/GIT1/PAK complex.

(**a**) Modulation of PAK1 phosphorylation by AXL activation or inhibition. Lysates of cells either treated with 1μM R428 for one hour or serum starved and treated with GAS6 for indicated time were analyzed with the indicated antibodies. (**b**) βPIX recruitment to FA is AXL modulated. Representative confocal images of Hs578T cells plated on coverslips and either treated with DMSO or 1μM R428, transfected with 100nM of siCTRL or siAXL or serum-starved and treated with GAS6 for 20min. Cells were then fixed, permeabilized and stained for PXN (green), βPIX (red) and Dapi (blue). Dashed boxes are used to depict the location of the zoomed images. (**c**) Quantification of the mean grey value of βPIX at PXN-FA shown in (b). *** $P < 0.0001$. Scale bar, 20μm. (**d-e**) Number of FAs is modulated by GIT1/βPIX/PAK1/CDC42/RAC1 expression levels. Quantification of the FA number per cell in Hs578T (d) or MDA-MB-231 (e) cells transfected with the indicated siRNA. ** $P < 0.005$ *** $P \leq 0.0001$ (n=3 experiments with 30 cells per condition). (**f**) PEAK1 interacts with βPIX. Lysates of 293T cells expressing the indicated plasmids were used for anti-Myc immunoprecipitation. Levels of GFP-βPIX is detected via western blotting. (**g**) PEAK1 regulates βPIX localization at FA sites Representative confocal images of MDA-MB-231 cells transfected with either 100nM siCTRL or siPEAK1. PLA kit was used to analyze the localization of βPIX at PXN-FAs. (**h**) Quantifications of the number of PLA signals per cell per condition. ** $P < 0.05$.

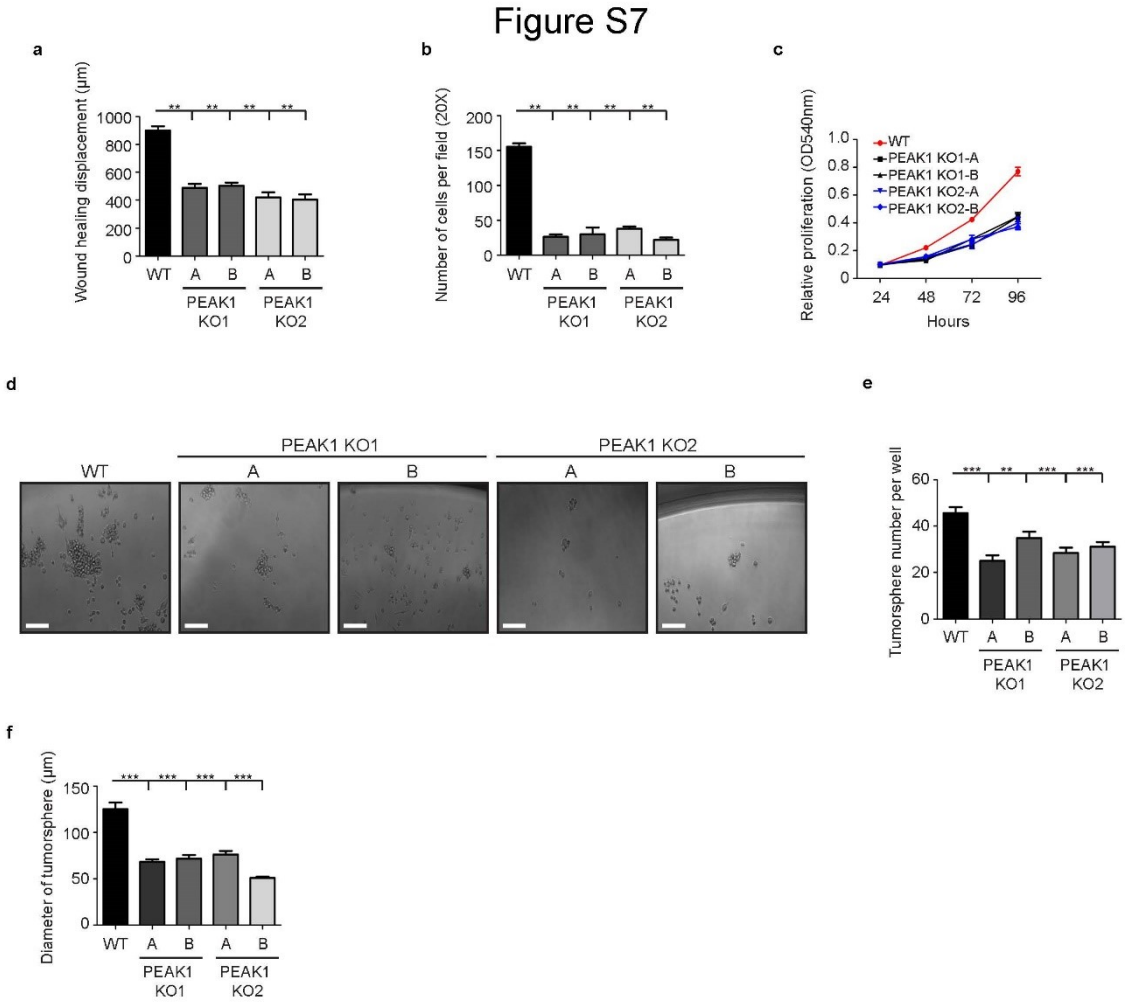

Figure 3. S7 PEAK1 is required for wound healing, proliferation and tumorsphere formation *in vitro*.

(**a**) Quantifications of MDA-MB-231 CRISPR WT or PEAK1 KO1 or KO2 clones displacement in a wound healing assay. ** $P < 0.0001$ (n=3, 4 fields used at 10X per condition per experiment). (**b**) Boyden invasion assay performed with MDA-MB-231 CRISPR WT or PEAK1 KO1 or KO2 clones using Matrigel as a matrix. The number of cells invaded was counted via DAPI staining of the membrane. ** $P < 0.0001$ (n=3, 10 fields used at 10X per condition per experiment). (**c**) MTT proliferation assay done in MDA-MB-231 CRISPR WT or PEAK1 KO1 or KO2 clones. (**d**) Representative microscopy images of tumorsphere formation in MDA-MB-231 CRISPR WT or PEAK1 KO1 or KO2 clones after 7 days. Scale bar, 60µm. (**e-f**) Quantifications of the tumorsphere number (e) and size of the tumorsphere (f) in conditions shown in (d). ** $P < 0.01$, *** $P < 0.0001$ (n=3, 10 fields used at 40X per condition per experiment).

Table 3. SI: List of antibodies

Name of Antibody	Company	Catalog #	Purpose	Dilution
p-AXL Y702	Cell Signaling	5724	WB	1:500
p-AKT S473	Cell Signaling	9271	WB	1:1000
pPAK1 S144/pPAK2 S141	Cell Signaling	2606P	WB	1:1000
PAK1	Cell Signaling	2602	WB	1:1000
pEPHA2 Y588	Cell Signaling	12677	WB	1:500
pGSK3B S9	Cell Signaling	5558	WB	1:1000
pJUN S243	Cell Signaling	2994	WB	1:500
pMYPT1 T696	Cell Signaling	5163	WB	1:500
pERK1/2 T202/Y204	Cell Signaling	4376	WB	1:1000
pCRKII Y251	Abcam	ab215751	WB	1:1000
pPXN Y118	Cell Signaling	2541	WB	1:500
pVCL Y822	Abcam	ab200825	WB	1:500
pSTMN1 S38	Cell Signaling	4191	WB	1:500
pCRMP2 T514	Cell Signaling	9397	WB	1:500
Paxillin	BD Transduction Laboratories	612405	WB	1:2000
Paxillin	BD Transduction Laboratories	612405	IF/PLA	1:200
BPix	Cell Signaling	4515	IF/PLA	1:100
GIT1	Cell Signaling	2919	PLA	1:100
GIT1	Dr. Alan Rick Horwitz	-	IF	1:100
Alexa Fluor 633 Phalloidin	Thermo Fisher Scientific	A22284	IF	5:200
Alexa 488 conjugated anti-rabbit	Thermo Fisher Scientific	A21441	IF	1:1000
Alexa 568 conjugated anti-mouse	Thermo Fisher Scientific	A11031	IF	1:1000
Alexa 488 conjugated anti-mouse	Thermo Fisher Scientific	A21200	IF	1:1000
Alexa 568 conjugated anti-rabbit	Thermo Fisher Scientific	A11011	IF	1:1000
AXL	Genescript	-	WB	1:10000
AXL	Cell Signaling	8661	PLA	1:100
pY99	Santa Cruz	sc-7020	WB	1:1000
CasL	Santa Cruz	sc-33659	WB	1:1000
Tubulin	Sigma	T5168	WB	1:10000
FAK	Santa Cruz	sc-558	IF/PLA	1:100
GFP B-2	Santa Cruz	sc-9996	WB	1:2000
GFP B-2	Santa Cruz	sc-9996	IF	1:100
4G10 HRP	EMD Millipore	16-105	WB	1:10000
HA Y-11	Santa Cruz	sc-805	WB	1:1000
c-Myc 9E10	Santa Cruz	sc-40	WB	1:2000
c-Myc A-14	Santa Cruz	sc-789	IF	1:100
Rac1	EMD Millipore	05-389	WB	1:3000
Flag M2-HRP	Sigma	A8592	WB	1:10000
Sgk269 EB-8	Santa Cruz	sc-100403	IF/PLA	1:100
PEAK1	EMD Millipore	09-274	WB	1:500
CrkII	BD Transduction Laboratories	610035	WB	1:2000
CrkII	BD Transduction Laboratories	610035	PLA	1:100
Calnexin E-10	Santa Cruz	sc-46669	WB	1:1000
CSK	Dr. Andre Veillette	-	WB	1:1000
Anti-Mouse HRP	Sigma	A 4416	WB	1:5000
Anti-Rabbit HRP	Santa Cruz	sc-2357	WB	1:8000
Anti-Goat HRP	Santa Cruz	sc-2020	WB	1:8000

Table 3. SII: List of siRNA

Name	Name	Company	Sequence
siNEDD9	siGENOME SMARTpool Human NEDD9 siRNA	Dharmacon, GE Healthcare	5' AGGAACUGGCCUUUCGCAA 3' 5' CUACCAAAAUCAGGGAAUU 3' 5' CCUCUGGACUGAUGCAGCA 3' 5' CCAAGAACAAGAGGUAUAU 3'
siPEAK1	siGENOME SMARTpool Human PEAK1 siRNA	Dharmacon, GE Healthcare	5' CCAAAUCUCUCUUUACAUC 3' 5' GCUAAGAGCACACCUAAGA 3' 5' UAUCAAAGUUCCCAUUGUU 3' 5' GAAAGACCCAUCCAUAAAG 3'
siAXL	ON-TARGETplus Human AXL siRNA	Dharmacon, GE Healthcare	5' ACAGCGAGAUUUAUGACUA 3' 5' GGUACCGGCUGGCGUAUCA 3' 5' GACGAAAUCCUCUAUGUCA 3' 5' GAAGGAGACCCGUUAUGGA 3'
siCRKII	siGENOME SMARTpool Human CRKII siRNA	Dharmacon, GE Healthcare	5' GGACAGCGAAGGCAAGAGA 3' 5' GAAUAGGAGAUCAAGAGUU 3' 5' GGUGAGCUGGUAAAGGUUA 3' 5' GGACAAGCCUGAAGAGCAG 3'
siCTRL	siGENOME Non-targeting siRNA	Dharmacon, GE Healthcare	5' UAGCGACUAAACACAUCAA 3'
siGIT1	siGENOME SMARTpool Human GIT1 siRNA	Dharmacon, GE Healthcare	5' GGACGACGCCAUCUAUUCA 3' 5' GCACACCCAUUGACUAUGC 3' 5' GGACGCCACAUCUCCAUUG 3' 5' CCGCACACCCAUUGACUAU 3'
siβPIX	siGENOME SMARTpool Human βPIX siRNA	Dharmacon, GE Healthcare	5' GGAAGAAGAUGCUCAGAUU 3' 5' GAAGAGCCCUCCCAAAGGA 3' 5' UCAAAGAGCUCGAGAGACA 3' 5' GGAGGGCGAUGACAUUAAA 3'
siPAK1	siGENOME SMARTpool Human PAK1 siRNA	Dharmacon, GE Healthcare	5' CAUCAAAUAUCACUAAGUC 3' 5' CAACAAAGAACAAUCACUA 3' 5' AGAAAUACCAGCACUAUGA 3' 5' GUGAAAUGCUCUCGGCUAU 3'
siCDC42	siGENOME SMARTpool Human CDC42 siRNA	Dharmacon, GE Healthcare	5' GGAGAACCAUAUACUCUUG 3' 5' GAUUACGACCGCUGAGUUA 3' 5' GAUGACCCCUCUACUAUUG 3' 5' CGGAAUAUGUACCGACUGU 3'
siRAC1	siGENOME SMARTpool Human RAC1 siRNA	Dharmacon, GE Healthcare	5' UAAGGAGAUUGGUGCUGUA 3' 5' UAAAGACACGAUCGAGAAA 3' 5' CGGCACCACUGUCCCAACA 3' 5' AUGAAAGUGUCACGGGUAA 3'

Table 3. SIII: List of plasmids

	Plasmids	Purpose	Origin
1	pDONR221	The backbone to generate all pDONR vectors	Addgene
2	pcDNA-hGAS6-His	Used to generate #3	Dr. Eric Manser
3	pDONR221-hGAS6-His	Used to generate #4	This study
4	pDEST-pcDNA5-hGAS6-His	Recombinant Gas6 Media	This study
5	pEGFP-NEDD9	Used to generate #9, 12, 13	Dr. Erica Golemis
6	pcDNA3.1-HA-NEDD9	Immunoprecipitation	Dr. Erica Golemis
7	pcDNA3-NEDD9	Immunoprecipitation	Dr. Michel Tremblay
8	pOG44	NEDD9 BioID	Dr. AC Gingras
9	pDONR221-NEDD9 for N-ter tag	Used to generate #11	This study
10	pcDNA5-pcDEST-BirA-Flag-N-ter	Used to generate #11, 32, 33	Dr. AC Gingras
11	pcDNA5-pDEST-BirA*-Flag-N-ter NEDD9	NEDD9 BioID	This study
12	pGEX4T1-hNEDD9 SD	NEDD9 IVK	This study
13	pGEX4T1-hNEDD9 CT	NEDD9 IVK	This study
14	pGEX4T1 GST	IVK/GST-Pulldown	JF Cote Lab
15	pCIS2-HA-DOCK3	Immunoprecipitation	Dr. David Schubert
16	pCMV-sport6-mouse AXL-WT	Immunoprecipitation	Dr. Rob Screaton
17	pCMV-sport6-mouse AXL-KD	Immunoprecipitation	JF Cote Lab
18	pcDNA3 FAK D5 HA-Tag	Immunoprecipitation	JF Cote Lab
19	pCS-3MT-6Myc	Backbone to generate all pCS-6Myc vectors	Addgene
20	pRetroX-Sgk269 WT	Used to generate #27	Dr. Roger Daly
21	pDONR221-L1-PEAK1 WT (stop)-L2	Used to generate #34, 32	This study
22	pDONR221-L1-PEAK1 Y531F (stop)-L2	Used to generate #36	This study
23	pDONR221-L1-PEAK1 3PA (stop)-L2	Used to generate #35, 33	This study
24	pcDNA5-pDEST-BirA*-Flag-N-ter PEAK1 WT	PEAK1 BioID	This study
25	pcDNA5-pDEST-BirA*-Flag-N-ter PEAK1 3PA	PEAK1 BioID	This study
26	pCS-6Myc-hPEAK1	Immunoprecipitation	This study
27	pCS-6Myc-hPEAK1 3PA	Immunoprecipitation/ Immunofluorescence	This study
28	pCS-6Myc-hPEAK1 Y531F	Immunoprecipitation	This study
29	pECFP-Flag-GIT1	Immunoprecipitation	Addgene
30	pCMV5-HA- ARHGEF7	Used to generate #41	Dr. Liliana Attisano
31	pEGFP-C2-ARHGEF7	Immunoprecipitation	This study
32	pEGFP-C2 CRKII WT	Immunoprecipitation	JF Cote Lab
33	pGEX 4T1 GST-CRKII WT	GST-Pulldown	JF Cote Lab
34	pGEX 4T1 GST-CRKII W169L	GST-Pulldown	JF Cote Lab
35	pGEX 4T1 GST-CRKII W275L	GST-Pulldown	JF Cote Lab
36	pcDNA3-Myc CRKII	Immunoprecipitation	JF Cote Lab
37	pEGFP-PAXILLIN	Live cell imaging	Addgene
38	pGEX2TK GST-PAXILLIN 1-313	Paxillin IVK	Dr. Christopher E. Turner
39	pGEX2TK GST-PAXILLIN 329-559	Paxillin IVK	Dr. Christopher E. Turner
40	pXM139-CSK	Immunoprecipitation	Dr. Andre Veillette
41	pVSV-G	Lentiviral infection	Dr. Mathieu Ferron
42	pRSV-Rev	Lentiviral infection	Dr. Mathieu Ferron
43	pMDLg/Prre	Lentiviral infection	Dr. Mathieu Ferron
44	pCL-Ampho	Retroviral infection	Dr. Sylvain Meloche
45	MSCV Luciferase PGK-hygro	Stable Luciferase expression	Addgene
46	LentiCas9-Blast	Stable Cas9 expression	Addgene
47	PEAK1 gRNA (BRDN0001145890)	Crispr PEAK1 KO1	Addgene
48	PEAK1 gRNA (BRDN0001147244)	Crispr PEAK1 KO2	Addgene

Table 3. SIV: List of primers

Oligonucleotide name	Oligonucleotide sequence	Purpose
hGas6 Forward	5' GGGGACAAGTTTGTACAAAAAAGCAGGCTTAA TGGCCCCTTCGCTCT 3'	Gateway Cloning
hGas6 Reverse	5' GGGGACCACTTTGTACAAGAAAGCTGGGTTTCA GTGGTGGTGGTGGTGG 3'	Gateway Cloning
hNedd9 SD Forward	5' ATCTGGTTCCGCGTGGATCCATGCAGCAGACCT TTGGC 3'	Cloning
hNedd9 SD Reverse	5' TCACGATGCGGCCGCTCGAGCTGAGCTGGGG AGGCTG 3'	Cloning
hNedd9 CT Forward	5' ATCTGGTTCCGCGTGGATCCATGGATGACTACG ATTACGTCCAC 3'	Cloning
hNedd9 CT Reverse	5' TCACGATGCGGCCGCTCGAGTGCCATCTCCAGC AAAGAGCGC 3'	Cloning
hNedd9 Forward	5' GGGGACAAGTTTGTACAAAAAAGCAGGCTTCATG AAGTATAAGAATCTTATGG 3'	Gateway Cloning
hNedd9 Reverse	5' GGGG AC CAC TTT GTA CAA GAA AGC TGG GTC TTAGAACGTTGCCATCTCCAGCA 3'	Gateway Cloning
GFP-PIX Forward	5' CGAGCTCAAGCTTCGAATTCATGACCGATAATAG CAACAATCAACTGG 3'	HiFi Cloning
GFP-PIX Reverse	5' TCAGTTATCTAGATCCGGTGGATCCTTATAGATTG GTCTCATCCCAGGCAGG 3'	HiFi Cloning
hBcar3 Forward	5' GGGGACAAGTTTGTACAAAAAAGCAGGCTTCA TGGCTGCAGGAAAATTTGCAAG 3'	Gateway Cloning
hBcar3 Reverse	5' GGGGACCACTTTGTACAAGAAAGCTGGGTCTC AAAGCTCTGCCTGCTTTACAGG 3'	Gateway Cloning
hPEAK1 WT Forward	5' GGGGACAAGTTTGTACAAAAAAGCAGGCTTAATG TCTGCTTGTAACACCTTTACTGAAC 3'	Gateway Cloning
hPEAK1 WT Reverse	5' GGGGACCACTTTGTACAAGAAAGCTGGGTTTCA GAGCGGCCGCGT 3'	Gateway Cloning
hPEAK1 ΔN Forward	5' GGGGACAAGTTTGTACAAAAAAGCAGGCTTAAT GGTGGTCTCTTATGGACAAGG 3'	Gateway Cloning
PEAK1 Y531F Forward	5' ATTCGATTCCAAGAAGTATGGACTTCTAGCACCA GTCCAC 3'	Mutagenesis
PEAK1 Y531F Reverse	5' TTCTTGGAATCGAATTGCACTGGATTTTTGGAA 3'	Mutagenesis
PEAK1 3PA Forward	5' CCTACAGCAGCCGCACTGCCAAAGAAGATGATC ATAAGAGCCAATACAGA 3'	Mutagenesis
PEAK1 3PA Reverse	5' TGGCAGTGCGGCTGCTGTAGGTTGGGAAGCATT GGGTGC 3'	Mutagenesis

DISCUSSION

Among the members of the receptor tyrosine kinases that are known to be key players of cancer biology, AXL receptor tyrosine kinase has been recognized as a promoter of tumorigenesis and metastasis in many different cancer types. As mentioned previously, it has been correlated with cancer aggressiveness where its dysregulated expression leads to oncogenic signaling and has been strongly correlated with poor prognosis of the patients. In breast cancer patients, AXL expression is not exclusive to a specific subtype, however in breast cancer cell lines, AXL expression has been limited to TNBC where no expression of AXL was detected in luminal or HER2+ breast cancer cell lines [449]. TNBC cell lines display a mesenchymal and invasive phenotype and provide an EMT signature that is promoted by AXL expression. In fact, AXL expression across multiple tumor types has been associated with EMT, a process that is necessary at different steps throughout the invasion-metastatic cascade. Recently, our group has defined a central role for AXL in promoting HER2+ breast cancer metastasis *in vivo*, where AXL was required at multiple stages of the metastatic cascade, at intravasation, extravasation and metastatic growth [58]. Due to its expression correlation with drug resistance, several studies demonstrated that blocking AXL function renders the cells to be more responsive to therapy, whether it was chemo- or drug-targeted therapy. This proposes AXL as a potential and a promising target for therapy, yet the underlying mechanisms behind its invasive role remained elusive. AXL downstream signaling has proven to be very redundant to other RTKs, such as EGFR and PDGFR, and the current low resolution of AXL signaling does not justify AXL's invasive role. Hence, in this thesis, we were able to provide insights into why AXL is unique among other RTKs to be classified as a robust promoter of cell invasion and metastasis.

Our work in chapter 2 provides a novel signaling arm downstream of AXL activation that can lead to RAC-induced cell invasiveness in TNBC cell lines. Previous work from our group and others demonstrated DOCK as a mediator of cancer cell invasion downstream of other RTKs such as HER2, EGFR, and PDGFR, where phosphorylation of DOCK1 lead to its activation and cancer cell dissemination [286-288]. Since interfering with ELMO and DOCK1 expression has been shown to impair breast cancer cell invasion and metastasis, these proteins seem to be important regulators of RAC-dependent cancer cell invasion. Based on these data, we sought to search for kinases that can modulate the phosphorylation of the scaffold protein

ELMO, the binding partner of DOCK GEF proteins. Through a series of biochemical assays, AXL (along with MER and TYRO3) was found to directly phosphorylate ELMO proteins to promote RAC-induced cell invasion. We demonstrated that AXL interaction with ELMO proteins and phosphorylation of their carboxyl-terminal tyrosine residue is essential for breast cancer cell invasion. Since TNBC cells express ELMO1 and ELMO2 but not ELMO3, and AXL phosphorylates both on the same residue, our data suggest that ELMO1 and ELMO2 play similar and interchangeable roles in mediating cancer cell invasion. In addition, phosphorylation of ELMO by AXL on the specific c-terminal tyrosine residue (Y713 in ELMO2 or Y720 in ELMO1) seems to be critical for cancer cell invasion since the rescue of ELMO expression with the phospho-mutant of ELMO prevented cell invasion. Hence, this phosphorylation site of ELMO seems to play a role in transmitting signals downstream of AXL signaling to promote RAC-induced invasion. How this occurs still remains obscure.

Since ELMO is known to potentiate DOCK GEF activity on RAC, the phosphorylation site, which falls in the DOCK binding region on ELMO, might play a role in stabilizing RAC binding to DOCK or relieving DOCK from its autoinhibited state. Our group has previously reported the mechanism of ELMO regulation by exchanging between an open and closed conformation, which modulates RAC activity [274]. Hence, the phosphorylation on this tyrosine residue may prevent ELMO from being in a closed conformational state that will maintain its open conformational state leading to higher DOCK GEF activity and hence RAC activation. Herein, we report DOCK1 as the first GEF to be a signaling intermediate downstream of AXL that may play a role in AXL-induced metastasis. Using DOCK GEF inhibitor CPYPP, a small molecule inhibitor against all DOCK-A subfamily members (including DOCK1, DOCK2, and DOCK5), AXL-induced RAC activation was shown to be DOCK1 mediated. Since ELMO interacts with all DOCK-A subfamily members, AXL can also recruit DOCK5, which is highly expressed in TNBC cells, to mediate AXL-induced RAC activation.

Furthermore, another study in breast cancer has shown the ELMO/DOCK complex to play a role in cancer cell invasion and metastasis downstream of GPCR signaling [291]. In specific, CXCL12 stimulation of CXCR4 in cells induces ELMO1 association with Gαi2 to mediate downstream actin polymerization, migration, and invasion of breast cancer cells. This study reported ELMO1 expression to correlate with lymph node and distant metastasis in breast cancer patients. Interestingly, they investigated further the role of ELMO in breast cancer tumor

growth and metastasis *in vivo*. They found the injection of siRNA ELMO-depleted cells into fat-pads of mice did not affect tumor growth *in vivo*. Our data, however, suggested that depletion of ELMO levels by siRNA affects proliferation of TNBC cells which could not be rescued with ELMO phospho-mutant. This difference may be due to the transient effect of the siRNA depletion in cells on proliferation, whereas *in vivo* other factors in the tumor microenvironment may surpass and overcome this effect. Similarly, work from our group has shown DOCK1-null mammary tumors to have growth defect in comparison to the DOCK1-WT mammary tumors *in vivo*, suggesting a role for DOCK1 in promoting cell proliferation [288]. The noted difference in ELMO and DOCK1 effect on tumor growth *in vivo* in the two different studies could be due to the different types of cancer models used in the different studies where ELMO was studied in a TNBC model and DOCK1 was studied in HER2+ breast cancer model.

Furthermore, AXL expression in TNBC cells has been reported to be important in sustaining an EMT state and a stem-like phenotype [92]. Our data revealing a new role for ELMO/DOCK in modulating VIMENTIN expression, a known marker for EMT, is novel and could be TNBC specific since we previously reported DOCK1-null HER2+ mammary tumors did not alter EMT gene expression [288]. The mechanisms in which ELMO/DOCK proteins alter EMT gene expression to sustain an EMT state remains to be fully explored. Recently, a clinical study has reported that VIMENTIN+ and AXL high expression is a poor prognostic factor for primary breast cancer and that their expression might contribute to the breast cancer aggressiveness [498]. This allows us to suggest ELMO/DOCK proteins as signaling intermediates downstream of AXL not only to mediate RAC-induced cell invasion but also to sustain an EMT state by maintaining VIMENTIN expression.

Nonetheless, our work along with others emphasize further the role of the ELMO/DOCK complex as signaling intermediates downstream of RTKs and GPCRs to mediate RAC-induced cell invasion. This allows us to suggest ELMO proteins to be used as biomarkers for diagnosis and treatment of breast cancer metastasis, and DOCK proteins as potential drug targets to inhibit their GEF activity to prevent RAC-induced invasion and ultimately metastasis.

To further explore the mechanisms AXL attains to sustain its invasive role to promote metastasis, we characterized in chapter 3 AXL phosphoproteome using TNBC cells as a model. TNBC lacks any targeted therapy in clinic and many of TNBC patients that acquire resistance to chemotherapy, which is the only treatment present in the clinic, have an upregulation of AXL

expression [499]. Also, to our advantage, TNBC cells express high levels of AXL which allowed us to manipulate its activation status by serum starvation and GAS6 treatment. To note, GAS6's contribution to cancer progression is unclear. Some studies report that AXL promotes metastasis independently of GAS6, by heterodimerizing with other RTKs, such as HER2 to transphosphorylate it and induce its signaling [58]. Another evidence reports EGFR transactivation of AXL induces robust downstream signaling important for invasive motility that is not activated vigorously by EGFR itself [57]. Others, however, have shown AXL decoy receptor, MYD1, which has enhanced GAS6-binding properties, as a therapeutic approach to disrupt GAS6/AXL signaling, indicating a role for GAS6 in cancer progression [101]. In our experimental model, high levels of AXL phosphorylation are observed in our TNBC cells in chapter 2 and 3 without GAS6 stimulation, which could be due to the high levels of AXL expression that renders AXL to be constitutively active. Another explanation for the high AXL phosphorylation observed independently of GAS6 could be due to AXL diverse interactions with other cell surface proteins. For instance, a study demonstrated EGFR, which is highly expressed in TNBC cells, to diversify its signaling by heterodimerizing with AXL [57]. Nonetheless, AXL in TNBC cells is still responsive to GAS6 stimulation upon serum starvation. Hence, GAS6 stimulation was a good and advantageous tool for us to stimulate and control AXL phosphorylation in serum-starved TNBC cells in a timely manner, as shown in chapter 2 and 3.

AXL downstream signaling has been mainly demonstrated to promote the biological processes of cell survival and cell migration mediated by established signaling pathways such as MAPK, JNK, and ERK signaling. These signaling pathways contain shared signaling intermediates with other RTKs and are not sufficient to explain AXL's biological activity. Hence, it was of importance for us to address this critical gap in knowledge and determine AXL specific pathways and signaling intermediates that justify its pro-invasive role in cancer progression. Our GAS6-induced AXL phosphoproteome obtained by a quantitative proteomics approach in TNBC cells revealed for the first time many significantly enriched pathways that may explain how AXL facilitates cancer cell invasion and metastasis. We uncovered AXL activation to modulate significantly 51 signaling pathways using KEGG pathway analysis, with Focal Adhesions (FA) as our top hit. We report, in chapter 3, AXL to facilitate cancer cell invasion and metastasis by strongly modulating FA turnover. As previously mentioned, focal

adhesions are adhesion points or clusters that anchor the cell to the ECM. The dynamics or turnover of these adhesion clusters, composed of cytoskeletal and signaling proteins, is modulated by repetitive phosphorylation events that lead to their assembly or disassembly, which will ultimately allow the cell to move and maneuver around to disseminate and become invasive. In our phosphoproteomic data, we found AXL to modulate many proteins involved in FA dynamics, including scaffolds, adaptors, GEFs and GAPs, kinases and phosphatases. By extensively comparing our phosphoproteomic data to other phosphoproteomic datasets of activated RTKs, such as EGF-stimulated EGFR, we were able to conclude that modulation of FA proteins was unique to AXL. From this comparison, EGFR signaling seemed to modulate adherens junctions, known to initiate and stabilize cell-cell contact, more specifically and robustly than AXL. Moreover, the difference we obtain by comparing the different datasets between EGFR and AXL phosphomodulated pathways could be due to the different cell lines and approaches used to obtain these datasets. Since EGFR phosphoproteomic dataset was obtained from a screen that was performed in HeLa cells, it will be necessary however to treat our TNBC cells with EGF at different time points, similar to GAS6 stimulation, and perform a similar quantitative phosphoproteomic screen in order to confirm AXL robust modulation of FA proteins is indeed unique to AXL. Knowing our TNBC cells express high levels of EGFR and that EGFR uses AXL to diversify its signaling, we hypothesize that EGFR in TNBC cells may use AXL to modulate FA turnover to modulate cell motility. Since our group has uncovered a role for HER2 in transphosphorylation and activating AXL [58], it is worthy to define the differential AXL phosphoproteomes obtained upon EGF-induced AXL activation to uncover differential AXL signaling pathways activated in different contexts. This will reveal additional potential drug targets that can be used to limit AXL-induced cancer cell invasiveness and metastasis in different cancer contexts.

Furthermore, our work in chapter 3 revealed for the first time AXL to be localized at FA structures and this localization seemed to be dependent on AXL phosphorylation status. It still remains elusive and more work is required to investigate how AXL gets trafficked to such complexes. One possibility could be by AXL modulation of its own trafficking where AXL rich endosomes can be targeted and trafficked to signal at and modify FA structures. AXL could also be found and clustered at FA sites as a membrane protein. Furthermore, our work revealed a novel role for AXL in regulating FA turnover by increasing the disassembly rates of FAs

through the recruitment of βPIX/GIT1/PAK disassembly complex. Among the phospho-modulated FA proteins, AXL activation led to a robust tyrosine phosphorylation of NEDD9, and other CAS-family members, which modulated its CRKII/DOCK3 complex formation and its localization at FA structures. Previous studies have shown an essential role for NEDD9 scaffold complex in oncogene-driven transformation, tumor establishment, cancer cell dissemination and colonization of cancer cells in a foreign tissue by actively regulating cytoskeletal dynamics [500]. In fact, NEDD9 has been linked to the establishment of an EMT state where NEDD9 complex induces the downregulation of E-Cadherin and upregulation of EMT markers such as SNAIL and SLUG [501]. In turn, the EMT marker TWIST positively controls the expression of NEDD9 and DOCK3 to maintain a mesenchymal type movement [296]. In melanoma cells, NEDD9/DOCK3 complex was reported to play a role in cell plasticity by promoting a mesenchymal-type movement and RAC-induced cell invasion, and by inhibiting an amoeboid-type movement [502]. As per their role in FA dynamics, NEDD9 or BCAR1 have been previously reported to act as mechanosensors at FA structures yet the exact mechanism how NEDD9 or BCAR1 complex transmits signals to the FA structures to induce their turnover remained unknown [503].

Our proximity labeling coupled to proteomics approach, named BioID, allowed us to reveal novel interactors of NEDD9 that can explain how this scaffolding complex leads to FA turnover. By merging our AXL phosphoproteome and NEDD9 interactome, we revealed a novel mechanism in which AXL utilizes the NEDD9 complex to modulate FA disassembly. In specific a novel binding partner to this complex, PEAK1, was found in proximity to NEDD9 and robustly phospho-modulated by AXL. PEAK1 is a non-receptor tyrosine kinase that localizes to the actin cytoskeleton and FA structures and regulates their turnover [393, 456]. It was previously reported to be tyrosine phosphorylated by SRC kinase downstream of EGFR signaling to modulate phosphorylation of FA proteins [393]. However, the exact role of phosphorylated PEAK1 regulatory mechanism at FA was unknown. Our data revealed a novel role for phosphorylated PEAK1 at FA sites as a mediator of PXN phosphorylation and a scaffold for βPIX/GIT1/PAK disassembly complex. Our data on PEAK1-mediated PXN phosphorylation was very intriguing since PEAK1 is known to be a pseudokinase that lacks any enzymatic activity due to its divergence from canonical kinases in multiple of the conserved kinase motifs (the glycine-rich loop, HRD motif, and DFG motif) which renders PEAK not

capable of nucleotide binding [504]. Hence, we concluded that PEAK1 acts a scaffold for other kinases that can mediate PXN phosphorylation. PXN phosphorylation has been largely attributed to SRC and FAK kinases, and our data reporting PEAK1 scaffold as a mediator of PXN phosphorylation is novel.

In search of PEAK1 bound kinases using BioID, we revealed PEAK1 interactome to involve many FA proteins as well as putative kinase interactors such as PRAG1 and EPHA2. A previous study has reported PEAK1 to act in a heterodimer with its family member PRAG1 to induce downstream signaling [463]. In addition, PRAG1 was shown to induce tyrosine phosphorylation in human cells by associating with CSK kinase, yet no specific substrate was identified [462]. Our hypothesis that PEAK1, in complex with PRAG1, utilizes CSK kinase to induce PXN phosphorylation was further validated by our data demonstrating CSK-mediated PXN phosphorylation. In fact, a previous study has shown CSK to localize at FA structures when SRC kinases are activated to negatively regulate them [505]. Herein, we report PXN as a novel substrate of CSK kinase, coupled to PEAK1/PRAG1 pseudokinase complex, at FA structures to mediate their turnover. Our data also revealed the necessity of PEAK1 proline-rich region, which is CRKII binding site, for AXL-mediated PEAK1 phosphorylation and PEAK1-mediated PXN phosphorylation. In fact, our BioID data of PEAK1 mutant, which lacks CRKII binding, demonstrated PRAG1 loss of binding, further reinforcing the role of the proline-rich region of PEAK1 in binding PRAG1 to scaffold CSK for PXN phosphorylation.

Interestingly, EPHA2 loss of binding was also observed in our BioID data of PEAK1 mutant, suggesting that EPHA2 putative interaction with PEAK1 is mediated by CRKII, PRAG1 or other SH3 domain-containing proteins that interact with the proline-rich region of PEAK1. A recent study has demonstrated a role for EPHA2 in cell motility by modulating FA dynamics [470]. Since EPHA2 was also found to be phospho-modulated by AXL in our phosphoproteomics data, this led us to suggest a mechanism in which NEDD9/CRKII/PEAK1 complex mediates EPHA2 heterodimerization with AXL, where AXL can transactivate EPHA2 to mediate PEAK1 phosphorylation and regulation of FA turnover. Further work is needed to investigate if this mechanism holds true in our TNBC cells.

Altogether, our work on FA regulation in chapter 3 expands our knowledge in revealing a novel mechanism in which AXL can modulate cell migration and invasion to confer its pro-invasive role. A similar role for AXL in ovarian cancer was revealed where AXL converges

with β3 integrin to modulate cell adhesion by recruiting BCAR1 protein [98]. This emphasizes further the role of AXL in modulating cell adhesion to the ECM by hijacking the FA machinery. In addition, revealing a novel mechanism for an atypical pseudokinase/kinase complex in mediating PXN phosphorylation is a major breakthrough in the field of FA regulation. We reported PEAK1 to play a role *in vivo* in mediating TNBC tumor growth and metastasis using mouse xenograft models. Similarly, other studies also demonstrated a role for PEAK1 in facilitating tumor growth and metastasis *in vivo* of various cancer models such as TGFβ-induced breast cancer, NSCLC and KRAS-induced pancreatic cancer model [471, 506, 507]. Moreover, PEAK1 expression levels have been shown to be correlated with poor patient prognosis and survival in several types of cancers [471, 472]. Hence, revealing the scaffolding function of PEAK1 aids in developing strategies that can pharmacologically target its bound kinases or that can target its protein-protein interface to prevent its scaffolding function.

Moreover, the effect of AXL activation was not limited to FA dynamics but to many other significantly enriched biological processes. Our analysis of AXL phosphoproteomics data revealed a robust link between AXL activation and regulation of actin cytoskeleton. This may explain the role AXL plays in mesenchymal cells which are pro-migratory and pro-invasive in comparison to epithelial cells, where actin cytoskeleton remodeling is involved and required for the cell to attain a mesenchymal phenotype and to lose its epithelial integrity. Since the regulation of actin cytoskeleton proteins affects many biological processes, this significant phospho-modulation of actin cytoskeletal proteins by AXL may explain the various ways AXL sustains an EMT pro-invasive state. Within the regulation of actin cytoskeleton proteins, AXL was found to modulate many GEFs and GAPs, which are regulators of small GTPases. Interestingly, DOCK-A subfamily members of GEF proteins were found to be significantly phospho-modulated by AXL, which further confirms the role we defined for them in chapter 2 as signaling intermediates to promote RAC-induced cell invasion downstream of AXL activation. Other DOCK family members were also found to be significantly phospho-modulated by AXL such as DOCK9 and DOCK10 which are part of DOCK-D subfamily. In fact, a recent study has explored the role of DOCK9 in complex with DOCK4 in promoting the formation of endothelial cells filopodia protrusions necessary for tubule remodeling in angiogenesis [508]. This may reveal a new signaling intermediate downstream of AXL/VEGFR heterodimer to promote angiogenesis, a process AXL has been shown to play a role in during

metastasis. This is one example in which our AXL phosphoproteome could answer many longstanding questions about AXL's invasive function in cancer progression and during the metastatic cascade, which are worthy of further investigations.

In addition to GTPase regulation, other links with endocytosis and phagocytosis were revealed and found significantly modulated by AXL activation. AXL, along with MER and TYRO3, have been shown to play an important role in the phagocytosis of apoptotic cells by macrophages [123]. Our phosphoproteomic screen may reveal novel mechanisms in which AXL achieves this role. It will be important to investigate further the phagocytosis network downstream of AXL to probe its function in cancer cell invasiveness. As per endocytosis, this biological process is known to regulate RTKs activity [509]. It involves the vesicular trafficking of the RTKs into endosomes or cytoplasmic vesicles that are internalized at the cell surface upon ligand binding to subsequently sort the ligand-receptor complexes to either lysosomes for degradation, which will ultimately lead to RTK downregulation or recycling back to the membrane [509]. These processes usually rely on intrinsic motifs and post-translational modifications such as phosphorylation and ubiquitination. This process in cancer is known to be skewed where specific oncogenes are known to be biased for RTKs recycling rather than degradation to maintain their oncogenic signaling [510]. Two phospho-modulated ubiquitin ligases, NEDD4L and CBLB, that we reveal in our AXL phosphoproteome are known to ubiquitinate lysine residues in the intracellular domains of RTKs to induce their internalization and sorting for lysosomal or proteasomal degradation. However, in some cases, ubiquitination of specific lysine residues by these ligases can trigger proteasome-independent pathways such as signal transduction or endocytosis. For instance, previous reports demonstrated the p85 regulatory subunit of PI3K can be polyubiquitinated by CBLB ligase in T-cells without affecting its protein levels [511]. A previous study, however, has demonstrated a mechanism of GAS6-induced AXL ubiquitination by CBLB ligase to downregulate AXL [46]. Thus, it will be interesting to investigate whether AXL phospho-modulation of these ligases either leads to inhibiting or activating these ligases to trigger proteasome-dependent or independent pathways.

Other proteins involved in ubiquitin binding and vesicular trafficking of RTKs, such as STAM1/2 which are part of the ESCORT complex, have also been identified to be phospho-modulated by AXL activation. The phospho-modulation of these proteins may suggest a mechanism in which AXL can use to regulate its activity by inhibiting its lysosomal degradation

and promoting its recycling back to the membrane to continuously signal. Extensive studies have been performed to study the regulation of RTK's activity by endocytosis and vesicular traffickings, such as EGFR, ERBB2, FGFR and VEGFR [510], and accumulating evidence suggests that internalized EGFR continues to bind and phosphorylate downstream signaling proteins in pre-degradative intracellular compartments, leading to activation of signaling pathways distinct from the ones at the cell surface [510, 512]. In addition, other studies reported EGFR to maintain its tumor-promoting signaling pathways, similarly to other RTKs such as MET, FGFR, and VEGFR, while localized in the nucleus [512]. This nuclear translocation of EGFR was shown to be mediated by AXL in EGFR drug-resistant models [513]. Since nuclear EGFR was demonstrated to function as a co-transcription factor for several oncogenic genes such as cyclin d1, c-myc, and stat1, this brings us to suggest that AXL could also regulate its own translocation to the nucleus to act as a transcription factor to induce its associated EMT gene signature. It still remains elusive if regulation of AXL activity by endocytosis is similar to EGFR's mechanism of regulation or is unique to AXL. Further work is needed to investigate whether AXL maintains its oncogenic signaling at intracellular compartments such as endosomes and nucleus, during cancer progression to sustain its pro-invasive role.

Another indirect mechanism in which AXL can regulate endocytosis or phagocytosis could be via AXL's phospho-modulation of microtubule binding proteins. The modulation of microtubules and microtubule binding proteins is known to regulate the processes of endocytosis and phagocytosis [514]. Endocytic trafficking requires motor proteins that tether membranes or transport vesicles along actin and microtubules cytoskeleton [515]. They also facilitate the endosomal sorting and the generation of transport intermediates by providing a force to deform and assist in the scission of the membrane [516]. Motor proteins such as KIFs, and microtubule filament system proteins that stabilize or destabilize microtubules, such as MAPs, MARK2, STMN1, and MYPT1 are among the proteins involved in the regulation of microtubule dynamics and found to be phospho-modulated by AXL activation. Altogether, this may suggest another mechanism that justifies the role we uncovered for AXL in our phosphoproteomic analysis in modulating endocytosis and vesicular trafficking.

Furthermore, another KEGG pathway that is significantly modulated in our AXL phosphoproteome is RNA transport. It is a process that involves the transport of RNA from the nucleus to the cytoplasm which is fundamental for gene expression. AXL may alter the export

of specific transcripts of encoding proteins for survival and oncogenesis by modulating mRNA export factors such as NUP and DDX proteins, as well as RNA binding proteins which determine the spatiotemporal regulation of translation and guarantee the correct subcellular localization of the translated protein [517]. Since the process of RNA transport has been shown to be interlinked with vesicle trafficking [517], AXL's regulation of RNA transport could also be a secondary effect of AXL's regulation of endocytosis and vesicle trafficking.

Another mechanism in which AXL can regulate gene expression is through a process named RNA processing and in specific alternative splicing. Many proteins involved in this process were found to be significantly phospho-modulated by AXL in our phosphoproteomics dataset. Alternative splicing changes and mutations in splicing factors are reasons behind the variations observed in transcriptomes of tumors [518]. In addition, these alterations are known to be linked with tumor progression, metastasis, and therapy resistance. AXL's direct or indirect modulation of splicing proteins such as SRRM1 and SRRM2 can lead to their activation in splicing, as seen previously [519]. Phosphorylation of splicing proteins can lead to their stabilization by preventing their degradation and hence promoting alternative splicing of RNA. Alterations in alternative splicing can be essential for understanding drug resistance [518]. Previous work has shown that patients that did not respond to targeted treatment against BRAF mutations express another BRAF isoform that lacks specific exons [520]. Interestingly, a small molecule inhibitor against a pre-splicing factor reduced the growth of the drug-resistant cells [521]. Similarly, others have also shown resistance to immunotherapy in leukemia is due to alternative splicing [518]. Since AXL is correlated with drug resistance in many cancer types, further work is required to investigate whether AXL modulation of alternative splicing could be a novel mechanism in which AXL uses to drive resistance upon immuno-, chemo- and targeted therapy.

Due to AXL's invasive role in cancer and its correlation with drug resistance, there has been an increased interest in developing AXL inhibitors to be used in the clinic. Since AXL is rarely reported to act as the main driver of cancer, AXL inhibitors are mainly aimed to be used as combinational therapy. As of today, many AXL targeted drugs have been developed and some are used in clinical trials [522]. AXL inhibitors are ATP-competitive inhibitors and are classified in 3 different categories: single-target AXL inhibitors, dual MET/AXL inhibitors, and multi-target AXL inhibitors [522]. Multi-target AXL inhibitors have demonstrated to be the

most effective and more promising for future applications. Several preclinical studies have shown benefits in AXL inhibition in diverse scenarios [523]. Recently, a few specific AXL inhibitors have entered early-phase clinical trials including BGB324 and BPI-9016M [523]. In addition to those, a monoclonal antibody against AXL and AXL decoy receptor are currently in preclinical development. Altogether, this effort in developing AXL inhibitors and the ongoing clinical trials using them will determine the therapeutic potential of AXL targeting, yet a better understanding of AXL mechanisms, defined in chapter 3, will lead to more effective anti-cancer strategies.

Furthermore, our work in chapter 2 and chapter 3 defining AXL specific downstream signaling mechanisms required for AXL's role in cancer invasiveness will aid in designing rational combination therapies and in determining the mechanisms AXL attains to acquire therapy resistance. By targeting specific signaling intermediates of AXL, such as PEAK1 or DOCK1 with AXL inhibition, this may prove to be a more effective anticancer strategy for treatment. A recent study in our lab demonstrated that co-treatment with AXL and HER2 blocking agents inhibited HER2+ patient-derived xenografts tumorsphere growth [58]. Hence, it will be important to determine if inhibiting other signaling intermediates of AXL signaling with AXL inhibition, will render cancer cells to be more responsive and sensitive to therapy. This highlights the significance of our work covered in this thesis in understanding the mechanisms behind AXL's invasive role. Our work introduces several potential therapeutic drug targets to be used in the combination therapy which may hold promise.

References

1. Yeh, A.C. and S. Ramaswamy, *Mechanisms of Cancer Cell Dormancy--Another Hallmark of Cancer?* Cancer Res, 2015. **75**(23): p. 5014-22.
2. Hanahan, D. and R.A. Weinberg, *Hallmarks of cancer: the next generation.* Cell, 2011. **144**(5): p. 646-74.
3. Hanahan, D. and R.A. Weinberg, *The hallmarks of cancer.* Cell, 2000. **100**(1): p. 57-70.
4. Cavallaro, U. and G. Christofori, *Cell adhesion and signalling by cadherins and Ig-CAMs in cancer.* Nat Rev Cancer, 2004. **4**(2): p. 118-32.
5. Berx, G. and F. van Roy, *Involvement of members of the cadherin superfamily in cancer.* Cold Spring Harb Perspect Biol, 2009. **1**(6): p. a003129.
6. Talmadge, J.E. and I.J. Fidler, *AACR centennial series: the biology of cancer metastasis: historical perspective.* Cancer Res, 2010. **70**(14): p. 5649-69.
7. Valastyan, S. and R.A. Weinberg, *Tumor metastasis: molecular insights and evolving paradigms.* Cell, 2011. **147**(2): p. 275-92.
8. Thiery, J.P., et al., *Epithelial-mesenchymal transitions in development and disease.* Cell, 2009. **139**(5): p. 871-90.
9. Yang, J. and R.A. Weinberg, *Epithelial-mesenchymal transition: at the crossroads of development and tumor metastasis.* Dev Cell, 2008. **14**(6): p. 818-29.
10. Egeblad, M., E.S. Nakasone, and Z. Werb, *Tumors as organs: complex tissues that interface with the entire organism.* Dev Cell, 2010. **18**(6): p. 884-901.
11. Peinado, H., S. Lavotshkin, and D. Lyden, *The secreted factors responsible for pre-metastatic niche formation: old sayings and new thoughts.* Semin Cancer Biol, 2011. **21**(2): p. 139-46.
12. Coghlin, C. and G.I. Murray, *Current and emerging concepts in tumour metastasis.* J Pathol, 2010. **222**(1): p. 1-15.
13. Giancotti, F.G., *Mechanisms governing metastatic dormancy and reactivation.* Cell, 2013. **155**(4): p. 750-64.
14. Gomez-Cuadrado, L., et al., *Mouse models of metastasis: progress and prospects.* Dis Model Mech, 2017. **10**(9): p. 1061-1074.
15. Anderson, K.N., R.B. Schwab, and M.E. Martinez, *Reproductive risk factors and breast cancer subtypes: a review of the literature.* Breast Cancer Res Treat, 2014. **144**(1): p. 1-10.
16. Hu, Z., et al., *The molecular portraits of breast tumors are conserved across microarray platforms.* BMC Genomics, 2006. **7**: p. 96.
17. Ullrich, A. and J. Schlessinger, *Signal transduction by receptors with tyrosine kinase activity.* Cell, 1990. **61**(2): p. 203-12.
18. Templeton, A.J., et al., *Prognostic relevance of receptor tyrosine kinase expression in breast cancer: a meta-analysis.* Cancer Treat Rev, 2014. **40**(9): p. 1048-55.
19. Lemmon, M.A. and J. Schlessinger, *Cell signaling by receptor tyrosine kinases.* Cell, 2010. **141**(7): p. 1117-34.
20. Zeqiraj, E. and D.M. van Aalten, *Pseudokinases-remnants of evolution or key allosteric regulators?* Curr Opin Struct Biol, 2010. **20**(6): p. 772-81.
21. Du, Z. and C.M. Lovly, *Mechanisms of receptor tyrosine kinase activation in cancer.* Mol Cancer, 2018. **17**(1): p. 58.

22. Lapraz, F., et al., *RTK and TGF-beta signaling pathways genes in the sea urchin genome.* Dev Biol, 2006. **300**(1): p. 132-52.
23. Linger, R.M., et al., *TAM receptor tyrosine kinases: biologic functions, signaling, and potential therapeutic targeting in human cancer.* Adv Cancer Res, 2008. **100**: p. 35-83.
24. Graham, D.K., et al., *The TAM family: phosphatidylserine sensing receptor tyrosine kinases gone awry in cancer.* Nat Rev Cancer, 2014. **14**(12): p. 769-85.
25. Davra, V., et al., *Ligand Activation of TAM Family Receptors-Implications for Tumor Biology and Therapeutic Response.* Cancers (Basel), 2016. **8**(12).
26. Mercer, J. and A. Helenius, *Vaccinia virus uses macropinocytosis and apoptotic mimicry to enter host cells.* Science, 2008. **320**(5875): p. 531-5.
27. Chen, C., et al., *Mer receptor tyrosine kinase signaling participates in platelet function.* Arterioscler Thromb Vasc Biol, 2004. **24**(6): p. 1118-23.
28. Scott, R.S., et al., *Phagocytosis and clearance of apoptotic cells is mediated by MER.* Nature, 2001. **411**(6834): p. 207-11.
29. Caberoy, N.B., G. Alvarado, and W. Li, *Tubby regulates microglial phagocytosis through MerTK.* J Neuroimmunol, 2012. **252**(1-2): p. 40-8.
30. Caberoy, N.B., et al., *Galectin-3 is a new MerTK-specific eat-me signal.* J Cell Physiol, 2012. **227**(2): p. 401-7.
31. Caberoy, N.B., Y. Zhou, and W. Li, *Tubby and tubby-like protein 1 are new MerTK ligands for phagocytosis.* EMBO J, 2010. **29**(23): p. 3898-910.
32. Zagorska, A., et al., *Diversification of TAM receptor tyrosine kinase function.* Nat Immunol, 2014. **15**(10): p. 920-8.
33. N, A.G., et al., *Apoptotic cells promote their own clearance and immune tolerance through activation of the nuclear receptor LXR.* Immunity, 2009. **31**(2): p. 245-58.
34. Li, Y., et al., *The C-mer gene is induced by Epstein-Barr virus immediate-early protein BRLF1.* J Virol, 2004. **78**(21): p. 11778-85.
35. Rankin, E.B., et al., *Direct regulation of GAS6/AXL signaling by HIF promotes renal metastasis through SRC and MET.* Proc Natl Acad Sci U S A, 2014. **111**(37): p. 13373-8.
36. Mudduluru, G. and H. Allgayer, *The human receptor tyrosine kinase Axl gene--promoter characterization and regulation of constitutive expression by Sp1, Sp3 and CpG methylation.* Biosci Rep, 2008. **28**(3): p. 161-76.
37. Mudduluru, G., P. Vajkoczy, and H. Allgayer, *Myeloid zinc finger 1 induces migration, invasion, and in vivo metastasis through Axl gene expression in solid cancer.* Mol Cancer Res, 2010. **8**(2): p. 159-69.
38. Giles, K.M., et al., *Axl mediates acquired resistance of head and neck cancer cells to the epidermal growth factor receptor inhibitor erlotinib.* Mol Cancer Ther, 2013. **12**(11): p. 2541-58.
39. Png, K.J., et al., *A microRNA regulon that mediates endothelial recruitment and metastasis by cancer cells.* Nature, 2011. **481**(7380): p. 190-4.
40. Mudduluru, G., et al., *Regulation of Axl receptor tyrosine kinase expression by miR-34a and miR-199a/b in solid cancer.* Oncogene, 2011. **30**(25): p. 2888-99.
41. Mackiewicz, M., et al., *Identification of the receptor tyrosine kinase AXL in breast cancer as a target for the human miR-34a microRNA.* Breast Cancer Res Treat, 2011. **130**(2): p. 663-79.

42. Kaller, M., et al., *Genome-wide characterization of miR-34a induced changes in protein and mRNA expression by a combined pulsed SILAC and microarray analysis.* Mol Cell Proteomics, 2011. **10**(8): p. M111 010462.
43. Tsou, W.I., et al., *Receptor tyrosine kinases, TYRO3, AXL, and MER, demonstrate distinct patterns and complex regulation of ligand-induced activation.* J Biol Chem, 2014. **289**(37): p. 25750-63.
44. Varnum, B.C., et al., *Axl receptor tyrosine kinase stimulated by the vitamin K-dependent protein encoded by growth-arrest-specific gene 6.* Nature, 1995. **373**(6515): p. 623-6.
45. Sasaki, T., et al., *Structural basis for Gas6-Axl signalling.* EMBO J, 2006. **25**(1): p. 80-7.
46. Paolino, M., et al., *The E3 ligase Cbl-b and TAM receptors regulate cancer metastasis via natural killer cells.* Nature, 2014. **507**(7493): p. 508-12.
47. Braunger, J., et al., *Intracellular signaling of the Ufo/Axl receptor tyrosine kinase is mediated mainly by a multi-substrate docking-site.* Oncogene, 1997. **14**(22): p. 2619-31.
48. Wu, Y., N. Tibrewal, and R.B. Birge, *Phosphatidylserine recognition by phagocytes: a view to a kill.* Trends Cell Biol, 2006. **16**(4): p. 189-97.
49. Lew, E.D., et al., *Differential TAM receptor-ligand-phospholipid interactions delimit differential TAM bioactivities.* Elife, 2014. **3**.
50. Fujimori, T., et al., *The Axl receptor tyrosine kinase is a discriminator of macrophage function in the inflamed lung.* Mucosal Immunol, 2015. **8**(5): p. 1021-1030.
51. Meyer, A.S., A.J. Zweemer, and D.A. Lauffenburger, *The AXL Receptor is a Sensor of Ligand Spatial Heterogeneity.* Cell Syst, 2015. **1**(1): p. 25-36.
52. Seitz, H.M., et al., *Macrophages and dendritic cells use different Axl/Mertk/Tyro3 receptors in clearance of apoptotic cells.* J Immunol, 2007. **178**(9): p. 5635-42.
53. Lemke, G. and C.V. Rothlin, *Immunobiology of the TAM receptors.* Nat Rev Immunol, 2008. **8**(5): p. 327-36.
54. Bellosta, P., et al., *The receptor tyrosine kinase ARK mediates cell aggregation by homophilic binding.* Mol Cell Biol, 1995. **15**(2): p. 614-25.
55. Konishi, A., et al., *Hydrogen peroxide activates the Gas6-Axl pathway in vascular smooth muscle cells.* J Biol Chem, 2004. **279**(27): p. 28766-70.
56. Brown, J.E., et al., *Cross-phosphorylation, signaling and proliferative functions of the Tyro3 and Axl receptors in Rat2 cells.* PLoS One, 2012. **7**(5): p. e36800.
57. Meyer, A.S., et al., *The receptor AXL diversifies EGFR signaling and limits the response to EGFR-targeted inhibitors in triple-negative breast cancer cells.* Sci Signal, 2013. **6**(287): p. ra66.
58. Goyette, M.A., et al., *The Receptor Tyrosine Kinase AXL Is Required at Multiple Steps of the Metastatic Cascade during HER2-Positive Breast Cancer Progression.* Cell Rep, 2018. **23**(5): p. 1476-1490.
59. Ruan, G.X. and A. Kazlauskas, *Axl is essential for VEGF-A-dependent activation of PI3K/Akt.* EMBO J, 2012. **31**(7): p. 1692-703.
60. Salian-Mehta, S., M. Xu, and M.E. Wierman, *AXL and MET crosstalk to promote gonadotropin releasing hormone (GnRH) neuronal cell migration and survival.* Mol Cell Endocrinol, 2013. **374**(1-2): p. 92-100.
61. Elkabets, M., et al., *AXL mediates resistance to PI3Kalpha inhibition by activating the EGFR/PKC/mTOR axis in head and neck and esophageal squamous cell carcinomas.* Cancer Cell, 2015. **27**(4): p. 533-46.

62. Miller, M.A., et al., *Reduced Proteolytic Shedding of Receptor Tyrosine Kinases Is a Post-Translational Mechanism of Kinase Inhibitor Resistance.* Cancer Discov, 2016. **6**(4): p. 382-99.
63. Hafizi, S., et al., *Interaction of Axl receptor tyrosine kinase with C1-TEN, a novel C1 domain-containing protein with homology to tensin.* Biochem Biophys Res Commun, 2002. **299**(5): p. 793-800.
64. Hafizi, S., F. Ibraimi, and B. Dahlback, *C1-TEN is a negative regulator of the Akt/PKB signal transduction pathway and inhibits cell survival, proliferation, and migration.* FASEB J, 2005. **19**(8): p. 971-3.
65. Antony, J., et al., *The tumour suppressor OPCML promotes AXL inactivation by the phosphatase PTPRG in ovarian cancer.* EMBO Rep, 2018.
66. Shiozawa, Y., et al., *GAS6/AXL axis regulates prostate cancer invasion, proliferation, and survival in the bone marrow niche.* Neoplasia, 2010. **12**(2): p. 116-27.
67. Darby, C., et al., *ETK2 receptor tyrosine kinase promotes survival of factor-dependent FDC-P1 progenitor cells.* Exp Hematol, 2000. **28**(6): p. 716-25.
68. Ghosh, A.K., et al., *The novel receptor tyrosine kinase Axl is constitutively active in B-cell chronic lymphocytic leukemia and acts as a docking site of nonreceptor kinases: implications for therapy.* Blood, 2011. **117**(6): p. 1928-37.
69. Park, I.K., et al., *Inhibition of the receptor tyrosine kinase Axl impedes activation of the FLT3 internal tandem duplication in human acute myeloid leukemia: implications for Axl as a potential therapeutic target.* Blood, 2013. **121**(11): p. 2064-73.
70. Goruppi, S., et al., *Requirement of phosphatidylinositol 3-kinase-dependent pathway and Src for Gas6-Axl mitogenic and survival activities in NIH 3T3 fibroblasts.* Mol Cell Biol, 1997. **17**(8): p. 4442-53.
71. Ou, W.B., et al., *AXL regulates mesothelioma proliferation and invasiveness.* Oncogene, 2011. **30**(14): p. 1643-52.
72. Hong, C.C., et al., *Receptor tyrosine kinase AXL is induced by chemotherapy drugs and overexpression of AXL confers drug resistance in acute myeloid leukemia.* Cancer Lett, 2008. **268**(2): p. 314-24.
73. Linger, R.M., et al., *Mer or Axl receptor tyrosine kinase inhibition promotes apoptosis, blocks growth and enhances chemosensitivity of human non-small cell lung cancer.* Oncogene, 2013. **32**(29): p. 3420-31.
74. Leconet, W., et al., *Preclinical validation of AXL receptor as a target for antibody-based pancreatic cancer immunotherapy.* Oncogene, 2014. **33**(47): p. 5405-14.
75. Keating, A.K., et al., *Inhibition of Mer and Axl receptor tyrosine kinases in astrocytoma cells leads to increased apoptosis and improved chemosensitivity.* Mol Cancer Ther, 2010. **9**(5): p. 1298-307.
76. Ben-Batalla, I., et al., *Axl, a prognostic and therapeutic target in acute myeloid leukemia mediates paracrine crosstalk of leukemia cells with bone marrow stroma.* Blood, 2013. **122**(14): p. 2443-52.
77. Papadakis, E.S., et al., *Axl promotes cutaneous squamous cell carcinoma survival through negative regulation of pro-apoptotic Bcl-2 family members.* J Invest Dermatol, 2011. **131**(2): p. 509-17.
78. Lee, W.P., et al., *Akt is required for Axl-Gas6 signaling to protect cells from E1A-mediated apoptosis.* Oncogene, 2002. **21**(3): p. 329-36.

79. Demarchi, F., et al., *Gas6 anti-apoptotic signaling requires NF-kappa B activation.* J Biol Chem, 2001. **276**(34): p. 31738-44.
80. Dunne, P.D., et al., *AXL is a key regulator of inherent and chemotherapy-induced invasion and predicts a poor clinical outcome in early-stage colon cancer.* Clin Cancer Res, 2014. **20**(1): p. 164-75.
81. Paccez, J.D., et al., *The receptor tyrosine kinase Axl is an essential regulator of prostate cancer proliferation and tumor growth and represents a new therapeutic target.* Oncogene, 2013. **32**(6): p. 689-98.
82. Ammoun, S., et al., *Axl/Gas6/NFkappaB signalling in schwannoma pathological proliferation, adhesion and survival.* Oncogene, 2014. **33**(3): p. 336-46.
83. Allen, M.P., et al., *Adhesion-related kinase repression of gonadotropin-releasing hormone gene expression requires Rac activation of the extracellular signal-regulated kinase pathway.* J Biol Chem, 2002. **277**(41): p. 38133-40.
84. Allen, M.P., et al., *Novel mechanism for gonadotropin-releasing hormone neuronal migration involving Gas6/Ark signaling to p38 mitogen-activated protein kinase.* Mol Cell Biol, 2002. **22**(2): p. 599-613.
85. Vajkoczy, P., et al., *Dominant-negative inhibition of the Axl receptor tyrosine kinase suppresses brain tumor cell growth and invasion and prolongs survival.* Proc Natl Acad Sci U S A, 2006. **103**(15): p. 5799-804.
86. Gjerdrum, C., et al., *Axl is an essential epithelial-to-mesenchymal transition-induced regulator of breast cancer metastasis and patient survival.* Proc Natl Acad Sci U S A, 2010. **107**(3): p. 1124-9.
87. Vuoriluoto, K., et al., *Vimentin regulates EMT induction by Slug and oncogenic H-Ras and migration by governing Axl expression in breast cancer.* Oncogene, 2011. **30**(12): p. 1436-48.
88. Rankin, E.B., et al., *AXL is an essential factor and therapeutic target for metastatic ovarian cancer.* Cancer Res, 2010. **70**(19): p. 7570-9.
89. Holland, S.J., et al., *R428, a selective small molecule inhibitor of Axl kinase, blocks tumor spread and prolongs survival in models of metastatic breast cancer.* Cancer Res, 2010. **70**(4): p. 1544-54.
90. Asiedu, M.K., et al., *AXL induces epithelial-to-mesenchymal transition and regulates the function of breast cancer stem cells.* Oncogene, 2014. **33**(10): p. 1316-24.
91. Lee, H.J., et al., *Gas6/Axl pathway promotes tumor invasion through the transcriptional activation of Slug in hepatocellular carcinoma.* Carcinogenesis, 2014. **35**(4): p. 769-75.
92. Wilson, C., et al., *AXL inhibition sensitizes mesenchymal cancer cells to antimitotic drugs.* Cancer Res, 2014. **74**(20): p. 5878-90.
93. Antony, J., et al., *The GAS6-AXL signaling network is a mesenchymal (Mes) molecular subtype-specific therapeutic target for ovarian cancer.* Sci Signal, 2016. **9**(448): p. ra97.
94. Halmos, B. and E.B. Haura, *New twists in the AXL(e) of tumor progression.* Sci Signal, 2016. **9**(448): p. fs14.
95. Abu-Thuraia, A., et al., *Axl phosphorylates Elmo scaffold proteins to promote Rac activation and cell invasion.* Mol Cell Biol, 2015. **35**(1): p. 76-87.
96. Tu, Y., F. Li, and C. Wu, *Nck-2, a novel Src homology2/3-containing adaptor protein that interacts with the LIM-only protein PINCH and components of growth factor receptor kinase-signaling pathways.* Mol Biol Cell, 1998. **9**(12): p. 3367-82.

97. Yang, B., et al., *Mechanosensing Controlled Directly by Tyrosine Kinases.* Nano Lett, 2016. **16**(9): p. 5951-61.
98. Rea, K., et al., *Novel Axl-driven signaling pathway and molecular signature characterize high-grade ovarian cancer patients with poor clinical outcome.* Oncotarget, 2015. **6**(31): p. 30859-75.
99. Tai, K.Y., et al., *Axl promotes cell invasion by inducing MMP-9 activity through activation of NF-kappaB and Brg-1.* Oncogene, 2008. **27**(29): p. 4044-55.
100. Wu, X., et al., *AXL-GAS6 expression can predict for adverse prognosis in non-small cell lung cancer with brain metastases.* J Cancer Res Clin Oncol, 2017.
101. Kariolis, M.S., et al., *An engineered Axl 'decoy receptor' effectively silences the Gas6-Axl signaling axis.* Nat Chem Biol, 2014. **10**(11): p. 977-83.
102. Mc Cormack, O., et al., *Growth arrest-specific gene 6 expression in human breast cancer.* Br J Cancer, 2008. **98**(6): p. 1141-6.
103. Loges, S., et al., *Malignant cells fuel tumor growth by educating infiltrating leukocytes to produce the mitogen Gas6.* Blood, 2010. **115**(11): p. 2264-73.
104. Lee-Sherick, A.B., et al., *Aberrant Mer receptor tyrosine kinase expression contributes to leukemogenesis in acute myeloid leukemia.* Oncogene, 2013. **32**(46): p. 5359-68.
105. Iida, K., et al., *Cell softening in malignant progression of human lung cancer cells by activation of receptor tyrosine kinase AXL.* Sci Rep, 2017. **7**(1): p. 17770.
106. Zhang, S., et al., *The prognostic role of Gas6/Axl axis in solid malignancies: a meta-analysis and literature review.* Onco Targets Ther, 2018. **11**: p. 509-519.
107. Lozneanu, L., et al., *Computational and Immunohistochemical Analyses Highlight AXL as a Potential Prognostic Marker for Ovarian Cancer Patients.* Anticancer Res, 2016. **36**(8): p. 4155-63.
108. Chien, C.W., et al., *Targeting TYRO3 inhibits epithelial-mesenchymal transition and increases drug sensitivity in colon cancer.* Oncogene, 2016. **35**(45): p. 5872-5881.
109. Tanaka, K., et al., *Impact of Expression of Vimentin and Axl in Breast Cancer.* Clin Breast Cancer, 2016.
110. Lambert, A.W., D.R. Pattabiraman, and R.A. Weinberg, *Emerging Biological Principles of Metastasis.* Cell, 2017. **168**(4): p. 670-691.
111. Del Pozo Martin, Y., et al., *Mesenchymal Cancer Cell-Stroma Crosstalk Promotes Niche Activation, Epithelial Reversion, and Metastatic Colonization.* Cell Rep, 2015. **13**(11): p. 2456-69.
112. Sosa, M.S., P. Bragado, and J.A. Aguirre-Ghiso, *Mechanisms of disseminated cancer cell dormancy: an awakening field.* Nat Rev Cancer, 2014. **14**(9): p. 611-22.
113. Yumoto, K., et al., *Axl is required for TGF-beta2-induced dormancy of prostate cancer cells in the bone marrow.* Sci Rep, 2016. **6**: p. 36520.
114. Jung, Y., et al., *Endogenous GAS6 and Mer receptor signaling regulate prostate cancer stem cells in bone marrow.* Oncotarget, 2016. **7**(18): p. 25698-711.
115. Burstyn-Cohen, T., M.J. Heeb, and G. Lemke, *Lack of protein S in mice causes embryonic lethal coagulopathy and vascular dysgenesis.* J Clin Invest, 2009. **119**(10): p. 2942-53.
116. Melaragno, M.G., Y.W. Fridell, and B.C. Berk, *The Gas6/Axl system: a novel regulator of vascular cell function.* Trends Cardiovasc Med, 1999. **9**(8): p. 250-3.

117. Fraineau, S., et al., *The vitamin K-dependent anticoagulant factor, protein S, inhibits multiple VEGF-A-induced angiogenesis events in a Mer- and SHP2-dependent manner.* Blood, 2012. **120**(25): p. 5073-83.
118. Holland, S.J., et al., *Multiple roles for the receptor tyrosine kinase axl in tumor formation.* Cancer Res, 2005. **65**(20): p. 9294-303.
119. Li, Y., et al., *Axl as a potential therapeutic target in cancer: role of Axl in tumor growth, metastasis and angiogenesis.* Oncogene, 2009. **28**(39): p. 3442-55.
120. Lu, Q., et al., *Tyro-3 family receptors are essential regulators of mammalian spermatogenesis.* Nature, 1999. **398**(6729): p. 723-8.
121. Duncan, J.L., et al., *An RCS-like retinal dystrophy phenotype in mer knockout mice.* Invest Ophthalmol Vis Sci, 2003. **44**(2): p. 826-38.
122. Rothlin, C.V., et al., *TAM receptors are pleiotropic inhibitors of the innate immune response.* Cell, 2007. **131**(6): p. 1124-36.
123. Lu, Q. and G. Lemke, *Homeostatic regulation of the immune system by receptor tyrosine kinases of the Tyro 3 family.* Science, 2001. **293**(5528): p. 306-11.
124. Chiu, K.C., et al., *Polarization of tumor-associated macrophages and Gas6/Axl signaling in oral squamous cell carcinoma.* Oral Oncol, 2015. **51**(7): p. 683-9.
125. Bottai, G., et al., *AXL-associated tumor inflammation as a poor prognostic signature in chemotherapy-treated triple-negative breast cancer patients.* Npj Breast Cancer, 2016. **2**: p. 16033.
126. Cook, R.S., et al., *MerTK inhibition in tumor leukocytes decreases tumor growth and metastasis.* J Clin Invest, 2013. **123**(8): p. 3231-42.
127. Schmid, E.T., et al., *AXL receptor tyrosine kinase is required for T cell priming and antiviral immunity.* Elife, 2016. **5**.
128. Carrera Silva, E.A., et al., *T cell-derived protein S engages TAM receptor signaling in dendritic cells to control the magnitude of the immune response.* Immunity, 2013. **39**(1): p. 160-70.
129. Zhao, G.J., et al., *Growth Arrest-Specific 6 Enhances the Suppressive Function of CD4+CD25+ Regulatory T Cells Mainly through Axl Receptor.* Mediators Inflamm, 2017. **2017**: p. 6848430.
130. Bosurgi, L., et al., *Paradoxical role of the proto-oncogene Axl and Mer receptor tyrosine kinases in colon cancer.* Proc Natl Acad Sci U S A, 2013. **110**(32): p. 13091-6.
131. Lin, J.Z., et al., *Targeting AXL overcomes resistance to docetaxel therapy in advanced prostate cancer.* Oncotarget, 2017. **8**(25): p. 41064-41077.
132. Oien, D.B., et al., *Cisplatin and Pemetrexed Activate AXL and AXL Inhibitor BGB324 Enhances Mesothelioma Cell Death from Chemotherapy.* Front Pharmacol, 2017. **8**: p. 970.
133. Li, Y., et al., *Inhibition of Mer and Axl receptor tyrosine kinases leads to increased apoptosis and improved chemosensitivity in human neuroblastoma.* Biochem Biophys Res Commun, 2015. **457**(3): p. 461-6.
134. Ludwig, K.F., et al., *Small-Molecule Inhibition of Axl Targets Tumor Immune Suppression and Enhances Chemotherapy in Pancreatic Cancer.* Cancer Res, 2018. **78**(1): p. 246-255.
135. Zhao, Y., et al., *Differential expression of Axl and correlation with invasion and multidrug resistance in cancer cells.* Cancer Invest, 2012. **30**(4): p. 287-94.

136. Kasikara, C., et al., *Phosphatidylserine Sensing by TAM Receptors Regulates AKT-Dependent Chemoresistance and PD-L1 Expression.* Mol Cancer Res, 2017. **15**(6): p. 753-764.
137. Dufies, M., et al., *Mechanisms of AXL overexpression and function in Imatinib-resistant chronic myeloid leukemia cells.* Oncotarget, 2011. **2**(11): p. 874-85.
138. Xie, S., et al., *Mer receptor tyrosine kinase is frequently overexpressed in human non-small cell lung cancer, confirming resistance to erlotinib.* Oncotarget, 2015. **6**(11): p. 9206-19.
139. Zhang, Z., et al., *Activation of the AXL kinase causes resistance to EGFR-targeted therapy in lung cancer.* Nat Genet, 2012. **44**(8): p. 852-60.
140. Bae, S.Y., et al., *Targeting the degradation of AXL receptor tyrosine kinase to overcome resistance in gefitinib-resistant non-small cell lung cancer.* Oncotarget, 2015. **6**(12): p. 10146-60.
141. Brand, T.M., et al., *AXL mediates resistance to cetuximab therapy.* Cancer Res, 2014. **74**(18): p. 5152-64.
142. Liu, L., et al., *Novel mechanism of lapatinib resistance in HER2-positive breast tumor cells: activation of AXL.* Cancer Res, 2009. **69**(17): p. 6871-8.
143. Debruyne, D.N., et al., *ALK inhibitor resistance in ALK(F1174L)-driven neuroblastoma is associated with AXL activation and induction of EMT.* Oncogene, 2016. **35**(28): p. 3681-91.
144. Balaji, K., et al., *AXL Inhibition Suppresses the DNA Damage Response and Sensitizes Cells to PARP Inhibition in Multiple Cancers.* Mol Cancer Res, 2017. **15**(1): p. 45-58.
145. Gustafsson, A., H.K.M. Fritz, and B. Dahlback, *Gas6-Axl signaling in presence of Sunitinib is enhanced, diversified and sustained in renal tumor cells, resulting in tumor-progressive advantages.* Exp Cell Res, 2017. **355**(1): p. 47-56.
146. Zhou, L., et al., *Targeting MET and AXL overcomes resistance to sunitinib therapy in renal cell carcinoma.* Oncogene, 2016. **35**(21): p. 2687-97.
147. Sharma, P., et al., *Primary, Adaptive, and Acquired Resistance to Cancer Immunotherapy.* Cell, 2017. **168**(4): p. 707-723.
148. Aguilera, T.A., et al., *Reprogramming the immunological microenvironment through radiation and targeting Axl.* Nat Commun, 2016. **7**: p. 13898.
149. Skinner, H.D., et al., *Integrative Analysis Identifies a Novel AXL-PI3 Kinase-PD-L1 Signaling Axis Associated with Radiation Resistance in Head and Neck Cancer.* Clin Cancer Res, 2017. **23**(11): p. 2713-2722.
150. Guo, Z., et al., *Axl inhibition induces the antitumor immune response which can be further potentiated by PD-1 blockade in the mouse cancer models.* Oncotarget, 2017. **8**(52): p. 89761-89774.
151. Kasikara, C., et al., *Phosphatidylserine Sensing by TAM Receptors Regulates AKT-dependent Chemoresistance and PD-L1 Expression.* Mol Cancer Res, 2017.
152. Lee, S.H. and R. Dominguez, *Regulation of actin cytoskeleton dynamics in cells.* Mol Cells, 2010. **29**(4): p. 311-25.
153. Oda, T., et al., *The nature of the globular- to fibrous-actin transition.* Nature, 2009. **457**(7228): p. 441-5.
154. Hussey, P.J., T. Ketelaar, and M.J. Deeks, *Control of the actin cytoskeleton in plant cell growth.* Annu Rev Plant Biol, 2006. **57**: p. 109-25.

155. Itoh, G. and S. Yumura, *A novel mitosis-specific dynamic actin structure in Dictyostelium cells.* J Cell Sci, 2007. **120**(Pt 24): p. 4302-9.
156. McMahon, H.T. and J.L. Gallop, *Membrane curvature and mechanisms of dynamic cell membrane remodelling.* Nature, 2005. **438**(7068): p. 590-6.
157. Puppo, A., et al., *Alteration of the cortical actin cytoskeleton deregulates Ca2+ signaling, monospermic fertilization, and sperm entry.* PLoS One, 2008. **3**(10): p. e3588.
158. Yamaguchi, H. and J. Condeelis, *Regulation of the actin cytoskeleton in cancer cell migration and invasion.* Biochim Biophys Acta, 2007. **1773**(5): p. 642-52.
159. Pollard, T.D. and G.G. Borisy, *Cellular motility driven by assembly and disassembly of actin filaments.* Cell, 2003. **112**(4): p. 453-65.
160. Schutt, C.E., et al., *The structure of crystalline profilin-beta-actin.* Nature, 1993. **365**(6449): p. 810-6.
161. Fedorov, A.A., et al., *Structure determination of yeast cofilin.* Nat Struct Biol, 1997. **4**(5): p. 366-9.
162. Chereau, D., et al., *Actin-bound structures of Wiskott-Aldrich syndrome protein (WASP)-homology domain 2 and the implications for filament assembly.* Proc Natl Acad Sci U S A, 2005. **102**(46): p. 16644-9.
163. Takenawa, T. and S. Suetsugu, *The WASP-WAVE protein network: connecting the membrane to the cytoskeleton.* Nat Rev Mol Cell Biol, 2007. **8**(1): p. 37-48.
164. Zigmond, S.H., *Formin-induced nucleation of actin filaments.* Curr Opin Cell Biol, 2004. **16**(1): p. 99-105.
165. Raftopoulou, M. and A. Hall, *Cell migration: Rho GTPases lead the way.* Dev Biol, 2004. **265**(1): p. 23-32.
166. Hall, A., *Small GTP-binding proteins and the regulation of the actin cytoskeleton.* Annu Rev Cell Biol, 1994. **10**: p. 31-54.
167. Dawson, J.C., J.A. Legg, and L.M. Machesky, *Bar domain proteins: a role in tubulation, scission and actin assembly in clathrin-mediated endocytosis.* Trends Cell Biol, 2006. **16**(10): p. 493-8.
168. Pylypenko, O., et al., *The PX-BAR membrane-remodeling unit of sorting nexin 9.* EMBO J, 2007. **26**(22): p. 4788-800.
169. Shimada, A., et al., *Curved EFC/F-BAR-domain dimers are joined end to end into a filament for membrane invagination in endocytosis.* Cell, 2007. **129**(4): p. 761-72.
170. Scita, G., et al., *IRSp53: crossing the road of membrane and actin dynamics in the formation of membrane protrusions.* Trends Cell Biol, 2008. **18**(2): p. 52-60.
171. Schultz, J., et al., *SMART, a simple modular architecture research tool: identification of signaling domains.* Proc Natl Acad Sci U S A, 1998. **95**(11): p. 5857-64.
172. Wennerberg, K. and C.J. Der, *Rho-family GTPases: it's not only Rac and Rho (and I like it).* J Cell Sci, 2004. **117**(Pt 8): p. 1301-12.
173. Jaffe, A.B. and A. Hall, *Rho GTPases: biochemistry and biology.* Annu Rev Cell Dev Biol, 2005. **21**: p. 247-69.
174. Bishop, A.L. and A. Hall, *Rho GTPases and their effector proteins.* Biochem J, 2000. **348 Pt 2**: p. 241-55.
175. Ridley, A.J. and A. Hall, *The small GTP-binding protein rho regulates the assembly of focal adhesions and actin stress fibers in response to growth factors.* Cell, 1992. **70**(3): p. 389-99.

176. Ridley, A.J., et al., *The small GTP-binding protein rac regulates growth factor-induced membrane ruffling.* Cell, 1992. **70**(3): p. 401-10.
177. Etienne-Manneville, S. and A. Hall, *Rho GTPases in cell biology.* Nature, 2002. **420**(6916): p. 629-35.
178. Grise, F., A. Bidaud, and V. Moreau, *Rho GTPases in hepatocellular carcinoma.* Biochim Biophys Acta, 2009. **1795**(2): p. 137-51.
179. Page, R.D., *TreeView: an application to display phylogenetic trees on personal computers.* Comput Appl Biosci, 1996. **12**(4): p. 357-8.
180. Pruyne, D. and A. Bretscher, *Polarization of cell growth in yeast. I. Establishment and maintenance of polarity states.* J Cell Sci, 2000. **113 (Pt 3)**: p. 365-75.
181. Lin, D., et al., *A mammalian PAR-3-PAR-6 complex implicated in Cdc42/Rac1 and aPKC signalling and cell polarity.* Nat Cell Biol, 2000. **2**(8): p. 540-7.
182. Joberty, G., et al., *The cell-polarity protein Par6 links Par3 and atypical protein kinase C to Cdc42.* Nat Cell Biol, 2000. **2**(8): p. 531-9.
183. Vasioukhin, V., et al., *Directed actin polymerization is the driving force for epithelial cell-cell adhesion.* Cell, 2000. **100**(2): p. 209-19.
184. Jacinto, A., A. Martinez-Arias, and P. Martin, *Mechanisms of epithelial fusion and repair.* Nat Cell Biol, 2001. **3**(5): p. E117-23.
185. Lee, T., et al., *Essential roles of Drosophila RhoA in the regulation of neuroblast proliferation and dendritic but not axonal morphogenesis.* Neuron, 2000. **25**(2): p. 307-16.
186. Wong, W.T., et al., *Rapid dendritic remodeling in the developing retina: dependence on neurotransmission and reciprocal regulation by Rac and Rho.* J Neurosci, 2000. **20**(13): p. 5024-36.
187. Yamanaka, T., et al., *PAR-6 regulates aPKC activity in a novel way and mediates cell-cell contact-induced formation of the epithelial junctional complex.* Genes Cells, 2001. **6**(8): p. 721-31.
188. O'Brien, L.E., et al., *Rac1 orientates epithelial apical polarity through effects on basolateral laminin assembly.* Nat Cell Biol, 2001. **3**(9): p. 831-8.
189. Sugihara, K., et al., *The exocyst complex binds the small GTPase RalA to mediate filopodia formation.* Nat Cell Biol, 2002. **4**(1): p. 73-8.
190. Moskalenko, S., et al., *The exocyst is a Ral effector complex.* Nat Cell Biol, 2002. **4**(1): p. 66-72.
191. Small, J.V., et al., *The lamellipodium: where motility begins.* Trends Cell Biol, 2002. **12**(3): p. 112-20.
192. Ng, J., et al., *Rac GTPases control axon growth, guidance and branching.* Nature, 2002. **416**(6879): p. 442-7.
193. Worthylake, R.A., et al., *RhoA is required for monocyte tail retraction during transendothelial migration.* J Cell Biol, 2001. **154**(1): p. 147-60.
194. Allen, W.E., et al., *A role for Cdc42 in macrophage chemotaxis.* J Cell Biol, 1998. **141**(5): p. 1147-57.
195. Condeelis, J., *How is actin polymerization nucleated in vivo?* Trends Cell Biol, 2001. **11**(7): p. 288-93.
196. Albert, M.L., J.I. Kim, and R.B. Birge, *alphavbeta5 integrin recruits the CrkII-Dock180-rac1 complex for phagocytosis of apoptotic cells.* Nat Cell Biol, 2000. **2**(12): p. 899-905.

197. Wittmann, T. and C.M. Waterman-Storer, *Cell motility: can Rho GTPases and microtubules point the way?* J Cell Sci, 2001. **114**(Pt 21): p. 3795-803.
198. Brock, J., et al., *Healing of incisional wounds in the embryonic chick wing bud: characterization of the actin purse-string and demonstration of a requirement for Rho activation.* J Cell Biol, 1996. **135**(4): p. 1097-107.
199. Lu, Y. and J. Settleman, *The Drosophila Pkn protein kinase is a Rho/Rac effector target required for dorsal closure during embryogenesis.* Genes Dev, 1999. **13**(9): p. 1168-80.
200. Stronach, B.E. and N. Perrimon, *Stress signaling in Drosophila.* Oncogene, 1999. **18**(45): p. 6172-82.
201. Knust, E., *Drosophila morphogenesis: movements behind the edge.* Curr Biol, 1997. **7**(9): p. R558-61.
202. Sakurada, S., et al., *Rho activation in excitatory agonist-stimulated vascular smooth muscle.* Am J Physiol Cell Physiol, 2001. **281**(2): p. C571-8.
203. Fukata, Y., M. Amano, and K. Kaibuchi, *Rho-Rho-kinase pathway in smooth muscle contraction and cytoskeletal reorganization of non-muscle cells.* Trends Pharmacol Sci, 2001. **22**(1): p. 32-9.
204. van Nieuw Amerongen, G.P., et al., *Activation of RhoA by thrombin in endothelial hyperpermeability: role of Rho kinase and protein tyrosine kinases.* Circ Res, 2000. **87**(4): p. 335-40.
205. Caron, E. and A. Hall, *Identification of two distinct mechanisms of phagocytosis controlled by different Rho GTPases.* Science, 1998. **282**(5394): p. 1717-21.
206. Bokoch, G.M., *Regulation of cell function by Rho family GTPases.* Immunol Res, 2000. **21**(2-3): p. 139-48.
207. deBakker, C.D., et al., *Phagocytosis of apoptotic cells is regulated by a UNC-73/TRIO-MIG-2/RhoG signaling module and armadillo repeats of CED-12/ELMO.* Curr Biol, 2004. **14**(24): p. 2208-16.
208. Hoppe, A.D. and J.A. Swanson, *Cdc42, Rac1, and Rac2 display distinct patterns of activation during phagocytosis.* Mol Biol Cell, 2004. **15**(8): p. 3509-19.
209. Patel, J.C., A. Hall, and E. Caron, *Vav regulates activation of Rac but not Cdc42 during FcgammaR-mediated phagocytosis.* Mol Biol Cell, 2002. **13**(4): p. 1215-26.
210. May, R.C., et al., *Involvement of the Arp2/3 complex in phagocytosis mediated by FcgammaR or CR3.* Nat Cell Biol, 2000. **2**(4): p. 246-8.
211. Olson, M.F., A. Ashworth, and A. Hall, *An essential role for Rho, Rac, and Cdc42 GTPases in cell cycle progression through G1.* Science, 1995. **269**(5228): p. 1270-2.
212. Cantrell, D., *Lymphocyte signalling: a coordinating role for Vav?* Curr Biol, 1998. **8**(15): p. R535-8.
213. Glassford, J., et al., *Vav is required for cyclin D2 induction and proliferation of mouse B lymphocytes activated via the antigen Receptor.* J Biol Chem, 2001. **276**(44): p. 41040-8.
214. Welsh, C.F., et al., *Timing of cyclin D1 expression within G1 phase is controlled by Rho.* Nat Cell Biol, 2001. **3**(11): p. 950-7.
215. Olson, M.F., H.F. Paterson, and C.J. Marshall, *Signals from Ras and Rho GTPases interact to regulate expression of p21Waf1/Cip1.* Nature, 1998. **394**(6690): p. 295-9.
216. Stowers, L., et al., *Regulation of the polarization of T cells toward antigen-presenting cells by Ras-related GTPase CDC42.* Proc Natl Acad Sci U S A, 1995. **92**(11): p. 5027-31.

217. Chiang, S.H., et al., *Insulin-stimulated GLUT4 translocation requires the CAP-dependent activation of TC10.* Nature, 2001. **410**(6831): p. 944-8.
218. Rossman, K.L., C.J. Der, and J. Sondek, *GEF means go: turning on RHO GTPases with guanine nucleotide-exchange factors.* Nat Rev Mol Cell Biol, 2005. **6**(2): p. 167-80.
219. Hodge, R.G. and A.J. Ridley, *Regulating Rho GTPases and their regulators.* Nat Rev Mol Cell Biol, 2016. **17**(8): p. 496-510.
220. Cook, D.R., K.L. Rossman, and C.J. Der, *Rho guanine nucleotide exchange factors: regulators of Rho GTPase activity in development and disease.* Oncogene, 2014. **33**(31): p. 4021-35.
221. Gadea, G. and A. Blangy, *Dock-family exchange factors in cell migration and disease.* Eur J Cell Biol, 2014. **93**(10-12): p. 466-77.
222. Laurin, M. and J.F. Cote, *Insights into the biological functions of Dock family guanine nucleotide exchange factors.* Genes Dev, 2014. **28**(6): p. 533-47.
223. Moon, S.Y. and Y. Zheng, *Rho GTPase-activating proteins in cell regulation.* Trends Cell Biol, 2003. **13**(1): p. 13-22.
224. Garcia-Mata, R., E. Boulter, and K. Burridge, *The 'invisible hand': regulation of RHO GTPases by RHOGDIs.* Nat Rev Mol Cell Biol, 2011. **12**(8): p. 493-504.
225. DerMardirossian, C. and G.M. Bokoch, *GDIs: central regulatory molecules in Rho GTPase activation.* Trends Cell Biol, 2005. **15**(7): p. 356-63.
226. Boulter, E. and R. Garcia-Mata, *RhoGDI: A rheostat for the Rho switch.* Small GTPases, 2010. **1**(1): p. 65-68.
227. Michaelson, D., et al., *Differential localization of Rho GTPases in live cells: regulation by hypervariable regions and RhoGDI binding.* J Cell Biol, 2001. **152**(1): p. 111-26.
228. Katayama, M., et al., *The posttranslationally modified C-terminal structure of bovine aortic smooth muscle rhoA p21.* J Biol Chem, 1991. **266**(19): p. 12639-45.
229. Navarro-Lerida, I., et al., *A palmitoylation switch mechanism regulates Rac1 function and membrane organization.* EMBO J, 2012. **31**(3): p. 534-51.
230. Nishimura, A. and M.E. Linder, *Identification of a novel prenyl and palmitoyl modification at the CaaX motif of Cdc42 that regulates RhoGDI binding.* Mol Cell Biol, 2013. **33**(7): p. 1417-29.
231. Berzat, A.C., et al., *Transforming activity of the Rho family GTPase, Wrch-1, a Wnt-regulated Cdc42 homolog, is dependent on a novel carboxyl-terminal palmitoylation motif.* J Biol Chem, 2005. **280**(38): p. 33055-65.
232. Chenette, E.J., N.Y. Mitin, and C.J. Der, *Multiple sequence elements facilitate Chp Rho GTPase subcellular location, membrane association, and transforming activity.* Mol Biol Cell, 2006. **17**(7): p. 3108-21.
233. Tong, J., et al., *Phosphorylation of Rac1 T108 by extracellular signal-regulated kinase in response to epidermal growth factor: a novel mechanism to regulate Rac1 function.* Mol Cell Biol, 2013. **33**(22): p. 4538-51.
234. Chang, F., et al., *Tyrosine phosphorylation of Rac1: a role in regulation of cell spreading.* PLoS One, 2011. **6**(12): p. e28587.
235. Kwon, T., et al., *Akt protein kinase inhibits Rac1-GTP binding through phosphorylation at serine 71 of Rac1.* J Biol Chem, 2000. **275**(1): p. 423-8.
236. Tu, S., et al., *Epidermal growth factor-dependent regulation of Cdc42 is mediated by the Src tyrosine kinase.* J Biol Chem, 2003. **278**(49): p. 49293-300.

237. Forget, M.A., et al., *Phosphorylation states of Cdc42 and RhoA regulate their interactions with Rho GDP dissociation inhibitor and their extraction from biological membranes.* Biochem J, 2002. **361**(Pt 2): p. 243-54.
238. Rolli-Derkinderen, M., et al., *Phosphorylation of serine 188 protects RhoA from ubiquitin/proteasome-mediated degradation in vascular smooth muscle cells.* Circ Res, 2005. **96**(11): p. 1152-60.
239. Guilluy, C., et al., *Ste20-related kinase SLK phosphorylates Ser188 of RhoA to induce vasodilation in response to angiotensin II Type 2 receptor activation.* Circ Res, 2008. **102**(10): p. 1265-74.
240. Cao, Z., et al., *SUMOylation of RhoGDIalpha is required for its repression of cyclin D1 expression and anchorage-independent growth of cancer cells.* Mol Oncol, 2014. **8**(2): p. 285-96.
241. Riento, K., et al., *RhoE function is regulated by ROCK I-mediated phosphorylation.* EMBO J, 2005. **24**(6): p. 1170-80.
242. Madigan, J.P., et al., *Regulation of Rnd3 localization and function by protein kinase C alpha-mediated phosphorylation.* Biochem J, 2009. **424**(1): p. 153-61.
243. Riou, P., et al., *14-3-3 proteins interact with a hybrid prenyl-phosphorylation motif to inhibit G proteins.* Cell, 2013. **153**(3): p. 640-53.
244. Alan, J.K., et al., *Regulation of the Rho family small GTPase Wrch-1/RhoU by C-terminal tyrosine phosphorylation requires Src.* Mol Cell Biol, 2010. **30**(17): p. 4324-38.
245. Castillo-Lluva, S., et al., *SUMOylation of the GTPase Rac1 is required for optimal cell migration.* Nat Cell Biol, 2010. **12**(11): p. 1078-85.
246. Wang, H.R., et al., *Regulation of cell polarity and protrusion formation by targeting RhoA for degradation.* Science, 2003. **302**(5651): p. 1775-9.
247. Wei, J., et al., *A new mechanism of RhoA ubiquitination and degradation: roles of SCF(FBXL19) E3 ligase and Erk2.* Biochim Biophys Acta, 2013. **1833**(12): p. 2757-2764.
248. Berthold, J., et al., *Characterization of RhoBTB-dependent Cul3 ubiquitin ligase complexes--evidence for an autoregulatory mechanism.* Exp Cell Res, 2008. **314**(19): p. 3453-65.
249. Lonjedo, M., et al., *The Rho family member RhoE interacts with Skp2 and is degraded at the proteasome during cell cycle progression.* J Biol Chem, 2013. **288**(43): p. 30872-82.
250. Dart, A.E., et al., *PAK4 promotes kinase-independent stabilization of RhoU to modulate cell adhesion.* J Cell Biol, 2015. **211**(4): p. 863-79.
251. Oberoi, T.K., et al., *IAPs regulate the plasticity of cell migration by directly targeting Rac1 for degradation.* EMBO J, 2012. **31**(1): p. 14-28.
252. Zhao, J., et al., *SCF E3 ligase F-box protein complex SCF(FBXL19) regulates cell migration by mediating Rac1 ubiquitination and degradation.* FASEB J, 2013. **27**(7): p. 2611-9.
253. Bijkerk, R., et al., *MicroRNA-155 functions as a negative regulator of RhoA signaling in TGF-beta-induced endothelial to mesenchymal transition.* Microrna, 2012. **1**(1): p. 2-10.
254. Huang, B., et al., *MiRNA-125a-3p is a negative regulator of the RhoA-actomyosin pathway in A549 cells.* Int J Oncol, 2013. **42**(5): p. 1734-42.

255. Liu, M., et al., *miR-185 targets RhoA and Cdc42 expression and inhibits the proliferation potential of human colorectal cells.* Cancer Lett, 2011. **301**(2): p. 151-60.
256. Park, S.Y., et al., *miR-29 miRNAs activate p53 by targeting p85 alpha and CDC42.* Nat Struct Mol Biol, 2009. **16**(1): p. 23-9.
257. Cote, J.F. and K. Vuori, *GEF what? Dock180 and related proteins help Rac to polarize cells in new ways.* Trends Cell Biol, 2007. **17**(8): p. 383-93.
258. Kobayashi, S., et al., *Membrane recruitment of DOCK180 by binding to PtdIns(3,4,5)P3.* Biochem J, 2001. **354**(Pt 1): p. 73-8.
259. Sanematsu, F., et al., *Phosphatidic acid-dependent recruitment and function of the Rac activator DOCK1 during dorsal ruffle formation.* J Biol Chem, 2013. **288**(12): p. 8092-100.
260. Fukui, Y., et al., *Haematopoietic cell-specific CDM family protein DOCK2 is essential for lymphocyte migration.* Nature, 2001. **412**(6849): p. 826-31.
261. Sanematsu, F., et al., *DOCK180 is a Rac activator that regulates cardiovascular development by acting downstream of CXCR4.* Circ Res, 2010. **107**(9): p. 1102-5.
262. Laurin, M., et al., *The atypical Rac activator Dock180 (Dock1) regulates myoblast fusion in vivo.* Proc Natl Acad Sci U S A, 2008. **105**(40): p. 15446-51.
263. Kunisaki, Y., et al., *DOCK2 is a Rac activator that regulates motility and polarity during neutrophil chemotaxis.* J Cell Biol, 2006. **174**(5): p. 647-52.
264. Hasegawa, H., et al., *DOCK180, a major CRK-binding protein, alters cell morphology upon translocation to the cell membrane.* Mol Cell Biol, 1996. **16**(4): p. 1770-6.
265. Klemke, R.L., et al., *CAS/Crk coupling serves as a "molecular switch" for induction of cell migration.* J Cell Biol, 1998. **140**(4): p. 961-72.
266. Cheresh, D.A., J. Leng, and R.L. Klemke, *Regulation of cell contraction and membrane ruffling by distinct signals in migratory cells.* J Cell Biol, 1999. **146**(5): p. 1107-16.
267. Ellis, R.E., D.M. Jacobson, and H.R. Horvitz, *Genes required for the engulfment of cell corpses during programmed cell death in Caenorhabditis elegans.* Genetics, 1991. **129**(1): p. 79-94.
268. Wu, Y.C. and H.R. Horvitz, *C. elegans phagocytosis and cell-migration protein CED-5 is similar to human DOCK180.* Nature, 1998. **392**(6675): p. 501-4.
269. Gumienny, T.L., et al., *CED-12/ELMO, a novel member of the CrkII/Dock180/Rac pathway, is required for phagocytosis and cell migration.* Cell, 2001. **107**(1): p. 27-41.
270. Wu, Y.C., et al., *C. elegans CED-12 acts in the conserved crkII/DOCK180/Rac pathway to control cell migration and cell corpse engulfment.* Dev Cell, 2001. **1**(4): p. 491-502.
271. Katoh, H. and M. Negishi, *RhoG activates Rac1 by direct interaction with the Dock180-binding protein Elmo.* Nature, 2003. **424**(6947): p. 461-4.
272. Grimsley, C.M., et al., *Characterization of a novel interaction between ELMO1 and ERM proteins.* J Biol Chem, 2006. **281**(9): p. 5928-37.
273. Elliott, M.R., et al., *Unexpected requirement for ELMO1 in clearance of apoptotic germ cells in vivo.* Nature, 2010. **467**(7313): p. 333-7.
274. Patel, M., A. Pelletier, and J.F. Cote, *Opening up on ELMO regulation: New insights into the control of Rac signaling by the DOCK180/ELMO complex.* Small GTPases, 2011. **2**(5): p. 268-275.
275. Komander, D., et al., *An alpha-helical extension of the ELMO1 pleckstrin homology domain mediates direct interaction to DOCK180 and is critical in Rac signaling.* Mol Biol Cell, 2008. **19**(11): p. 4837-51.

276. Grimsley, C.M., et al., *Dock180 and ELMO1 proteins cooperate to promote evolutionarily conserved Rac-dependent cell migration.* J Biol Chem, 2004. **279**(7): p. 6087-97.
277. Margaron, Y., N. Fradet, and J.F. Cote, *ELMO recruits actin cross-linking family 7 (ACF7) at the cell membrane for microtubule capture and stabilization of cellular protrusions.* J Biol Chem, 2013. **288**(2): p. 1184-99.
278. Brugnera, E., et al., *Unconventional Rac-GEF activity is mediated through the Dock180-ELMO complex.* Nat Cell Biol, 2002. **4**(8): p. 574-82.
279. Lu, M., et al., *PH domain of ELMO functions in trans to regulate Rac activation via Dock180.* Nat Struct Mol Biol, 2004. **11**(8): p. 756-62.
280. Makino, Y., et al., *Elmo1 inhibits ubiquitylation of Dock180.* J Cell Sci, 2006. **119**(Pt 5): p. 923-32.
281. Lu, M., et al., *A Steric-inhibition model for regulation of nucleotide exchange via the Dock180 family of GEFs.* Curr Biol, 2005. **15**(4): p. 371-7.
282. Patel, M., et al., *An evolutionarily conserved autoinhibitory molecular switch in ELMO proteins regulates Rac signaling.* Curr Biol, 2010. **20**(22): p. 2021-7.
283. Patel, M., et al., *The Arf family GTPase Arl4A complexes with ELMO proteins to promote actin cytoskeleton remodeling and reveals a versatile Ras-binding domain in the ELMO proteins family.* J Biol Chem, 2011. **286**(45): p. 38969-79.
284. Yokoyama, N., et al., *Identification of tyrosine residues on ELMO1 that are phosphorylated by the Src-family kinase Hck.* Biochemistry, 2005. **44**(24): p. 8841-9.
285. Feng, H., et al., *Activation of Rac1 by Src-dependent phosphorylation of Dock180(Y1811) mediates PDGFRalpha-stimulated glioma tumorigenesis in mice and humans.* J Clin Invest, 2011. **121**(12): p. 4670-84.
286. Feng, H., et al., *Phosphorylation of dedicator of cytokinesis 1 (Dock180) at tyrosine residue Y722 by Src family kinases mediates EGFRvIII-driven glioblastoma tumorigenesis.* Proc Natl Acad Sci U S A, 2012. **109**(8): p. 3018-23.
287. Feng, H., et al., *EGFRvIII stimulates glioma growth and invasion through PKA-dependent serine phosphorylation of Dock180.* Oncogene, 2014. **33**(19): p. 2504-12.
288. Laurin, M., et al., *Rac-specific guanine nucleotide exchange factor DOCK1 is a critical regulator of HER2-mediated breast cancer metastasis.* Proc Natl Acad Sci U S A, 2013. **110**(18): p. 7434-9.
289. Miyamoto, Y., et al., *Akt and PP2A reciprocally regulate the guanine nucleotide exchange factor Dock6 to control axon growth of sensory neurons.* Sci Signal, 2013. **6**(265): p. ra15.
290. Smith, H.W., P. Marra, and C.J. Marshall, *uPAR promotes formation of the p130Cas-Crk complex to activate Rac through DOCK180.* J Cell Biol, 2008. **182**(4): p. 777-90.
291. Li, H., et al., *Association between Galphai2 and ELMO1/Dock180 connects chemokine signalling with Rac activation and metastasis.* Nat Commun, 2013. **4**: p. 1706.
292. Fritsch, R., et al., *RAS and RHO families of GTPases directly regulate distinct phosphoinositide 3-kinase isoforms.* Cell, 2013. **153**(5): p. 1050-63.
293. Friedl, P. and K. Wolf, *Tumour-cell invasion and migration: diversity and escape mechanisms.* Nat Rev Cancer, 2003. **3**(5): p. 362-74.
294. Taddei, M.L., et al., *Microenvironment and tumor cell plasticity: an easy way out.* Cancer Lett, 2013. **341**(1): p. 80-96.

295. Sanz-Moreno, V., et al., *Rac activation and inactivation control plasticity of tumor cell movement.* Cell, 2008. **135**(3): p. 510-23.
296. Yang, W.H., et al., *RAC1 activation mediates Twist1-induced cancer cell migration.* Nat Cell Biol, 2012. **14**(4): p. 366-74.
297. Kobayashi, M., et al., *Dock4 forms a complex with SH3YL1 and regulates cancer cell migration.* Cell Signal, 2014. **26**(5): p. 1082-8.
298. Hiramoto, K., M. Negishi, and H. Katoh, *Dock4 is regulated by RhoG and promotes Rac-dependent cell migration.* Exp Cell Res, 2006. **312**(20): p. 4205-16.
299. Hiramoto-Yamaki, N., et al., *Ephexin4 and EphA2 mediate cell migration through a RhoG-dependent mechanism.* J Cell Biol, 2010. **190**(3): p. 461-77.
300. Chambers, A.F., A.C. Groom, and I.C. MacDonald, *Dissemination and growth of cancer cells in metastatic sites.* Nat Rev Cancer, 2002. **2**(8): p. 563-72.
301. Lauffenburger, D.A. and A.F. Horwitz, *Cell migration: a physically integrated molecular process.* Cell, 1996. **84**(3): p. 359-69.
302. Ridley, A.J., et al., *Cell migration: integrating signals from front to back.* Science, 2003. **302**(5651): p. 1704-9.
303. Sanz-Moreno, V. and C.J. Marshall, *The plasticity of cytoskeletal dynamics underlying neoplastic cell migration.* Curr Opin Cell Biol, 2010. **22**(5): p. 690-6.
304. Sahai, E., *Illuminating the metastatic process.* Nat Rev Cancer, 2007. **7**(10): p. 737-49.
305. Fidler, I.J., *The pathogenesis of cancer metastasis: the 'seed and soil' hypothesis revisited.* Nat Rev Cancer, 2003. **3**(6): p. 453-8.
306. Ngan, E., et al., *Emerging roles for LPP in metastatic cancer progression.* J Cell Commun Signal, 2018. **12**(1): p. 143-156.
307. Friedl, P. and K. Wolf, *Plasticity of cell migration: a multiscale tuning model.* J Cell Biol, 2010. **188**(1): p. 11-9.
308. Friedl, P. and S. Alexander, *Cancer invasion and the microenvironment: plasticity and reciprocity.* Cell, 2011. **147**(5): p. 992-1009.
309. Friedl, P. and K. Wolf, *Proteolytic interstitial cell migration: a five-step process.* Cancer Metastasis Rev, 2009. **28**(1-2): p. 129-35.
310. Sheetz, M.P., et al., *Cell migration as a five-step cycle.* Biochem Soc Symp, 1999. **65**: p. 233-43.
311. Welf, E.S. and J.M. Haugh, *Signaling pathways that control cell migration: models and analysis.* Wiley Interdiscip Rev Syst Biol Med, 2011. **3**(2): p. 231-40.
312. Estecha, A., et al., *Moesin orchestrates cortical polarity of melanoma tumour cells to initiate 3D invasion.* J Cell Sci, 2009. **122**(Pt 19): p. 3492-501.
313. Poincloux, R., et al., *Contractility of the cell rear drives invasion of breast tumor cells in 3D Matrigel.* Proc Natl Acad Sci U S A, 2011. **108**(5): p. 1943-8.
314. Friedl, P., et al., *Migration of highly aggressive MV3 melanoma cells in 3-dimensional collagen lattices results in local matrix reorganization and shedding of alpha2 and beta1 integrins and CD44.* Cancer Res, 1997. **57**(10): p. 2061-70.
315. Ladoux, B., R.M. Mege, and X. Trepat, *Front-Rear Polarization by Mechanical Cues: From Single Cells to Tissues.* Trends Cell Biol, 2016. **26**(6): p. 420-433.
316. Parsons, J.T., A.R. Horwitz, and M.A. Schwartz, *Cell adhesion: integrating cytoskeletal dynamics and cellular tension.* Nat Rev Mol Cell Biol, 2010. **11**(9): p. 633-43.

317. Gupton, S.L. and C.M. Waterman-Storer, *Spatiotemporal feedback between actomyosin and focal-adhesion systems optimizes rapid cell migration.* Cell, 2006. **125**(7): p. 1361-74.
318. Abercrombie, M., J.E. Heaysman, and S.M. Pegrum, *The locomotion of fibroblasts in culture. II. "RRuffling".* Exp Cell Res, 1970. **60**(3): p. 437-44.
319. Cramer, L.P., M. Siebert, and T.J. Mitchison, *Identification of novel graded polarity actin filament bundles in locomoting heart fibroblasts: implications for the generation of motile force.* J Cell Biol, 1997. **136**(6): p. 1287-305.
320. Wu, Y.I., et al., *A genetically encoded photoactivatable Rac controls the motility of living cells.* Nature, 2009. **461**(7260): p. 104-8.
321. Meller, J., L. Vidali, and M.A. Schwartz, *Endogenous RhoG is dispensable for integrin-mediated cell spreading but contributes to Rac-independent migration.* J Cell Sci, 2008. **121**(Pt 12): p. 1981-9.
322. van Rheenen, J., J. Condeelis, and M. Glogauer, *A common cofilin activity cycle in invasive tumor cells and inflammatory cells.* J Cell Sci, 2009. **122**(Pt 3): p. 305-11.
323. Chesarone, M.A., A.G. DuPage, and B.L. Goode, *Unleashing formins to remodel the actin and microtubule cytoskeletons.* Nat Rev Mol Cell Biol, 2010. **11**(1): p. 62-74.
324. Ren, G., M.S. Crampton, and A.S. Yap, *Cortactin: Coordinating adhesion and the actin cytoskeleton at cellular protrusions.* Cell Motil Cytoskeleton, 2009. **66**(10): p. 865-73.
325. Mullins, R.D., J.A. Heuser, and T.D. Pollard, *The interaction of Arp2/3 complex with actin: nucleation, high affinity pointed end capping, and formation of branching networks of filaments.* Proc Natl Acad Sci U S A, 1998. **95**(11): p. 6181-6.
326. Lai, F.P., et al., *Arp2/3 complex interactions and actin network turnover in lamellipodia.* EMBO J, 2008. **27**(7): p. 982-92.
327. Mattila, P.K. and P. Lappalainen, *Filopodia: molecular architecture and cellular functions.* Nat Rev Mol Cell Biol, 2008. **9**(6): p. 446-54.
328. Machesky, L.M. and A. Li, *Fascin: Invasive filopodia promoting metastasis.* Commun Integr Biol, 2010. **3**(3): p. 263-70.
329. Ahmed, S., W.I. Goh, and W. Bu, *I-BAR domains, IRSp53 and filopodium formation.* Semin Cell Dev Biol, 2010. **21**(4): p. 350-6.
330. Hotulainen, P., et al., *Defining mechanisms of actin polymerization and depolymerization during dendritic spine morphogenesis.* J Cell Biol, 2009. **185**(2): p. 323-39.
331. Johnston, S.A., et al., *Arp2/3 complex activity in filopodia of spreading cells.* BMC Cell Biol, 2008. **9**: p. 65.
332. Bear, J.E. and F.B. Gertler, *Ena/VASP: towards resolving a pointed controversy at the barbed end.* J Cell Sci, 2009. **122**(Pt 12): p. 1947-53.
333. Bohil, A.B., B.W. Robertson, and R.E. Cheney, *Myosin-X is a molecular motor that functions in filopodia formation.* Proc Natl Acad Sci U S A, 2006. **103**(33): p. 12411-6.
334. Campellone, K.G. and M.D. Welch, *A nucleator arms race: cellular control of actin assembly.* Nat Rev Mol Cell Biol, 2010. **11**(4): p. 237-51.
335. Gupton, S.L. and F.B. Gertler, *Filopodia: the fingers that do the walking.* Sci STKE, 2007. **2007**(400): p. re5.
336. Chen, W.T., *Proteolytic activity of specialized surface protrusions formed at rosette contact sites of transformed cells.* J Exp Zool, 1989. **251**(2): p. 167-85.

337. Buccione, R., G. Caldieri, and I. Ayala, *Invadopodia: specialized tumor cell structures for the focal degradation of the extracellular matrix.* Cancer Metastasis Rev, 2009. **28**(1-2): p. 137-49.
338. Eddy, R.J., et al., *Tumor Cell Invadopodia: Invasive Protrusions that Orchestrate Metastasis.* Trends Cell Biol, 2017. **27**(8): p. 595-607.
339. Poincloux, R., F. Lizarraga, and P. Chavrier, *Matrix invasion by tumour cells: a focus on MT1-MMP trafficking to invadopodia.* J Cell Sci, 2009. **122**(Pt 17): p. 3015-24.
340. Schoumacher, M., et al., *Actin, microtubules, and vimentin intermediate filaments cooperate for elongation of invadopodia.* J Cell Biol, 2010. **189**(3): p. 541-56.
341. Ayala, I., et al., *Faciogenital dysplasia protein Fgd1 regulates invadopodia biogenesis and extracellular matrix degradation and is up-regulated in prostate and breast cancer.* Cancer Res, 2009. **69**(3): p. 747-52.
342. Lizarraga, F., et al., *Diaphanous-related formins are required for invadopodia formation and invasion of breast tumor cells.* Cancer Res, 2009. **69**(7): p. 2792-800.
343. Pichot, C.S., et al., *Cdc42-interacting protein 4 promotes breast cancer cell invasion and formation of invadopodia through activation of N-WASp.* Cancer Res, 2010. **70**(21): p. 8347-56.
344. Klemke, R.L., *Trespassing cancer cells: 'fingerprinting' invasive protrusions reveals metastatic culprits.* Curr Opin Cell Biol, 2012. **24**(5): p. 662-9.
345. Iwaya, K., et al., *Correlation between liver metastasis of the colocalization of actin-related protein 2 and 3 complex and WAVE2 in colorectal carcinoma.* Cancer Sci, 2007. **98**(7): p. 992-9.
346. Choi, S., et al., *Proteomic profiling of human cancer pseudopodia for the identification of anti-metastatic drug candidates.* Sci Rep, 2018. **8**(1): p. 5858.
347. Le Clainche, C. and M.F. Carlier, *Regulation of actin assembly associated with protrusion and adhesion in cell migration.* Physiol Rev, 2008. **88**(2): p. 489-513.
348. Charras, G. and E. Paluch, *Blebs lead the way: how to migrate without lamellipodia.* Nat Rev Mol Cell Biol, 2008. **9**(9): p. 730-6.
349. Bovellan, M., et al., *Death-associated protein kinase (DAPK) and signal transduction: blebbing in programmed cell death.* FEBS J, 2010. **277**(1): p. 58-65.
350. Tinevez, J.Y., et al., *Role of cortical tension in bleb growth.* Proc Natl Acad Sci U S A, 2009. **106**(44): p. 18581-6.
351. Kardash, E., et al., *A role for Rho GTPases and cell-cell adhesion in single-cell motility in vivo.* Nat Cell Biol, 2010. **12**(1): p. 47-53; sup pp 1-11.
352. Hannemann, S., et al., *The Diaphanous-related Formin FHOD1 associates with ROCK1 and promotes Src-dependent plasma membrane blebbing.* J Biol Chem, 2008. **283**(41): p. 27891-903.
353. Geiger, B., J.P. Spatz, and A.D. Bershadsky, *Environmental sensing through focal adhesions.* Nat Rev Mol Cell Biol, 2009. **10**(1): p. 21-33.
354. Truong, H. and E.H. Danen, *Integrin switching modulates adhesion dynamics and cell migration.* Cell Adh Migr, 2009. **3**(2): p. 179-81.
355. Hynes, R.O., *Integrins: bidirectional, allosteric signaling machines.* Cell, 2002. **110**(6): p. 673-87.
356. Martin, K.H., et al., *Integrin connections map: to infinity and beyond.* Science, 2002. **296**(5573): p. 1652-3.

357. Galbraith, C.G. and M.P. Sheetz, *Forces on adhesive contacts affect cell function.* Curr Opin Cell Biol, 1998. **10**(5): p. 566-71.
358. Liu, S., D.A. Calderwood, and M.H. Ginsberg, *Integrin cytoplasmic domain-binding proteins.* J Cell Sci, 2000. **113 (Pt 20)**: p. 3563-71.
359. Petit, V. and J.P. Thiery, *Focal adhesions: structure and dynamics.* Biol Cell, 2000. **92**(7): p. 477-94.
360. Humphries, J.D., et al., *Vinculin controls focal adhesion formation by direct interactions with talin and actin.* J Cell Biol, 2007. **179**(5): p. 1043-57.
361. Horwitz, A., et al., *Interaction of plasma membrane fibronectin receptor with talin--a transmembrane linkage.* Nature, 1986. **320**(6062): p. 531-3.
362. Geiger, B., et al., *Transmembrane crosstalk between the extracellular matrix--cytoskeleton crosstalk.* Nat Rev Mol Cell Biol, 2001. **2**(11): p. 793-805.
363. Goksoy, E., et al., *Structural basis for the autoinhibition of talin in regulating integrin activation.* Mol Cell, 2008. **31**(1): p. 124-33.
364. Nayal, A., D.J. Webb, and A.F. Horwitz, *Talin: an emerging focal point of adhesion dynamics.* Curr Opin Cell Biol, 2004. **16**(1): p. 94-8.
365. Ziegler, W.H., et al., *Integrin connections to the cytoskeleton through talin and vinculin.* Biochem Soc Trans, 2008. **36**(Pt 2): p. 235-9.
366. Bois, P.R., et al., *The vinculin binding sites of talin and alpha-actinin are sufficient to activate vinculin.* J Biol Chem, 2006. **281**(11): p. 7228-36.
367. Webb, D.J., J.T. Parsons, and A.F. Horwitz, *Adhesion assembly, disassembly and turnover in migrating cells -- over and over and over again.* Nat Cell Biol, 2002. **4**(4): p. E97-100.
368. Broussard, J.A., D.J. Webb, and I. Kaverina, *Asymmetric focal adhesion disassembly in motile cells.* Curr Opin Cell Biol, 2008. **20**(1): p. 85-90.
369. Deakin, N.O. and C.E. Turner, *Paxillin comes of age.* J Cell Sci, 2008. **121**(Pt 15): p. 2435-44.
370. Burridge, K. and M. Chrzanowska-Wodnicka, *Focal adhesions, contractility, and signaling.* Annu Rev Cell Dev Biol, 1996. **12**: p. 463-518.
371. Nobes, C.D. and A. Hall, *Rho, rac, and cdc42 GTPases regulate the assembly of multimolecular focal complexes associated with actin stress fibers, lamellipodia, and filopodia.* Cell, 1995. **81**(1): p. 53-62.
372. Nicholson-Dykstra, S., H.N. Higgs, and E.S. Harris, *Actin dynamics: growth from dendritic branches.* Curr Biol, 2005. **15**(9): p. R346-57.
373. Hotulainen, P. and P. Lappalainen, *Stress fibers are generated by two distinct actin assembly mechanisms in motile cells.* J Cell Biol, 2006. **173**(3): p. 383-94.
374. Vicente-Manzanares, M., et al., *Segregation and activation of myosin IIB creates a rear in migrating cells.* J Cell Biol, 2008. **183**(3): p. 543-54.
375. del Rio, A., et al., *Stretching single talin rod molecules activates vinculin binding.* Science, 2009. **323**(5914): p. 638-41.
376. Ezratty, E.J., et al., *Clathrin mediates integrin endocytosis for focal adhesion disassembly in migrating cells.* J Cell Biol, 2009. **187**(5): p. 733-47.
377. Ezratty, E.J., M.A. Partridge, and G.G. Gundersen, *Microtubule-induced focal adhesion disassembly is mediated by dynamin and focal adhesion kinase.* Nat Cell Biol, 2005. **7**(6): p. 581-90.

378. Premont, R.T., et al., *The GIT/PIX complex: an oligomeric assembly of GIT family ARF GTPase-activating proteins and PIX family Rac1/Cdc42 guanine nucleotide exchange factors.* Cell Signal, 2004. **16**(9): p. 1001-11.
379. Hiroyasu, S., et al., *Loss of beta-PIX inhibits focal adhesion disassembly and promotes keratinocyte motility via myosin light chain activation.* J Cell Sci, 2017. **130**(14): p. 2329-2343.
380. Kuo, J.C., et al., *Analysis of the myosin-II-responsive focal adhesion proteome reveals a role for beta-Pix in negative regulation of focal adhesion maturation.* Nat Cell Biol, 2011. **13**(4): p. 383-93.
381. Wilson, E., et al., *RhoJ interacts with the GIT-PIX complex and regulates focal adhesion disassembly.* J Cell Sci, 2014. **127**(Pt 14): p. 3039-51.
382. Lim, Y., et al., *PyK2 and FAK connections to p190Rho guanine nucleotide exchange factor regulate RhoA activity, focal adhesion formation, and cell motility.* J Cell Biol, 2008. **180**(1): p. 187-203.
383. Kiyokawa, E. and M. Matsuda, *Regulation of focal adhesion and cell migration by ANKRD28-DOCK180 interaction.* Cell Adh Migr, 2009. **3**(3): p. 281-4.
384. Tomar, A., et al., *A FAK-p120RasGAP-p190RhoGAP complex regulates polarity in migrating cells.* J Cell Sci, 2009. **122**(Pt 11): p. 1852-62.
385. Schmalzigaug, R., et al., *GIT1 utilizes a focal adhesion targeting-homology domain to bind paxillin.* Cell Signal, 2007. **19**(8): p. 1733-44.
386. Defilippi, P., P. Di Stefano, and S. Cabodi, *p130Cas: a versatile scaffold in signaling networks.* Trends Cell Biol, 2006. **16**(5): p. 257-63.
387. Sawada, Y., et al., *Force sensing by mechanical extension of the Src family kinase substrate p130Cas.* Cell, 2006. **127**(5): p. 1015-26.
388. Iwahara, T., et al., *CrkII regulates focal adhesion kinase activation by making a complex with Crk-associated substrate, p130Cas.* Proc Natl Acad Sci U S A, 2004. **101**(51): p. 17693-8.
389. Stoletov, K.V., C. Gong, and B.I. Terman, *Nck and Crk mediate distinct VEGF-induced signaling pathways that serve overlapping functions in focal adhesion turnover and integrin activation.* Exp Cell Res, 2004. **295**(1): p. 258-68.
390. Zaidel-Bar, R., et al., *A paxillin tyrosine phosphorylation switch regulates the assembly and form of cell-matrix adhesions.* J Cell Sci, 2007. **120**(Pt 1): p. 137-48.
391. Brown, M.C. and C.E. Turner, *Paxillin: adapting to change.* Physiol Rev, 2004. **84**(4): p. 1315-39.
392. Nayal, A., et al., *Paxillin phosphorylation at Ser273 localizes a GIT1-PIX-PAK complex and regulates adhesion and protrusion dynamics.* J Cell Biol, 2006. **173**(4): p. 587-9.
393. Bristow, J.M., et al., *Dynamic phosphorylation of tyrosine 665 in pseudopodium-enriched atypical kinase 1 (PEAK1) is essential for the regulation of cell migration and focal adhesion turnover.* J Biol Chem, 2013. **288**(1): p. 123-31.
394. Parsons, J.T., *Focal adhesion kinase: the first ten years.* J Cell Sci, 2003. **116**(Pt 8): p. 1409-16.
395. Tomar, A. and D.D. Schlaepfer, *Focal adhesion kinase: switching between GAPs and GEFs in the regulation of cell motility.* Curr Opin Cell Biol, 2009. **21**(5): p. 676-83.
396. Mitra, S.K., D.A. Hanson, and D.D. Schlaepfer, *Focal adhesion kinase: in command and control of cell motility.* Nat Rev Mol Cell Biol, 2005. **6**(1): p. 56-68.

397. Legate, K.R., et al., *ILK, PINCH and parvin: the tIPP of integrin signalling.* Nat Rev Mol Cell Biol, 2006. **7**(1): p. 20-31.
398. Mitra, S.K. and D.D. Schlaepfer, *Integrin-regulated FAK-Src signaling in normal and cancer cells.* Curr Opin Cell Biol, 2006. **18**(5): p. 516-23.
399. Peacock, J.G., et al., *The Abl-related gene tyrosine kinase acts through p190RhoGAP to inhibit actomyosin contractility and regulate focal adhesion dynamics upon adhesion to fibronectin.* Mol Biol Cell, 2007. **18**(10): p. 3860-72.
400. Giannone, G. and M.P. Sheetz, *Substrate rigidity and force define form through tyrosine phosphatase and kinase pathways.* Trends Cell Biol, 2006. **16**(4): p. 213-23.
401. Burridge, K., S.K. Sastry, and J.L. Sallee, *Regulation of cell adhesion by protein-tyrosine phosphatases. I. Cell-matrix adhesion.* J Biol Chem, 2006. **281**(23): p. 15593-6.
402. Zheng, Y., et al., *FAK phosphorylation by ERK primes ras-induced tyrosine dephosphorylation of FAK mediated by PIN1 and PTP-PEST.* Mol Cell, 2009. **35**(1): p. 11-25.
403. Espejo, R., et al., *PTP-PEST controls motility, adherens junction assembly, and Rho GTPase activity in colon cancer cells.* Am J Physiol Cell Physiol, 2010. **299**(2): p. C454-63.
404. Lin, S.Y., et al., *The protein-tyrosine phosphatase SHP-1 regulates the phosphorylation of alpha-actinin.* J Biol Chem, 2004. **279**(24): p. 25755-64.
405. Yu, D.H., et al., *Protein-tyrosine phosphatase Shp-2 regulates cell spreading, migration, and focal adhesion.* J Biol Chem, 1998. **273**(33): p. 21125-31.
406. de Oliveira, M.V., et al., *SHP-2 regulates myogenesis by coupling to FAK signaling pathway.* FEBS Lett, 2009. **583**(18): p. 2975-81.
407. Zhang, Z., et al., *Phosphorylated alpha-actinin and protein-tyrosine phosphatase 1B coregulate the disassembly of the focal adhesion kinase x Src complex and promote cell migration.* J Biol Chem, 2006. **281**(3): p. 1746-54.
408. Liang, F., et al., *The role of protein-tyrosine phosphatase 1B in integrin signaling.* J Biol Chem, 2005. **280**(26): p. 24857-63.
409. O'Bryan, J.P., et al., *axl, a transforming gene isolated from primary human myeloid leukemia cells, encodes a novel receptor tyrosine kinase.* Mol Cell Biol, 1991. **11**(10): p. 5016-31.
410. Stitt, T.N., et al., *The anticoagulation factor protein S and its relative, Gas6, are ligands for the Tyro 3/Axl family of receptor tyrosine kinases.* Cell, 1995. **80**(4): p. 661-70.
411. Nagata, K., et al., *Identification of the product of growth arrest-specific gene 6 as a common ligand for Axl, Sky, and Mer receptor tyrosine kinases.* J Biol Chem, 1996. **271**(47): p. 30022-7.
412. O'Bryan, J.P., et al., *The transforming receptor tyrosine kinase, Axl, is post-translationally regulated by proteolytic cleavage.* J Biol Chem, 1995. **270**(2): p. 551-7.
413. Hall, M.O., et al., *Both protein S and Gas6 stimulate outer segment phagocytosis by cultured rat retinal pigment epithelial cells.* Exp Eye Res, 2005. **81**(5): p. 581-91.
414. Wu, Y., et al., *A role for Mer tyrosine kinase in alphavbeta5 integrin-mediated phagocytosis of apoptotic cells.* J Cell Sci, 2005. **118**(Pt 3): p. 539-53.
415. Caberoy, N.B., et al., *Identification of tubby and tubby-like protein 1 as eat-me signals by phage display.* Exp Cell Res, 2010. **316**(2): p. 245-57.

416. Nakano, T., et al., *Cell adhesion to phosphatidylserine mediated by a product of growth arrest-specific gene 6.* J Biol Chem, 1997. **272**(47): p. 29411-4.
417. Burchert, A., et al., *Determinants for transformation induced by the Axl receptor tyrosine kinase.* Oncogene, 1998. **16**(24): p. 3177-87.
418. Budagian, V., et al., *A promiscuous liaison between IL-15 receptor and Axl receptor tyrosine kinase in cell death control (Retracted Article. See vol 30, pg 627, 2011).* Embo Journal, 2005. **24**(24): p. 4260-4270.
419. Fridell, Y.W., et al., *Differential activation of the Ras/extracellular-signal-regulated protein kinase pathway is responsible for the biological consequences induced by the Axl receptor tyrosine kinase.* Mol Cell Biol, 1996. **16**(1): p. 135-45.
420. Lemke, G. and Q. Lu, *Macrophage regulation by Tyro 3 family receptors.* Curr Opin Immunol, 2003. **15**(1): p. 31-6.
421. D'Cruz, P.M., et al., *Mutation of the receptor tyrosine kinase gene Mertk in the retinal dystrophic RCS rat.* Hum Mol Genet, 2000. **9**(4): p. 645-51.
422. Shieh, Y.S., et al., *Expression of axl in lung adenocarcinoma and correlation with tumor progression.* Neoplasia, 2005. **7**(12): p. 1058-64.
423. Holland, S.J., et al., *R428, a Selective Small Molecule Inhibitor of Axl Kinase, Blocks Tumor Spread and Prolongs Survival in Models of Metastatic Breast Cancer.* Cancer Research, 2010. **70**(4): p. 1544-1554.
424. Ye, X., et al., *An anti-Axl monoclonal antibody attenuates xenograft tumor growth and enhances the effect of multiple anticancer therapies.* Oncogene, 2010. **29**(38): p. 5254-64.
425. Cote, J.F. and K. Vuori, *Identification of an evolutionarily conserved superfamily of DOCK180-related proteins with guanine nucleotide exchange activity.* J Cell Sci, 2002. **115**(Pt 24): p. 4901-13.
426. Meller, N., et al., *Zizimin1, a novel Cdc42 activator, reveals a new GEF domain for Rho proteins.* Nat Cell Biol, 2002. **4**(9): p. 639-47.
427. Feng, H., et al., *EGFRvIII stimulates glioma growth and invasion through PKA-dependent serine phosphorylation of Dock180.* Oncogene, 2013.
428. Jansson, D., et al., *Glucose controls CREB activity in islet cells via regulated phosphorylation of TORC2.* Proc Natl Acad Sci U S A, 2008. **105**(29): p. 10161-6.
429. Verma, A., et al., *Targeting Axl and Mer kinases in cancer.* Mol Cancer Ther, 2011. **10**(10): p. 1763-73.
430. Weinger, J.G., et al., *In brain, Axl recruits Grb2 and the p85 regulatory subunit of PI3 kinase; in vitro mutagenesis defines the requisite binding sites for downstream Akt activation.* J Neurochem, 2008. **106**(1): p. 134-46.
431. Nielsen-Preiss, S.M., et al., *Adhesion-related kinase induction of migration requires phosphatidylinositol-3-kinase and ras stimulation of rac activity in immortalized gonadotropin-releasing hormone neuronal cells.* Endocrinology, 2007. **148**(6): p. 2806-14.
432. Nishikimi, A., et al., *Blockade of inflammatory responses by a small-molecule inhibitor of the Rac activator DOCK2.* Chem Biol, 2012. **19**(4): p. 488-97.
433. Childs, G. and J.E. Segall, *Twists and turns of invasion.* Nat Cell Biol, 2012. **14**(4): p. 337-9.
434. Zhang, Y.X., et al., *AXL is a potential target for therapeutic intervention in breast cancer progression.* Cancer Res, 2008. **68**(6): p. 1905-15.

435. Hamoud, N., et al., *G-protein coupled receptor BAI3 promotes myoblast fusion in vertebrates.* Proc Natl Acad Sci U S A, 2014. **111**(10): p. 3745-50.
436. Duchek, P., et al., *Guidance of cell migration by the Drosophila PDGF/VEGF receptor.* Cell, 2001. **107**(1): p. 17-26.
437. Liu, Z.C., N. Odell, and E.R. Geisbrecht, *Drosophila importin-7 functions upstream of the Elmo signaling module to mediate the formation and stability of muscle attachments.* J Cell Sci, 2013. **126**(Pt 22): p. 5210-23.
438. Mahajan, N.P. and H.S. Earp, *An SH2 domain-dependent, phosphotyrosine-independent interaction between Vav1 and the Mer receptor tyrosine kinase: a mechanism for localizing guanine nucleotide-exchange factor action.* J Biol Chem, 2003. **278**(43): p. 42596-603.
439. Cote, J.F., et al., *A novel and evolutionarily conserved PtdIns(3,4,5)P3-binding domain is necessary for DOCK180 signalling.* Nat Cell Biol, 2005. **7**(8): p. 797-807.
440. Dai, W., et al., *Molecular cloning of a novel receptor tyrosine kinase, tif, highly expressed in human ovary and testis.* Oncogene, 1994. **9**(3): p. 975-9.
441. Steeg, P.S., *Targeting metastasis.* Nat Rev Cancer, 2016. **16**(4): p. 201-18.
442. Bauer, K.R., et al., *Descriptive analysis of estrogen receptor (ER)-negative, progesterone receptor (PR)-negative, and HER2-negative invasive breast cancer, the so-called triple-negative phenotype: a population-based study from the California cancer Registry.* Cancer, 2007. **109**(9): p. 1721-8.
443. Penault-Llorca, F. and G. Viale, *Pathological and molecular diagnosis of triple-negative breast cancer: a clinical perspective.* Ann Oncol, 2012. **23 Suppl 6**: p. vi19-22.
444. Anders, C.K. and L.A. Carey, *Biology, metastatic patterns, and treatment of patients with triple-negative breast cancer.* Clin Breast Cancer, 2009. **9 Suppl 2**: p. S73-81.
445. Lamouille, S., J. Xu, and R. Derynck, *Molecular mechanisms of epithelial-mesenchymal transition.* Nat Rev Mol Cell Biol, 2014. **15**(3): p. 178-96.
446. Sarrio, D., et al., *Epithelial-mesenchymal transition in breast cancer relates to the basal-like phenotype.* Cancer Res, 2008. **68**(4): p. 989-97.
447. Jeong, H., et al., *Epithelial-mesenchymal transition in breast cancer correlates with high histological grade and triple-negative phenotype.* Histopathology, 2012. **60**(6B): p. E87-95.
448. Lemke, G., *Biology of the TAM receptors.* Cold Spring Harb Perspect Biol, 2013. **5**(11): p. a009076.
449. D'Alfonso, T.M., et al., *Axl receptor tyrosine kinase expression in breast cancer.* J Clin Pathol, 2014. **67**(8): p. 690-6.
450. Ong, S.E., et al., *Stable isotope labeling by amino acids in cell culture, SILAC, as a simple and accurate approach to expression proteomics.* Mol Cell Proteomics, 2002. **1**(5): p. 376-86.
451. Olsen, J.V., et al., *Global, in vivo, and site-specific phosphorylation dynamics in signaling networks.* Cell, 2006. **127**(3): p. 635-48.
452. Engholm-Keller, K., et al., *Multidimensional strategy for sensitive phosphoproteomics incorporating protein prefractionation combined with SIMAC, HILIC, and TiO(2) chromatography applied to proximal EGF signaling.* J Proteome Res, 2011. **10**(12): p. 5383-97.
453. Kim, M., et al., *Comparative oncogenomics identifies NEDD9 as a melanoma metastasis gene.* Cell, 2006. **125**(7): p. 1269-81.

454. Hanks, S.K. and T.R. Polte, *Signaling through focal adhesion kinase.* Bioessays, 1997. **19**(2): p. 137-45.
455. Roux, K.J., et al., *A promiscuous biotin ligase fusion protein identifies proximal and interacting proteins in mammalian cells.* J Cell Biol, 2012. **196**(6): p. 801-10.
456. Wang, Y., et al., *Pseudopodium-enriched atypical kinase 1 regulates the cytoskeleton and cancer progression [corrected].* Proc Natl Acad Sci U S A, 2010. **107**(24): p. 10920-5.
457. Kelber, J.A. and R.L. Klemke, *PEAK1, a novel kinase target in the fight against cancer.* Oncotarget, 2010. **1**(3): p. 219-23.
458. Croucher, D.R., et al., *Involvement of Lyn and the atypical kinase SgK269/PEAK1 in a basal breast cancer signaling pathway.* Cancer Res, 2013. **73**(6): p. 1969-80.
459. Zheng, Y., et al., *Temporal regulation of EGF signalling networks by the scaffold protein Shc1.* Nature, 2013. **499**(7457): p. 166-71.
460. Lamorte, L., et al., *Crk associates with a multimolecular Paxillin/GIT2/beta-PIX complex and promotes Rac-dependent relocalization of Paxillin to focal contacts.* Mol Biol Cell, 2003. **14**(7): p. 2818-31.
461. Hagel, M., et al., *The adaptor protein paxillin is essential for normal development in the mouse and is a critical transducer of fibronectin signaling.* Mol Cell Biol, 2002. **22**(3): p. 901-15.
462. Lecointre, C., et al., *Dimerization of the Pragmin Pseudo-Kinase Regulates Protein Tyrosine Phosphorylation.* Structure, 2018. **26**(4): p. 545-554 e4.
463. Liu, L., et al., *Homo- and Heterotypic Association Regulates Signaling by the SgK269/PEAK1 and SgK223 Pseudokinases.* J Biol Chem, 2016. **291**(41): p. 21571-21583.
464. Zhao, Z.S., et al., *Coupling of PAK-interacting exchange factor PIX to GIT1 promotes focal complex disassembly.* Mol Cell Biol, 2000. **20**(17): p. 6354-63.
465. Feng, Q., et al., *Phosphorylation of the cool-1/beta-Pix protein serves as a regulatory signal for the migration and invasive activity of Src-transformed cells.* J Biol Chem, 2010. **285**(24): p. 18806-16.
466. Manser, E., et al., *PAK kinases are directly coupled to the PIX family of nucleotide exchange factors.* Mol Cell, 1998. **1**(2): p. 183-92.
467. Manser, E., et al., *A brain serine/threonine protein kinase activated by Cdc42 and Rac1.* Nature, 1994. **367**(6458): p. 40-6.
468. Bagrodia, S. and R.A. Cerione, *Pak to the future.* Trends Cell Biol, 1999. **9**(9): p. 350-5.
469. Korshunov, V.A., *Axl-dependent signalling: a clinical update.* Clin Sci (Lond), 2012. **122**(8): p. 361-8.
470. Chen, Z., et al., *Spatially modulated ephrinA1:EphA2 signaling increases local contractility and global focal adhesion dynamics to promote cell motility.* Proc Natl Acad Sci U S A, 2018. **115**(25): p. E5696-E5705.
471. Agajanian, M., et al., *PEAK1 Acts as a Molecular Switch to Regulate Context-Dependent TGFbeta Responses in Breast Cancer.* PLoS One, 2015. **10**(8): p. e0135748.
472. Kelber, J.A., et al., *KRas induces a Src/PEAK1/ErbB2 kinase amplification loop that drives metastatic growth and therapy resistance in pancreatic cancer.* Cancer Res, 2012. **72**(10): p. 2554-64.

473. Vouri, M., et al., *Axl-EGFR receptor tyrosine kinase hetero-interaction provides EGFR with access to pro-invasive signalling in cancer cells.* Oncogenesis, 2016. **5**(10): p. e266.
474. Cote, J.F., C.E. Turner, and M.L. Tremblay, *Intact LIM 3 and LIM 4 domains of paxillin are required for the association to a novel polyproline region (Pro 2) of protein-tyrosine phosphatase-PEST.* J Biol Chem, 1999. **274**(29): p. 20550-60.
475. Cao, M.Y., et al., *Regulation of mouse PECAM-1 tyrosine phosphorylation by the Src and Csk families of protein-tyrosine kinases.* J Biol Chem, 1998. **273**(25): p. 15765-72.
476. Tyanova, S., T. Temu, and J. Cox, *The MaxQuant computational platform for mass spectrometry-based shotgun proteomics.* Nat Protoc, 2016. **11**(12): p. 2301-2319.
477. Couzens, A.L., et al., *Protein interaction network of the mammalian Hippo pathway reveals mechanisms of kinase-phosphatase interactions.* Sci Signal, 2013. **6**(302): p. rs15.
478. Youn, J.Y., et al., *High-Density Proximity Mapping Reveals the Subcellular Organization of mRNA-Associated Granules and Bodies.* Mol Cell, 2018. **69**(3): p. 517-532 e11.
479. Shteynberg, D., et al., *iProphet: multi-level integrative analysis of shotgun proteomic data improves peptide and protein identification rates and error estimates.* Mol Cell Proteomics, 2011. **10**(12): p. M111 007690.
480. Liu, G., et al., *ProHits: integrated software for mass spectrometry-based interaction proteomics.* Nat Biotechnol, 2010. **28**(10): p. 1015-7.
481. Keller, A., et al., *Empirical statistical model to estimate the accuracy of peptide identifications made by MS/MS and database search.* Anal Chem, 2002. **74**(20): p. 5383-92.
482. Nesvizhskii, A.I., et al., *A statistical model for identifying proteins by tandem mass spectrometry.* Anal Chem, 2003. **75**(17): p. 4646-58.
483. Zybailov, B., et al., *Statistical analysis of membrane proteome expression changes in Saccharomyces cerevisiae.* J Proteome Res, 2006. **5**(9): p. 2339-47.
484. Knight, J.D.R., et al., *ProHits-viz: a suite of web tools for visualizing interaction proteomics data.* Nat Methods, 2017. **14**(7): p. 645-646.
485. Shannon, P., et al., *Cytoscape: a software environment for integrated models of biomolecular interaction networks.* Genome Res, 2003. **13**(11): p. 2498-504.
486. Montojo, J., et al., *GeneMANIA Cytoscape plugin: fast gene function predictions on the desktop.* Bioinformatics, 2010. **26**(22): p. 2927-8.
487. Huntley, R.P., et al., *The GOA database: gene Ontology annotation updates for 2015.* Nucleic Acids Res, 2015. **43**(Database issue): p. D1057-63.
488. Chen, M.J., J.E. Dixon, and G. Manning, *Genomics and evolution of protein phosphatases.* Sci Signal, 2017. **10**(474).
489. Manning, G., et al., *The protein kinase complement of the human genome.* Science, 2002. **298**(5600): p. 1912-34.
490. Reimand, J., et al., *g:Profiler-a web server for functional interpretation of gene lists (2016 update).* Nucleic Acids Res, 2016. **44**(W1): p. W83-9.
491. Kanehisa, M. and S. Goto, *KEGG: kyoto encyclopedia of genes and genomes.* Nucleic Acids Res, 2000. **28**(1): p. 27-30.
492. Yu, G., et al., *clusterProfiler: an R package for comparing biological themes among gene clusters.* OMICS, 2012. **16**(5): p. 284-7.

493. Kumar, L. and E.F. M, *Mfuzz: a software package for soft clustering of microarray data.* Bioinformation, 2007. **2**(1): p. 5-7.
494. Schwammle, V. and O.N. Jensen, *A simple and fast method to determine the parameters for fuzzy c-means cluster analysis.* Bioinformatics, 2010. **26**(22): p. 2841-8.
495. O'Shea, J.P., et al., *pLogo: a probabilistic approach to visualizing sequence motifs.* Nat Methods, 2013. **10**(12): p. 1211-2.
496. Doench, J.G., et al., *Optimized sgRNA design to maximize activity and minimize off-target effects of CRISPR-Cas9.* Nat Biotechnol, 2016. **34**(2): p. 184-191.
497. Boimel, P.J., et al., *Contribution of CXCL12 secretion to invasion of breast cancer cells.* Breast Cancer Res, 2012. **14**(1): p. R23.
498. Tanaka, K., et al., *Impact of Expression of Vimentin and Axl in Breast Cancer.* Clin Breast Cancer, 2016. **16**(6): p. 520-526 e2.
499. Liedtke, C., et al., *Response to neoadjuvant therapy and long-term survival in patients with triple-negative breast cancer.* J Clin Oncol, 2008. **26**(8): p. 1275-81.
500. Guerrero, M.S., J.T. Parsons, and A.H. Bouton, *Cas and NEDD9 Contribute to Tumor Progression through Dynamic Regulation of the Cytoskeleton.* Genes Cancer, 2012. **3**(5-6): p. 371-81.
501. Kong, C., et al., *NEDD9 is a positive regulator of epithelial-mesenchymal transition and promotes invasion in aggressive breast cancer.* PLoS One, 2011. **6**(7): p. e22666.
502. Ahn, J., V. Sanz-Moreno, and C.J. Marshall, *The metastasis gene NEDD9 product acts through integrin beta3 and Src to promote mesenchymal motility and inhibit amoeboid motility.* J Cell Sci, 2012. **125**(Pt 7): p. 1814-26.
503. Branis, J., et al., *The role of focal adhesion anchoring domains of CAS in mechanotransduction.* Sci Rep, 2017. **7**: p. 46233.
504. Ha, B.H. and T.J. Boggon, *The crystal structure of pseudokinase PEAK1 (Sugen kinase 269) reveals an unusual catalytic cleft and a novel mode of kinase fold dimerization.* J Biol Chem, 2018. **293**(5): p. 1642-1650.
505. Li, L., M. Okura, and A. Imamoto, *Focal adhesions require catalytic activity of Src family kinases to mediate integrin-matrix adhesion.* Mol Cell Biol, 2002. **22**(4): p. 1203-17.
506. Fujimura, K., et al., *A hypusine-eIF5A-PEAK1 switch regulates the pathogenesis of pancreatic cancer.* Cancer Res, 2014. **74**(22): p. 6671-81.
507. Ding, C., et al., *Overexpression of PEAK1 contributes to epithelial-mesenchymal transition and tumor metastasis in lung cancer through modulating ERK1/2 and JAK2 signaling.* Cell Death Dis, 2018. **9**(8): p. 802.
508. Abraham, S., et al., *A Rac/Cdc42 exchange factor complex promotes formation of lateral filopodia and blood vessel lumen morphogenesis.* Nat Commun, 2015. **6**: p. 7286.
509. Wiley, H.S. and P.M. Burke, *Regulation of receptor tyrosine kinase signaling by endocytic trafficking.* Traffic, 2001. **2**(1): p. 12-8.
510. Goh, L.K. and A. Sorkin, *Endocytosis of receptor tyrosine kinases.* Cold Spring Harb Perspect Biol, 2013. **5**(5): p. a017459.
511. Fang, D., et al., *Cbl-b, a RING-type E3 ubiquitin ligase, targets phosphatidylinositol 3-kinase for ubiquitination in T cells.* J Biol Chem, 2001. **276**(7): p. 4872-8.
512. Han, W. and H.W. Lo, *Landscape of EGFR signaling network in human cancers: biology and therapeutic response in relation to receptor subcellular locations.* Cancer Lett, 2012. **318**(2): p. 124-34.

513. Brand, T.M., et al., *The receptor tyrosine kinase AXL mediates nuclear translocation of the epidermal growth factor receptor.* Sci Signal, 2017. **10**(460).
514. Mellman, I. and Y. Yarden, *Endocytosis and cancer.* Cold Spring Harb Perspect Biol, 2013. **5**(12): p. a016949.
515. Murray, J.W. and A.W. Wolkoff, *Roles of the cytoskeleton and motor proteins in endocytic sorting.* Adv Drug Deliv Rev, 2003. **55**(11): p. 1385-403.
516. Granger, E., et al., *The role of the cytoskeleton and molecular motors in endosomal dynamics.* Semin Cell Dev Biol, 2014. **31**: p. 20-9.
517. Hautbergue, G.M., *RNA Nuclear Export: From Neurological Disorders to Cancer.* Adv Exp Med Biol, 2017. **1007**: p. 89-109.
518. Singh, B. and E. Eyras, *The role of alternative splicing in cancer.* Transcription, 2017. **8**(2): p. 91-98.
519. Fan, Y.J., et al., *Multifunctional RNA processing protein SRm160 induces apoptosis and regulates eye and genital development in Drosophila.* Genetics, 2014. **197**(4): p. 1251-65.
520. Poulikakos, P.I., et al., *RAF inhibitor resistance is mediated by dimerization of aberrantly spliced BRAF(V600E).* Nature, 2011. **480**(7377): p. 387-90.
521. Salton, M., et al., *Inhibition of vemurafenib-resistant melanoma by interference with pre-mRNA splicing.* Nat Commun, 2015. **6**: p. 7103.
522. Shen, Y., et al., *Axl inhibitors as novel cancer therapeutic agents.* Life Sci, 2018. **198**: p. 99-111.
523. Gay, C.M., K. Balaji, and L.A. Byers, *Giving AXL the axe: targeting AXL in human malignancy.* Br J Cancer, 2017. **116**(4): p. 415-423.

Appendix 1: Datasets of CHAPTER 3

- **Dataset I**
- **Dataset II**
- **Dataset III**
- **Dataset IV**
- **Dataset V**
- **Dataset VI**